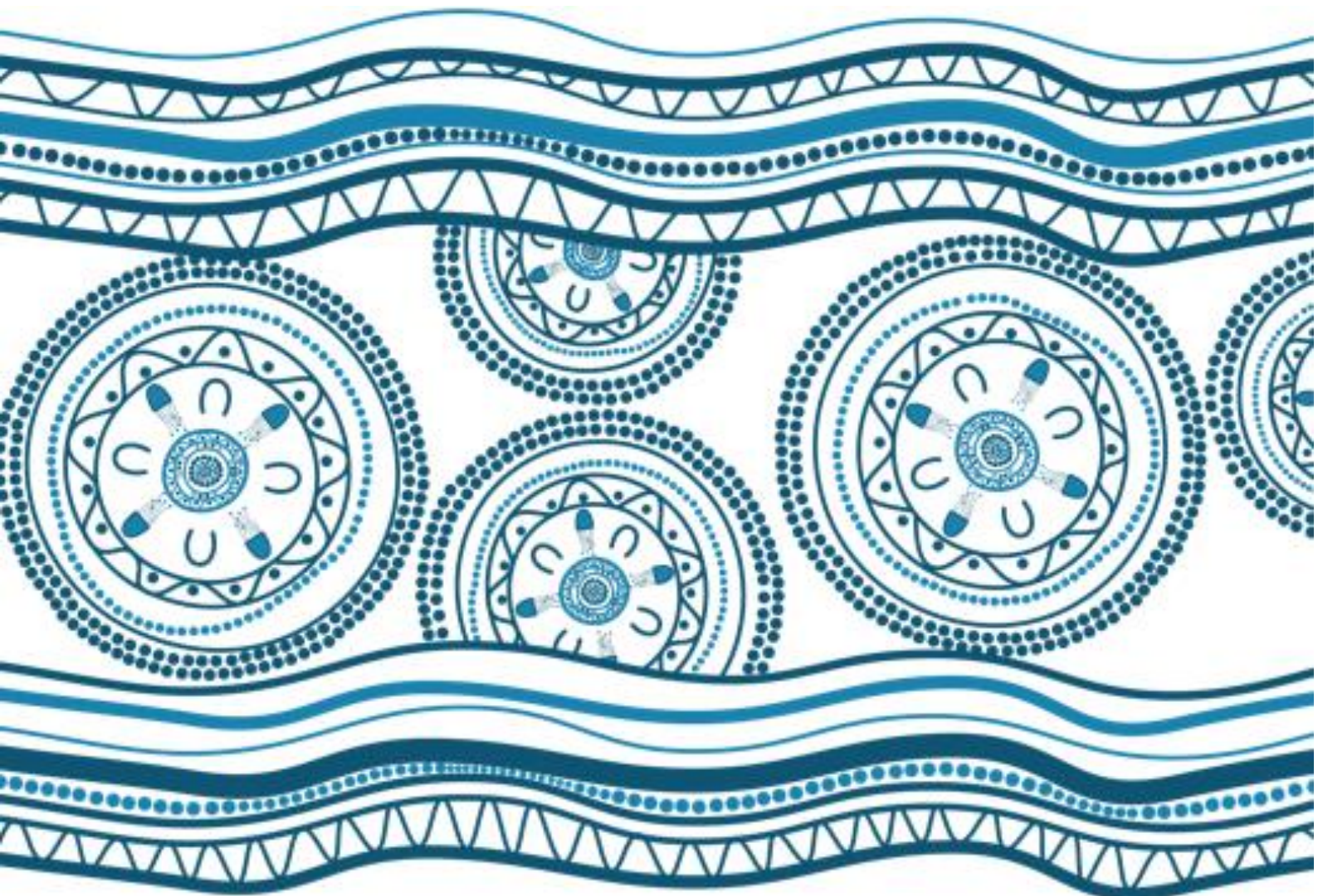


Appendix T

Coastal Processes Memorandum



BLANK PAGE

Our Ref: AWE200187:CJS
Contact: Chris Scraggs

23 June 2021

Arup
Barrack Place,
151 Clarence Street
Sydney NSW 2000

Attention: Thomas Dunlop

Cardno (NSW/ACT) Pty Ltd
ABN 95 001 145 035

Level 9 - The Forum
203 Pacific Highway
St Leonards NSW 2065
PO Box 19

Phone +61 2 9496 7700
Fax +61 2 9439 5170

www.cardno.com

Dear Thomas,

KAMAY FERRY WHARVES PROJECT IMPACTS TO COASTAL PROCESSES

Preamble

In order to support the EIS process, Arup has requested that Cardno provide an interpretation of the coastal modelling carried out during the design phase. Specifically, information has been requested in relation to potential impacts on coastal processes, potential suspended sediment plumes generated during construction and potential scouring due to propeller wash effects.

The purpose of this assessment has been to address the matters raised in SEAR 5 (1) (b), which states the following:

5. Environmentally Sensitive Lands and Processes

The project is designed, constructed and operated to avoid or minimise impacts on protected and sensitive lands.

The project is designed, constructed and operated to avoid or minimise future exposure to coastal hazards and processes.

- 1. Environmentally sensitive land and processes (and the impact of processes on the project) including, but not limited to:*

(b) hydrodynamic and coastal processes (including disruptions to wave direction, dune stability, sediment movement, scouring and erosion of the shoreline and seabed etc.) associated with adopted risk mitigation actions.

This letter presents the outcomes of Cardno's assessment.

Background

Most of the features of the Kurnell and La Perouse sites have been formed over the past 10,000 years of the Holocene period (Roy and Crawford, 1979); during a period of substantial sea level rise. Relative to that period, sea level is now stable. However, natural and human-caused changes to the shoreline areas continue and are predominantly caused by storm waves, particularly when they occur during periods of high water level. Notably, these sites are affected from time-to-time when:

- At Kurnell offshore waves propagate from ENE
- At La Perouse, offshore waves propagate from the SSE

Typical storm events that have affected these sites are May 1974, August 1986, May 1997 and June 2016 (Kurnell).

Existing Conditions

Waves – Swell

Swell waves are ocean waves to which no further wind energy is being added. In a severe Tasman Sea storm, even the highest offshore waves may still be developing; but as they propagate to Kurnell and La Perouse that wave growth process ceases and they essentially become swell.

Both sites are relatively sheltered from ocean waves and are only affected on rare occasions when high waves from ENE (Kurnell) or SSE (La Perouse) occur at times of high water levels. Both sites may also be affected on rare occasions by high local sea waves caused by westerly sector winds. Wave climate investigations undertaken for this project are described in **Appendix C (Coastal Modelling Report)**. **Figure 1** provides a wave height rose for Kurnell Site A, developed from 20 years of recorded offshore Sydney region wave data, which was applied to a calibrated wave model (**Appendix C**). This result shows that wave heights (H_s) near the proposed Kurnell ferry berth rarely exceed 0.5m and propagate from a directional window of about NNE to NE near the berth.

Figure 2 provides the equivalent information near the proposed La Perouse ferry berth site. Again, H_s rarely exceeds 0.5m, but significant wave refraction has led to incident wave direction there being from the WSW to W sector, approximately.

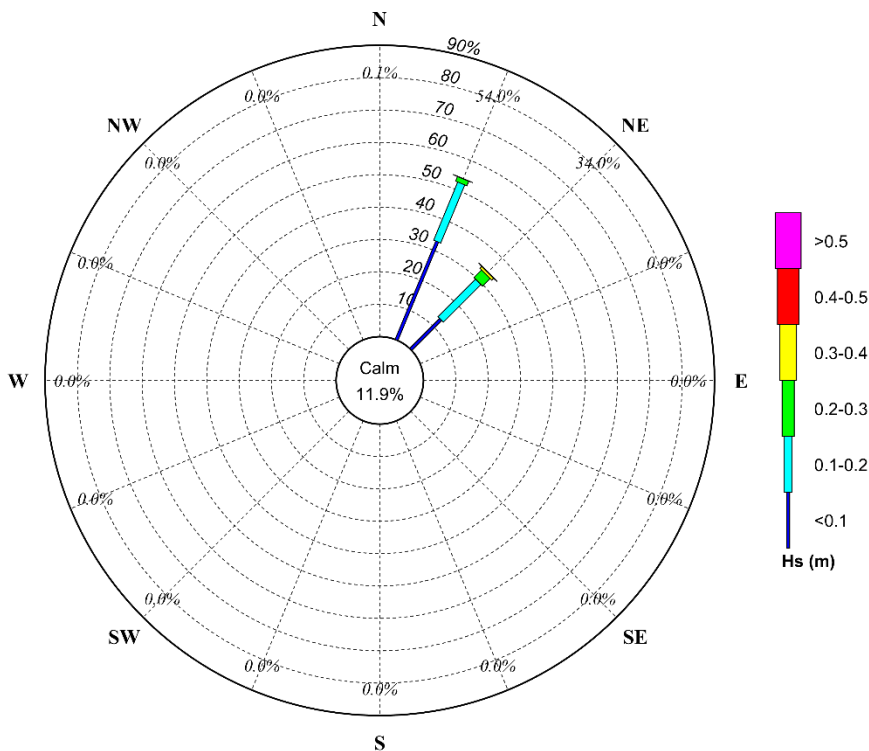


Figure 1 - Swell Wave Rose (Significant Wave Height by Peak Wave Direction) at Kurnell

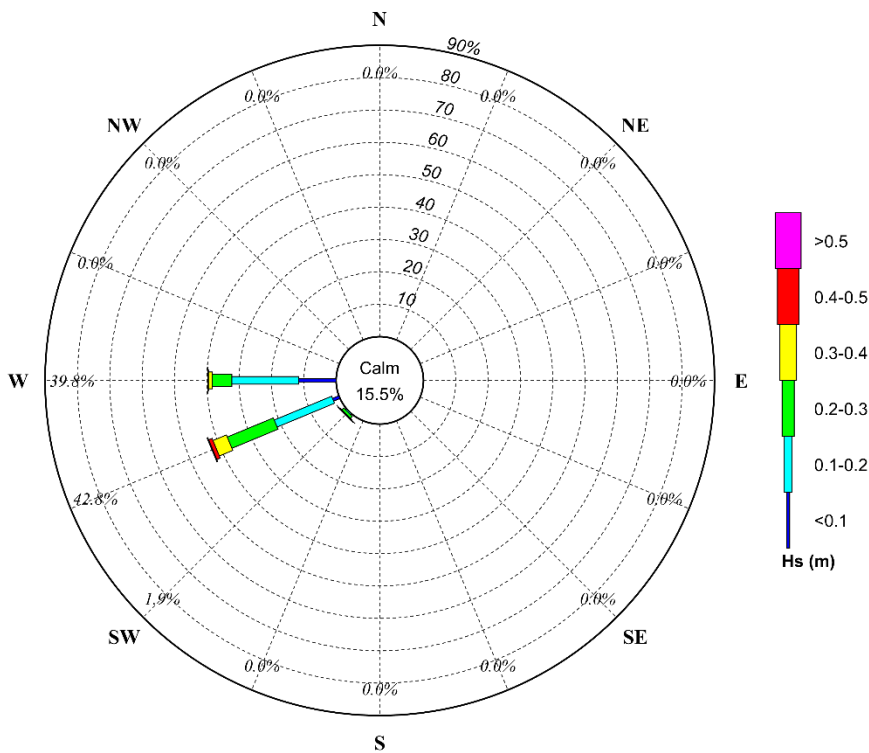


Figure 2 - Swell Wave Rose (Significant Wave Height by Peak Wave Direction) at La Perouse

Waves – Local Sea

Local sea, or wind waves, are waves that are still developing under the prevailing winds. Both Kurnell and La Perouse berth sites are exposed to fetches in the order of 5-6km from the general western sector, but also from other directions.

Figure 3 shows that on rare occasions local sea caused by north-westerly winds can cause waves with $H_s > 0.5m$ at the Kurnell berth site. Waves having $H_s \geq 0.3m$ can occur from a wide range of directions at the proposed Kurnell berth.

Figure 4 shows that the La Perouse berth site is affected by wind waves that may exceed $H_s = 0.5m$ on rare occasions, predominantly from the west, but also from within the SSW to W sector.

At 200-years ARI, design wave conditions are:

- Kurnell – H_s (m)/ T_p (s) swell 0.9/16; sea – 1.1/3.5
- La Perouse – H_s (m)/ T_p (s) swell 1.2/15; sea – 0.9/2.6

Hence La Perouse is affected slightly more than Kurnell by swell, but less by local sea.

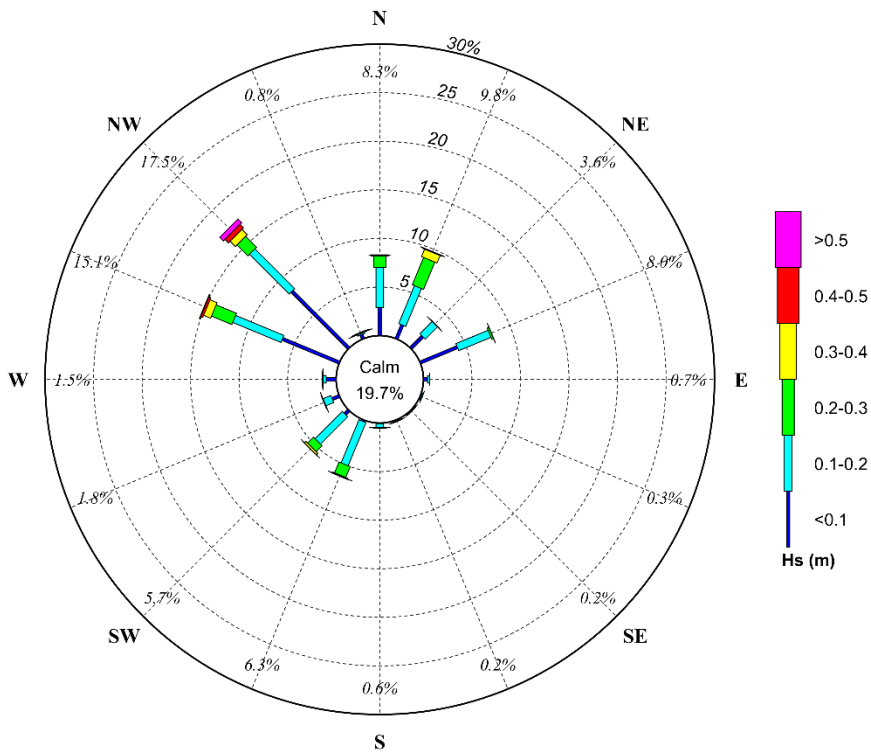


Figure 3 - Sea Wave Rose (Significant Wave Height by Peak Wave Direction) at Kurnell

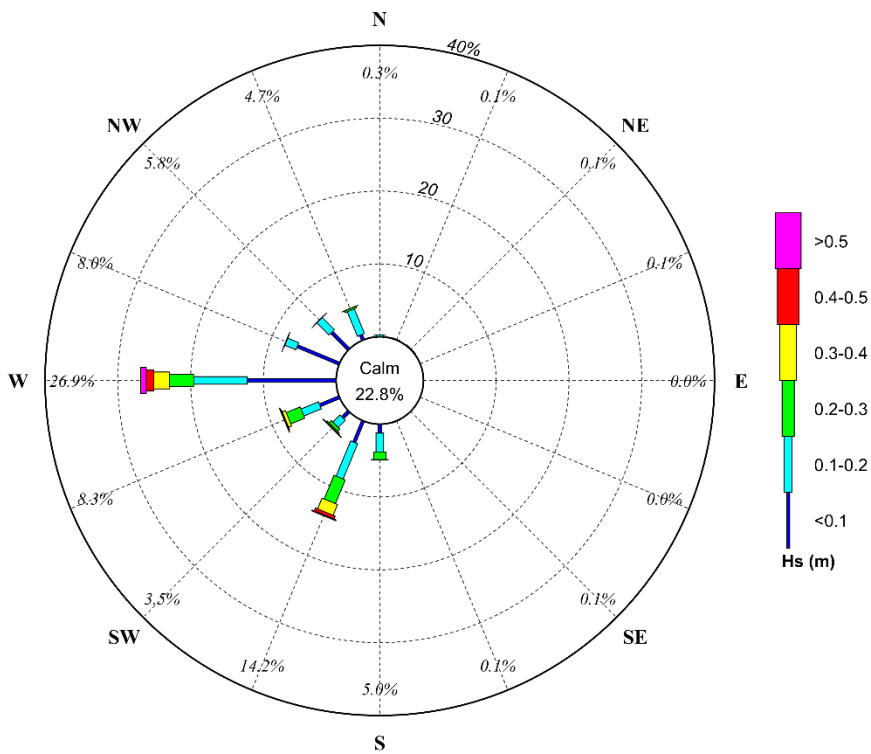


Figure 4 - Sea Wave Rose (Significant Wave Height by Peak Wave Direction) at La Perouse

Currents

Ocean currents within Botany Bay are caused predominantly by the astronomical tides. However, flooding in the Georges River can also affect the bay currents, but less so at the ferry berth sites. Strong winds, especially during neap tides, can also affect bay currents, mainly near Kurnell.

Appendix C undertook current modelling for this project. That work showed that large scale eddy formations can affect both sites, especially during periods of lower current speeds.

Figure 5 provides current speed and direction roses at both of the proposed berth sites. Current speeds are relatively much higher at Kurnell, up to about 0.25m/s, compared with peak current speeds near La Perouse peaking at 0.05m/s. At both sites the current directions are highly focussed, but asymmetrical. That is, at both sites, ebb tide currents are much stronger than flood tide currents.

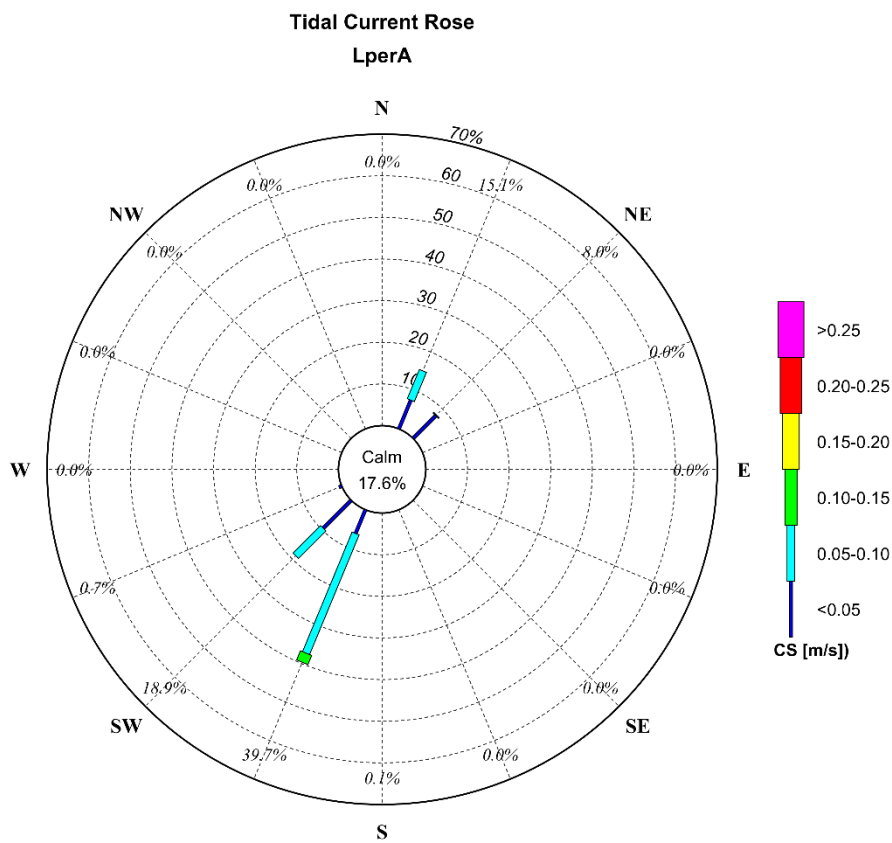
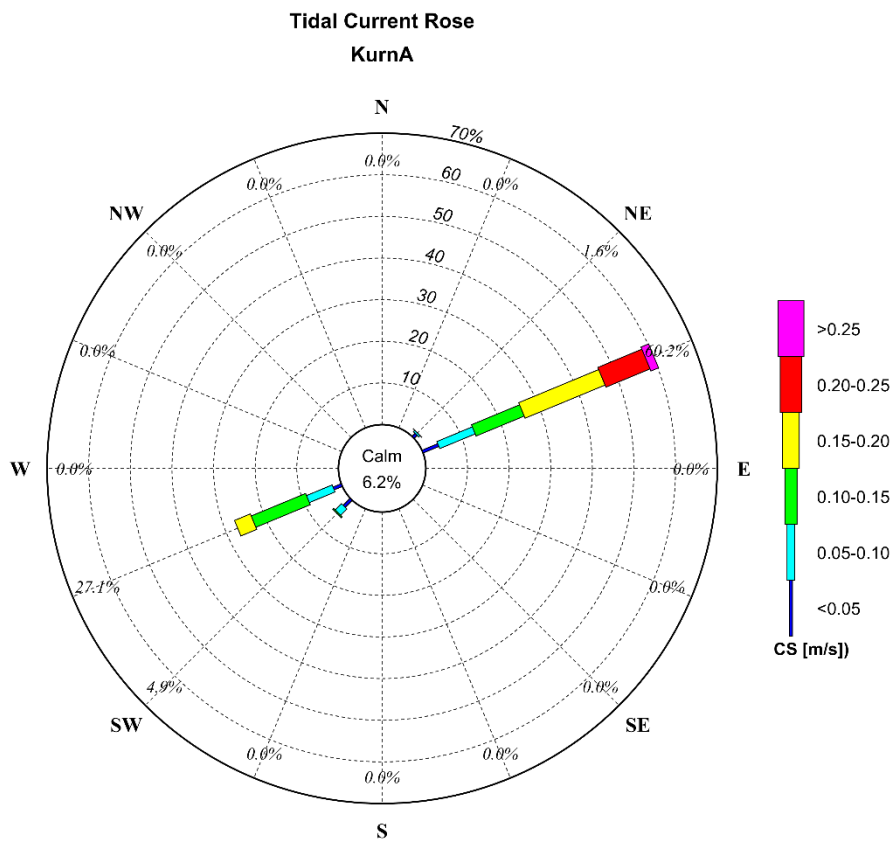


Figure 5 - Tidal Current Roses at Kurnell (top) and La Perouse (bottom)

Sediment Plumes

The construction phase of the Botany Bay ferries project will involve piled jetty construction at the Kurnell and La Perouse sites, together with the construction of a temporary causeway at Kurnell to assist with jetty construction. These tasks will cause short term suspended sediment plumes. Some aspects of the construction phase are described in ARUP (2020a). They are summarised below, including some assumptions that Cardno have made to develop conceptual suspended sediment plume cases.

Pile Driving

A large number of piles are required at both sites to support the access jetties and wharves. Although there is underlying rock at both sites, Cardno have assumed that piles will be driven into sand at both sites. This process will displace/disturb the bottom sediments and thereby lead to the production of suspended sediment plumes – basically from the fines content (<65µm, about).

Although ARUP have undertaken geotechnical investigations at both sites, there is no seabed particle size distribution information available from that work. Based on previous EIS investigations undertaken for infrastructure projects in Botany Bay (Parallel Runway, Port Botany developments, EA cable crossing, Sydney De-Salination Plant project, for example), Cardno has adopted a fines content of 10% at both the Kurnell and La Perouse sites. This is likely to be a conservative position at these sites.

Cardno have assumed:

- Pile embedment of 5m in 2 hours, diameter 0.6m
- 10% of fines released as suspended sediments (Barnard, 1980).

Applying the results of the Botany Bay regional current modelling described in **Appendix C**:

- Spring tide current speed of 0.25m/s at Kurnell wharf
- Spring tide current speed of 0.05m/s at La Perouse wharf

and physically realistic horizontal and vertical dispersion coefficients, together with a fall velocity related to silt of diameter 70µm – typical, the plume results presented in **Appendix A** have been determined.

Tables A.1 and **A.2** show that suspended sediment concentrations arising from pile driving will be very low, remain near the seabed and not be visible at the sea surface. They will not extend beyond 50m in physically realistic terms.

Causeway Construction

ARUP (2020a) provides some details of the temporary causeway that is proposed for construction at Kurnell.

This will be a low level structure formed of a quarry run core protected by sand-filled GSC bags acting as armour. Based on ARUP's indicative data, the structure will be about 75m long with a 5m wide core and be 2.5m high. Based on Cardno's previous similar analyses undertaken for breakwater construction at Wallaroo in South Australia, about 1.5% of the core material, upper limit, will become fine dust during the loading, transport and tipping processes.

Adopting a delivery rate of 50t/hour, a fine silt production rate of 0.21kg/s has been determined. Because the core material falls through the full water column, this silt has been introduced into the water column at four heights above the seabed in a 4m water depth – depth will vary, but suspended sediment concentrations will be highest in more shallow water.

Table A.3 shows that some suspended sediment might be detected at the surface within 20m from the tipping point, but any visible plume will disappear within 50m from the tipping point. Note, also, that the analytical model is steady-state and assumes that the tipping process will be continuous. Depending upon the extent of constructed works, there may only be five truck loads per hour. Hence the plume development process will be very intermittent and less visible than predicted.

Based on the estimated volume of core, loss as fines and the estimated plume extents, an average deposition depth of 1mm has been calculated, noting that the regional wave energy will be sufficient to disperse these fine sediments more widely very quickly.

The application of silt curtains would be impractical, and it is also unlikely that installation being restricted to periods of ebb tide would be practical as a mitigation strategy.

Potential Shoreline Effects

At both of these sites there is the potential for wave action to affect shoreline sediments.

Appendix D (Shoreline Impact Assessment) describes the likely effects of a (then) proposed permanent causeway to be constructed at Kurnell as part of the access structure to the proposed Kurnell berth. This structure was to extend to the -2m AHD contour from the back-beach location, about 140m long. However, this structure is proposed no longer, but a temporary causeway of about 70m length is proposed to assist with construction of a new jetty for access to the Kurnell berth.

Based on historical aerial photographs, and the generally rocky form of the inter-tidal beach area at Kurnell, **Appendix D** concluded that longshore transport is very low in this area. This is confirmed through examination of historical beach changes near the small rock groyne that lies further west, but east of the Caltex jetty. That structure was built in the mid-1970s and shows no identifiable sand accumulation there.

Note that the back-beach area at the proposed Kurnell ferry site has been formed as a perched sandy beach that is quite vulnerable to ENE storm events, for example June 2016. That event caused considerable beach width loss that may not recover; at least in the short term.

However, the presence of the temporary causeway will affect the very local structure of wave propagation near itself – both by diffraction and reflection. These changes will cause local re-alignments of the shoreline both sides of the temporary causeway. These changes can occur quite quickly - based on Cardno's experience during the construction of the breakwater at Yarra Bay on the northern side of the Bay in the mid-1970s. However, once removed following jetty construction, the shoreline will gradually return to its previous quasi-equilibrium form.

Because the jetties and berths proposed for both structures will be constructed on relatively widely-spaced piles, they will have no effect on the Kurnell and La Perouse shorelines.

Note also that there are no sand dunes in the immediate area of the La Perouse jetty. Moreover, the La Perouse facilities will not change the local wave conditions, and hence not affect any dunes in nearby Frenchmans Bay. Note that any dune sands near the Kurnell jetty are protected by an existing geotextile sand-filled bag revetment to the east of the jetty and a rock revetment on its western side.

At-Berth Scour

The seabed at both ferry berth sites is predominantly sandy, with some seagrass identified at both sites, see **Figures 6** and **7**. Additionally, the sandy seabeds may be underlain by sandstone bedrock, which can be seen at the shorelines in **Figures 6** and **7**. Details are available in ARUP (2020b) – based on borehole data. At La Perouse sandstone was encountered at about -5.5m AHD and at the Kurnell berth site at about -11m AHD. Hence there is scope for propeller caused scour at both wharf sites. That outcome will need to be considered in wharf pile design and will likely cause some seagrass loss over the width of the arrival departure swath – where it occurs over that swath area.

Kamay Ferry Terminals



Figure 6 – Seagrass Map at Kurnell

Kamay Ferry Terminals



Figure 7 – Seagrass Map at La Perouse

Propeller caused currents may reach speeds of 0.5 to 1m/s – typical, based on PIANC (2015) and Cardno's measured current data from field experiments undertaken at Manly Wharf East for TfNSW, see **Appendix B**. These current speeds are sufficiently high to cause seabed scour. Their effects will be greater at low tide than at high tide.

Although no pre-ferry-operations seabed survey was undertaken at Manly Wharf East, the form of the seabed indicates that about 1 to 2m of seabed scour has occurred there – see **Figures B.3** and **B.4**.

Similar conditions will occur at La Perouse and Kurnell and similar scour can be expected at those sites. After some initial, short-term seabed disturbance there will be no suspended sediment plumes arising from operational activity.

Cross Bay Propeller Effects

The proposed operating area of the ferry as it traverses the bay is shown below in **Figure 8**. The majority of this swept path is across the existing Port Botany Shipping Channel. The commercial traffic that uses this shipping channel has not caused any significant bank erosion or scour over the years. Given the scale of the ships using the channel compared to the proposed ferry, it is unlikely that there will be any perceivable bed scouring due to the ferry operations as it traverses the bay.



Figure 8 – Ferry Swept Path

Conclusions

The outcomes of this coastal processes assessment are summarised as follow for the construction and operation phases:

Construction Phase

- Although the temporary causeway to be built at Kurnell would act as a barrier to the low net rate of westward sand transport, and thereby cause some temporary, localised shoreline change, once the causeway has been removed the shoreline will return gradually to its present state. The effects would be similar to those caused by the abutment structure of the existing viewing platform.
- Construction vessels would move irregularly over the entire work area. Hence, whilst the propellers will cause some identifiable wash, seabed disturbance would be limited to the work area and not develop a significant scour hole. The level of propeller wash will be similar that caused by other vessels that operate in shallow water in Botany Bay
- During construction of the temporary causeway there would be a minor release of suspended sediments to the local bay area. This suspended sediment would be caused by truck-loads of tipped rock that arrive at intervals. Hence there would be time for the suspended sediments of one load to disperse/ resettle on the seabed before the arrival of another truck load. Estimated concentrations will be no higher than those that occur naturally in Botany Bay – notably during major floods in the Cooks and Georges Rivers.
- Sediment deposition arising from this construction work would be dispersed and be indistinguishable from natural processes that cause siltation in the bay.
- Piling for jetty construction would not cause identifiable plumes of suspended sediments and lead to no identifiable sediment deposition.

Operation Phase

- Because the two wharves will be constructed on openly-spaced piles, they will not affect tidal currents or wave propagation; and hence have no effect on coastal processes.
- The size and speed of the ferries will be too small/low to cause waves that lead to shoreline damage. Additionally, vessels will slow-down as they approach the wharves, with the two wharves being in the order of 100m from the shoreline at both sites. This 100m distance from the shorelines will provide sufficient distance from each shoreline to ensure that boat waves would diminish in height sufficiently to prevent shoreline damage. Note also that the inter-tidal shorelines at both sites are essentially rocky, but at Kurnell there are back-beach protection works.
- The ferries at both sites would berth in water depths of about 3.5m to 4.5m. It is therefore likely that propeller wash from the ferries, and to some extent other commercial and recreational vessels that might use these wharves, would create scour holes at both wharf sites. The extent of scour would depend on the final ferry specifications, frequency of ferry services and operational controls; as well as any underlying rock. Jetty design will include scour allowances to ensure their safe design.
- Note also that there are no sand dunes in the immediate area of the La Perouse jetty. Moreover, the La Perouse facilities will not change the local wave conditions, and hence not affect any dunes in nearby Frenchmans Bay. Note that any dune sands near the Kurnell jetty are protected by an existing geotextile sand-filled bag revetment to the east of the jetty and a rock revetment on its western side.

References

- ARUP (2020a): Technical Advice Note, Constructability Report (Concept Phase).
- ARUP (2020b): Kamay Ferry Wharves Project. Overwater Geotechnical Investigations Factual Report.
- Barnard, W.D (1978): Prediction and Control of Dredged Material Dispersion around Dredging and Open-Water Pipeline Disposal Operations. Technical Report DS-78-13, US Army Engineers Waterway Experiment Station, Vicksburg, MS.
- Kuo, A Y, Welch, C S and Lukens, R J (1985): Dredge Induced Turbidity Plume Model. ASCE Jnl WPC & O Eng, Vol. III, No. 3, pp476-494.
- PIANC (2015): Guidelines for Protecting Berthing Structures from Scour caused by Ships. Report No. 180, Brussels, Belgium.
- Roy, P and Crawford (1979): Holocene Geological Evolution of Southern Botany Bay - Kurnell Region, Central NSW Coast. Records of the Geological Survey of NSW 20(2): pp159-250.

Appendix A

Suspended Sediment Plume Results

Table A-1 Concentration of Suspended Silt (mg/litre) – Kurnell Jetty and Wharf Piling – Current Speed 0.25m/s

Elevation above Sea Bed (m)	Distance Downstream from Pile Driving (m)									
	20	40	60	80	100	120	140	160	180	100
4.0	4.0	0	0	0	0	0	0	0	0	0
3.0	3.0	0	0	0	0	0	0	0	0	0
2.0	2.0	0	0	0	0	0	0	0	0	0
1.0	1.0	0.1	0.1	0	0	0	0	0	0	0
0.5	0.5	0.9	0.3	0.1	0	0	0	0	0	0

Table A-2 Concentration of Suspended Silt (mg/litre) – La Perouse Jetty and Wharf Piling– Current Speed 0.05m/s

Elevation above Sea Bed (m)	Distance Downstream from Pile Driving (m)									
	20	40	60	80	100	120	140	160	180	100
4.0	0	0	0	0	0	0	0	0	0	0
3.0	0	0	0	0	0	0	0	0	0	0
2.0	0	0	0	0	0	0	0	0	0	0
1.0	0.2	0.1	0	0	0	0	0	0	0	0
0.5	1.0	0.2	0	0	0	0	0	0	0	0

Table A-3 Concentration of Suspended Silt (mg/litre) – Kurnell Jetty Core Tipping – Current Speed 0.25m/s

Elevation above Sea Bed (m)	Distance Downstream from Core Tipping (m)									
	20	40	60	80	100	120	140	160	180	200
4.0	2.2	1.1	0.6	0.3	0.2	0.1	0.1	0	0	0
3.0	22	11	5.6	3.0	1.7	1.0	0.6	0.4	0.2	0.1
2.0	22	15	11	8.2	5.7	3.9	2.6	1.7	1.1	0.7
1.0	22	15	12	10	8.7	7.1	5.5	4.2	3.1	2.2
0.5	20	15	12	10	9.1	7.9	6.7	5.4	4.3	3.3

Appendix B
Typical Ferry Wake Currents

On behalf of RMS, now TfNSW, Cardno undertook field investigations and calculations to determine the order of currents caused by ferries at Manly east wharf. This work formed part of studies related to seabed scour and seagrass loss at that site.

To establish a dataset of ferry wash measurements to be used as part of numerical model calibration, Captain Cook Cruises provided their 29 m LOA multi-hulled catamaran vessel, Nancy Wake – see **OB.1**. The vessel specifications of Nancy Wake are presented in **OB.1**.



Figure B.1 Nancy Wake – Captain Cook Cruises

Table B.1 Vessel Specifications for the Nancy Wake – Captain Cook Cruises

Parameter	Units	Value
Length Overall (LOA)	m	29.2
Number of Engines/ Propellers	-	2
Single Engine Power	kW	670
Propeller Type	Twin Screw - Fixed Pitch	
Propeller Dimensions (diameter x pitch)	m	0.79 x 0.87
Centreline of Propeller Boss from Waterline	m	1.3 (based on similar vessels)
Horizontal Distance Between Propeller Axis	m	≈ 5.8
Draft	m	1.4
Beam	m	8.0

Propeller Wash Currents

ADCP Field Measurements

RMS arranged for a ferry (the Nancy Wake, see above), to be used to undertake onsite measurements of ferry wash currents at Manly East Wharf. This exercise took place on 12 December 2018, beginning about 1030. Measurements were undertaken over a period of about 4 hours on a near windless day, during which, the tidal elevation ranged between 0.17 and 0.85 m AHD.

The investigations involved a vessel mounted ADCP that undertook a number of transects across the ferry wash stream between Manly East Wharf and Manly Cove East shoreline. Vertical measurement bins (over the water column) were set at 0.5 m and GPS units were used to log the horizontal coordinates of the ferry and ADCP boat.

These experiments began with two moored, stationary position cases – stern-in and bow-in, the former uncommon in normal operations (advised by the ferry master). The purpose of these cases was to develop near ‘steady-state’ propeller wash conditions and record the current structure along transects transverse to the wash stream. That data was then used to ‘calibrate’ the numerical momentum sources applied in the hydrodynamic model representation of ferry propeller wash. During these stationary test cases, the vessel was moored to the pier and the ferry engine power was set at 25 to 30% of full power. Cardno were advised by the ferry master that this was generally higher than normally used – presumed in calm weather conditions.

For ‘stern-in’ stationary scenarios, observed current were in the order of 1 m/s, generally consistent throughout the water column, over a beam width of about 10 – 20 m with their magnitude decreasing with distance away from the propellers

For the ‘bow-in’ stationary scenarios, observed currents at similar transect locations were significantly lower. Although ADCP measurements indicate current speed magnitudes of up to 1 m/s due to localised turbulence, current speeds were generally of the order of approximately 0.5 to 0.7 m/s throughout the water column and across the stream. Furthermore, the lateral spread of these larger current speeds is also observed to be lower.

Other test cases involved ‘normal’ arrival and departure manoeuvres with transects being observed about 10 m landward from the wharf. Current speeds were lower in these cases.

Empirical Estimates

In addition to the ADCP field measurements, the structure of the propeller wash was estimated through the use of empirical equations. Based on the specified vessel parameters (e.g. engine power, propeller diameter, and applied engine power), the current structure was determined for unconfined conditions, that is, without the influence of the bounding seabed or water surface. Consequently, differences between the measured current fields and those of the empirical formulations were observed. Nonetheless, empirical estimations are useful for ‘truthing’ measured and modelled results; but not appropriate for the purpose of model propeller stream calibration – also being for infinite depth conditions.

Estimated current speeds along the depth of the propeller axis and near-bed level of the Manly Wharf East (-4.6 m AHD) are presented in **0**. The empirical wash fields indicated that current speeds exceeding the threshold for sediment movement (~0.3 m/s) extended to a distance of approximately 90 m from the propeller for both assessed cases. Furthermore, peak bed velocities are of the order of 0.6 - 0.7 m/s and are located approximately 20 - 30 m away from the propellers. As expected, current speeds along the depth of the propeller axis are overall larger than those at the bed, particularly in the near-field region of the propellers.

Overall, the magnitudes of empirically derived propeller currents are of the same order of magnitude as those observed during the field investigation. It should be noted that marginally higher current speeds of up to 1 m/s were recorded over the full depth of the water column by the ADCP, approximately 30-50 m away from the vessel propeller during the ‘bow-in’ stationary berthing condition. It is likely that the increased current speeds are, however, partially attributed to the decrease in water depth as the wash field propagates out of the deeper scour hole and into the shallower nearshore areas where the measurements were recorded.

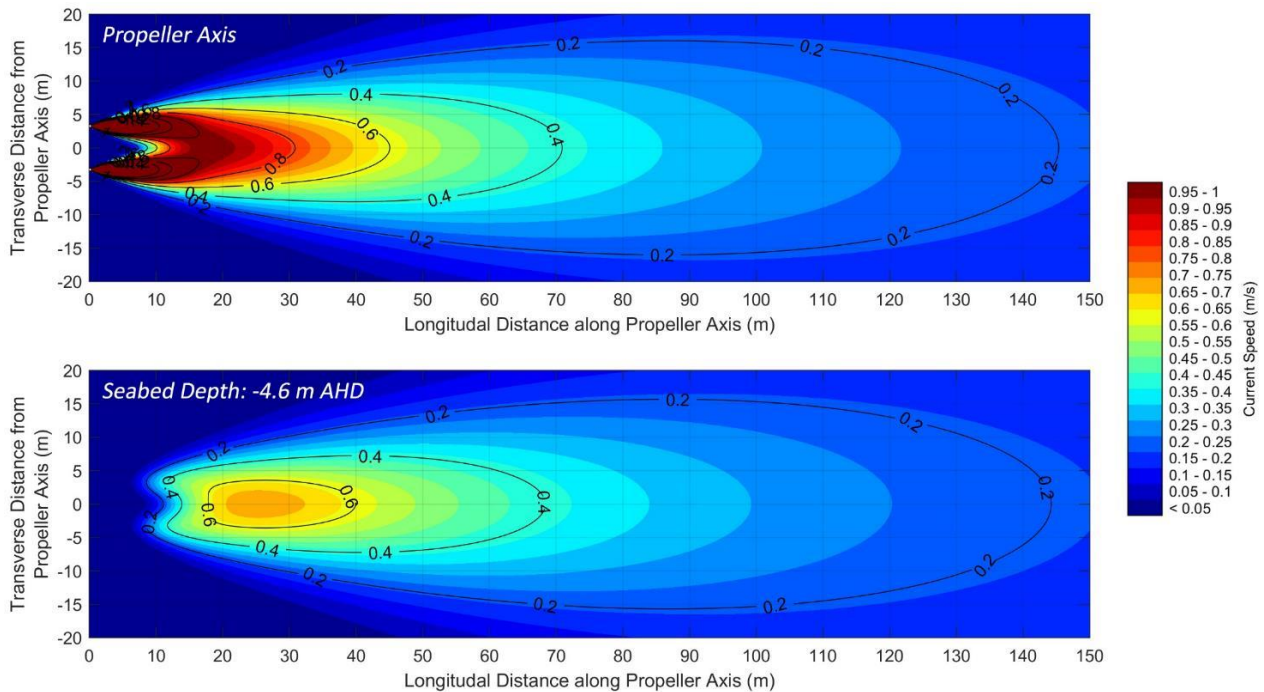


Figure B.2 'Dutch Method' Unconfined Propeller Current Field – *Propeller Axis (top) and -4.6 m AHD (bottom)*

At Manly Wharf East, two bathymetric transects, longitudinal to the axis of the propeller were assessed to investigate the seabed elevations and characteristics of the vessel scour within the ferry berthing area. The location of these transects is presented in **0**.

The bathymetric transects (**0**) indicate that seabed elevations underneath the footprint of the vessel hull are approximately -4 to -5 m AHD, gradually extending up to a relatively flat nearshore area, at -2 m AHD where seagrass meadows are located. To the best of Cardno's knowledge, no survey data is available prior to the servicing of the Manly East Wharf by catamaran ferries and consequently the prior seabed elevations are unknown. However, based on the presence of low sand wave formations, typical of propeller induced scour, and the planform shape of the bathymetric contours, orientated with the axis of the ferry propellers, it is highly likely that the berthing manoeuvres over recent years have contributed to the formation of a landward progressing scour hole.

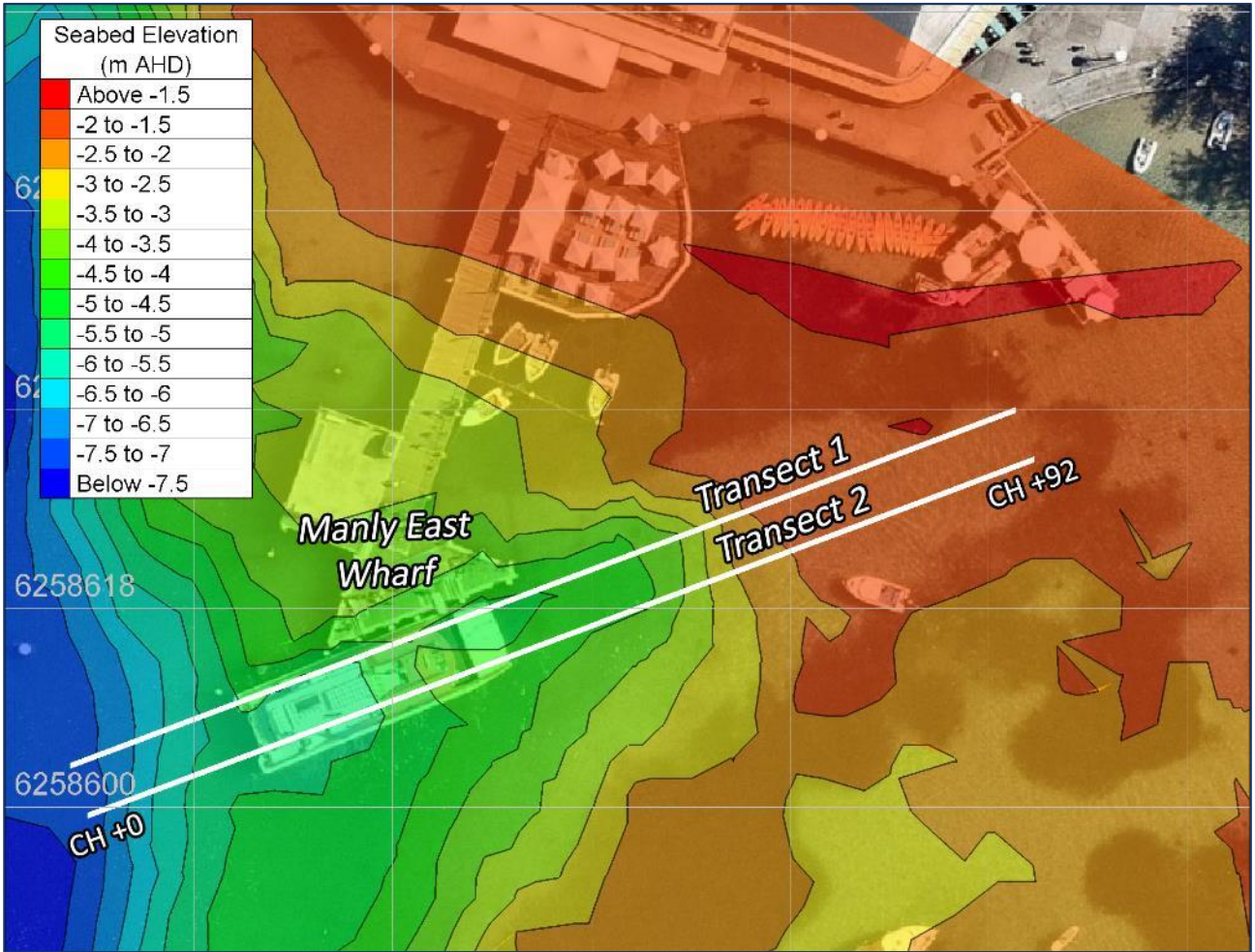


Figure B.3 Location of Bathymetric Transects

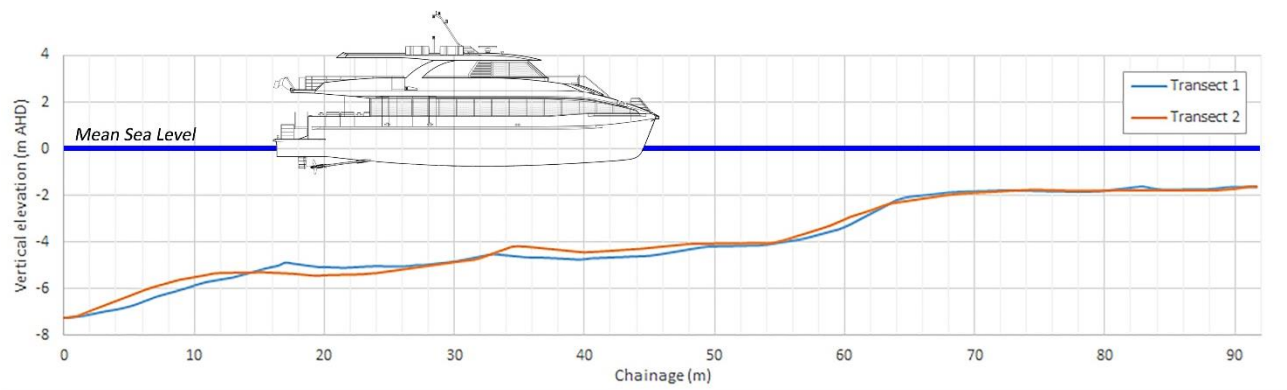


Figure B.4 Bathymetric Transects through Ferry Propeller Axis (29 m vessel to scale)

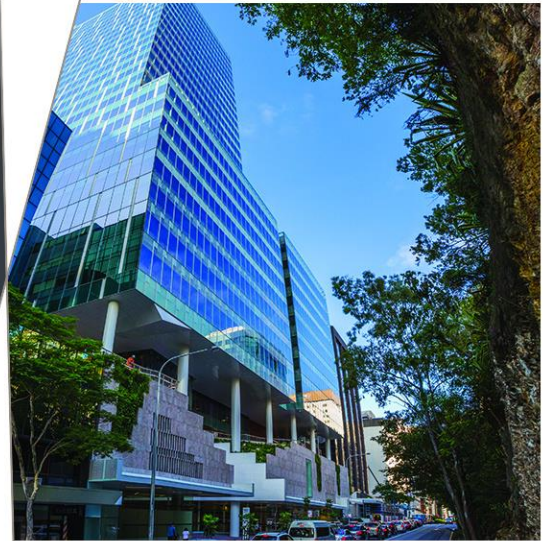
Appendix C

Coastal Modelling Report (2020)

Coastal Modelling Report

Kamay Ferry Wharves Project
(Strategic Phase)

AWE200187



Prepared for
Arup

29 July 2020

Arup Reference
KFW01-ARUP-BPW-EN-RPT-00001

Contact Information

Cardno (NSW/ACT) Pty Ltd

ABN 95 001 145 035

Level 9 - The Forum

203 Pacific Highway

St Leonards NSW 2065

Australia

www.cardno.com

Phone +61 2 9496 7700

Fax +61 2 9439 5170

Author(s):



Chris Scraggs

Principal Coastal Engineer

Approved By:



Doug Treloar

Senior Principal Coastal Engineer

Document Information

Prepared for	Arup
Project Name	Kamay Ferry Wharves Project (Strategic Phase)
File Reference	AWE200187_R001_Coastal ModellingReport.docm
Job Reference	AWE200187
Date	29 July 2020
Version Number	2

Effective Date 29/07/2020

Date Approved 29/07/2020

Document History

Version	Effective Date	Description of Revision	Prepared by	Reviewed by
A	12/03/2020	Draft issued for Review	CS	PDT
0	21/03/2020	Issued for Use	CS	PDT
1	23/06/2020	Final Review Issue	CS	PDT
2	28/07/2020	Final – Reissued	CS	PDT

© Cardno. Copyright in the whole and every part of this document belongs to Cardno and may not be used, sold, transferred, copied or reproduced in whole or in part in any manner or form or in or on any media to any person other than by agreement with Cardno.

This document is produced by Cardno solely for the benefit and use by the client in accordance with the terms of the engagement. Cardno does not and shall not assume any responsibility or liability whatsoever to any third party arising out of any use or reliance by any third party on the content of this document.

Our report is based on information made available by the client. The validity and comprehensiveness of supplied information has not been independently verified and, for the purposes of this report, it is assumed that the information provided to Cardno is both complete and accurate. Whilst, to the best of our knowledge, the information contained in this report is accurate at the date of issue, changes may occur to the site conditions, the site context or the applicable planning framework. This report should not be used after any such changes without consulting the provider of the report or a suitably qualified person.

Table of Contents

1	Introduction	1
	1.1 General	1
	1.2 Project Description	2
	1.3 Scope of this Study	2
2	Project Datum and Conventions	4
	2.1 Units	4
	2.2 Coordinate system	4
	2.3 Vertical Reference Level	4
	2.4 Time Reference	4
	2.5 Direction Convention	4
	2.6 Average Recurrence Interval	4
3	Physical Processes	6
4	Data	7
	4.1 Bathymetric Data	7
	4.2 Wave Data	7
	4.3 Wind Data	8
5	Offshore Wave Climate	16
6	Nearshore Wave Model	20
	6.1 Wave Modelling System	20
	6.2 Wave Model Calibration	20
	6.3 SWAN Model Simulations	24
7	Nearshore Wave Climate	1
	7.1 Swell Waves	1
	7.2 Sea Waves	7
8	Storm Hindcast Modelling	13
	8.1 WaveWatchIII Modelling	13
	8.2 Site Specific Wind Data Reanalysis	14
	8.3 Storm Wave Hindcast Modelling	16
9	Design Wave Criteria	17
	9.1 Extreme Wave Parameters	17
	9.2 Limitations of Extreme Value Analysis	24
	9.3 Design Wave Crest Levels	25
10	Hydrodynamic Modelling	26
	10.1 Current Modelling System	26
	10.2 Model Set-up	27
	10.3 Hydrodynamic Simulations	27
11	Concluding Remarks	31
12	References	32

Appendices

Appendix A	Physical Processes
Appendix B	Glossary of Terms
Appendix C	Preliminary Layouts
Appendix D	Kurnell Wave Climate
Appendix E	La Perouse Wave Climate
Appendix F	Crossing Points Wave Climate
Appendix G	Sea Wave Modelling Plots

Tables

Table 2-1	Probability of Equalling or Exceeding Different ARI Events for Given Design Lives	5
Table 4-1	Design Wind Speeds over Water in Botany Bay	12
Table 4-2	3-Second Gust Wind Speeds	13
Table 4-3	30-Second Gust Wind Speeds	14
Table 4-4	1 Hour Average Wind Speeds	15
Table 5-1	Frequency of Occurrence of Significant Wave Height by Direction, Offshore Botany Bay WRB	17
Table 5-2	Frequency of Occurrence of Peak Wave Period by Direction, Offshore Botany Bay WRB	17
Table 5-3	Frequency of Occurrence of Significant Wave Height by Peak Wave Period, Offshore Botany Bay WRB	18
Table 6-1	Wave Model Calibration Metrics	24
Table 6-2	Model Output Locations	27
Table 7-1	Occurrence of Significant Wave Height by Peak Wave Direction at Kurnell Location A	1
Table 7-2	Occurrence of Significant Wave Height by Peak Wave Period at Kurnell Location A	1
Table 7-3	Occurrence of Significant Wave Height by Peak Wave Direction at La Perouse Location A	3
Table 7-4	Occurrence of Significant Wave Height by Peak Wave Period at La Perouse Location A	3
Table 7-5	Occurrence of Significant Wave Height by Peak Wave Direction at Crossing Point 5	5
Table 7-6	Occurrence of Significant Wave Height by Peak Wave Period at Crossing Point 5	5
Table 7-7	Occurrence of Significant Wave Height (Sea) by Peak Wave Direction at Kurnell Location A	7
Table 7-8	Occurrence of Significant Wave Height (Sea) by Peak Wave Period at Kurnell Location A	7
Table 7-9	Occurrence of Significant Wave Height (Sea) by Peak Wave Direction at La Perouse Location A	9
Table 7-10	Occurrence of Significant Wave Height (Sea) by Peak Wave Period at La Perouse Location A	9
Table 7-11	Occurrence of Significant Wave Height (Sea) by Peak Wave Direction at Crossing Point 5	11
Table 7-12	Occurrence of Significant Wave Height (Sea) by Peak Wave Period at Crossing Point 5	11
Table 8-1	WaveWatchIII Storm Events – 1970 - 1980	14
Table 8-2	Summary of the Peak Wave Conditions from the Hindcast Wave Modelling	16
Table 9-1	Design Significant Wave Height Criteria at Kurnell, in m	17
Table 9-2	Associated Peak Wave Periods at Kurnell	18

Table 9-3	Design Sea Wave Heights at Kurnell	19
Table 9-4	Design Sea Wave Periods at Kurnell	20
Table 9-5	Design Significant Wave Height Criteria at La Perouse, in m	21
Table 9-6	Associated Peak Wave Period at La Perouse	22
Table 9-7	Design Sea Wave Heights at La Perouse	23
Table 9-8	Design Sea Wave Periods at La Perouse	24
Table 9-9	Present Day Design Wave Crest Levels	25

Figures

Figure 1-1	Locality Plan	1
Figure 4-1	Annual Wind Rose for Sydney Airport	9
Figure 4-2	Seasonal Wind Roses for Sydney Airport	10
Figure 4-3	Sydney Wind Probability of Exceedance	11
Figure 5-1	Botany Bay Waverider Buoy Wave Rose (Significant Wave Height by Wave Direction)	16
Figure 5-2	Botany Bay Waverider Buoy Wave Rose (Peak Wave Period Height by Wave Direction)	17
Figure 5-3	Seasonal Wave Height Roses offshore of Botany Bay	18
Figure 5-4	Seasonal Wave Period Roses - Offshore Botany Bay	19
Figure 6-1	SWAN Model Grid and Bathymetry, every 15 th Grid Line Shown	22
Figure 6-2	Wave Model Calibration at the Kurnell Waverider Buoy (June 01 to December 31 2016)	23
Figure 6-3	Wave Model Calibration at the Kurnell Waverider Buoy (January 01 to June 01 2017)	23
Figure 6-4	Wave Model Calibration at the Yarra Bay Waverider Buoy	24
Figure 6-5	Kurnell Output Locations	25
Figure 6-6	La Perouse Output Locations	26
Figure 6-7	Crossing Output locations	27
Figure 6-8	Modelled Significant Wave Height and Direction, Swell Waves from the ENE	28
Figure 6-9	Modelled Significant Wave Height and Direction, Swell Waves from the East	29
Figure 6-10	Modelled Significant Wave Height and Direction, Swell Waves from the SSE	30
Figure 6-11	Modelled Significant (Sea) Wave Height and Direction, 1-Year ARI Wind from the West	31
Figure 6-12	Modelled Significant (Sea) Wave Height and Direction, 1-Year ARI Wind from the Northwest	32
Figure 7-1	Swell Wave Rose (Significant Wave Height by Peak Wave Direction) at Kurnell Location A	2
Figure 7-2	Swell Wave Rose (Significant Wave Height by Peak Wave Direction) at La Perouse Location A 4	
Figure 7-3	Swell Wave Rose (Significant Wave Height by Peak Wave Direction) at Crossing Point 5	6
Figure 7-4	Sea Wave Rose (Significant Wave Height by Peak Wave Direction) at Kurnell Location A	8
Figure 7-5	Sea Wave Rose (Significant Wave Height by Peak Wave Direction) at La Perouse Location A 10	
Figure 7-6	Sea Wave Rose (Significant Wave Height by Peak Wave Direction) at Crossing Point 5	12
Figure 10-1	Botany and Woollooware Bays Hydrodynamic Model Set-up	27
Figure 10-2	Map of Peak Ebbing Currents during the Simulation Period	28
Figure 10-3	Map of Peak Flooding Currents during the Simulation Period	29
Figure 10-4	Tidal Current Roses at Kurnell (top) and La Perouse (bottom)	30

1 Introduction

1.1 General

Transport for NSW, (TfNSW), are investigating the feasibility of re-instating a passenger ferry route between Kurnell and La Perouse in Botany Bay (**Figure 1-1**). Arup have been engaged by Transport to develop a business case for the project, and Cardno have been engaged by Arup to prepare design water level, wave, current and wind data to assist with their design tasks.

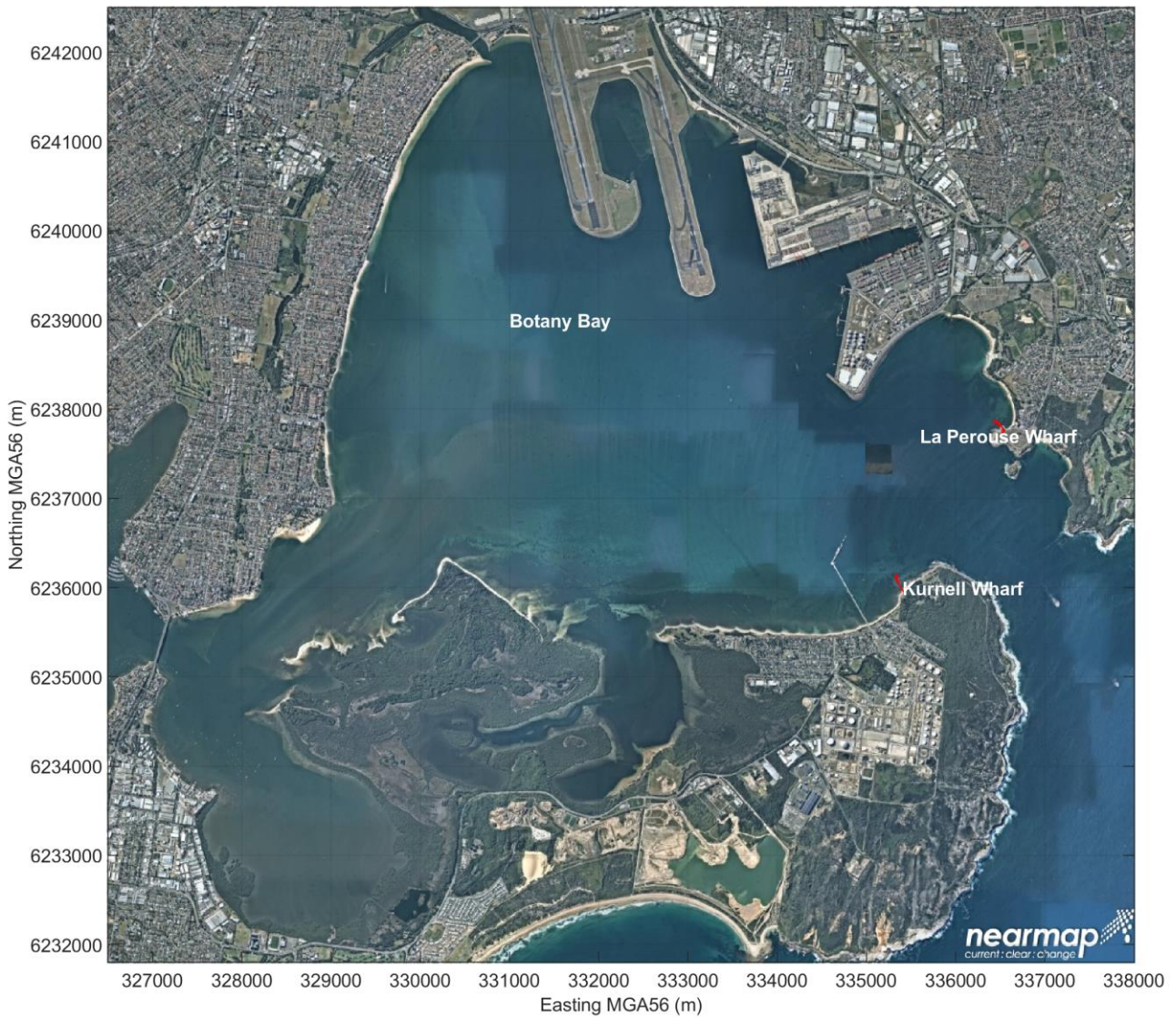


Figure 1-1 Locality Plan

1.2 Project Description

La Perouse and the Kurnell Peninsula are located on the northern and southern sides of the ocean entrance to Botany Bay, respectively, which lies approximately 14 km south of the Sydney CBD. Both sites have a diverse variety of land uses, including residential, commercial and industrial precincts, as well as the Kamay Botany Bay National Park at Kurnell. Both the La Perouse and Kurnell areas contain a rich array of items of historical, cultural and environmental value. A passenger ferry service between these two localities had previously operated between 1890 and 1974, when services ceased following severe damage to both wharves after a major storm event in late May 1974. As a result, the wharves were decommissioned. The trip had been a short 20-minute crossing.

In 2016, Transport for NSW (TfNSW) completed a [Feasibility Study^{\[1\]}](#) that investigated the viability of reinstating the wharves and ferry service. The study concluded that reinstating the wharves would provide numerous indirect social, economic, cultural and tourism benefits for La Perouse, Kurnell and the wider Sydney area. Separately, in 2018, the Office of Environment and Heritage (now the Department of Planning, Industry and Environment) completed the [Kamay Botany Bay National Park Master Plan^{\[2\]}](#) (Master Plan), which looks to deliver on the vision to make the 'Kurnell Precinct' of Kamay Botany Bay National Park 'a place of significance to all Australians that contributes to their sense of identity as Australians.'

On 28th April 2018, the Prime Minister and Federal Treasurer announced \$50 million in funding towards Stage 1 of the Master Plan with contributions coming from both the Commonwealth (\$25 million) and NSW (\$25 million) Governments. Stage 1 of the Master Plan includes the re-establishment of the wharves at La Perouse and Kurnell.

^[1] <https://www.transport.nsw.gov.au/sites/default/files/media/documents/2017/ferry-wharves-la-perouse-kurnell-feasibility-study-report.pdf>

^[2] <https://www.environment.nsw.gov.au/research-and-publications/publications-search/kamay-botany-bay-national-park-kurnell-master-plan>

TfNSW has now established a project team to undertake the planning, design, assessment (business case and environmental impact assessments), and delivery of the reinstatement of the La Perouse and Kurnell wharves and associated infrastructure (the Kamay Ferry Wharves Project).

A range of site investigations will be undertaken to better inform the design and environmental assessment, and key stakeholders and the community will be consulted throughout the project phases.

The Project scope of work includes:

- the reconstruction of fit-for-purpose maritime infrastructure at La Perouse and Kurnell suitable for the berthing of passenger ferries, tourism related commercial vessels and recreational vessels; and the
- construction of fit-for-purpose land-side amenities that are specifically required to facilitate the safe and efficient operation of the infrastructure referred to above, including, (but not limited to), carparks, passenger waiting areas/shelters, ticketing facilities, toilets, pathways from car parking and transport connections, and gate/security provisions.

At this stage, the Project does not involve the specific procurement of a passenger ferry service between the wharves.

Construction is expected to be completed before the end of 2023.

The preliminary layout provided to Cardno by ARUP for this study provides presented in **Appendix C**.

1.3 Scope of this Study

Arup requested the following Scope of Work requirements for the data output locations shown in **Appendices D, E and F**.

1.3.1 Wave and Current Data

For Locations 1 to 5, the following information was required:

- a) Frequency tables and roses of sea and swell Hm0 and direction;
- b) Wind-wave direction-height occurrence matrices covering the principal directions W, NW, N, NE, E, which can be used to determine 1, 20, 50, 100 and 1000-years ARI parameters;

- c) Significant threshold exceedance durations associated with the wind waves from each direction – directional wave height persistence analyses;
- d) Time-series of H_{m0} , T_p , T_m , T_s , peak wave direction, mean wave direction and directional spreading at each point for sea and swell waves for a one year simulation period in ASCII files;
- g) Advice on design combinations of wind and swell waves;
- h) Advice on tidal current velocities and directions; and
- i) Current rose plots and directional frequency of occurrence tables.

1.3.2 Wind Data

The following wind information is required for the site:

Wind occurrence matrix covering principal directions S, SW, W, NW, N, NE, E, SE for 1, 20, 50, 100, 1000 and 2500-years ARI parameters at a height of 10m above MSL and including the 3-second gust, 30-second gust, 10-minute mean and 1-hourly mean speeds for each direction and ARI.

1.3.3 Modelling Requirements

The wave model system used in the study was to be calibrated and be capable of reproducing the relevant wave physics to accurately determine wave conditions at the two sites.

Exceedance curves and design wind and wave conditions were derived from a dataset of sufficient length to accurately determine extreme conditions out to the 100-years ARI risk level. For local wind waves this data period was from 1939 to 2019. For swell this data period was from 1992 to 2019, as well some specific storm events prior to 1992. Advice was to be given on the accuracy of extrapolating the results past the 100-years ARI. More discussion on this matter is provided below.

2 Project Datum and Conventions

2.1 Units

The SI System of Units has been used.

2.2 Coordinate system

All coordinates are in MGA zone 56 and are based on the GDA94 spheroid.

2.3 Vertical Reference Level

All elevations are in meters and referenced to Australian Height Datum (AHD), unless otherwise noted.

2.4 Time Reference

All data related to time are given in Eastern Standard Time (EST), which is GMT + 10 hours.

2.5 Direction Convention

Flow: Flow directions refer to the direction towards which the flow occurs. Directions of the flow are always given clockwise with respect to true north. The unit is degrees.

Wave direction: The direction from which the wave is coming (i.e. coming from convention), and is measured clockwise from true north. A wave with a direction of 0° is coming from the north, and 90° is coming from the east etc.

Wind direction: The direction from which the wind is blowing (i.e. coming from convention), and is measured clockwise from true north. A wind with a direction of 0° is coming from the north, and 90° is coming from the east etc.

2.6 Average Recurrence Interval

This report presents an overview of the met-ocean conditions at La Perouse and Kurnell. The met-ocean conditions are presented in the form of statistics, wind and wave roses and extreme value estimates.

This report defines extreme met-ocean conditions based upon an average recurrence (or return) interval (ARI). The ARI is defined as the average interval of time, normally in years, in which the condition would be expected to be exceeded once. Design events are typically defined in this manner. For example, a 50-years ARI event is, on average, exceeded once every 50 years. It should be noted that it is possible, although not probable, that this extreme event could be exceeded during the first year of the life of the structure, or may not be exceeded at all over the life of the structure. **Table 2-1** presents the probability of occurrence of events up to the 1,000-years ARI event for given design lives. For a 50 years design life there is an approximate 40% probability that a 100-years ARI event or larger will occur within the design lifetime of the structure. A 1,000-years ARI event has a 5% chance of occurring (or being exceeded) during a typical 50-years design life of a coastal structure.

Table 2-1 Probability of Equalling or Exceeding Different ARI Events for Given Design Lives

Average Recurrence Interval Event	Probability of Occurrence in 1 year Period	Probability of Occurrence in 2 years Period	Probability of Occurrence in 5 years period	Probability of Occurrence in 10 years Period	Probability of Occurrence in 25 years Period	Probability of Occurrence in 50 years Period	Probability of Occurrence in 100 years Period
1 year	63.2%	86.5%	99.3%	100.0%	100.0%	100.0%	100.0%
2 years	39.3%	63.2%	91.8%	99.3%	100.0%	100.0%	100.0%
5 years	18.1%	33.0%	63.2%	86.5%	99.3%	100.0%	100.0%
10 years	9.5%	18.1%	39.3%	63.2%	91.8%	99.3%	100.0%
25 years	3.9%	7.7%	18.1%	33.0%	63.2%	86.5%	98.2%
50 years	2.0%	3.9%	9.5%	18.1%	39.3%	63.2%	86.5%
100 years	1.0%	2.0%	4.9%	9.5%	22.1%	39.3%	63.2%
200 years	0.5%	1.0%	2.5%	4.9%	11.8%	22.1%	39.3%
300 years	0.3%	0.7%	1.7%	3.3%	8.0%	15.4%	28.3%
400 years	0.2%	0.5%	1.2%	2.5%	6.1%	11.8%	22.1%
500 years	0.2%	0.4%	1.0%	2.0%	4.9%	9.5%	18.1%
1000 years	0.1%	0.2%	0.5%	1.0%	2.5%	4.9%	9.5%

3 Physical Processes

Appendix A describes the physical processes relevant to this investigation. A glossary of terms is presented in **Appendix B**. **Appendix A** also includes some definitions.

The dominant processes at both sites are ocean waves, tidal currents and winds. They are described in some detail in the Appendices.

4 Data

A range of data items were required to set-up, calibrate and operate the wave and current models applied to this investigation. They are described below.

4.1 Bathymetric Data

Bathymetric and topographic data for this investigation has been derived from the recent LIDAR survey of the NSW coastal area, provided in digital form for most of Botany Bay (State Government of NSW and Department of Planning, Industry and Environment, 2019). Data for offshore regions and the Georges River were obtained from AUS charts 198 and 199.

Site specific survey data in the immediate vicinities of the Kurnell and La Perouse sites and collected for this project was also used to define the bathymetry in the project areas. The resulting model bathymetry setup is provided in **Figure 6-1** (SWAN), and **Figure 10-1** (Delft3D) to datum AHD.

4.2 Wave Data

Wave data has been recorded at Botany Bay by the Port Authority of NSW (PANSW), and its predecessor bodies, since 1971. The principal location is offshore in a depth of about 80m using a Datawell Waverider buoy that transmits a signal onshore for processing and storage. In the early 1970's this was done using paper tape and records were taken about four times a day. Continuous records are taken now, thereby providing a better definition of peak storm wave parameters. These analyses provide data in terms of Hs and Tz, together with other parameters. Wave direction is a particularly important parameter for wave propagation into Botany Bay, but has only been recorded at this site since 2012.

PANSW have recorded wave data at other sites within Botany Bay for shorter periods, notably near the Caltex submarine berth, and at a site in Yarra Bay. Both of these sites were used for wave model calibration for this investigation. PANSW provided their full directional offshore Waverider buoy data set Kurnell and Yarra Bay Waverider buoy data for this investigation.

Other offshore wave data has also been recorded by Manly Hydraulics Laboratory at Long Reef to the north of Botany Bay. That installation includes recorded wave direction. Comparison between the analysed Long Reef and Botany Bay wave data shows that 'actual' offshore wave directions (Long Reef) are more southerly, on a probability of occurrence basis, than has been estimated for the Botany Bay data using hindcast methods (Kulmar, 1995).

For the purposes of this study all wave energy recorded at the PANSW offshore Waverider buoy has been classified as swell, even though there will generally be some local sea present. In severe storms, where wave growth may still be occurring to the higher waves, those waves should physically be described as sea, but the distinction is not important to this investigation.

For this study, wave height and period data recorded at the offshore Botany Bay Waverider buoy was used from 2012 to 2019 – provided by the Port Authority of NSW. Data prior to 2012 was obtained from a number of sources, including hindcast data from Cardno's NSW coastal hindcast wave model, and measurements collected at the Long Reef Buoy. Hence an almost continuous period of about 28 years of data (1992 to 2019, but with some data gaps), was prepared and was used for preparation of swell wave height parameters in terms of joint occurrence of Hs and Tz and Hs and direction at each of the nominated output locations, as well as persistence.

The preparation of design wave parameters required the identification of storm events over the period from 1971 to 2019. In order to determine offshore wave directions for those events, when recorded wave direction was not available, Cardno used a global wave model based on WaveWatch III and wind field data available from NOAA. This model system includes a nested model of the whole NSW coastline. Wind fields for identified or known storm events were then modelled. In most cases the only output of this modelling that was used for this study was wave direction near the peak of storm events. However, for some events, such as the very severe storms of May and June, 1974, there was no recorded offshore wave data available – Waverider buoy out of the water being serviced. In those cases the WaveWatch III data was used to describe wave height, period and direction parameters.

4.3 Wind Data

Wind affects both the wave and current climates in Botany Bay. Wind data has been recorded at Sydney Airport since 1939 (Monypenny *et al.*, 1997). The location and impact of airport development have changed since then. From 1939 to 16 August, 1994, a Dines anemometer was used to record 10-minute averages of wind speed and direction. Since the early 1960's, at least, this anemometer was located on a 10m mast near the intersection of the east-west and north-south runways. Recommended WMO clearances from buildings and other obstructions were maintained. During its period of service, the Dines anemometer was maintained well.

Since 16 August, 1994, wind data at the airport has been recorded using a Synchrotec anemometer installed on a 10m mast near the threshold of the main north-south runway, which is more exposed than the previous Dines anemometer site.

Analyses of these wind records by Monypenny and Middleton, 1997 showed that there had been a gradual error (reduction) in wind speed recorded by the Dines anemometer. This reduction amounted to 2.6m/s by August, 1994. Monypenny and Middleton, 1997 advise that a simplified linear adjustment be made to Sydney airport wind speeds up to 16 August, 1994 and this adjustment was made for this study. Data to January, 2020 was obtained from the Bureau of Meteorology. Wind speed was adjusted as advised by Monypenny and Middleton, 1997.

Other wind data was also obtained from the Bureau of Meteorology for an anemometer site on the Caltex jetty. It covers the period from April 2000 to September 2012. This record is not of sufficient length to be used to describe the wind climate at the jetty in terms of very infrequent conditions. Hence correlation analyses were undertaken to relate the Kurnell wind speeds and directions to the longer term airport data. This was undertaken using 16 directional sectors. The relationships developed from these analyses were then used to transform the 73 years of airport wind data to an equivalent 73 years of wind data (10-minute averages) to an over water dataset close to the site.

4.3.1 Wind Climate

Shorter period local sea waves within Botany Bay are generated by winds blowing across the water body. Local sea wave conditions will be affected by fetch (the distance across the water body over which the wind blows), as well as the wind speed and direction. Consequently, assessment of local sea wave conditions required an understanding of the wind climate of Sydney.

Figure 4-1 depicts the directionality of the local wind conditions across Sydney, as recorded at the Sydney Airport anemometer. Considered on an annual basis, the local winds are somewhat omnidirectional, although the prevailing directions do vary throughout the year. Overall, "calm" conditions occur around 5% of the time.

Figure 4-2 depicts the seasonality of local wind conditions. These wind roses show that southerlies and easterlies tend to dominate during summer period, while westerlies tend to prevail during winter, with autumn and spring serving as transition periods.

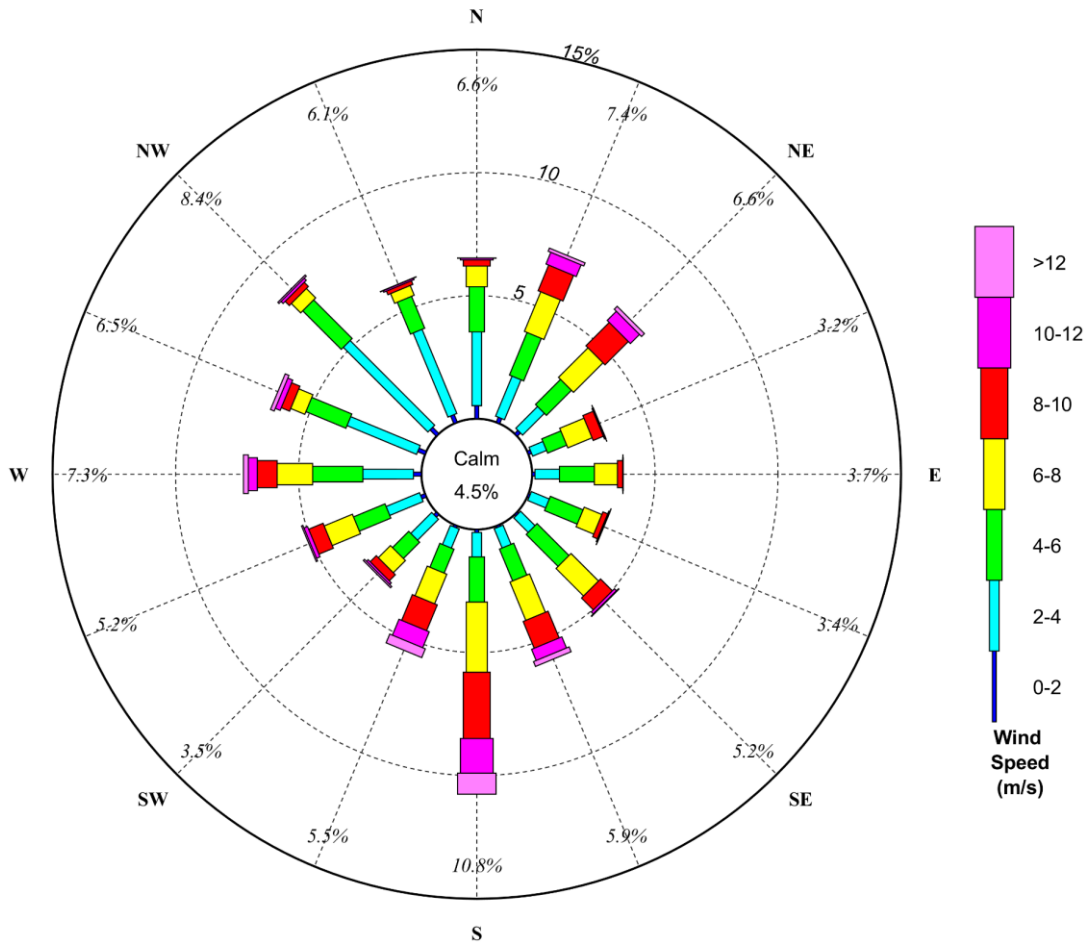


Figure 4-1 Annual Wind Rose for Sydney Airport

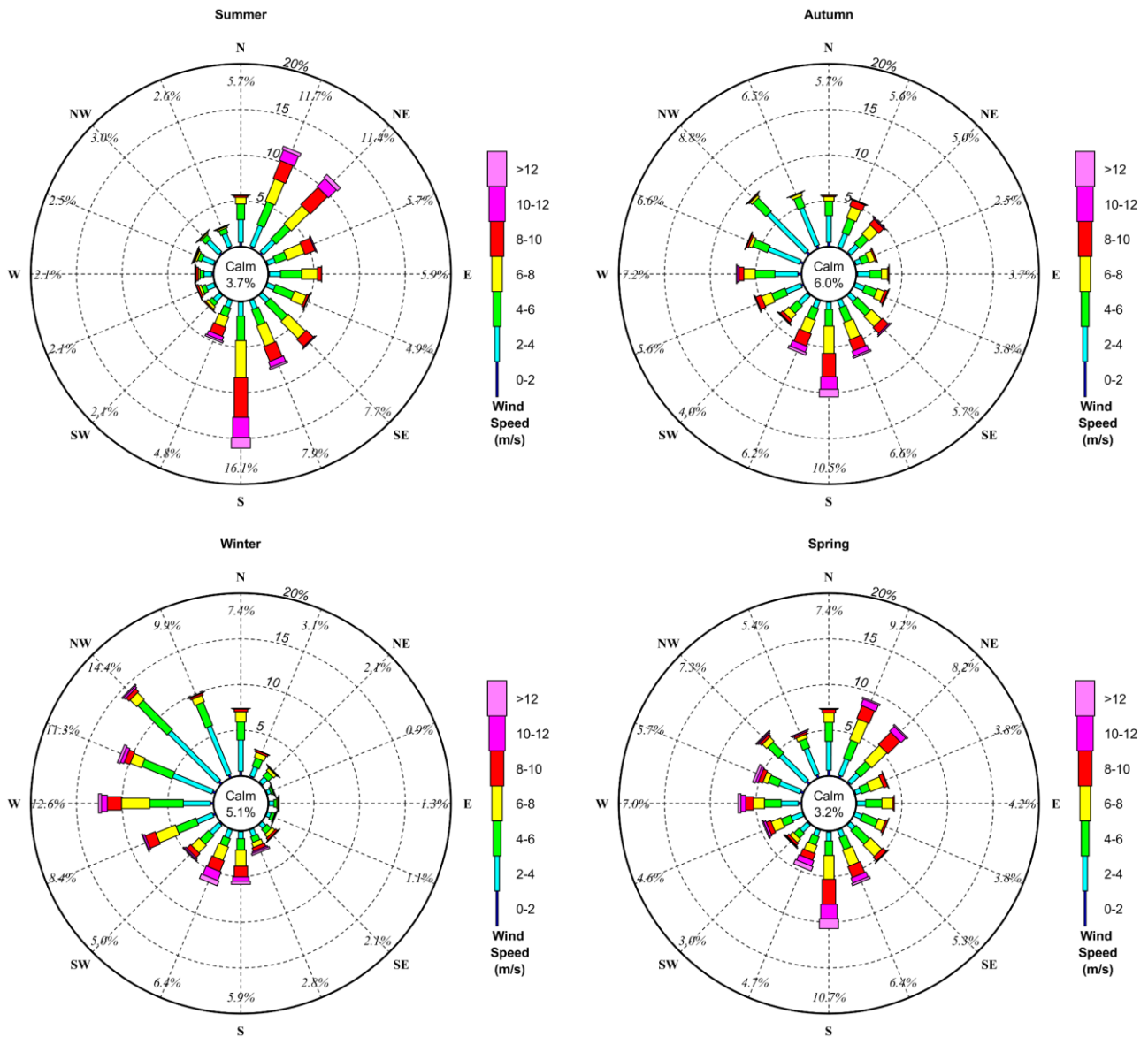


Figure 4-2 Seasonal Wind Roses for Sydney Airport

Figure 4-3 describes the probability of exceedance of given wind speeds. The plot indicates that the median wind speed is around 5 m/s (or ≈10 knots). Similarly, the plot shows that a 9 m/s wind speed is exceeded around 10% of the time and 14 m/s is exceeded around 1% of the time.

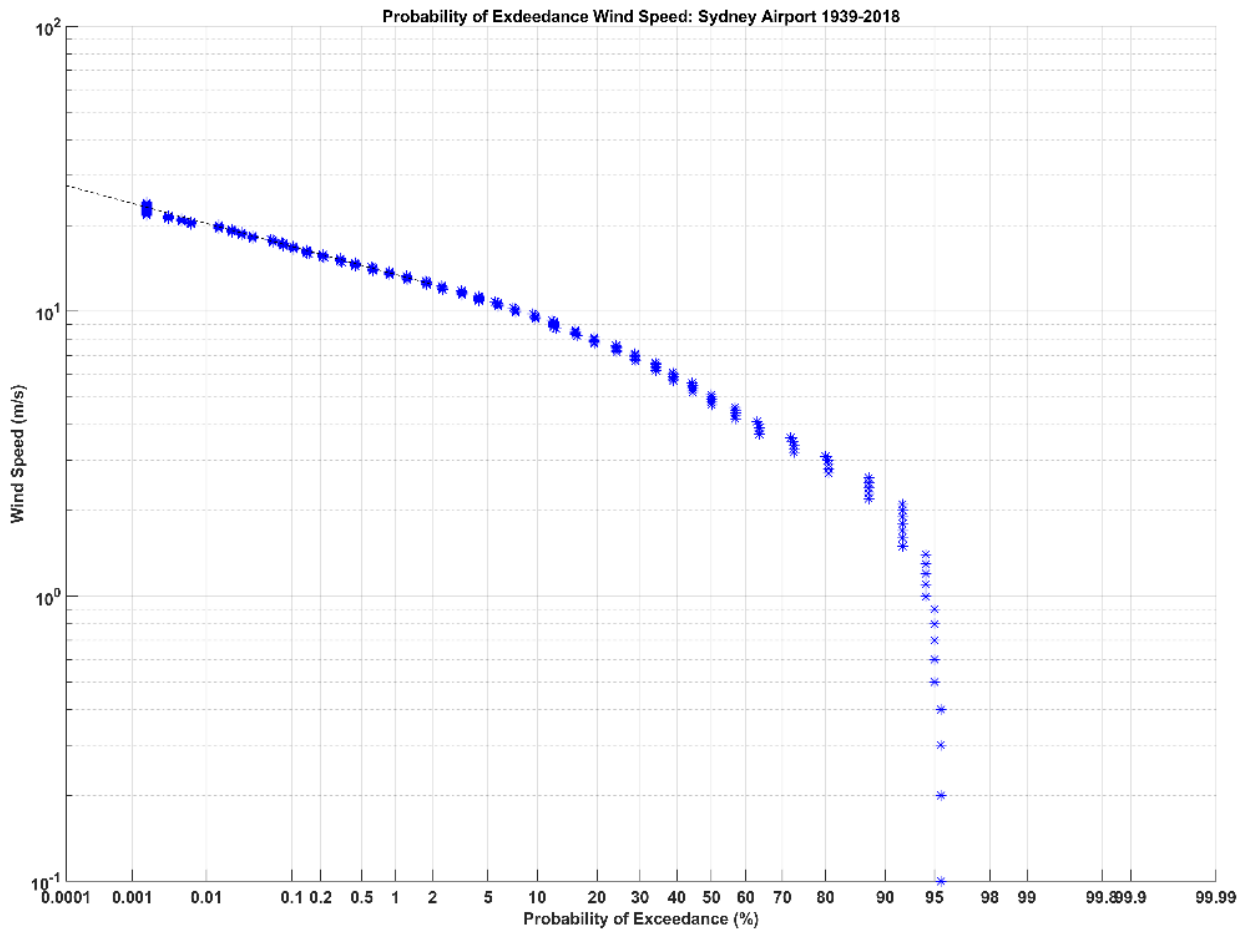


Figure 4-3 Sydney Wind Probability of Exceedance

4.3.2 Extreme Wind Speeds

This wind data was then analysed in terms of independent wind storm events in eight directional octants. Where a storm produced peak speeds in more than one octant, both results were accepted in order to provide a directional wind speed climate. Independent events required 72 hours of separation between peaks. Whilst it is acknowledged that some storms have longer durations, for example, August, 1986, this is a reasonable general position to adopt. The results are presented in **Table 4-1**. Relationships presented in WMO, 2008 were used to calculate wind speeds for other averaging intervals, see **Tables 4-2 to 4-4**. These tables also include the 95% confidence limits determined as part of the extremal analyses.

Data has been prepared for a range of speed averaging intervals.

Table 4-1 Design Wind Speeds over Water in Botany Bay

10-minutes Average Wind Speed (m/s) (Including 95% Confidence Limits)							
ARI (years)	1	20	50	100	500	1000	2500
S	22.2	26.3	28.5	31.4	33.3	35.0	36.4
	21.0	25.0	26.4	27.3	29.4	30.3	31.5
	19.8	23.5	24.2	25.0	25.3	25.6	26.6
SW	18.3	22.0	24.0	26.5	29.0	29.4	30.9
	17.4	20.6	21.8	22.6	24.5	25.3	26.5
	16.5	19.5	19.6	19.7	19.8	20.0	20.8
W	21.3	25.1	26.6	28.9	30.8	31.8	33.6
	20.4	23.9	25.1	25.9	27.9	28.7	30.0
	19.5	22.8	23.4	24.1	25.0	25.5	26.3
NW	18.8	20.8	21.9	22.6	24.1	24.3	25.1
	18.3	20.2	20.8	21.3	22.2	22.7	23.3
	17.8	19.6	19.9	20.0	20.3	20.5	21.5
N	14.6	16.4	17.2	17.8	19.2	19.5	20.3
	14.1	15.9	16.5	16.9	17.9	18.3	19.0
	13.7	15.3	15.7	16.0	16.6	16.8	17.5
NE	17.6	19.0	19.6	20.0	21.1	21.3	21.8
	17.4	18.7	19.2	19.5	20.2	20.7	21.0
	17.2	18.3	18.5	18.6	19.3	19.4	19.9
E	11.9	15.3	16.7	17.9	20.0	20.9	22.3
	10.8	14.0	15.1	15.9	17.8	18.6	19.8
	9.7	12.7	13.4	13.9	15.6	16.5	17.5
SE	14.7	17.7	19.6	20.8	23.4	25.1	26.4
	13.8	16.6	17.6	18.3	19.7	20.5	21.6
	12.8	15.4	15.6	15.9	16.0	16.1	16.9

Table 4-2 3-Second Gust Wind Speeds

3-Second Gust (m/s) - $F_s = 1.38$ (Including 95% Confidence Limits)							
ARI (years)	1	20	50	100	500	1000	2500
S	30.6	36.3	39.3	43.3	46.0	48.3	50.2
	29.0	34.5	36.4	37.6	40.4	41.7	43.6
	27.3	32.4	33.4	34.5	34.9	35.3	36.7
SW	25.3	30.4	33.1	36.6	40.0	40.6	42.6
	24.0	28.5	30.1	31.2	33.7	35.0	36.4
	22.8	26.9	27.0	27.2	27.3	27.6	28.7
W	29.4	34.6	36.7	39.9	42.5	43.9	46.4
	28.1	33.0	34.6	35.8	38.5	39.6	41.1
	26.9	31.5	32.3	33.3	34.5	35.2	36.3
NW	25.9	28.7	30.2	31.2	33.3	33.5	34.6
	25.2	27.8	28.7	29.3	30.6	31.4	32.2
	24.6	27.0	27.5	27.6	28.0	28.3	29.7
N	20.1	22.6	23.7	24.6	26.5	26.9	28.0
	19.4	21.9	22.7	23.3	24.7	25.2	26.0
	18.9	21.1	21.7	22.1	22.9	23.2	24.3
NE	24.3	26.2	27.0	27.6	29.1	29.4	30.1
	24.0	25.8	26.4	26.9	27.9	28.5	29.1
	23.7	25.3	25.5	25.7	26.6	26.8	27.5
E	16.4	21.1	23.0	24.7	27.6	28.8	30.8
	14.9	19.3	20.8	22.0	24.6	25.7	27.0
	13.4	17.5	18.5	19.2	21.5	22.8	24.2
SE	20.3	24.4	27.0	28.7	32.3	34.6	36.4
	19.0	22.9	24.3	25.3	27.2	28.3	29.6
	19.7	21.3	21.5	21.9	22.1	22.2	23.3

Table 4-3 30-Second Gust Wind Speeds

ARI (years)	30-Second Gust (m/s) - $F_s = 1.18$ (Including 95% Confidence Limits)						
	1	20	50	100	500	1000	2500
S	26.2	31.0	33.6	37.1	39.3	41.3	43.0
	24.8	29.5	31.1	32.2	34.6	35.7	37.2
	23.4	27.7	28.6	29.5	29.9	30.2	31.4
SW	21.6	26.0	28.3	31.3	34.2	34.7	36.5
	20.5	24.4	25.7	26.7	28.8	29.9	31.1
	19.5	23.0	23.1	23.2	23.4	23.6	24.5
W	25.1	29.6	31.4	34.1	36.3	37.5	39.6
	24.0	28.2	29.6	30.6	32.9	33.8	35.2
	23.0	26.9	27.6	28.4	29.5	30.1	31.0
NW	22.2	24.5	25.8	26.7	28.4	28.7	29.6
	21.5	23.8	24.5	25.1	26.2	26.8	27.6
	21.0	23.1	27.5	23.6	24.0	24.2	25.4
N	17.2	19.4	20.3	21.0	22.7	23.0	24.0
	16.6	18.7	19.4	20.0	21.1	21.6	22.3
	16.2	18.1	18.5	18.9	19.6	19.8	20.7
NE	20.8	22.4	23.1	23.6	24.9	25.1	25.7
	20.5	22.0	22.6	23.0	23.8	24.4	24.9
	20.3	21.6	21.8	21.9	22.8	22.9	23.5
E	14.0	18.1	19.7	21.1	23.6	24.7	26.3
	12.7	16.5	17.8	18.8	21.0	21.9	23.1
	11.4	15.0	15.8	16.4	18.4	19.5	20.7
SE	17.3	20.9	23.1	24.5	27.6	29.6	31.2
	16.2	19.6	20.8	21.6	23.2	24.2	25.4
	15.1	18.2	18.4	18.8	18.9	19.0	19.9

Table 4-4 1 Hour Average Wind Speeds

ARI (years)	1-Hour Average (m/s) - $F_s = 0.952$ (Including 95% Confidence Limits)						
	1	20	50	100	500	1000	2500
S	21.1	25.0	27.1	29.9	31.7	33.3	34.7
	20.0	23.8	25.1	26.0	27.9	28.8	30.1
	18.8	22.4	23.0	23.8	24.1	24.4	25.3
SW	17.4	20.9	22.8	25.2	27.6	28.0	29.4
	16.5	19.7	20.8	21.6	23.2	24.1	25.1
	15.7	18.6	18.7	18.8	18.8	19.0	19.8
W	20.3	24.0	25.3	27.5	29.3	30.3	32.0
	19.4	22.7	23.9	24.7	26.6	27.3	28.4
	18.6	21.7	22.3	22.9	23.8	24.3	25.0
NW	17.9	19.8	20.8	21.5	22.9	23.1	23.9
	17.4	19.2	19.8	20.2	21.1	21.6	22.3
	16.9	18.7	18.9	19.0	19.3	19.5	20.5
N	13.9	15.6	16.4	16.9	18.3	18.6	19.3
	13.4	15.1	15.7	16.1	17.0	17.4	18.0
	13.0	14.6	14.9	15.2	15.8	16.0	16.7
NE	16.8	18.0	18.7	19.0	20.1	20.3	20.8
	16.5	17.8	18.2	18.6	19.2	19.7	20.2
	16.4	17.4	17.6	17.7	18.4	18.5	18.9
E	11.3	14.6	15.9	17.0	19.0	19.9	21.2
	10.3	13.3	14.4	15.2	16.9	17.7	18.7
	9.2	12.1	12.8	13.2	14.9	15.7	16.7
SE	14.0	16.9	18.7	19.8	22.3	23.9	25.1
	13.1	15.8	16.8	17.4	18.8	19.6	20.4
	12.2	14.7	14.9	15.1	15.2	15.3	16.1

These peak event wind speeds are generally lower than those presented in the Australian wind code, AS1170. This outcome arises, to some extent, because the wind data used in the preparation of the wind code design parameters are based on data from more than one anemometer site in a region. Hence, for a selected data period, more storm events occur, thereby raising the design wind speeds. This effect will be different for different directions. Moreover, the definition of the 100-years ARI wind speed in the wind Code is somewhat different, being the wind speed that only has a 5% likelihood of being exceeded once in 100-years, on average.

5 Offshore Wave Climate

The offshore wave data described in **Section 4.2** has been analysed to describe wave conditions offshore of Botany Bay. **Figures 5-1** and **5-2** present significant wave height and peak wave period roses, which have been derived from the combined wave time-series dataset. Waves offshore of Botany Bay predominantly come from the south to the south-east sectors, which account for over 65% of the annual wave climate. For the remaining time, waves generally approach from the north east to the east south east sectors, and rarely from directions outside of these ranges.

Frequency of occurrence tables of significant wave height by direction, peak wave period by direction and significant wave height by peak wave period are presented below in **Tables 5-1**, **5-2** and **5-3**. These tables indicate that the predominant wave direction is from the SSE and significant wave heights are most frequently between 1 and 1.5m. Large wave events (>3m Hs), occur on average for 5.5% of the time, occurring between directions from the east-northeast to the south-southwest, although most frequently occurring from the south-south-east and the south. Peak wave periods are commonly between 7 and 11 seconds and commonly occur with offshore Hs values between 1 and 2m.

Seasonal wave roses are presented in **Figures 5.3** and **5.4**. These figures show that there is a slight variation in wave directionality throughout the year. During winter, the waves tend to be more predominant from the south-south-east and have longer periods, whereas during summer wave direction is fairly evenly distributed between northeast and south.

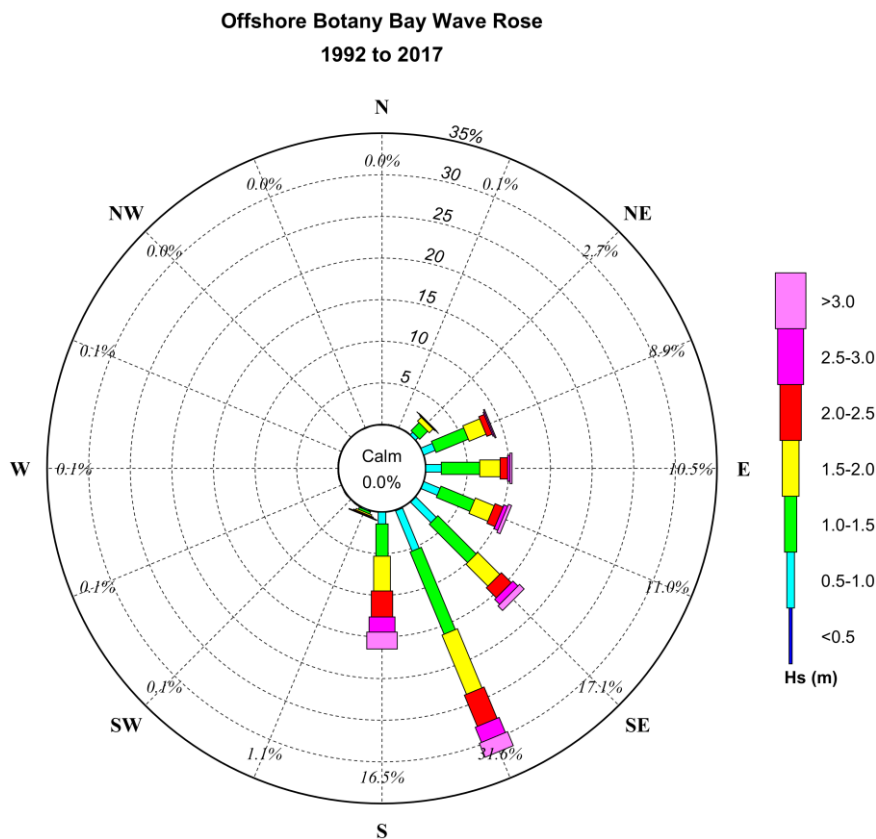


Figure 5-1 Botany Bay Waverider Buoy Wave Rose (Significant Wave Height by Wave Direction)

Offshore Botany Bay Wave Period Rose
1992 to 2017

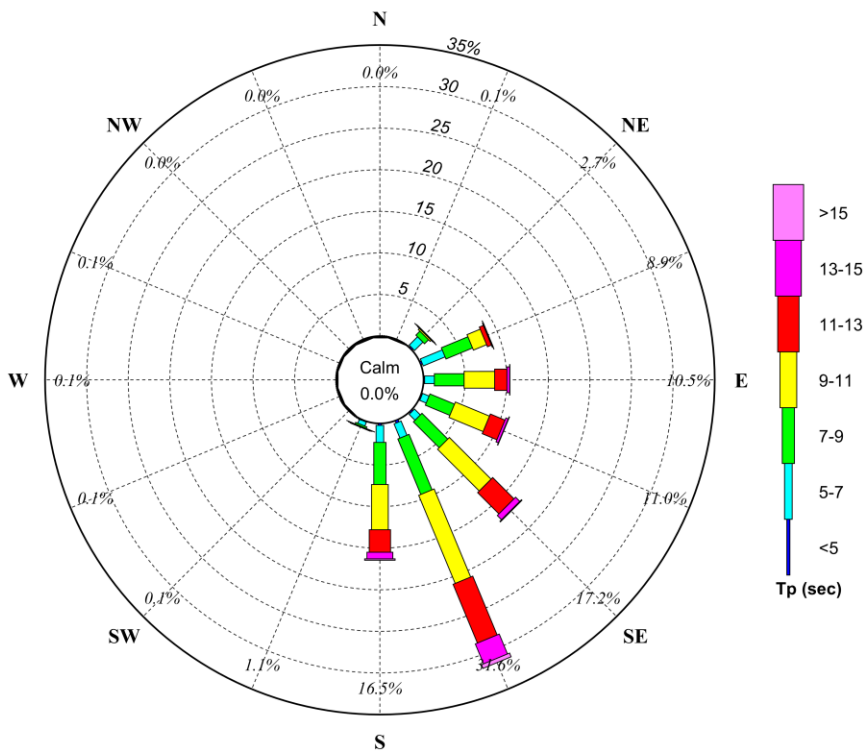


Figure 5-2 Botany Bay Waverider Buoy Wave Rose (Peak Wave Period Height by Wave Direction)

Table 5-1 Frequency of Occurrence of Significant Wave Height by Direction, Offshore Botany Bay WRB

Hs (m)		Wave Direction Bins (Coming From °N)															Total	Cum. Total	
From	To	N	NNE	NE	ENE	E	ESE	SE	SSE	S	SSW	SW	WSW	W	WNW	NW			NNW
Calm (<0.25 m)		0.0%															0.0%	0.0%	
0.25	0.50	-	-	-	0.0%	0.0%	0.0%	0.1%	0.1%	0.0%	-	-	-	-	-	-	-	0.3%	0.3%
0.50	1.00	-	0.0%	0.5%	1.5%	1.9%	2.1%	3.5%	5.2%	1.4%	0.2%	0.1%	0.0%	0.1%	0.1%	0.0%	0.0%	16.6%	17.0%
1.00	1.50	-	0.0%	1.4%	4.2%	4.6%	4.4%	6.5%	10.7%	3.9%	0.3%	0.0%	0.0%	0.0%	-	-	-	36.0%	53.0%
1.50	2.00	-	0.0%	0.7%	2.2%	2.5%	2.5%	3.7%	7.7%	4.2%	0.2%	-	-	-	-	-	-	23.8%	76.8%
2.00	2.50	-	-	0.2%	0.7%	0.9%	1.1%	1.7%	4.1%	3.1%	0.2%	-	-	-	-	-	-	11.9%	88.7%
2.50	3.00	-	-	0.0%	0.2%	0.3%	0.5%	0.9%	2.0%	1.8%	0.1%	-	-	-	-	-	-	5.8%	94.5%
>3.0		-	-	-	0.1%	0.3%	0.4%	0.8%	1.8%	2.0%	0.1%	-	-	-	-	-	-	5.5%	100%
Total		0.0%	0.1%	2.7%	8.9%	10.5%	11.0%	17.1%	31.6%	16.5%	1.1%	0.1%	0.1%	0.1%	0.1%	0.0%	0.0%	100%	

Table 5-2 Frequency of Occurrence of Peak Wave Period by Direction, Offshore Botany Bay WRB

Tp (sec)		Wave Direction Bins (Coming From °N)															Total	Cum. Total	
From	To	N	NNE	NE	ENE	E	ESE	SE	SSE	S	SSW	SW	WSW	W	WNW	NW			NNW
<5		-	0.0%	0.2%	0.2%	0.1%	0.1%	0.2%	0.3%	0.2%	0.1%	0.0%	0.0%	0.0%	0.0%	0.0%	-	1.7%	1.7%
5	7	-	0.0%	1.4%	2.9%	1.2%	0.9%	1.0%	1.9%	2.1%	0.5%	0.0%	0.0%	0.0%	-	-	-	12.0%	13.7%
7	9	-	0.0%	0.7%	3.5%	3.6%	3.2%	4.4%	7.2%	5.1%	0.3%	0.0%	0.0%	0.0%	-	-	-	28.0%	41.7%
9	11	-	0.0%	0.2%	1.7%	3.7%	4.4%	7.1%	11.5%	5.4%	0.1%	0.0%	0.0%	0.0%	0.0%	0.0%	-	34.3%	75.9%
11	13	-	0.0%	0.1%	0.5%	1.5%	1.9%	3.6%	7.7%	2.7%	0.0%	0.0%	0.0%	0.0%	0.0%	-	-	18.2%	94.1%
13	15	-	-	0.0%	0.1%	0.4%	0.3%	0.7%	2.6%	0.8%	0.0%	-	-	-	-	-	-	5.0%	99.2%
>15		-	-	-	-	0.0%	0.0%	0.0%	0.1%	0.5%	0.2%	-	-	-	-	-	-	0.8%	100%
Total		0.0%	0.1%	2.7%	8.9%	10.5%	11.0%	17.2%	31.6%	16.5%	1.1%	0.1%	0.1%	0.1%	0.1%	0.0%	0.0%	100%	

Table 5-3 Frequency of Occurrence of Significant Wave Height by Peak Wave Period, Offshore Botany Bay WRB

Hs (m)		Wave Period Bins (Tp, sec)									Total	Cum. Total
		<3	3	5	7	9	11	13	15	>17		
From	To		5	7	9	11	13	15	17			
Calm (<0.25)		0.0%	0.0%	0.0%	-	0.0%	-	-	-	-	0.0%	0.0%
0.25	0.50	0.0%	0.0%	0.0%	0.0%	0.1%	0.1%	0.0%	0.0%	-	0.3%	0.3%
0.50	1.00	0.0%	0.8%	1.8%	4.1%	5.2%	3.6%	1.0%	0.2%	0.0%	16.6%	17.0%
1.00	1.50	-	0.9%	5.8%	10.4%	11.2%	5.7%	1.7%	0.3%	0.0%	36.0%	53.0%
1.50	2.00	-	0.1%	3.2%	7.3%	8.4%	3.7%	1.0%	0.1%	0.0%	23.8%	76.8%
2.00	2.50	-	-	1.1%	3.8%	4.5%	2.0%	0.5%	0.1%	0.0%	11.9%	88.7%
2.50	3.00	-	-	0.2%	1.6%	2.4%	1.2%	0.3%	0.0%	0.0%	5.8%	94.5%
3.00	3.50	-	-	0.0%	0.6%	1.2%	0.6%	0.1%	0.0%	0.0%	2.7%	97.2%
3.50	4.00	-	-	-	0.2%	0.6%	0.4%	0.1%	0.0%	0.0%	1.4%	98.6%
4.00	4.50	-	-	-	0.1%	0.3%	0.3%	0.0%	0.0%	0.0%	0.7%	99.3%
4.50	5.00	-	-	-	0.0%	0.1%	0.1%	0.0%	0.0%	-	0.3%	99.7%
>5		-	-	-	0.0%	0.1%	0.2%	0.0%	0.0%	-	0.3%	100.0%
Total		0.0%	1.7%	12.1%	28.2%	34.3%	18.0%	4.9%	0.7%	0.1%	100%	

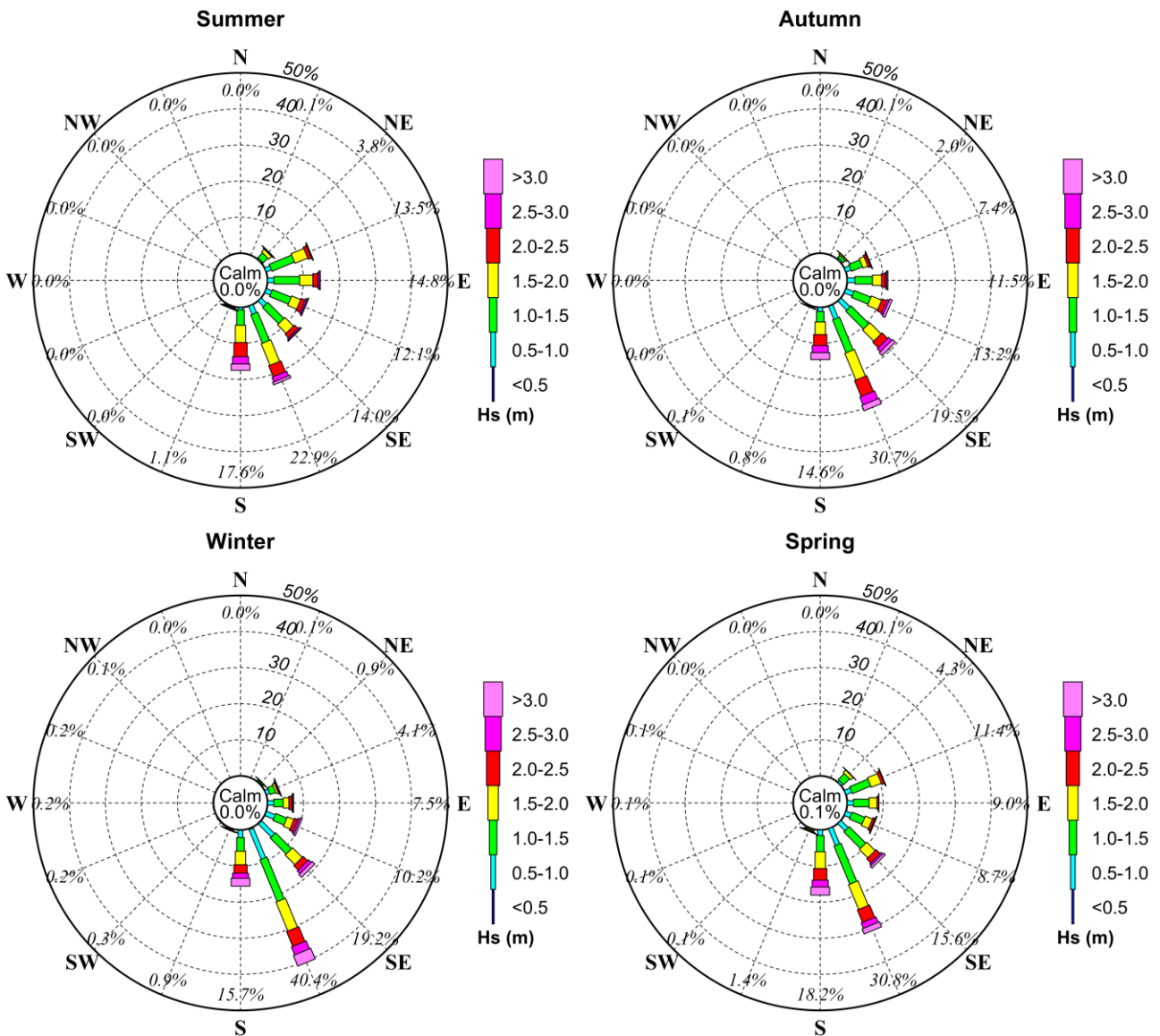


Figure 5-3 Seasonal Wave Height Roses offshore of Botany Bay

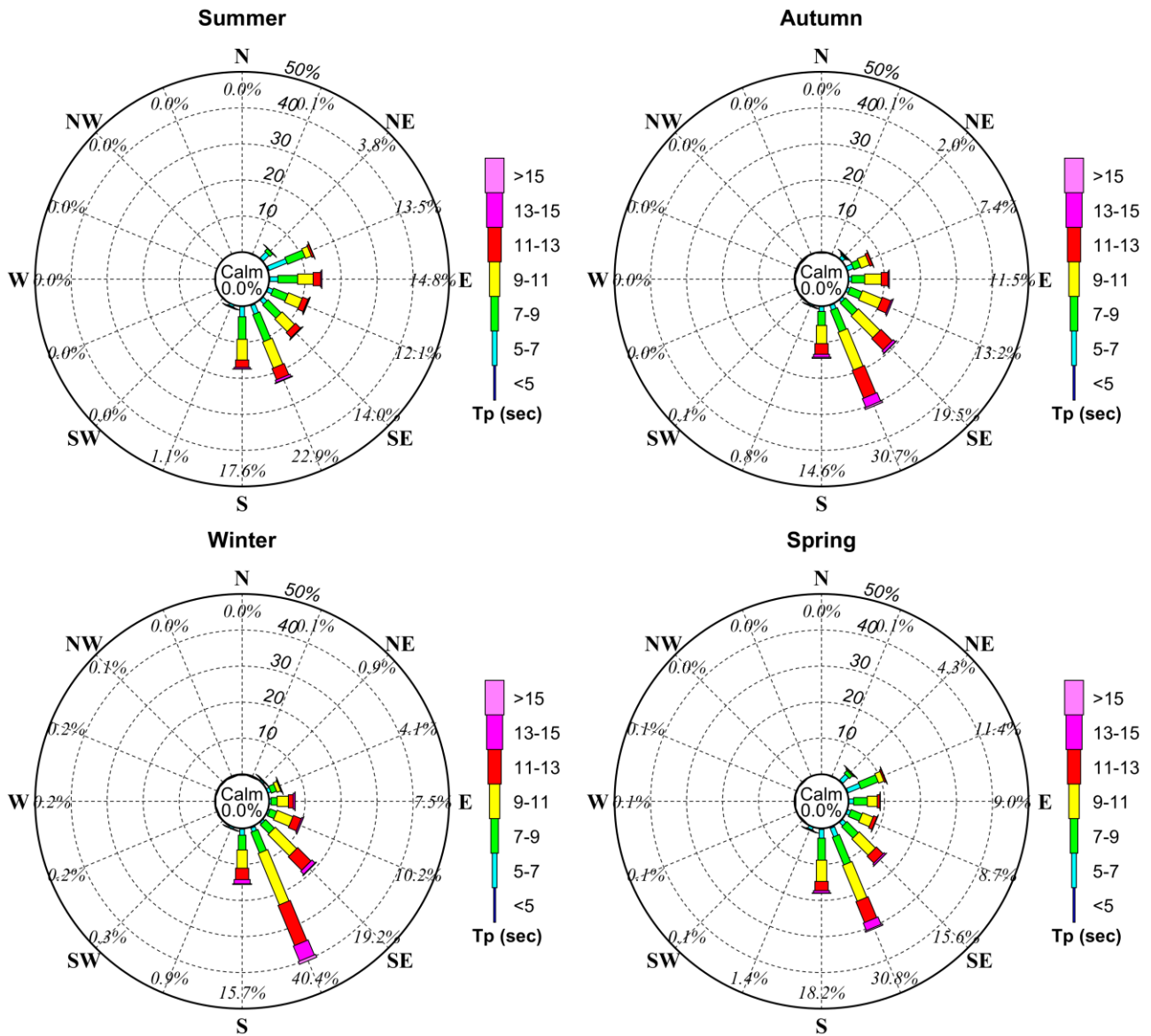


Figure 5-4 Seasonal Wave Period Roses - Offshore Botany Bay

6 Nearshore Wave Model

6.1 Wave Modelling System

The wave model Cardno used in this study to transfer offshore wave data to the nominated output locations at La Perouse and Kurnell is based on the third generation wind/wave modelling system, SWAN, which is incorporated as a module into the Delft3D modelling system. This model was developed at the Delft Technical University and includes wind input (wind-wave cases), combined sea and swell, offshore wave parameters (swell cases), refraction, shoaling, non-linear wave-wave interaction, a full directional spectral description of wave propagation, bed friction, white capping, currents and wave breaking. SWAN also models phase-averaged diffraction based on the model of Holthuijsen *et al.*, 1993.

SWAN includes a nested grid capability that allows coarser grids in deeper water and finer grids in shallow water, where better definition of seabed form and spatial depth variation are needed. Output from the model includes significant wave height, dominant wave direction, spectral peak and mean periods and (optionally) the full directional wave spectra at selected grid points. This model was used also for the wind wave (local sea), investigations.

Offshore waves were propagated into Botany Bay to nominated output locations to describe operational and design wave criteria.

Figure 6-1 describes the SWAN grid and bathymetry applied to this investigation.

6.2 Wave Model Calibration

The SWAN wave model has previously been calibrated in Botany Bay for local sea (Lawson and Treloar, 2003) and swell (Cardno, 2012 and Cardno, 2017). Model calibration increases the confidence in the reliability of the model to transfer recorded offshore wave data (Hs, Tp and Direction), to selected inshore locations.

Model calibration was undertaken in terms of comparisons between modelled and recorded wave parameters at the Yarra Bay and Kurnell Waverider buoy sites operated by PANSW. The period selected for this process was the full record at Yarra Bay, namely from 21/09/2016 to 03/02/2017 and a one year period at Kurnell being 1/6/2016 to 1/5/2017. Results are presented in **Figures 6-2, 6-3 and 6-4**. In this process the main calibration parameter was the adopted offshore directional spread.

The calibration plots indicate that the model is replicating the general trends at both sites. There appear to be slight positive biases during low wave events, with the model over-predicting significant wave heights by 10 to 20 cm. However, during the large storms (20/10/2016 to 26/10/2016 at Yarra Bay and June 2016 at Kurnell), the model matches the measurements quite well, noting that the confidence limits in recorded data are typically $\pm 15\%$.

6.2.1 Quantitative Model Diagnostics

The accuracy of the model is described by a range of quantitative validation metrics, specifically:-

- Model Skill;
- Bias;
- RMS Error;
- Scatter Index; and
- Correlation.

These error statistics were applied to calibrate the wave model system. The statistical error parameters and their equations are detailed below.

Model Skill

The model skill at simulating the measured conditions is given by Equation 6.1. This produces 0 in cases of no agreement and 1 for perfect agreement between the modelled and measured data (Willmott et al, 1985).

$$ModelSkill = 1 - \frac{\sum_{i=1}^N [M_i - O_i]^2}{\sum_{i=1}^N ([M_i - \bar{O}] + [O_i - \bar{O}])^2} \quad (6.1)$$

where:-

- O_i observed, or measured data (m for waves)
- M_i modelled data (m for waves)
- \bar{O}_i mean of observed data (m for waves)

Bias

The bias is a measure of the difference between the expected value and the true value of a parameter, and is calculated using **Equation 6.2**. An unbiased model has a zero bias. Otherwise the model is said to be positively or negatively biased, an indication as to whether the model is persistently over or under-predicting the physical conditions, respectively.

$$Bias = \frac{1}{N} \sum_{i=1}^N (M_i - O_i) \quad (6.2)$$

RMS Error

The RMS error, **Equation 6.3**, is also a measure of the difference between the expected value and the true value of a parameter. It provides a measure of the magnitude of the difference between the modelled and measured values.

$$RMS = \sqrt{\frac{1}{N} \sum_{i=1}^N [M_i - O_i]^2} \quad (6.3)$$

Scatter index

The scatter index is the RMS error normalised by the mean of the observations – see **Equation 6.4**. It provides an indication of the scatter of the data about the mean.

$$SI = \frac{\sqrt{\frac{1}{N} \sum_{i=1}^N ([M_i - \bar{M}] - [O_i - \bar{O}])^2}}{\bar{O}} \quad (6.4)$$

where:-

- \bar{M}_i mean of modelled data (m for waves)

Correlation

The correlation is usually reported as the R^2 value, – see **Equation 6.5**. It is a measure of the strength of the linear relationship between two variables. Values of R^2 can be between 0 and 1, where 0 indicates no linear relationship, 1 indicates a perfect linear relationship and values greater than 0.5 indicate a strong linear relationship.

$$R^2 = \frac{\sum_{i=1}^N [M_i - \bar{M}][O_i - \bar{O}]}{\sqrt{\sum_{i=1}^N [M_i - \bar{M}]^2 \sum_{i=1}^N [O_i - \bar{O}]^2}} \quad (6.5)$$

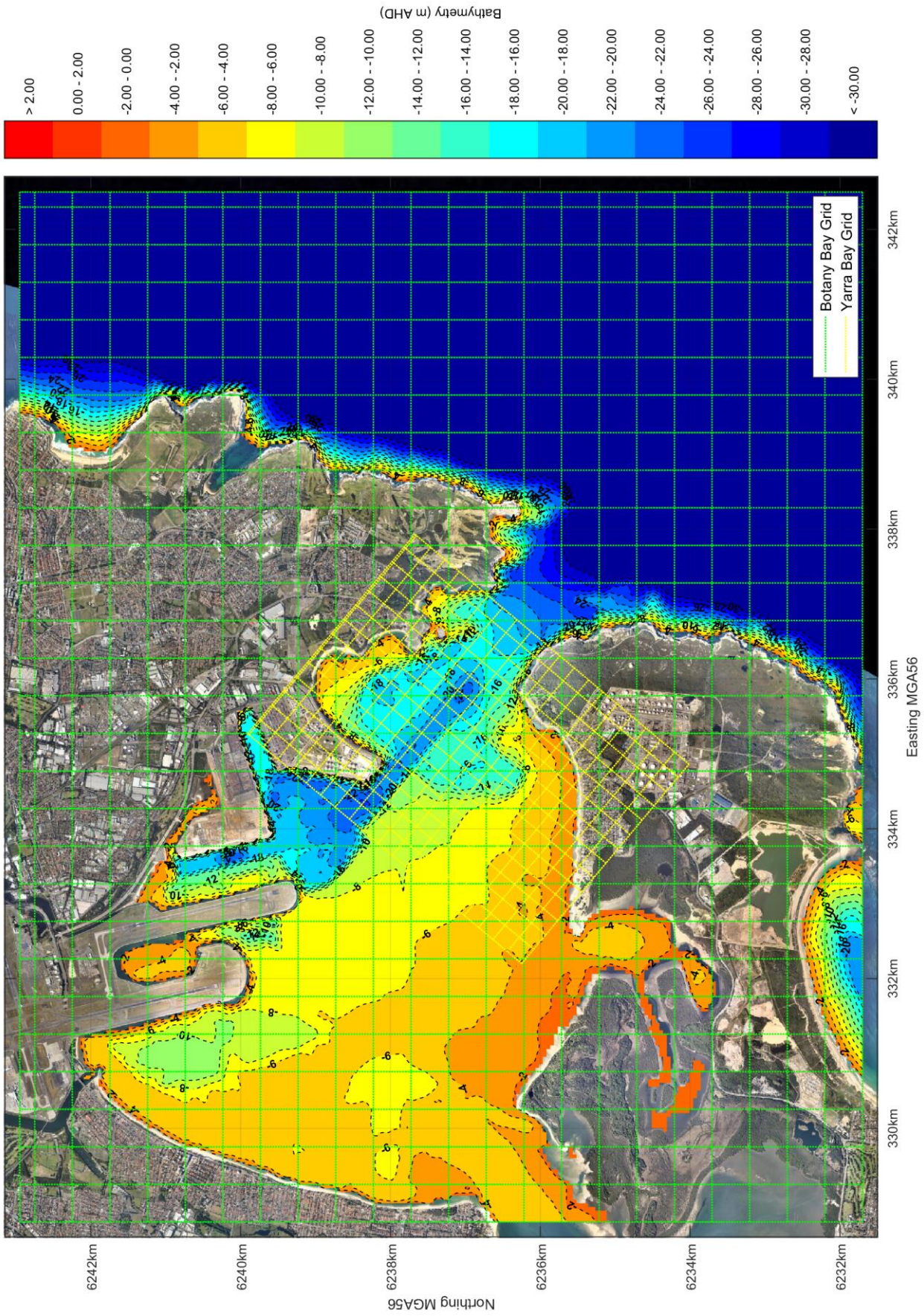


Figure 6-1 SWAN Model Grid and Bathymetry, every 15th Grid Line Shown

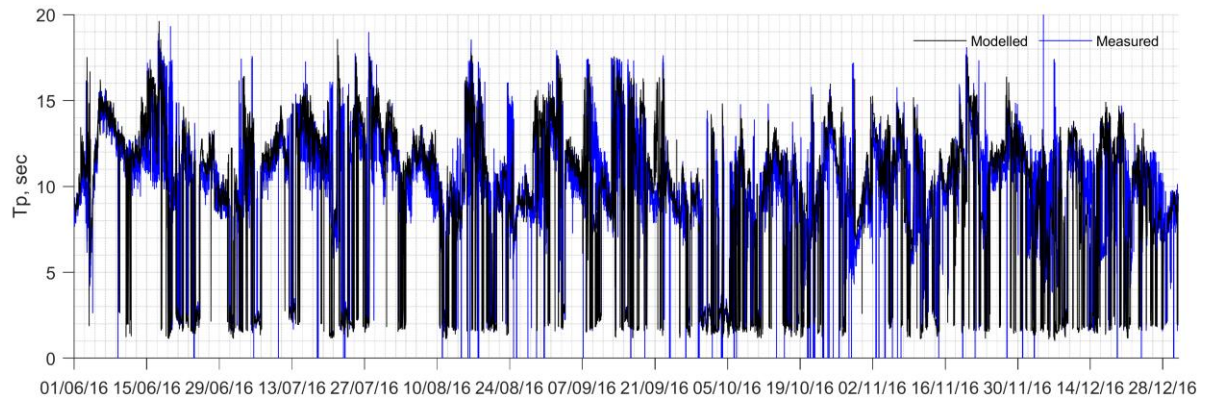
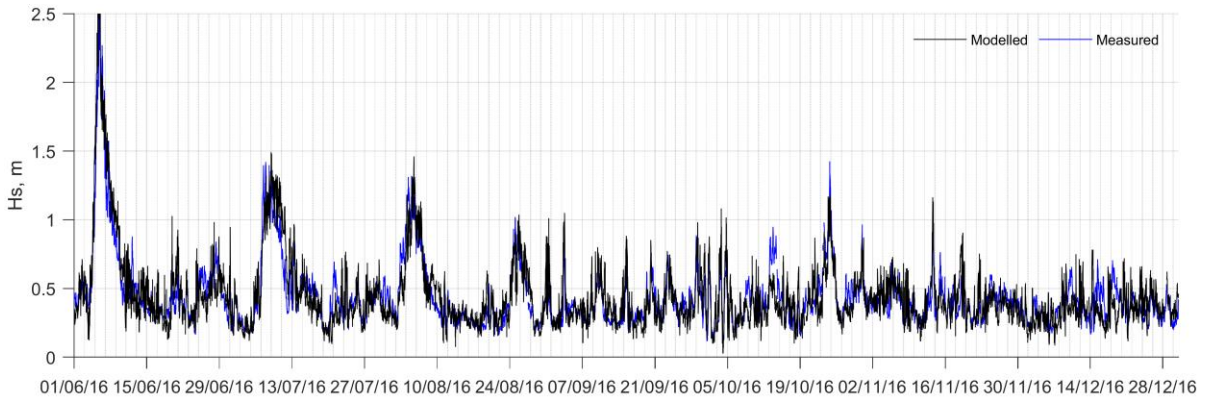


Figure 6-2 Wave Model Calibration at the Kumell Waverider Buoy (June 01 to December 31 2016)

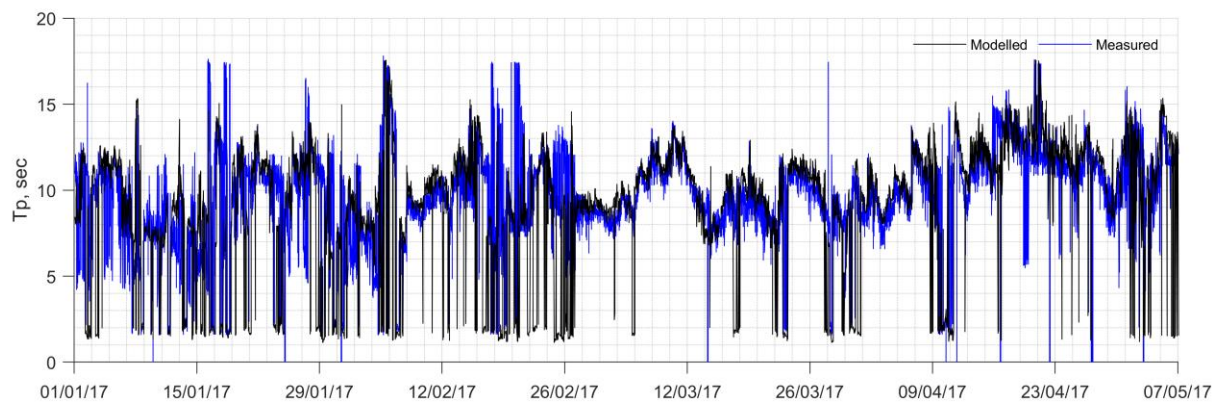
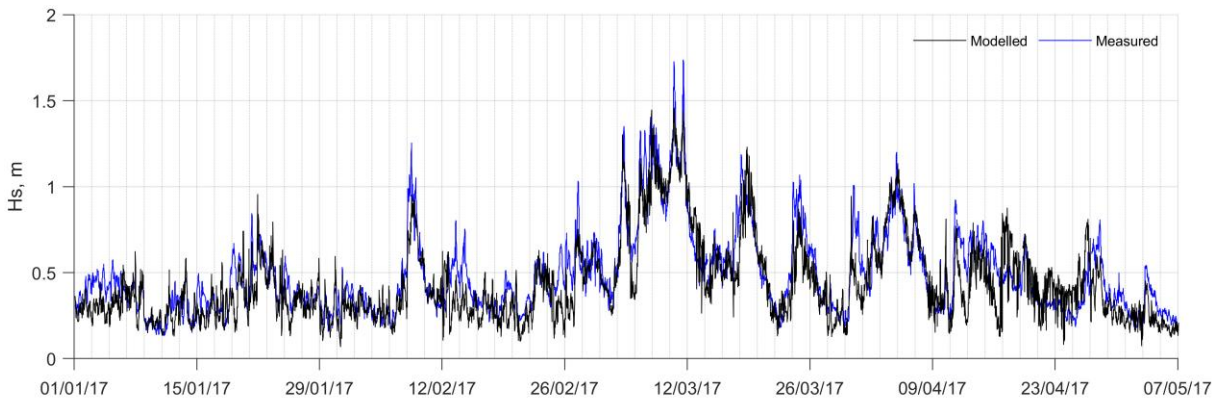


Figure 6-3 Wave Model Calibration at the Kumell Waverider Buoy (January 01 to June 01 2017)

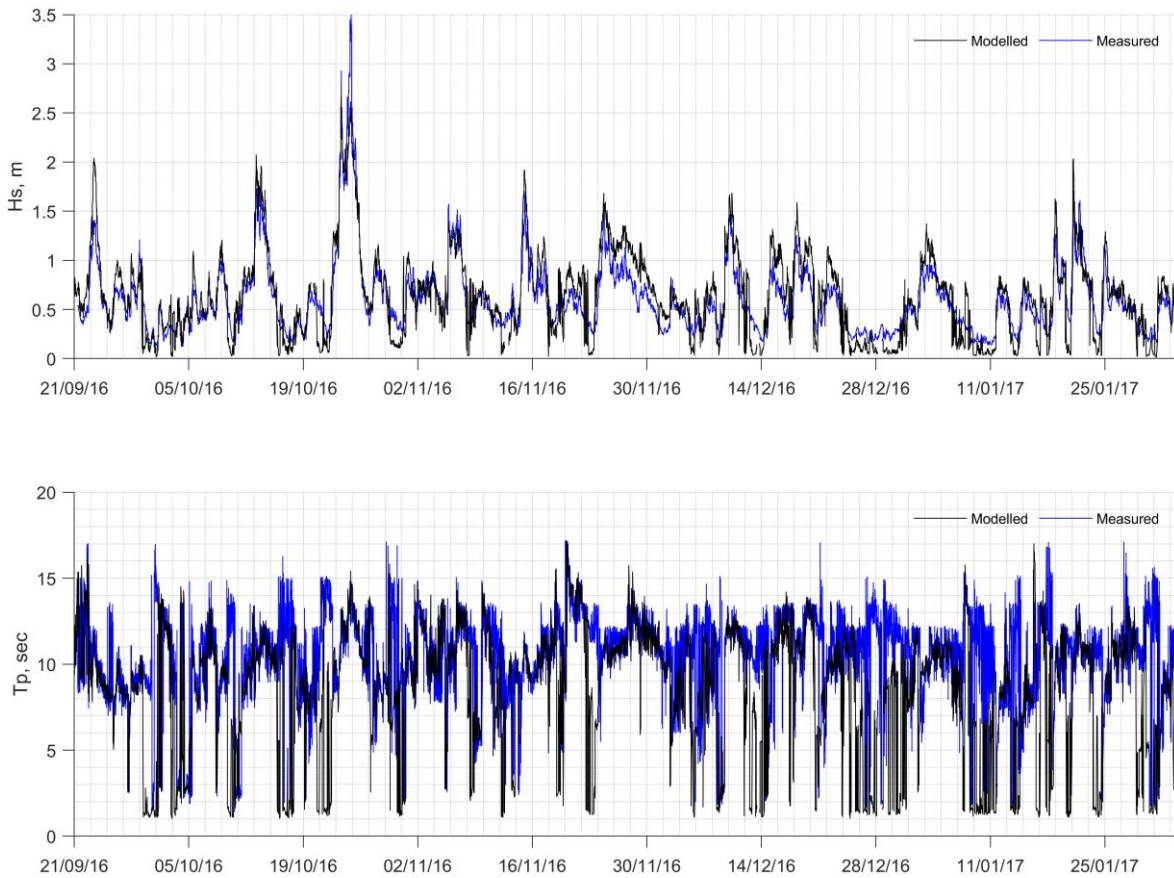


Figure 6-4 Wave Model Calibration at the Yarra Bay Waverider Buoy

Table 6-1 Wave Model Calibration Metrics

Wave Buoy	RMSE (m)	Bias (measured-model) (m)	Scatter Index	Correlation Coefficient
Kurnell	0.14	0.01	0.28	0.84
Yarra Bay	0.20	-0.05	0.33	0.89

These results, although variable, show that the SWAN model describes wave propagation from offshore to the Kurnell and Yarra Bay areas well.

6.3 SWAN Model Simulations

The propagation of waves into the La Perouse and Kurnell ferry wharf locations was investigated by applying the SWAN wave model to prepare wave transfer coefficients for a full suite of offshore wave heights, periods and directions, namely:

- Peak wave periods (T_p) ranging from 2s to 20s - at 2s intervals;
- Wave Directions from north, clockwise through to south- at 11.25 degree intervals;
- Offshore significant wave heights (H_s) of 0.5m, and every 1m between 1m and 8m; and

- Water levels varying between -1m and 1m AHD at 0.5m intervals

This resulted in a total of 7,650 basic wave simulations.

The results of this SWAN wave modelling provided matrices of wave coefficients and near shore wave directions at the selected model output locations shown on **Figures 6-5 to 6-7**, also presented in **Table 6-2**. These resulting simulation cases provided a reliable basis for the transfer of the offshore Waverider buoy data to inshore swell time-series at the nominated output locations.

Maps of the modelled significant wave height in Botany bay under a 1m offshore wave height and 12 second peak period for directions of ENE, E and SSE are presented in **Figures 6-8, 6-9 and 6-10**. Similar plots showing the significant wave height and peak wave direction under the 1 in 1-year ARI winds from the west and north-west are presented in **Figures 6-11 and 6-12**.

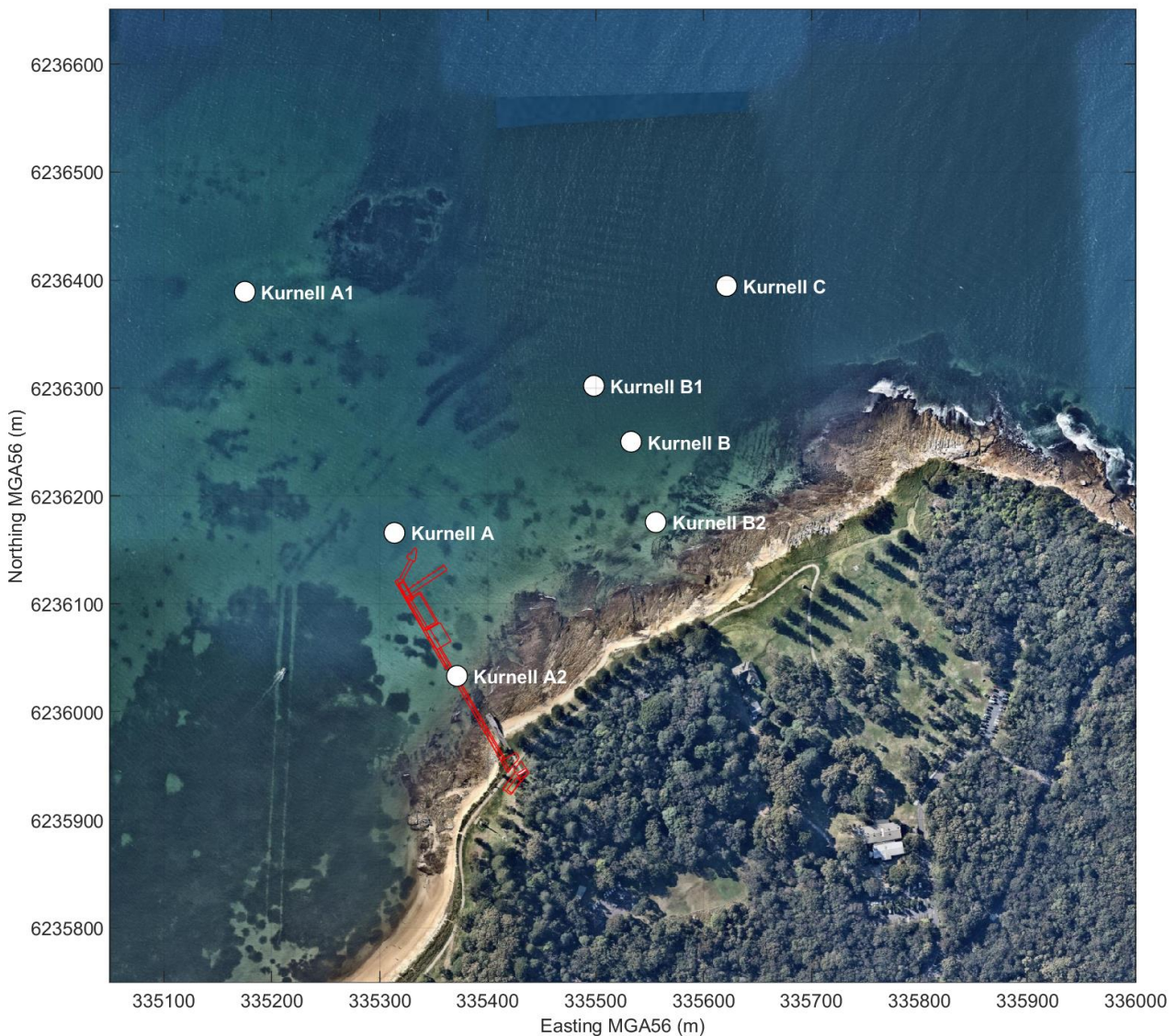


Figure 6-5 Kurnell Output Locations

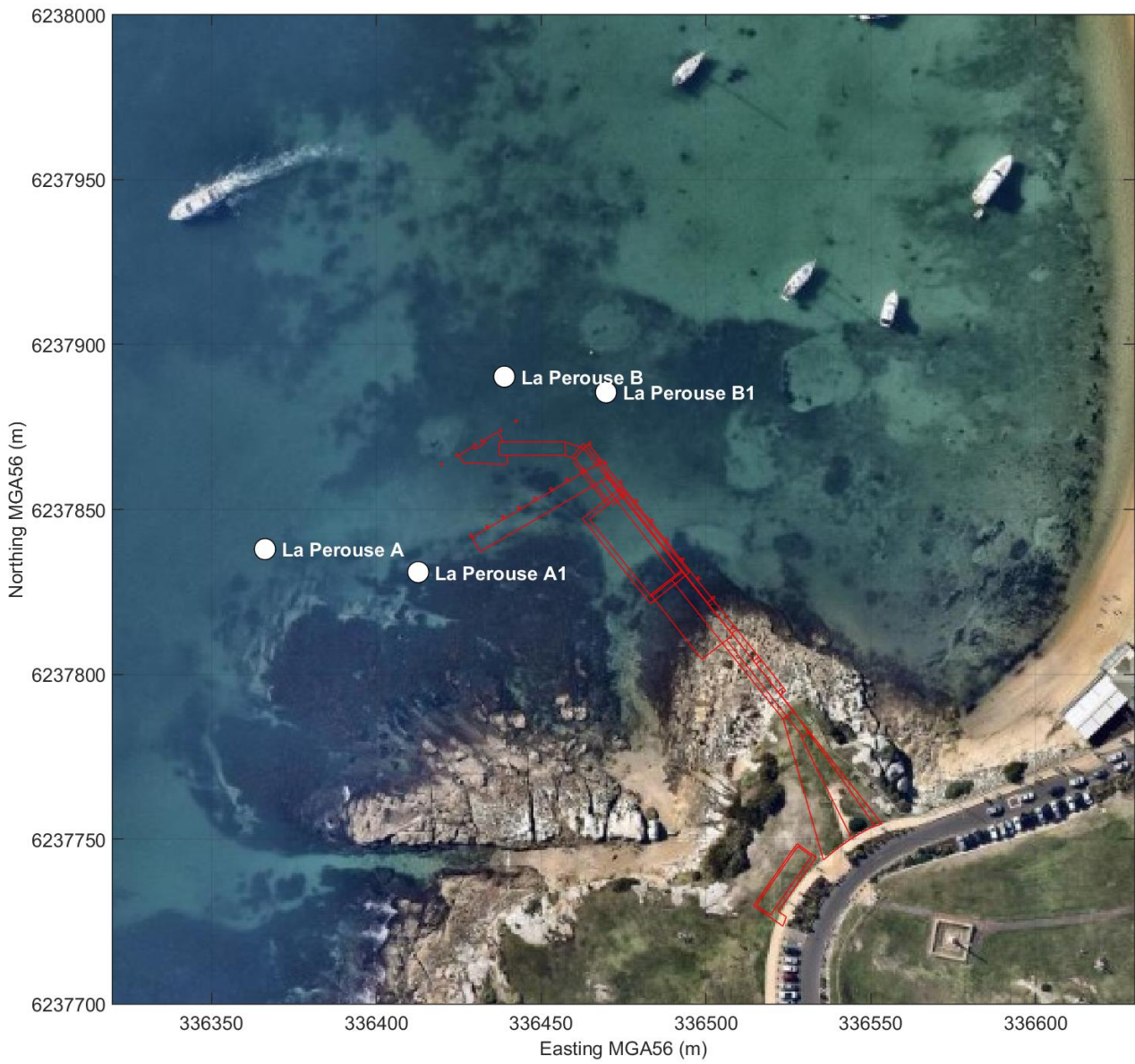


Figure 6-6 La Perouse Output Locations

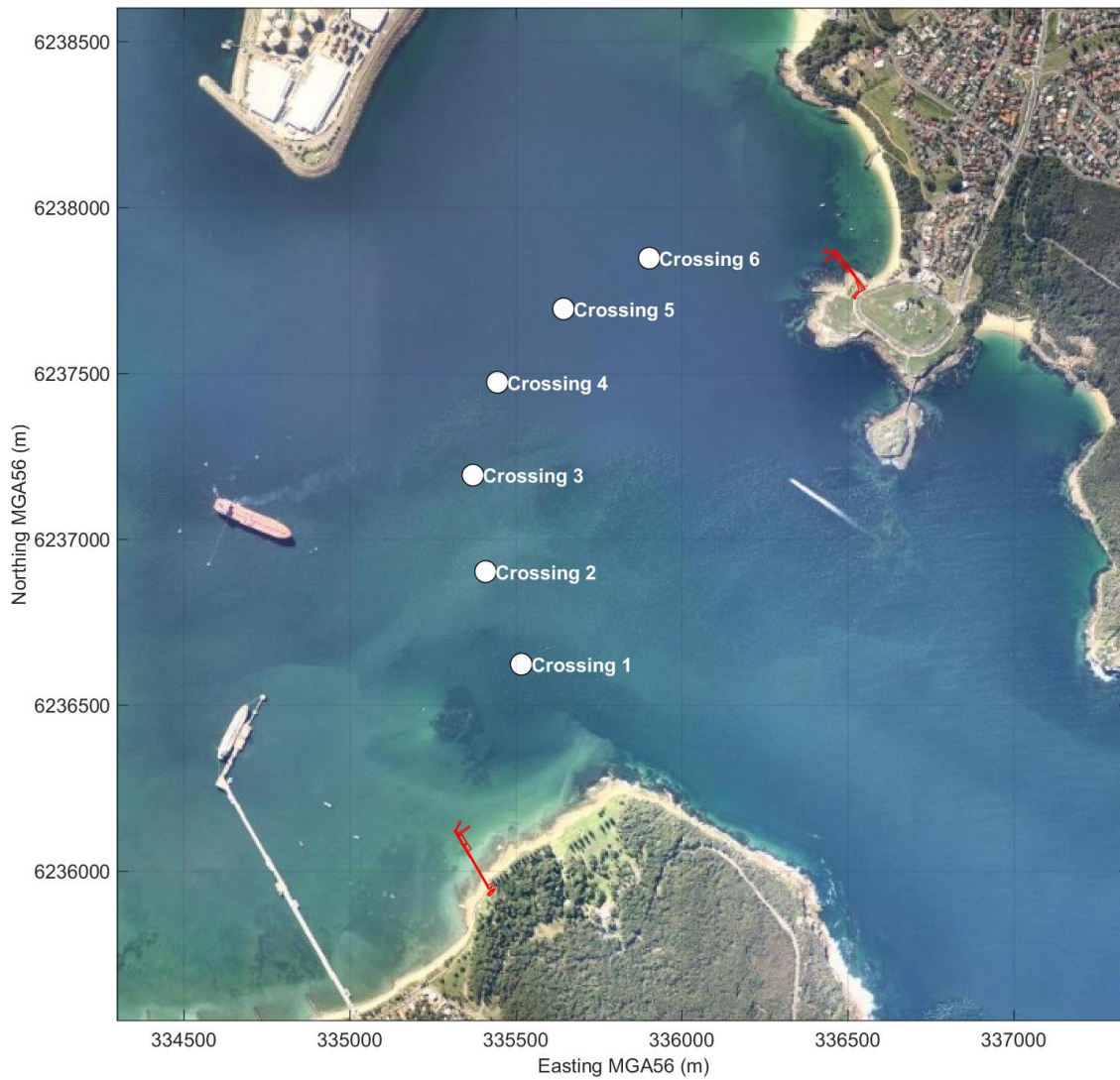


Figure 6-7 Crossing Output locations

Table 6-2 Model Output Locations

Location	Easting	Northing	Location	Easting	Northing
Kurnell A	335,313.5	6,236,166.1	La Perouse B	336,438.8	6,237,890.3
Kurnell A1	335,175.0	6,236,389.0	La Perouse B1	336,469.7	6,237,885.5
Kurnell A2	335,371.5	6,236,033.6	Crossing 1	335,516.6	6,236,622.6
Kurnell B	335,532.7	6,236,249.9	Crossing 2	335,409.0	6,236,902.1
Kurnell B1	335,498.4	6,236,301.9	Crossing 3	335,370.9	6,237,192.8
Kurnell B2	335,555.6	6,236,175.8	Crossing 4	335,444.6	6,237,472.6
Kurnell C	335,621.2	6,236,394.5	Crossing 5	335,643.7	6,237,694.2
La Perouse A	336,366.3	6,237,837.9	Crossing 6	335,902.0	6,237,846.8
La Perouse A1	336,412.7	6,237,831.0			

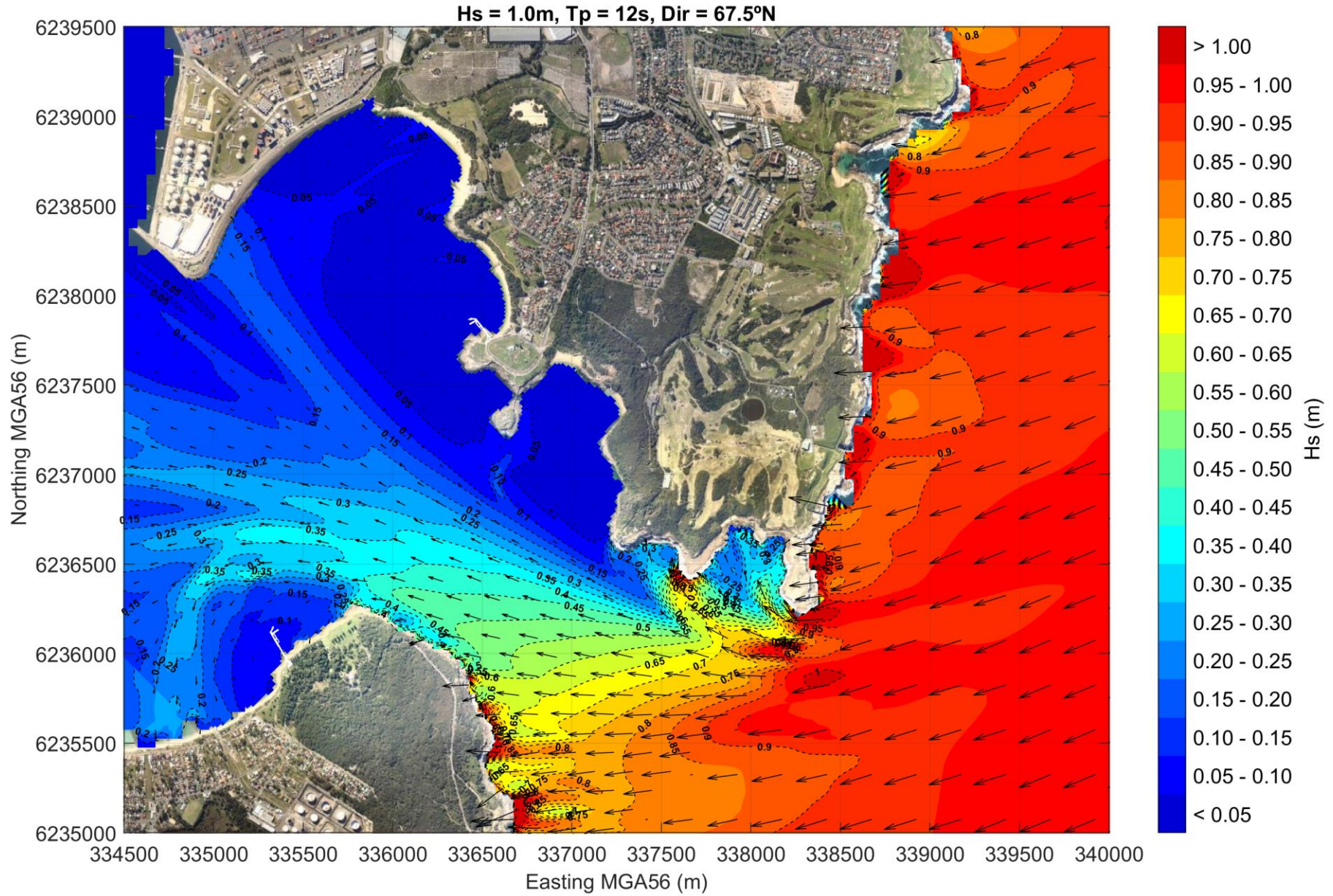


Figure 6-8 Modelled Significant Wave Height and Direction, Swell Waves from the ENE

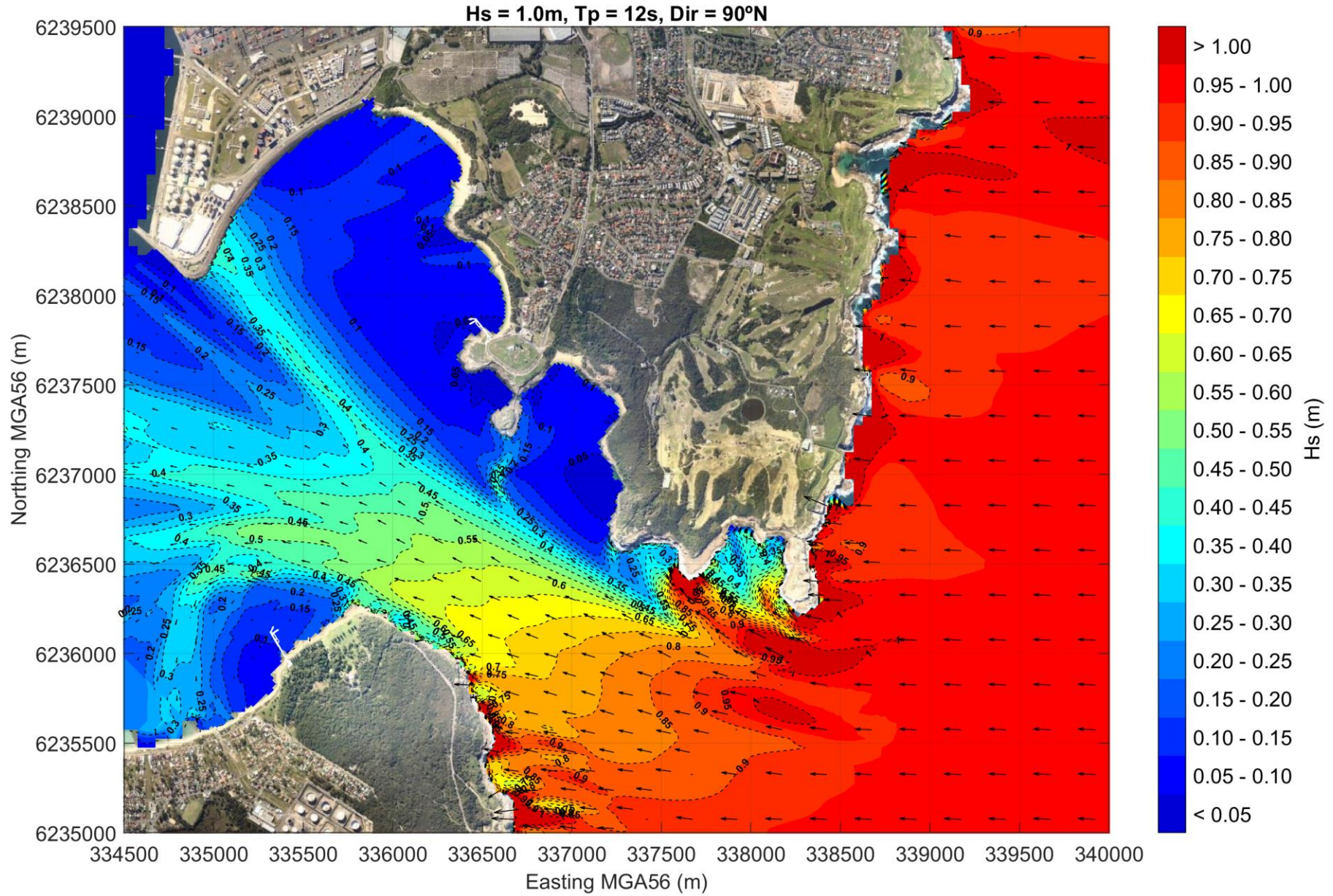


Figure 6-9 Modelled Significant Wave Height and Direction, Swell Waves from the East

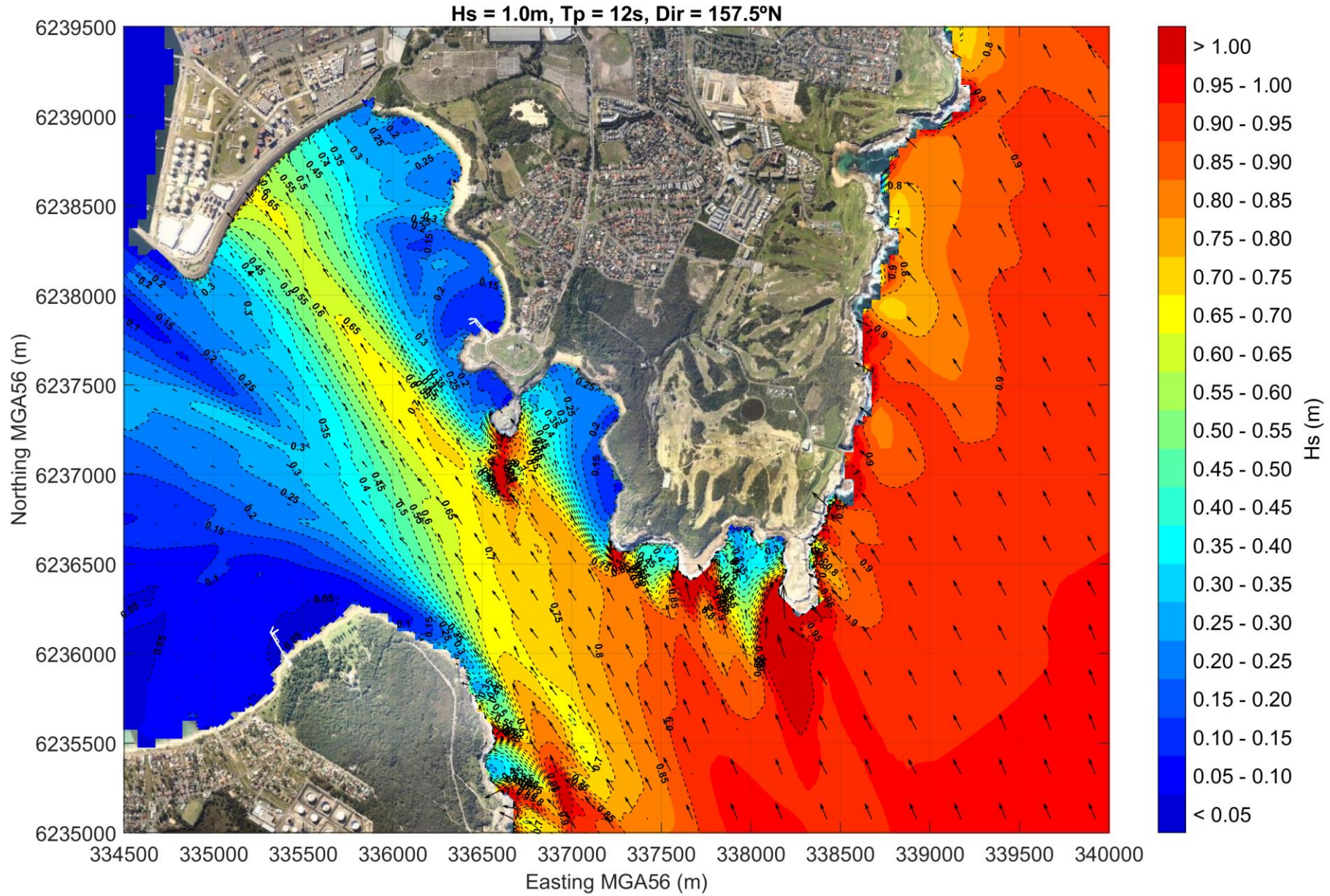


Figure 6-10 Modelled Significant Wave Height and Direction, Swell Waves from the SSE

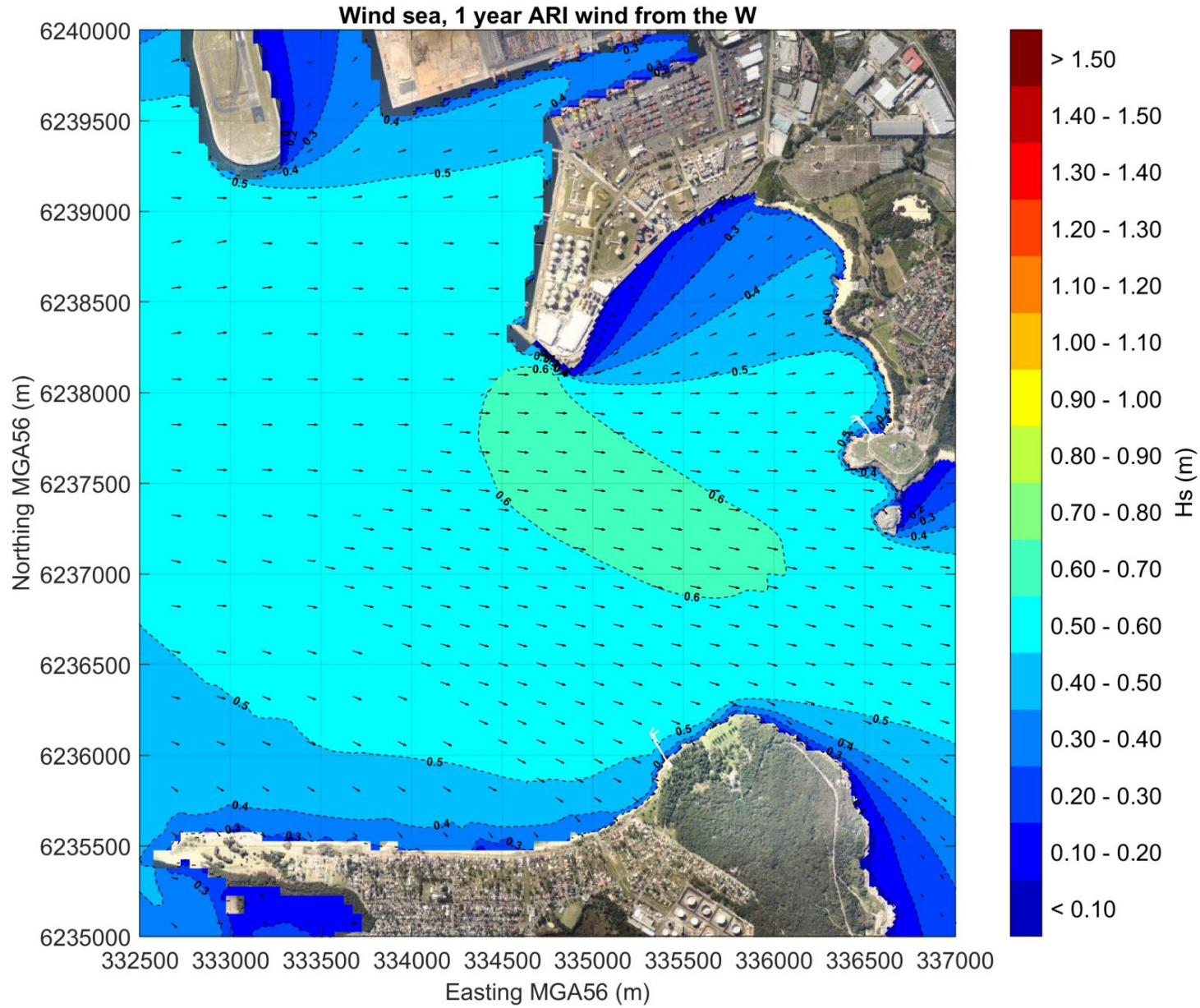


Figure 6-11 Modelled Significant (Sea) Wave Height and Direction, 1-Year ARI Wind from the West

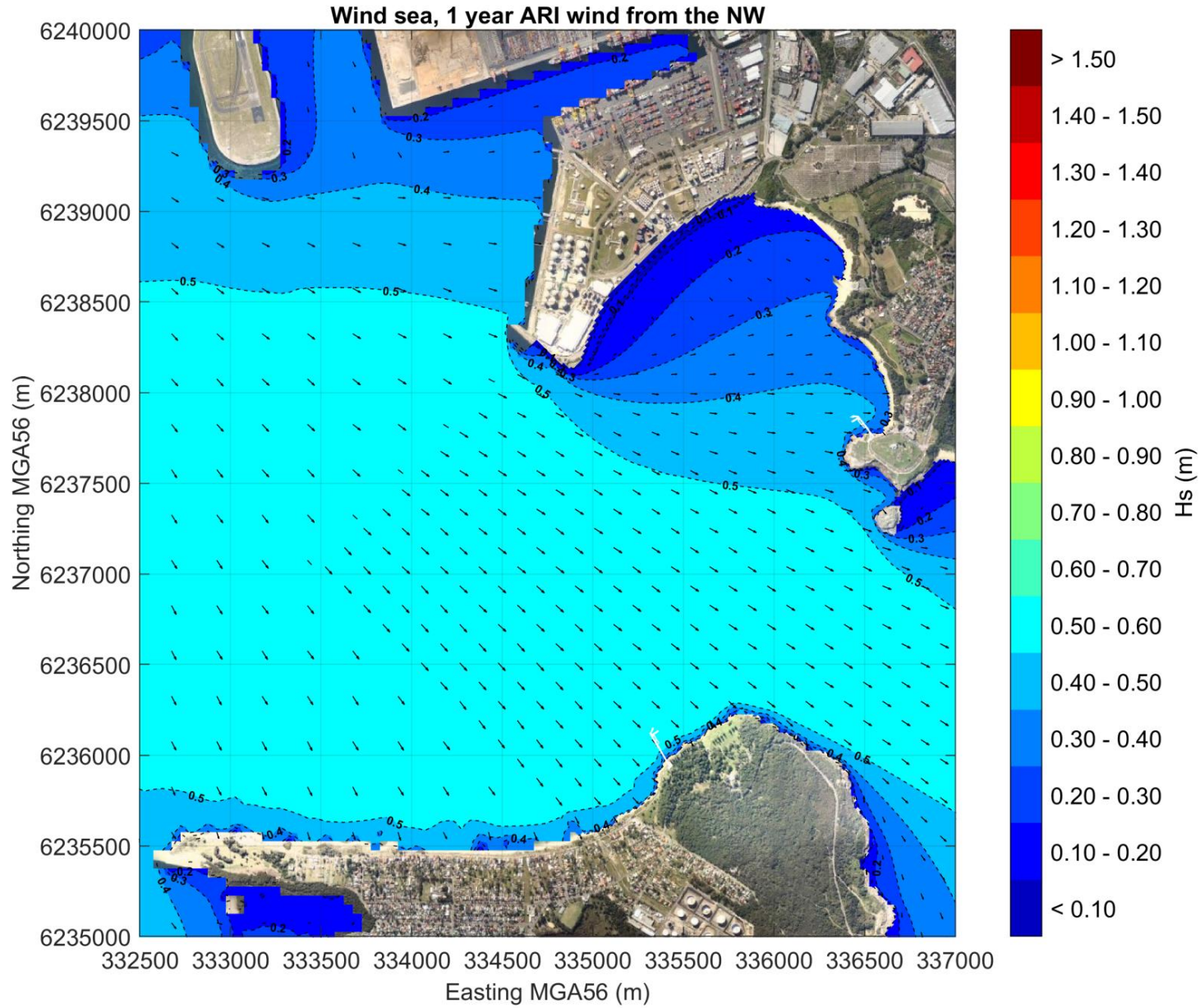


Figure 6-12 Modelled Significant (Sea) Wave Height and Direction, 1-Year ARI Wind from the Northwest

7 Nearshore Wave Climate

A time-series of sea and swell wave conditions at each of the model output points has been derived by applying the modelled transformation coefficients to the offshore wave dataset. The results at the Kurnell Jetty, La Perouse Jetty and Crossing Point 5 are discussed below.

7.1 Swell Waves

7.1.1 Kurnell

A wave rose of the hindcast swell wave conditions at Kurnell Location A is presented in **Figure 7-1**. This figure shows that swell wave conditions at this location are expected to be fairly unidirectional (between NNE and NE), and are generally less than 0.3m in height (Hs). Peak wave periods vary between 2 and 20 seconds, but are typically in the range of 7 to 13 seconds.

Tables 6-1 and **6-2** provide the joint occurrence of significant wave height and peak wave direction and peak wave period at Kurnell Location A; **Appendix D** provides the tables for all seven output Locations.

Table 7-1 Occurrence of Significant Wave Height by Peak Wave Direction at Kurnell Location A

Hs (m)		Direction Bins															Total	P<Hs	P>Hs	
		N	NNE	NE	ENE	E	ESE	SE	SSE	S	SSW	SW	WSW	W	WNW	NW				NNW
<0.05		0.21%	8.34%	2.94%	0.41%	-	-	-	-	-	-	-	-	-	-	-	-	11.9%	11.9%	88.1%
0.05	0.1	0.09%	32.91%	13.14%	0.03%	-	-	-	-	-	-	-	-	-	-	-	-	46.2%	58.1%	41.9%
0.1	0.2	-	19.44%	16.44%	-	-	-	-	-	-	-	-	-	-	-	-	-	35.9%	93.9%	6.1%
0.2	0.3	-	1.56%	3.36%	-	-	-	-	-	-	-	-	-	-	-	-	-	4.9%	98.9%	1.1%
0.3	0.4	-	0.10%	0.81%	-	-	-	-	-	-	-	-	-	-	-	-	-	0.9%	99.8%	0.2%
0.4	0.5	-	0.00%	0.19%	-	-	-	-	-	-	-	-	-	-	-	-	-	0.2%	100%	0.0%
>0.5		-	-	0.05%	-	-	-	-	-	-	-	-	-	-	-	-	-	0.0%	100%	0.0%
Sum		0.3%	62.3%	36.9%	0.4%	0.0%	0.0%	0.0%	0.0%	0.0%	0.0%	0.0%	0.0%	0.0%	0.0%	0.0%	0.0%	100%		

Table 7-2 Occurrence of Significant Wave Height by Peak Wave Period at Kurnell Location A

Hs (m)		Peak Wave Period Bins (sec)									Total	P<Hs	P>Hs
		<3	3	5	7	9	11	13	15	>17			
From	To		5	7	9	11	13	15	17				
Calm (<0.05)		0.01%	0.87%	3.63%	2.23%	2.52%	1.57%	0.87%	0.17%	0.02%	11.9%	11.9%	88.1%
0.05	0.1	-	0.15%	5.15%	12.40%	14.00%	8.95%	4.43%	0.96%	0.13%	46.2%	58.1%	41.9%
0.1	0.2	-	-	0.85%	7.39%	13.21%	9.65%	3.74%	0.90%	0.14%	35.9%	93.9%	6.1%
0.2	0.3	-	-	-	0.61%	1.77%	1.77%	0.62%	0.11%	0.04%	4.9%	98.8%	1.2%
0.3	0.4	-	-	-	0.03%	0.30%	0.42%	0.12%	0.03%	0.01%	0.9%	99.8%	0.2%
0.4	0.5	-	-	-	-	0.05%	0.11%	0.03%	-	-	0.2%	99.9%	0.1%
>0.5		-	-	-	-	-	0.03%	0.01%	-	-	0.0%	100%	0.0%
Sum		0.0%	1.0%	9.6%	22.7%	31.9%	22.5%	9.8%	2.2%	0.3%	100.0%		

**Kurnell Swell Wave Rose
 Location A, 1998 to 2018**

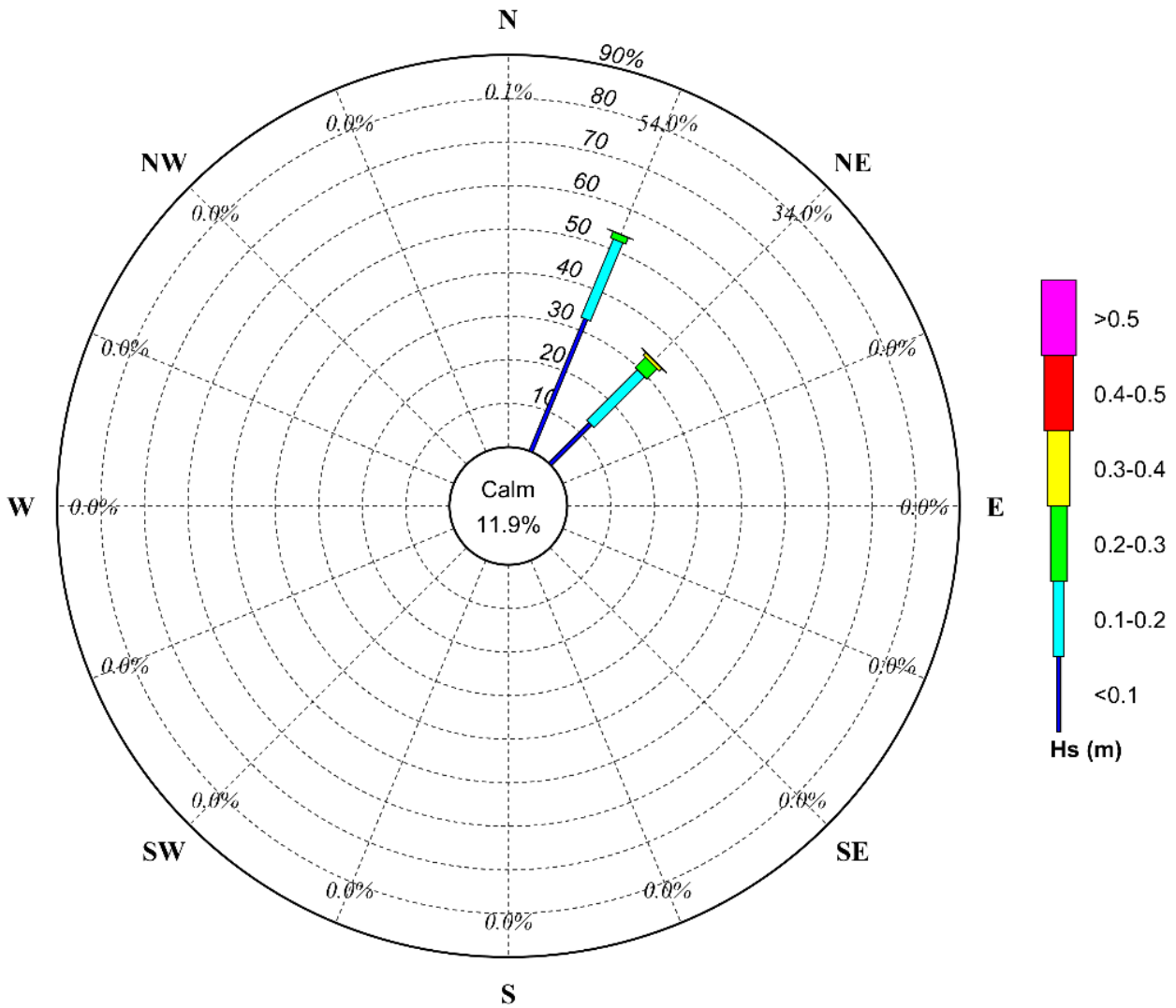


Figure 7-1 Swell Wave Rose (Significant Wave Height by Peak Wave Direction) at Kurnell Location A

7.1.2 La Perouse

A wave rose of the hindcast swell wave conditions at La Perouse Location A is presented in **Figure 7-2**. This figure shows that swell wave conditions at this location are expected to be fairly unidirectional (between WSW and W), and generally less than 0.4m in height (Hs). Peak wave periods vary between 2 and 20 seconds, but are typically in the range of 7 to 13 seconds.

Tables 7-3 and 7-4 provide the joint occurrence of significant wave height by peak wave direction and peak wave period at La Perouse Location A, **Appendix E** provides the tables for all four La Perouse output locations.

Table 7-3 Occurrence of Significant Wave Height by Peak Wave Direction at La Perouse Location A

Hs (m)		Direction Bins														Total	P<Hs	P>Hs	
		N	NNE	NE	ENE	E	ESE	SE	SSE	S	SSW	SW	WSW	W	WNW				NW
<0.05		-	-	-	-	-	-	-	-	-	-	0.13%	15.20%	0.13%	-	-	15.5%	15.5%	84.5%
0.05	0.1	-	-	-	-	-	-	-	-	-	0.04%	2.17%	11.59%	0.04%	-	-	13.8%	29.3%	70.7%
0.1	0.2	-	-	-	-	-	-	-	-	-	0.46%	19.23%	20.70%	-	-	-	40.4%	69.7%	30.3%
0.2	0.3	-	-	-	-	-	-	-	-	-	0.94%	15.43%	6.07%	-	-	-	22.4%	92.1%	7.9%
0.3	0.4	-	-	-	-	-	-	-	-	-	0.34%	4.54%	1.21%	-	-	-	6.1%	98.2%	1.8%
0.4	0.5	-	-	-	-	-	-	-	-	-	0.08%	1.17%	0.25%	-	-	-	1.5%	99.7%	0.3%
>0.5		-	-	-	-	-	-	-	-	-	0.01%	0.26%	0.02%	-	-	-	0.3%	100%	0.0%
Sum		0.0%	0.0%	0.0%	0.0%	0.0%	0.0%	0.0%	0.0%	0.0%	1.9%	42.9%	55.0%	0.2%	0.0%	0.0%	100%		

Table 7-4 Occurrence of Significant Wave Height by Peak Wave Period at La Perouse Location A

Hs (m)		Peak Wave Period Bins (sec)									Total	P<Hs	P>Hs
		<3	3	5	7	9	11	13	15	>17			
From	To		5	7	9	11	13	15	17				
Calm (<0.05)		0.02%	0.79%	3.74%	3.60%	3.84%	2.46%	0.81%	0.19%	0.02%	15.5%	15.5%	84.5%
0.05	0.1	-	0.59%	0.82%	2.23%	4.48%	3.77%	1.62%	0.30%	0.03%	13.8%	29.3%	70.7%
0.1	0.2	-	2.48%	2.94%	8.64%	12.23%	9.32%	3.66%	0.97%	0.15%	40.4%	69.7%	30.3%
0.2	0.3	-	0.68%	2.53%	6.02%	7.60%	3.97%	1.27%	0.31%	0.06%	22.4%	92.1%	7.9%
0.3	0.4	-	0.01%	0.28%	1.45%	2.52%	1.35%	0.34%	0.10%	0.03%	6.1%	98.2%	1.8%
0.4	0.5	-	-	-	0.20%	0.60%	0.54%	0.13%	0.02%	-	1.5%	99.7%	0.3%
>0.5		-	-	-	-	0.10%	0.13%	0.04%	-	-	0.3%	100%	0.0%
Sum		0.0%	4.5%	10.3%	22.2%	31.4%	21.5%	7.9%	1.9%	0.3%	100%		

La Perouse Swell Wave Rose
Location A, 1998 to 2018

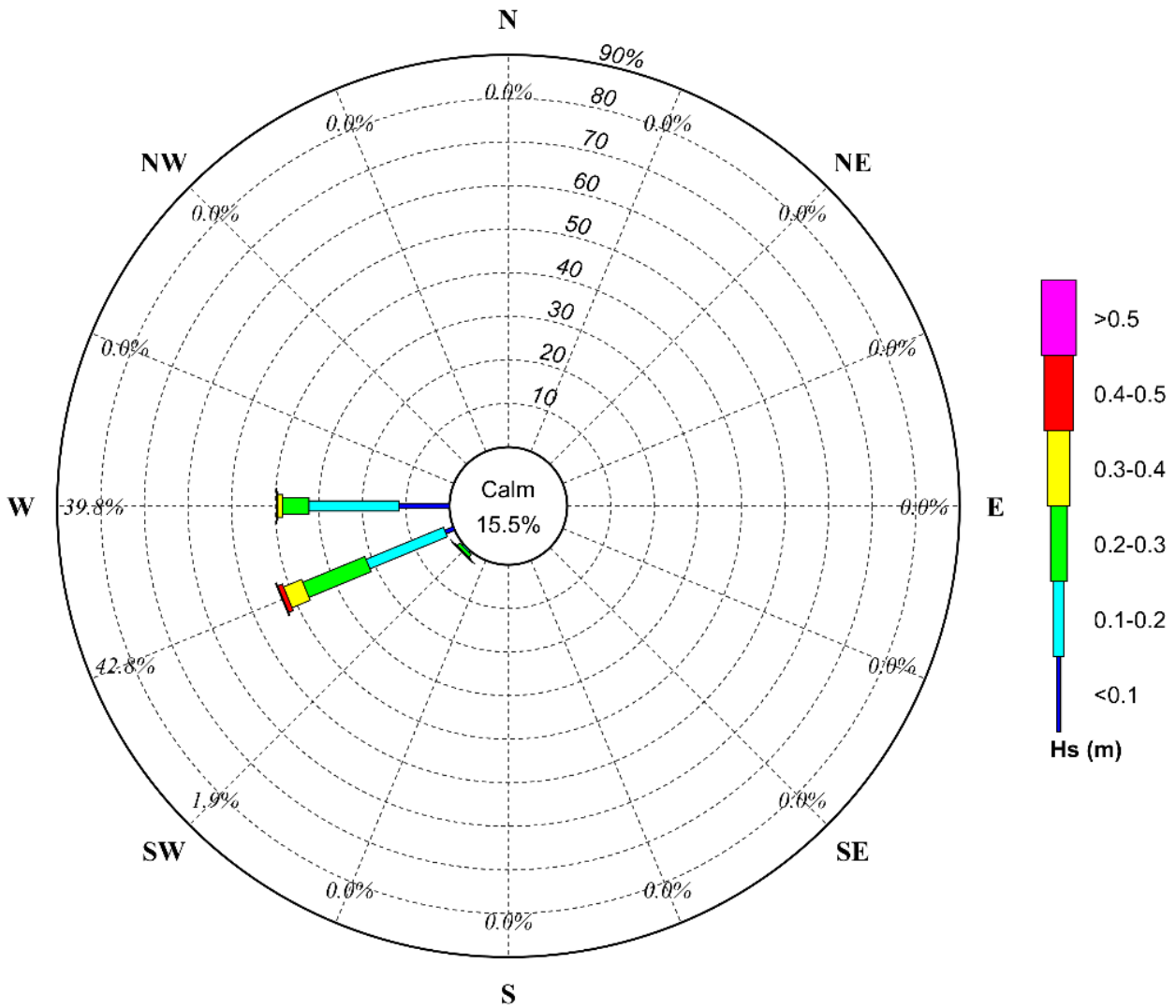


Figure 7-2 Swell Wave Rose (Significant Wave Height by Peak Wave Direction) at La Perouse Location A

7.1.3 Crossing Points

Wave conditions in open water between Kurnell and La Perouse can vary significantly during a storm event. Based on the selected output locations from the model simulations, the largest swell waves would generally be experienced in the vicinity of Crossing Point 5, which is to the north of the Botany Bay shipping channel.

A wave rose of the hindcast swell wave conditions at Crossing Point 5 is presented in **Figure 7-3**. This figure shows that swell wave conditions at this point are expected to be fairly unidirectional (from the SE), and generally less than 1.5m in height (Hs). Larger wave events do occur, with the model predicting that the significant wave height at this crossing point exceeds 2.5m for 0.5% of the time. Peak wave periods vary between 2 and 20 seconds, but are typically in the range of 7 to 13 seconds.

Tables 7-5 and **7-6** provide the joint occurrence of significant wave height by peak wave direction and peak wave period at Crossing Point 5, **Appendix F** provides the tables for all six output crossing points.

Table 7-5 Occurrence of Significant Wave Height by Peak Wave Direction at Crossing Point 5

Hs (m)		Direction Bins															Total	P<Hs	P>Hs	
		N	NNE	NE	ENE	E	ESE	SE	SSE	S	SSW	SW	WSW	W	WNW	NW				NNW
<0.1		-	-	-	-	-	-	7.34%	0.00%	-	-	-	-	-	-	-	-	7.3%	7.3%	92.7%
0.10	0.25	-	-	-	-	-	-	8.91%	0.24%	-	-	-	-	-	-	-	-	9.2%	16.5%	83.5%
0.25	0.50	-	-	-	-	-	-	15.02%	2.87%	-	-	-	-	-	-	-	-	17.9%	34.4%	65.6%
0.50	0.75	-	-	-	-	-	-	19.99%	4.72%	-	-	-	-	-	-	-	-	24.7%	59.1%	40.9%
0.75	1.00	-	-	-	-	-	-	15.49%	4.01%	-	-	-	-	-	-	-	-	19.5%	78.6%	21.4%
1.00	1.25	-	-	-	-	-	-	7.95%	2.66%	-	-	-	-	-	-	-	-	10.6%	89.2%	10.8%
1.25	1.50	-	-	-	-	-	-	3.67%	1.47%	-	-	-	-	-	-	-	-	5.1%	94.3%	5.7%
1.50	1.75	-	-	-	-	-	-	1.84%	0.74%	-	-	-	-	-	-	-	-	2.6%	96.9%	3.1%
1.75	2.00	-	-	-	-	-	-	0.93%	0.41%	-	-	-	-	-	-	-	-	1.3%	98.3%	1.7%
2.00	2.25	-	-	-	-	-	-	0.54%	0.24%	-	-	-	-	-	-	-	-	0.8%	99.0%	1.0%
2.25	2.50	-	-	-	-	-	-	0.30%	0.12%	-	-	-	-	-	-	-	-	0.4%	99.5%	0.5%
>2.5		-	-	-	-	-	-	0.44%	0.11%	-	-	-	-	-	-	-	-	0.5%	100%	0.0%
Sum		0.0%	0.0%	0.0%	0.0%	0.0%	0.0%	82.4%	17.6%	0.0%	0.0%	0.0%	0.0%	0.0%	0.0%	0.0%	0.0%	100%		

Table 7-6 Occurrence of Significant Wave Height by Peak Wave Period at Crossing Point 5

Hs (m)		Peak Wave Period Bins (sec)									Total	P<Hs	P>Hs
		<3	3	5	7	9	11	13	15	>17			
From	To		5	7	9	11	13	15	17				
Calm (<0.1)		0.01%	0.64%	2.29%	1.54%	1.63%	0.76%	0.36%	0.08%	0.02%	7.3%	7.3%	92.7%
0.10	0.25	-	0.28%	1.33%	2.03%	2.68%	2.03%	0.64%	0.14%	-	9.1%	16.5%	83.5%
0.25	0.50	-	0.75%	2.16%	3.30%	5.15%	4.34%	1.81%	0.36%	0.03%	17.9%	34.4%	65.6%
0.50	0.75	-	0.06%	2.78%	6.02%	7.54%	5.47%	2.21%	0.56%	0.09%	24.7%	59.1%	40.9%
0.75	1.00	-	-	1.11%	4.86%	6.87%	4.48%	1.63%	0.47%	0.07%	19.5%	78.6%	21.4%
1.00	1.25	-	-	0.19%	2.17%	4.24%	2.80%	0.94%	0.23%	0.04%	10.6%	89.2%	10.8%
1.25	1.50	-	-	-	0.85%	2.10%	1.53%	0.51%	0.12%	0.02%	5.1%	94.3%	5.7%
1.50	1.75	-	-	-	0.28%	1.07%	0.90%	0.25%	0.07%	0.01%	2.6%	96.9%	3.1%
1.75	2.00	-	-	-	0.08%	0.52%	0.53%	0.15%	0.03%	0.02%	1.3%	98.3%	1.7%
2.00	2.25	-	-	-	0.03%	0.28%	0.33%	0.10%	0.02%	0.01%	0.8%	99.0%	1.0%
2.25	2.50	-	-	-	-	0.13%	0.20%	0.06%	0.01%	-	0.4%	99.4%	0.6%
>2.5		-	-	-	-	0.14%	0.28%	0.10%	0.02%	-	0.5%	100.0%	0.0%
Sum		0.0%	1.7%	9.9%	21.2%	32.4%	23.7%	8.7%	2.1%	0.3%	100.0%		

Swell Wave Rose
Crossing 5, 1998 to 2018

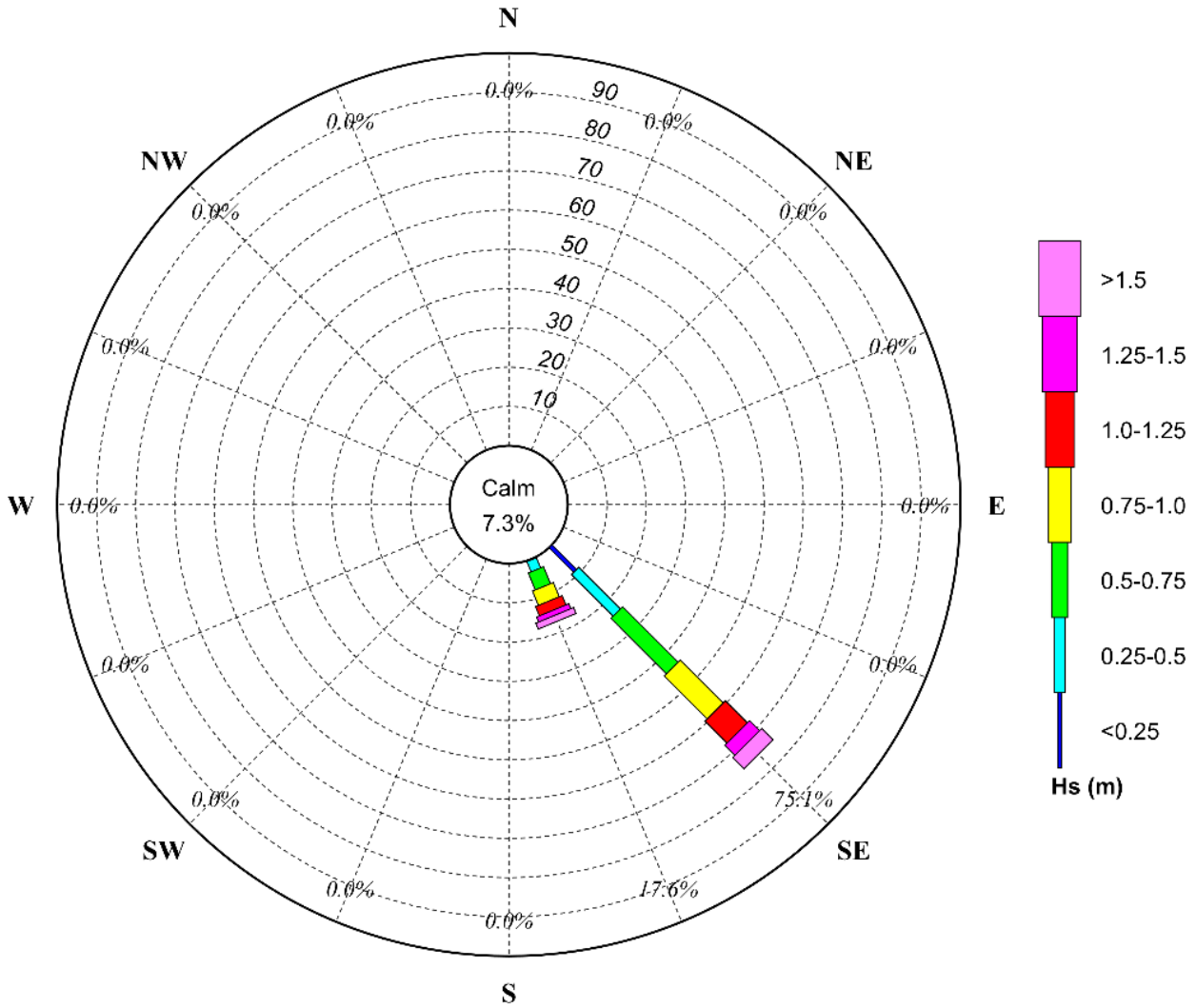


Figure 7-3 Swell Wave Rose (Significant Wave Height by Peak Wave Direction) at Crossing Point 5

7.2 Sea Waves

7.2.1 Kurnell

A wave rose of the hindcast locally wind generated (sea) wave conditions at Kurnell Location A is presented in **Figure 7-4**. This figure shows that sea wave conditions at this location predominantly come from the northern directions (WNW to ENE). The largest sea waves tend to come from the NW. Peak wave periods rarely exceed 2.5 seconds.

Tables 7-7 and **7-8** provide the joint occurrence of significant sea wave height by peak wave direction and peak wave period at Kurnell Location A, **Appendix D** provides the tables for all seven output locations.

Table 7-7 Occurrence of Significant Wave Height (Sea) by Peak Wave Direction at Kurnell Location A

Hs (m)		Direction Bins															Total	P<Hs	P>Hs	
		N	NNE	NE	ENE	E	ESE	SE	SSE	S	SSW	SW	WSW	W	WNW	NW				NNW
<0.05		1.45%	1.09%	1.39%	3.26%	0.01%	-	-	-	-	-	-	-	-	4.50%	2.71%	5.27%	19.7%	19.7%	80.3%
0.05	0.1	2.92%	1.56%	1.75%	4.16%	0.43%	0.12%	0.06%	0.06%	0.07%	0.18%	0.59%	0.82%	1.04%	6.37%	8.31%	0.48%	28.9%	48.6%	51.4%
0.1	0.2	4.13%	4.23%	1.80%	3.60%	0.24%	0.13%	0.12%	0.14%	0.40%	4.81%	3.98%	0.87%	0.36%	5.39%	5.79%	0.23%	36.2%	84.8%	15.2%
0.2	0.3	1.16%	3.05%	0.04%	0.20%	0.01%	0.01%	0.01%	0.01%	0.08%	1.22%	0.87%	0.07%	0.06%	2.28%	1.60%	0.05%	10.7%	95.5%	4.5%
0.3	0.4	0.14%	0.84%	0.0%	0.03%	-	-	0.00%	0.00%	0.01%	0.12%	0.23%	0.01%	0.01%	0.79%	0.79%	0.01%	3.0%	98.5%	1.5%
0.4	0.5	0.00%	0.09%	0.00%	0.00%	-	-	-	-	0.00%	0.01%	0.03%	0.00%	0.00%	0.24%	0.52%	0.00%	0.9%	99.4%	0.6%
>0.5		-	0.01%	-	-	-	-	-	-	-	0.00%	0.01%	-	-	0.06%	0.54%	0.00%	0.6%	100%	0.0%
Sum		9.8%	10.9%	5.0%	11.2%	0.7%	0.3%	0.2%	0.2%	0.6%	6.3%	5.7%	1.8%	1.5%	19.6%	20.3%	6.0%	100%		

Table 7-8 Occurrence of Significant Wave Height (Sea) by Peak Wave Period at Kurnell Location A

Hs (m)		Peak Wave Period Bins (sec)							Total	P<Hs	P>Hs
		<1.5	1.5	2.0	2.5	3.0	3.5	>4			
From	To	2.0	2.5	3.0	3.5	4.0					
Calm (<0.05)		16.35%	3.33%	-	-	-	-	-	19.7%	19.7%	80.3%
0.05	0.1	18.07%	10.83%	-	-	-	-	-	28.9%	48.6%	51.4%
0.1	0.2	18.94%	17.28%	-	-	-	-	-	36.2%	84.8%	15.2%
0.2	0.3	1.00%	8.13%	1.59%	-	-	-	-	10.7%	95.5%	4.5%
0.3	0.4	-	0.50%	2.46%	0.01%	-	-	-	3.0%	98.5%	1.5%
0.4	0.5	-	0.04%	0.37%	0.49%	-	-	-	0.9%	99.4%	0.6%
>0.5		-	-	0.01%	0.44%	0.16%	-	-	0.6%	100.0%	0.0%
Sum		54.4%	40.1%	4.4%	0.9%	0.2%	0.0%	0.0%	100.0%		

**Kurnell Sea Wave Rose
Location A, 1998 to 2018**

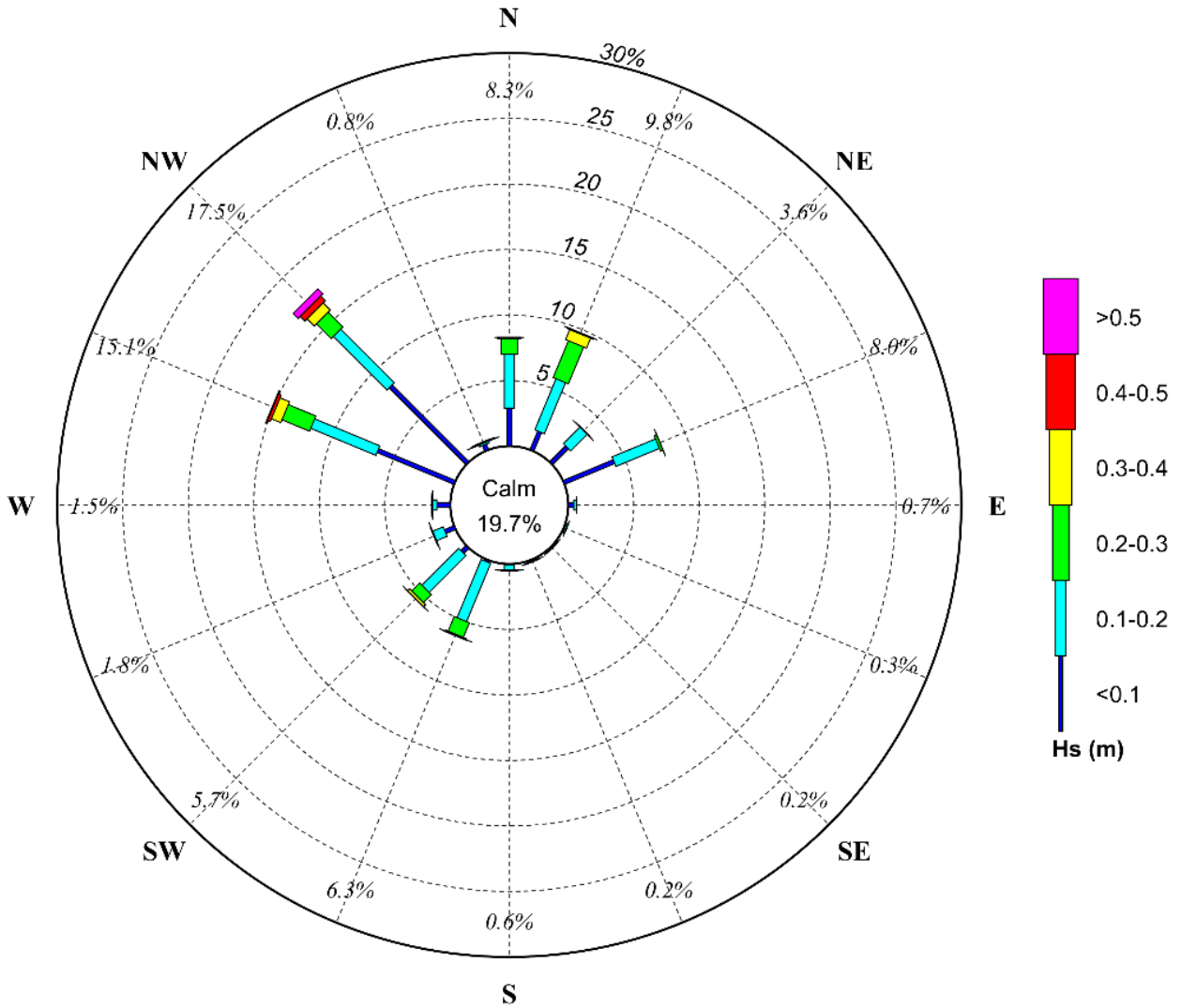


Figure 7-4 Sea Wave Rose (Significant Wave Height by Peak Wave Direction) at Kurnell Location A

7.2.2 La Perouse

A wave rose of the hindcast sea wave conditions at La Perouse Location A is presented in **Figure 7-5**. This figure shows that sea wave conditions at this location typically come from directions between south and west and are generally less than 0.4m in height (Hs). Peak wave periods vary between 2 and 4 seconds, but are typically less than 2.5 seconds.

Tables 7-9 and 7-10 provide the joint occurrence of significant wave height by peak wave direction and peak wave period at La Perouse Location A, **Appendix E** provides the tables for all four output locations.

Table 7-9 Occurrence of Significant Wave Height (Sea) by Peak Wave Direction at La Perouse Location A

Hs (m)		Direction Bins															Total	P<Hs	P>Hs	
		N	NNE	NE	ENE	E	ESE	SE	SSE	S	SSW	SW	WSW	W	WNW	NW				NNW
<0.05		-	-	-	-	-	-	-	-	3.06%	3.00%	1.30%	3.12%	6.51%	3.80%	0.95%	1.07%	22.8%	22.8%	77.2%
0.05	0.1	0.01%	0.01%	0.01%	0.01%	0.00%	0.01%	0.02%	0.09%	1.25%	3.22%	1.24%	2.93%	12.20%	6.28%	3.36%	0.79%	31.4%	54.2%	45.8%
0.1	0.2	0.25%	0.12%	0.11%	0.04%	0.03%	0.03%	0.03%	0.01%	2.58%	5.24%	1.41%	2.61%	7.41%	1.64%	2.37%	3.67%	27.6%	81.8%	18.2%
0.2	0.3	0.00%	-	0.00%	-	-	-	-	-	1.08%	3.54%	0.47%	2.08%	3.35%	0.08%	0.05%	0.27%	10.9%	92.7%	7.3%
0.3	0.4	-	-	-	-	-	-	-	-	0.05%	1.62%	0.20%	0.49%	2.14%	0.01%	0.01%	0.00%	4.5%	97.3%	2.7%
0.4	0.5	-	-	-	-	-	-	-	-	-	0.45%	0.11%	0.15%	1.03%	0.00%	0.00%	-	1.7%	99.0%	1.0%
>0.5		-	-	-	-	-	-	-	-	-	0.13%	0.05%	0.06%	0.76%	-	-	-	1.0%	100.0%	0.0%
Sum		0.3%	0.1%	0.1%	0.1%	0.0%	0.0%	0.1%	0.1%	8.0%	17.2%	4.8%	11.4%	33.4%	11.8%	6.7%	5.8%	100.0%		

Table 7-10 Occurrence of Significant Wave Height (Sea) by Peak Wave Period at La Perouse Location A

Hs (m)		Peak Wave Period Bins (sec)							Total	P<Hs	P>Hs
		<1.5	1.5	2.0	2.5	3.0	3.5	>4			
From	To		2.0	2.5	3.0	3.5	4.0				
Calm (<0.05)		19.37%	3.44%	-	-	-	-	-	22.8%	22.8%	77.2%
0.05	0.1	21.29%	9.67%	0.45%	-	-	-	-	31.4%	54.2%	45.8%
0.1	0.2	12.60%	10.82%	3.03%	1.11%	-	-	-	27.6%	81.8%	18.2%
0.2	0.3	-	7.32%	2.69%	0.75%	0.18%	-	-	10.9%	92.7%	7.3%
0.3	0.4	-	0.21%	3.97%	0.19%	0.15%	-	-	4.5%	97.2%	2.8%
0.4	0.5	-	-	0.79%	0.88%	0.05%	0.02%	-	1.7%	99.0%	1.0%
>0.5		-	-	0.01%	0.75%	0.22%	0.02%	-	1.0%	100.0%	0.0%
Sum		53.3%	31.5%	11.0%	3.7%	0.6%	0.0%	0.0%	100.0%		

La Perouse Sea Wave Rose
Location A, 1998 to 2018

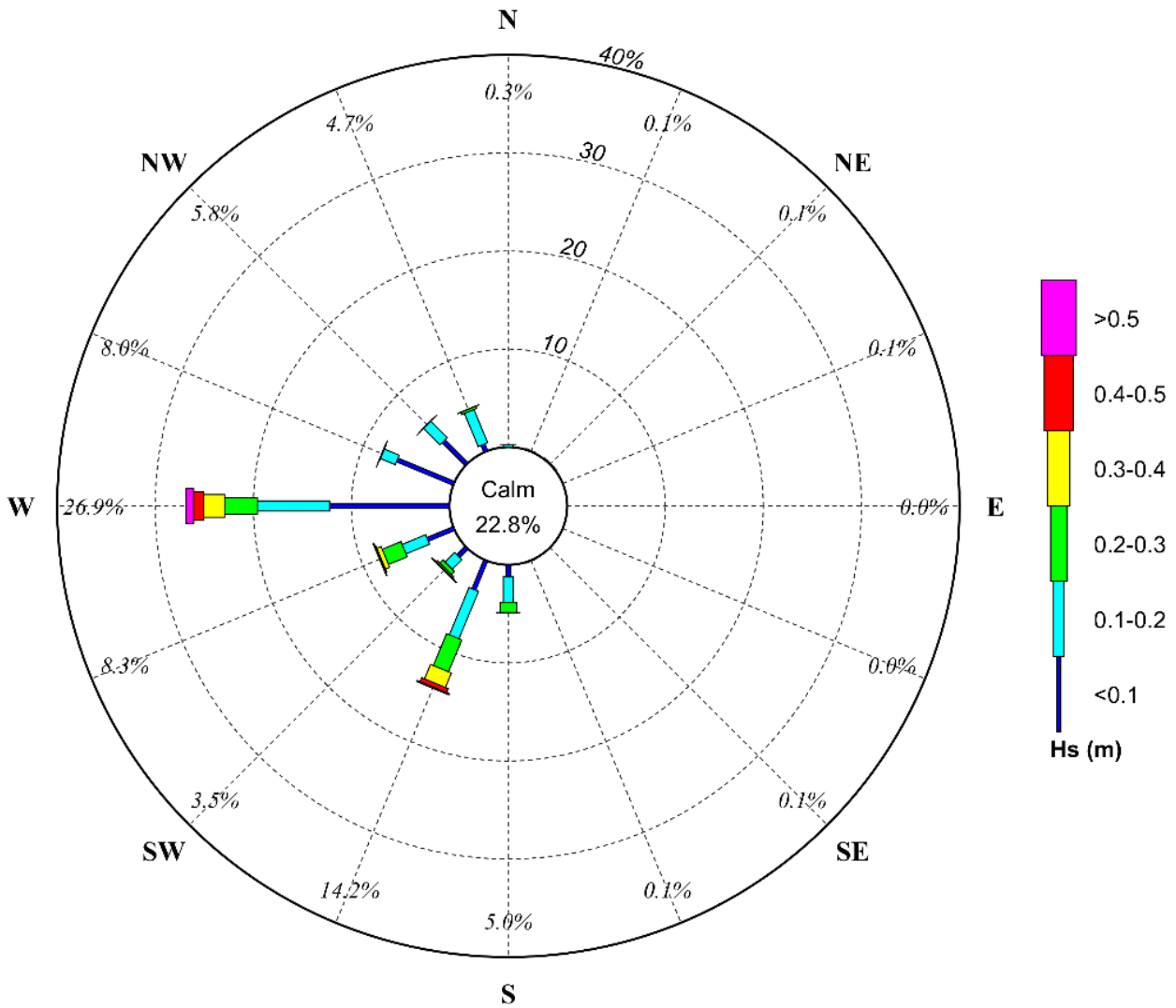


Figure 7-5 Sea Wave Rose (Significant Wave Height by Peak Wave Direction) at La Perouse Location A

7.2.3 Crossing Points

A wave rose of the hindcast swell wave conditions at Crossing Point 5 is presented in **Figure 7-6**. This figure shows that sea wave conditions at this point typically come from the south-east and also the west. Sea waves are generally less than 0.5m in height (Hs), with peak wave periods predominantly less than 3 seconds.

Tables 7-11 and **7-12** provide the joint occurrence of significant wave height and peak wave direction and peak wave period at Crossing Point 5, **Appendix F** provides the tables for all six output crossing points.

Table 7-11 Occurrence of Significant Wave Height (Sea) by Peak Wave Direction at Crossing Point 5

Hs (m)		Direction Bins															Total	P<Hs	P>Hs	
		N	NNE	NE	ENE	E	ESE	SE	SSE	S	SSW	SW	WSW	W	WNW	NW				NNW
<0.05		0.14%	0.12%	0.01%	0.01%	0.02%	0.15%	1.83%	0.73%	0.05%	0.03%	0.04%	0.61%	1.66%	3.36%	0.44%	0.18%	9.4%	9.4%	90.6%
0.05	0.1	0.43%	0.38%	0.02%	0.03%	0.05%	0.31%	4.96%	1.31%	0.07%	0.06%	0.06%	1.10%	3.78%	9.40%	1.44%	0.49%	23.9%	33.3%	66.7%
0.1	0.2	4.57%	2.13%	0.13%	0.12%	0.18%	0.37%	6.63%	3.20%	0.13%	0.09%	0.12%	1.36%	4.50%	3.89%	1.43%	2.81%	31.7%	65.0%	35.0%
0.2	0.3	1.79%	3.48%	0.00%	0.00%	0.00%	0.01%	4.00%	3.97%	0.10%	0.07%	0.08%	0.55%	3.91%	0.62%	0.01%	0.32%	18.9%	83.9%	16.1%
0.3	0.4	0.00%	0.07%	0.02%	0.00%	0.00%	0.00%	2.54%	2.77%	0.06%	0.03%	0.03%	0.08%	2.23%	0.12%	0.00%	0.00%	8.0%	91.8%	8.2%
0.4	0.5	-	0.00%	0.00%	-	-	-	1.74%	1.40%	0.02%	0.01%	0.02%	0.02%	1.13%	0.05%	-	-	4.4%	96.2%	3.8%
>0.5		-	0.00%	-	-	-	-	1.31%	1.46%	0.02%	0.01%	0.01%	0.01%	0.78%	0.18%	-	-	3.8%	100.0%	0.0%
Sum		6.9%	6.2%	0.2%	0.2%	0.3%	0.8%	23.0%	14.8%	0.5%	0.3%	0.4%	3.7%	18.0%	17.6%	3.3%	3.8%	100.0%		

Table 7-12 Occurrence of Significant Wave Height (Sea) by Peak Wave Period at Crossing Point 5

Hs (m)		Peak Wave Period Bins (sec)						Total	P<Hs	P>Hs	
		<1.5	1.5	2.0	2.5	3.0	3.5				>4
From	To		2.0	2.5	3.0	3.5	4.0				
Calm (<0.05)		5.67%	3.71%	-	-	-	-	-	9.4%	9.4%	90.6%
0.05	0.1	14.01%	9.87%	-	-	-	-	-	23.9%	33.3%	66.7%
0.1	0.2	14.53%	17.14%	0.02%	-	-	-	-	31.7%	65.0%	35.0%
0.2	0.3	3.84%	7.98%	7.10%	-	-	-	-	18.9%	83.9%	16.1%
0.3	0.4	-	0.48%	6.56%	0.92%	-	-	-	8.0%	91.8%	8.2%
0.4	0.5	-	-	1.34%	3.04%	-	-	-	4.4%	96.2%	3.8%
>0.5		-	-	0.08%	2.63%	0.98%	0.08%	-	3.8%	100.0%	0.0%
Sum		38.1%	39.2%	15.1%	6.6%	1.0%	0.1%	0.0%	100.0%		

Sea Wave Rose
Crossing 5, 1998 to 2018

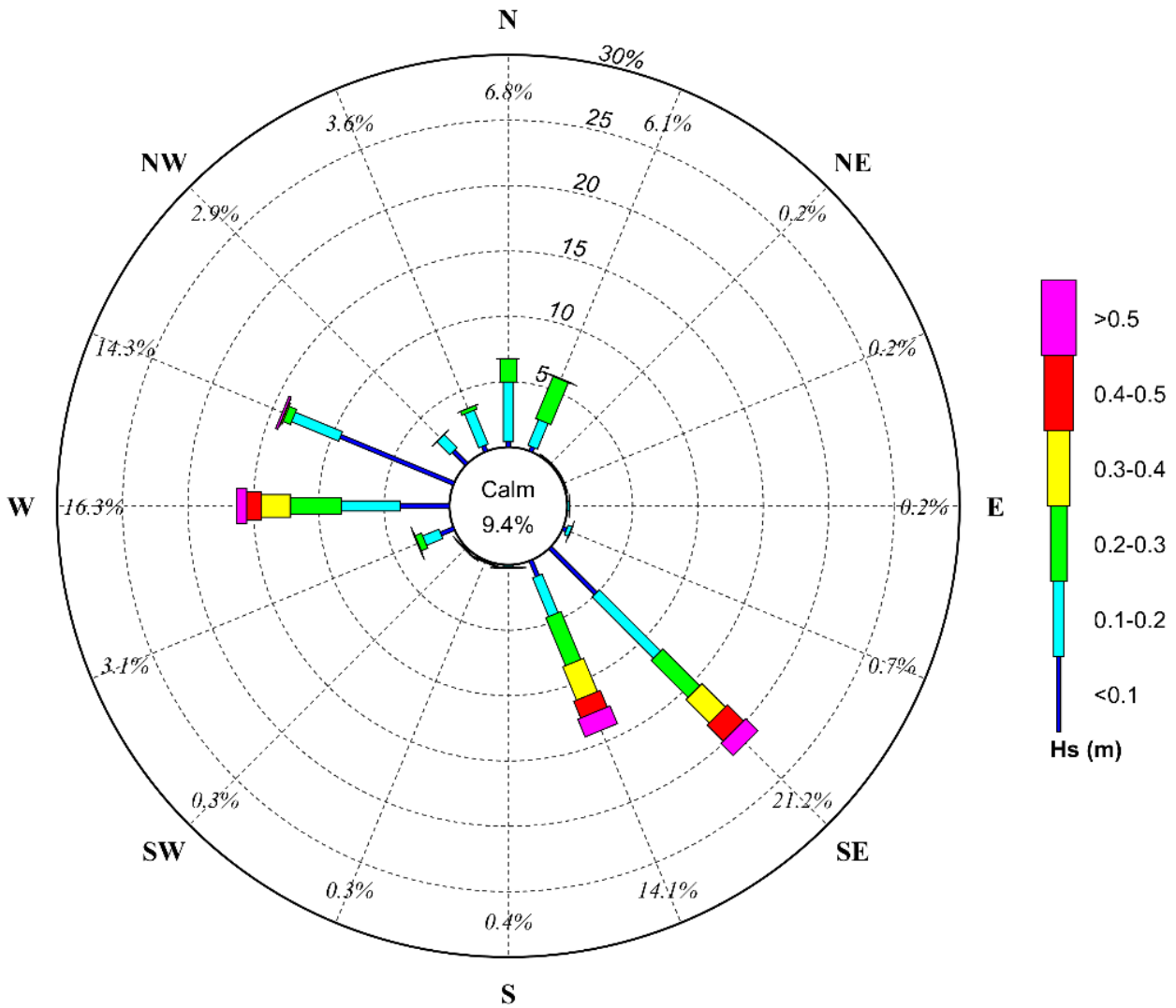


Figure 7-6 Sea Wave Rose (Significant Wave Height by Peak Wave Direction) at Crossing Point 5

8 Storm Hindcast Modelling

Part of this study involved developing design wave criteria within Botany Bay. This task required a long term dataset to derive reliable extreme value estimates. The stormiest period in recent history occurred during the 1970s, which is prior to the collection of any directional wave measurements in NSW. To estimate the wave conditions during this period, Cardno's WaveWatch III model has been applied to hindcast wave conditions for selected, known severe storms over this period.

8.1 WaveWatchIII Modelling

This section of the report describes the development of a global hindcast wind field data set, with particular focus on the NSW coast, offshore Botany Bay. Cardno (NSW/ACT) applied hindcast wind fields for the period 1970 to 1980 to assist with this wave hindcast study for Botany Bay; mainly to determine offshore wave directions for those storms for which offshore wave direction was not available from Long Reef or Botany Bay. The wind fields were applied to a WaveWatchIII (WWIII) spectral wave model for the assessment of peak storm wave parameters offshore of Botany Bay.

8.1.1 Project Scope

The tasks consisted of the following:-

- Compilation of available global hindcast wind fields for the period 1970 to 1980;
- Analysis and application of bias correction based on comparisons to the improved Climate Forecast System Reanalysis winds (available from 1979) over concurrent periods;
- Re-analysis and verification of the hindcast wind fields using measured wind data over the coastal zone (that is, close to land);
- Identification of storm events during the period 1970 to 1980;
- Development of adjusted wind fields for input to the WaveWatchIII model;
- Wave hindcast modelling of the 1970s storms in the global WaveWatchIII model; and
- Nearshore wave modelling to estimate peak storm wave parameters at the project sites;

8.1.2 Datasets

The following datasets were applied in this study.

1. NCEP/NCAR Reanalysis 1

The NCEP/NCAR Reanalysis 1 (NCEP Reanalysis) data set is a freely available global hindcast database of gridded atmospheric parameters developed by the National Centre for Environmental Prediction (NCEP), USA. Reanalysis data was obtained from the NOAA/OAR/ESRL PSD, Boulder, Colorado, USA, via their web site (<http://www.esrl.noaa.gov/psd/>). Surface winds (at 10m elevation) are available on a global grid of 2.5 degree x 2.5 degree resolution (144 x 73). Values of wind speed are provided as instantaneous records 4 times daily (at 0Z, 6Z, 12Z, 18Z) over the period 1948 to 2012.

2. NCEP Climate Forecast System Reanalysis

The Climate Forecast System Reanalysis (CFSR) comprises a high resolution, global coupled model that describes the interactions between the Earth's atmosphere, oceans and land. Developed by NCEP, gridded output from the model is made available at hourly time-steps and 0.5° horizontal resolution (see <http://cfs.ncep.noaa.gov/cfsr/>). Surface winds (at 10m elevation) are provided as instantaneous records every hour over the period 1979 to 2010. NCEP state that the CFSR data is a superior product to other available re-analysis products.

3. Sydney Airport Measured Winds

Measured wind data was purchased from the Bureau of Meteorology (BoM) from the Airport Meteorological Office (AMO) at Sydney Airport. The station provides half-hourly wind measurements from October 1948 to the present. An analysis of this wind data by Moneypenny and Middleton, 1997 (via Lawson & Treloar, 2003) showed that the initial anemometer, which operated until 1994, imparted a gradual error (reduction) in wind speed readings that amounted to 2.6m/s by August 1994. To correct this, a linear adjustment has been made for this study, in keeping with the recommendations.

No other adjustments were made to the data, with the available information suggesting that measurements recorded during the 1970s were taken from a 10m mast with sufficient exposure to the open coast (that is, under high wind speed conditions adjustments for atmospheric boundary layer and air-sea temperature differences can be neglected).

8.1.3 1970s Storm Events

Storm identification was completed by selecting peak wave height records over the period of available measured wave data from the Botany Bay offshore WRB. Upon inspection of the storm list it was noted that the severe storms of May/June 1974 were not included. This was a result of there being no recorded wave data during these storms – the offshore Waverider buoy was being serviced. A second attempt at storm identification was carried out based on wind speed to infill the selection of large storms during the period 1970 to 1980.

A predominant feature of severe storm events offshore of Botany Bay is the significant southerly component of the wind speed leading up to or during the peak wave conditions. To this end, the V-wind component of the NCEP reanalysis data was investigated at the nearest overwater grid location to Botany Bay. Wind events that resulted in gale force winds (>17.5m/s) with a southerly component of greater than 15m/s were identified and extracted. This resulted in nine storms being added to the storm listing and included the severe storms of May/June 1974. A storm listing is provided in **Table 8-1**.

Table 8-1 WaveWatchIII Storm Events – 1970 - 1980

Storm ID	Time of Storm Peak	Start Date	End Date
Storm_06May70	06 May 1970 18:00	26 Apr 1970 00:00	10 May 1970 00:00
Storm_25Jul71	25 Jul 1971 14:37	15 Jul 1971 00:00	29 Jul 1971 00:00
Storm_14Dec71	14 Dec 1971 18:00	04 Dec 1971 00:00	18 Dec 1971 00:00
Storm_09Mar72	09 Mar 1972 00:00	28 Feb 1972 00:00	13 Mar 1972 00:00
Storm_26Mar72	26 Mar 1972 02:58	16 Mar 1972 00:00	30 Mar 1972 00:00
Storm_23Jun72	23 Jun 1972 06:00	13 Jun 1972 00:00	27 Jun 1972 00:00
Storm_16Jun73	16 Jun 1973 09:03	06 Jun 1973 00:00	20 Jun 1973 00:00
Storm_20Feb74	20 Feb 1974 06:46	10 Feb 1974 00:00	24 Feb 1974 00:00
Storm_01May74	01 May 1974 00:00	21 Apr 1974 00:00	05 May 1974 00:00
Storm_26May74	26 May 1974 12:00	16 May 1974 00:00	30 May 1974 00:00
Storm_09Jun74	09 Jun 1974 00:00	30 May 1974 00:00	13 Jun 1974 00:00
Storm_06Aug74	06 Aug 1974 20:55	27 Jul 1974 00:00	10 Aug 1974 00:00
Storm_26Sep74	26 Sep 1974 18:14	16 Sep 1974 00:00	30 Sep 1974 00:00
Storm_12Jun75	12 Jun 1975 14:40	02 Jun 1975 00:00	16 Jun 1975 00:00
Storm_21Jun75	21 Jun 1975 07:59	11 Jun 1975 00:00	25 Jun 1975 00:00
Storm_04Mar76	04 Mar 1976 12:00	23 Feb 1976 00:00	08 Mar 1976 00:00
Storm_17Jun76	17 Jun 1976 16:43	07 Jun 1976 00:00	21 Jun 1976 00:00
Storm_09Apr77	09 Apr 1977 20:58	30 Mar 1977 00:00	13 Apr 1977 00:00
Storm_10Jun77	10 Jun 1977 14:11	31 May 1977 00:00	14 Jun 1977 00:00
Storm_19Jun77	19 Jun 1977 00:00	09 Jun 1977 00:00	23 Jun 1977 00:00
Storm_29Jan78	29 Jan 1978 02:43	19 Jan 1978 00:00	02 Feb 1978 00:00
Storm_19Mar78	19 Mar 1978 08:54	09 Mar 1978 00:00	23 Mar 1978 00:00
Storm_01Jun78	01 Jun 1978 23:58	22 May 1978 00:00	05 Jun 1978 00:00
Storm_15Jun78	15 Jun 1978 08:52	05 Jun 1978 00:00	19 Jun 1978 00:00

8.2 Site Specific Wind Data Reanalysis

The general aim of this reanalysis study was to produce a continuous gridded wind field dataset covering the period 1970 to 1980 that is broadly consistent with the improved CFSR hindcast winds and available measured data (in terms of peak wind speed events), within the offshore region of Botany Bay. This outcome was achieved using the methods described below. This wind data was then applied to the WaveWatchIII model.

8.2.1 Hindcast Wind Comparisons

For the period 1970 to 1980, it is the NCEP reanalysis dataset that provides the only continuous coverage, albeit with less temporal and spatial resolution than more recent reanalysis products. However, the more recently developed CFSR reanalysis is considered to be the better hindcast dataset, based on advice from NCEP. Furthermore, it is the CFSR dataset that has been used for hindcast studies completed by Cardno,

along the NSW coast that covers the period 1979 to 2009. In order to provide consistency with this previous hindcast work, and to distil any improvements from the more recent reanalysis package, a direct comparison of the hindcast datasets over a 10-years period (1979 to 1989) was undertaken to identify any bias between the two wind data sets.

The following procedure was followed:-

1. Spatial and temporal interpolation of the CFSR winds over the NCEP reanalysis data period (that is, 2.5 degree spatial resolution at 6 hourly time-steps).
2. For each grid point within the Tasman Sea region, scatter plots of U-wind and V-wind components comparing NCEP reanalysis against CFSR reanalysis winds were generated.
3. A linear fit was derived for records above gale force magnitude (17.5m/s from either dataset). The slope of this fit provided a measure of the bias between the datasets during storm events (being a focus of the hindcast study).
4. Any calculated bias was then corrected by applying an adjustment to the NCEP reanalysis data.

8.2.2 Verification to Measured Data

Typically, comparisons between hindcast winds and measured data show that hindcast winds under-predict wind speeds over land and along the coastal fringe. Comparisons between the scaled NCEP winds (as described above) were therefore compared to available measured winds at Sydney Airport. As discussed above, the Sydney Airport site is considered an adequately exposed location and provides an appropriate dataset to compare with the hindcast winds.

The following procedure was followed for each identified storm event:-

1. Temporal interpolation of the BoM winds over the NCEP reanalysis time-steps (that is, at 6 hourly intervals).
2. Spatial interpolation of the scaled NCEP reanalysis winds to the Sydney Airport measurement location.
3. A coastal wind scaling factor was calculated so that the peak wind speed during each event matched the peak measured wind speed (typically in the order of a 5 to 25% increase) – that is, a storm-by-storm basis. The scaling of magnitude was independent of direction and hence the direction of the hindcast winds was preserved.
4. The hindcast winds were then scaled over the coastal region within an approximate 4 degrees region about Botany Bay.

8.2.3 Scaling of NCEP/NCAR Reanalysis 1 Winds

In general the adjustments made to the NCEP reanalysis winds resulted in more southerly wind conditions in the region to the south-east of Botany Bay and an increase of wind speeds over the NSW coastal fringe. Scaling of the NCEP winds was only applied over the Tasman Sea area.

8.3 Storm Wave Hindcast Modelling

The wind fields described in **Section 8.2** were then applied to Cardno's global WaveWatchIII (WW3) spectral wave model to derive time series of wave data offshore of Botany Bay. Each storm was then modelled through the nearshore wave model described in **Section 5** to estimate storm wave conditions at the project sites. A summary of the hindcast wave modelling results is presented in **Table 8-2**.

The locations selected to characterise Kurnell and La Perouse were selected to be:

Kurnell A– which is in a depth of 4.5m at datum AHD

La Perouse A – which is in a depth of 5.3m at datum AHD

Table 8-2 Summary of the Peak Wave Conditions from the Hindcast Wave Modelling

Storm ID	Offshore			Kurnell			La Perouse		
	Hs (m)	Tp (s)	Dir	Hs (m)	Tp (s)	Dir	Hs (m)	Tp (s)	Dir
Storm_06May70	4.50	11.2	165.4	0.48	11.7	302.5	0.81	11.1	272.5
Storm_25Jul71	5.38	10.7	158.7	0.39	9.8	232.5	0.76	9.1	277.5
Storm_14Dec71	4.22	8.9	155.1	0.35	9.1	42.5	0.70	8.8	277.5
Storm_09Mar72	4.57	10.2	142.2	0.44	10.6	47.5	0.68	10.3	277.5
Storm_26Mar72	3.75	8.6	155.7	0.27	1.9	17.5	0.61	8.5	277.5
Storm_23Jun72	6.67	11.2	153.0	0.49	11.6	37.5	0.96	11.1	272.5
Storm_16Jun73	5.51	13.8	163.5	0.39	10.9	302.5	0.76	10.2	277.5
Storm_20Feb74	5.22	11.4	79.9	0.33	10.2	37.5	0.71	9.9	227.5
Storm_01May74	7.52	12.8	150.1	0.50	13.4	37.5	0.93	11.6	227.5
Storm_26May74	11.41	14.7	150.4	0.60	15.8	37.5	1.03	13.1	277.5
Storm_09Jun74	4.62	12.3	163.2	0.46	11.8	47.5	0.86	12.6	277.5
Storm_06Aug74	6.38	12.1	156.7	0.67	3.0	312.5	0.81	3.2	272.5
Storm_26Sep74	5.60	11.7	165.2	0.38	10.9	37.5	0.78	10.2	227.5
Storm_12Jun75	5.30	11.5	161.8	0.45	11.8	37.5	0.91	10.9	272.5
Storm_21Jun75	7.42	12.7	128.6	0.74	13.7	47.5	0.86	10.8	227.5
Storm_04Mar76	6.17	11.2	144.6	0.43	12.3	42.5	0.72	11.8	277.5
Storm_17Jun76	5.27	11.5	150.9	0.42	11.9	42.5	0.81	11.4	277.5
Storm_09Apr77	5.07	11.4	163.0	0.41	2.5	302.5	0.66	10.0	277.5
Storm_10Jun77	5.03	11.3	157.9	0.54	2.9	307.5	0.66	9.0	277.5
Storm_19Jun77	5.07	10.1	160.2	0.38	10.9	37.5	0.78	10.2	277.5
Storm_29Jan78	5.20	11.4	156.8	0.51	11.0	42.5	0.94	12.8	277.5
Storm_19Mar78	6.50	12.2	125.1	0.57	10.5	47.5	0.62	10.2	277.5
Storm_01Jun78	7.37	12.7	144.6	0.66	13.3	47.5	0.88	13.4	277.5
Storm_15Jun78	6.57	11.4	155.6	0.41	11.7	37.5	0.78	11.1	277.5

9 Design Wave Criteria

9.1 Extreme Wave Parameters

Design wave parameters were estimated at the Kurnell and La Perouse jetty locations by determining peak wave heights (H_{m0}) for each hindcast event. These peak wave heights were then censored using a peak over threshold extremal analysis. This process is adopted to ensure that the adopted sample population of wave heights includes only events that are from an extremal population. For this analysis, an initial threshold equal to 50% of the largest significant wave height in the hindcast records at Kurnell and La Perouse was used. A second filter was then applied to select only the top 52 events (3 larger than the number of years covered by the dataset), if the peak over threshold filter resulted in a large number of events. This led to 52 extremal events at Kurnell and La Perouse over the 49 years of wave data. Additionally, correlation analyses were undertaken in order to describe parameters such as the peak wave period that would occur jointly with peak event wave heights at each nominated ARI.

9.1.1 Kurnell

The extreme wave conditions calculated for the Kurnell output sites are presented below in **Table 9-1**. This table indicates that the 100-years ARI significant wave height ranges between 0.7m (at Kurnell A2) and approximately 2m at the most exposed locations being Kurnell A1 and Kurnell C. Associated peak wave periods are presented in **Table 9-2**, and indicate that the 100s-year ARI significant wave heights have an associated peak wave period of approximately 16 seconds at all of the locations.

Table 9-1 Design Significant Wave Height Criteria at Kurnell, in m

H_s	Arup Data Output Points at Kurnell – H_s (m)						
	(Including 95% Confidence Limits)						
ARI (yr)	Kurnell A	Kurnell A1	Kurnell A2	Kurnell B	Kurnell B1	Kurnell B2	Kurnell C
1	0.61 +/- 0.01	1.05 +/- 0.03	0.60 +/- 0.01	0.62 +/- 0.01	0.64 +/- 0.01	0.59 +/- 0.01	1.03 +/- 0.02
2	0.65 +/- 0.02	1.24 +/- 0.06	0.62 +/- 0.02	0.69 +/- 0.04	0.70 +/- 0.03	0.65 +/- 0.02	1.22 +/- 0.06
5	0.70 +/- 0.03	1.44 +/- 0.09	0.64 +/- 0.03	0.79 +/- 0.06	0.80 +/- 0.05	0.73 +/- 0.05	1.41 +/- 0.09
10	0.75 +/- 0.04	1.57 +/- 0.11	0.66 +/- 0.04	0.87 +/- 0.07	0.88 +/- 0.07	0.78 +/- 0.06	1.54 +/- 0.12
20	0.77 +/- 0.06	1.69 +/- 0.14	0.66 +/- 0.06	0.95 +/- 0.1	0.96 +/- 0.09	0.84 +/- 0.08	1.66 +/- 0.14
25	0.79 +/- 0.07	1.73 +/- 0.15	0.67 +/- 0.06	0.98 +/- 0.11	0.98 +/- 0.10	0.86 +/- 0.09	1.7 +/- 0.15
50	0.81 +/- 0.07	1.85 +/- 0.19	0.68 +/- 0.07	1.05 +/- 0.13	1.06 +/- 0.13	0.93 +/- 0.11	1.82 +/- 0.19
75	0.82 +/- 0.09	1.92 +/- 0.22	0.69 +/- 0.07	1.09 +/- 0.14	1.10 +/- 0.14	0.97 +/- 0.13	1.89 +/- 0.21
100	0.83 +/- 0.09	1.97 +/- 0.24	0.70 +/- 0.08	1.12 +/- 0.15	1.13 +/- 0.15	0.99 +/- 0.13	1.93 +/- 0.22
200	0.86 +/- 0.11	2.08 +/- 0.28	0.71 +/- 0.09	1.19 +/- 0.18	1.20 +/- 0.17	1.06 +/- 0.16	2.04 +/- 0.26
500	0.90 +/- 0.12	2.22 +/- 0.33	0.76 +/- 0.11	1.28 +/- 0.21	1.29 +/- 0.21	1.14 +/- 0.18	2.18 +/- 0.31
1000	0.95 +/- 0.13	2.33 +/- 0.38	0.80 +/- 0.13	1.35 +/- 0.24	1.35 +/- 0.23	1.20 +/- 0.20	2.29 +/- 0.35

Table 9-2 Associated Peak Wave Periods at Kurnell

Tp (sec)	Arup Data Output Points at Kurnell – Tp (sec)						
	ARI (yr)	KurnA	KurnA1	KurnA2	KurnB	KurnB1	KurnB2
1	14.1	14.4	14.1	14.1	14.3	14.3	14.0
2	14.6	14.8	14.6	14.4	14.8	14.8	14.4
5	15.0	15.1	15.0	14.8	15.2	15.3	14.7
10	15.3	15.3	15.3	15.0	15.6	15.6	14.9
20	15.6	15.4	15.6	15.2	15.8	15.9	15.0
25	15.7	15.5	15.7	15.3	15.9	16.0	15.1
50	15.9	15.6	15.9	15.5	16.2	16.2	15.2
75	16.0	15.7	16.0	15.6	16.3	16.3	15.3
100	16.1	15.7	16.1	15.7	16.4	16.4	15.3
200	16.3	15.8	16.3	15.8	16.6	16.6	15.4
500	16.6	16.0	16.6	16.0	16.9	16.9	15.6
1000	16.7	16.1	16.8	16.2	17.0	17.0	15.7

$$* T_{H_s} = 0.93 \times T_p$$

Because both sites were damaged during the May 1974 ECL event, it is instructive to compare modelled peak storm H_{m0} at Kurnell with this ARI table; noting water level contributes also to overall ARI definition. The modelled peak event parameters at Kurnell were:

$H_{m0} = 0.6\text{m}$ – approximate 1-years ARI, based on **Table 9.1** and Location Kurnell A

$T_p = 16\text{ s}$

Water level = 1.43 m AHD – 100-years ARI (**Table A.2**)

Wave crest level for $H_{max} = +2.18\text{m AHD}$

Note that there is significant spatial variation in wave height at this site and caution is advised when selecting design criteria.

To assess the extreme sea waves at Kurnell, the extreme wind speeds outlined in **Table 4-1** were applied to the SWAN model and the results were extracted at the nominated output locations. The modelled significant wave heights at the output locations are provided below in **Table 9-3** and the peak wave periods are provided in **Table 9-4**. Contour plots of significant wave height from these simulations are provided in **Appendix G**. Note that in the shallower locations, the design sea waves are larger than those reported above in **Table 9-1**; however, with a much lower wave period.

Even though they are larger, the longer period waves will govern wave forces on vertical structures, piles and uplift on a jetty. For rock armoured structures, the longer period waves also govern, with a median rock size of approximately 220 kg required for the sea waves at Kurnell A, whereas the smaller swell waves would require a median rock armour mass of approximately 290 kg for the 1,000-years ARI event (based on Van-Der-Meer's formula, $S=2$, armour density = 2650 kg/m³ and a batter slope of 1 vertical to 1.5 horizontal).

Peak wave crest levels for sea waves are also smaller for sea waves, for example at the 1,000-years ARI, the wave crest level of the H_{max} is 1.52m above the still water level, whereas the sea wave H_{max} crest level is 1.17m above the still water level, according to Fenton's non-linear wave theory.

Table 9-3 Design Sea Wave Heights at Kurnell

H_s	Arup Data Output Points at Kurnell – H_s (m)						
	ARI (years)	Kurnell A	Kurnell A1	Kurnell A2	Kurnell B	Kurnell B1	Kurnell B2
1	0.61	0.62	0.55	0.62	0.64	0.59	0.65
2	0.68	0.69	0.61	0.69	0.70	0.65	0.72
5	0.76	0.77	0.68	0.76	0.78	0.73	0.79
10	0.82	0.82	0.73	0.81	0.83	0.78	0.85
20	0.88	0.88	0.78	0.87	0.89	0.83	0.91
25	0.90	0.90	0.80	0.88	0.90	0.85	0.93
50	0.96	0.95	0.85	0.94	0.96	0.90	0.98
75	1.00	0.98	0.87	0.96	0.99	0.93	1.01
100	1.03	1.01	0.89	0.99	1.01	0.95	1.04
200	1.09	1.06	0.94	1.04	1.06	1.00	1.09
500	1.17	1.13	1.00	1.10	1.13	1.07	1.16
1000	1.23	1.18	1.04	1.15	1.18	1.12	1.21

Table 9-4 Design Sea Wave Periods at Kurnell

Tp (sec)	Arup Data Output Points at Kurnell – Tp (sec)							
	ARI (years)	Kurnell A	Kurnell A1	Kurnell A2	Kurnell B	Kurnell B1	Kurnell B2	Kurnell C
1		2.8	2.8	2.8	2.8	2.9	2.8	2.9
2		2.9	2.9	3.0	3.0	3.0	2.9	3.0
5		3.1	3.1	3.1	3.1	3.1	3.1	3.1
10		3.2	3.1	3.2	3.1	3.2	3.2	3.2
20		3.2	3.2	3.3	3.2	3.2	3.3	3.3
25		3.3	3.2	3.3	3.2	3.2	3.3	3.3
50		3.4	3.3	3.4	3.3	3.3	3.4	3.4
75		3.4	3.3	3.5	3.3	3.4	3.4	3.4
100		3.4	3.4	3.5	3.4	3.4	3.4	3.4
200		3.5	3.4	3.6	3.4	3.4	3.5	3.5
500		3.6	3.5	3.7	3.5	3.5	3.6	3.6
1000		3.7	3.6	3.7	3.6	3.6	3.7	3.6

9.1.2 La Perouse

The extreme wave conditions calculated for the La Perouse output sites are presented below in **Table 9-5**. This table indicates that the 100-years ARI peak event significant wave height is approximately 1m at all of the output locations. Associated peak wave periods are presented in **Table 9-6**, and indicate that the 100-years ARI significant wave heights have an associated peak wave period of approximately 15 seconds at all of the locations.

Table 9-5 Design Significant Wave Height Criteria at La Perouse, in m

H_s	Arup Data Output Points at La Perouse– H_{m0} (m)			
	(Including 95% Confidence Limits)			
ARI (years)	La Perouse A	La Perouse A1	La Perouse B	La Perouse B1
1	0.62 +/- 0.02	0.70 +/- 0.01	0.59 +/- 0.02	0.50 +/- 0.02
2	0.72 +/- 0.03	0.78 +/- 0.03	0.68 +/- 0.03	0.65 +/- 0.03
5	0.81 +/- 0.04	0.86 +/- 0.04	0.77 +/- 0.04	0.75 +/- 0.04
10	0.88 +/- 0.05	0.91 +/- 0.04	0.83 +/- 0.05	0.81 +/- 0.05
20	0.93 +/- 0.06	0.96 +/- 0.05	0.89 +/- 0.06	0.85 +/- 0.04
25	0.95 +/- 0.06	0.97 +/- 0.05	0.91 +/- 0.06	0.87 +/- 0.05
50	1.00 +/- 0.07	1.01 +/- 0.05	0.96 +/- 0.07	0.91 +/- 0.06
75	1.03 +/- 0.08	1.04 +/- 0.06	0.98 +/- 0.07	0.93 +/- 0.06
100	1.05 +/- 0.09	1.06 +/- 0.07	1.00 +/- 0.07	0.95 +/- 0.07
200	1.10 +/- 0.10	1.10 +/- 0.08	1.05 +/- 0.09	0.98 +/- 0.08
500	1.16 +/- 0.12	1.15 +/- 0.09	1.11 +/- 0.10	1.02 +/- 0.09
1000	1.21 +/- 0.14	1.19 +/- 0.10	1.15 +/- 0.11	1.05 +/- 0.1

Table 9-6 Associated Peak Wave Period at La Perouse

Tp ARI (yr)	Arup Data Output Points at La Perouse – Tp (sec)			
	La Perouse A	La Perouse A1	La Perouse B	La Perouse B1
1	12.9	13.3	13.1	12.7
2	13.5	13.8	13.6	13.6
5	14.0	14.1	14.0	14.1
10	14.3	14.4	14.3	14.3
20	14.5	14.6	14.5	14.6
25	14.6	14.6	14.6	14.6
50	14.8	14.8	14.8	14.8
75	14.9	14.9	14.9	14.9
100	15.0	15.0	15.0	15.0
200	15.2	15.2	15.2	15.1
500	15.4	15.4	15.4	15.3
1000	15.6	15.5	15.5	15.4

$$* T_{H_s} = 0.93 \times T_p$$

Because both sites were damaged during the May 1974 ECL event, it is instructive to compare modelled peak storm H_{m0} at Kurnell with this ARI table; noting water level contributes also to overall ARI definition. The modelled peak event parameters at La Perouse were:

$H_{m0} = 0.81$ m – 10-years ARI, based on **Table 9.1** and Location La Perouse B1

$T_p = 16$ s

Water level = 1.43 m AHD – 100-years ARI (**Table A.2**)

Wave crest level for $H_{max} = 2.56$ m AHD

To assess the extreme sea waves at La Perouse, the extreme wind speeds outlined in **Table 4-1** were applied to the SWAN model and the results were extracted at the nominated output locations. The modelled significant wave heights at the output locations are provided below in **Table 9-7** and the peak wave periods are provided in **Table 9-8**. Contour plots of significant wave height from these simulations are provided in **Appendix G**.

Table 9-7 Design Sea Wave Heights at La Perouse

H_s	Arup Data Output Points at La Perouse– H_{m0} (m)			
	ARI (years)	La Perouse A	La Perouse A1	La Perouse B
1	0.55	0.52	0.53	0.52
2	0.60	0.58	0.59	0.57
5	0.67	0.63	0.64	0.63
10	0.72	0.68	0.69	0.67
20	0.76	0.72	0.73	0.71
25	0.79	0.75	0.76	0.74
50	0.84	0.79	0.81	0.78
75	0.88	0.82	0.84	0.81
100	0.89	0.83	0.85	0.82
200	0.92	0.86	0.88	0.86
500	0.98	0.92	0.94	0.92
1000	1.02	0.95	0.97	0.95

Table 9-8 Design Sea Wave Periods at La Perouse

Tp (sec)	Arup Data Output Points at La Perouse – Tp (sec)				
	ARI (years)	La Perouse A	La Perouse A1	La Perouse B	La Perouse B1
1		3.0	3.0	3.0	3.0
2		3.2	3.1	3.1	3.1
5		3.3	3.2	3.2	3.2
10		3.4	3.3	3.3	3.3
20		3.4	3.4	3.4	3.4
25		3.5	3.4	3.5	3.4
50		3.5	3.5	3.5	3.5
75		3.5	3.5	3.5	3.5
100		3.6	3.6	3.6	3.6
200		3.6	3.6	3.6	3.4
500		3.7	3.6	3.7	3.5
1000		3.8	3.7	3.8	3.5

9.2 Limitations of Extreme Value Analysis

It is important to note that spatial gradients in wave height at both of these locations are significant, for example, compare Kurnell A with Kurnell C. Although wave heights at both locations are relatively 'small' they may lead to design wave crest level differences of about 0.5m and associated differences in wave uplift pressures of 6 to 8 kPa. Hence a conservative design position should be adopted.

There is some subjectivity in selecting the sample peak event wave height populations, affected by the relatively short data duration (49 years) versus ARI analyses to 1,000-years. Adopting fewer data points would lead to greater uncertainty in the outcomes of the EVA. Provided that the sample populations are reliably from extremal populations, the narrow confidence limits are realistic. It is noted that uncertainty in design met-ocean parameters is addressed through load factors, see AS 4997. A common approach also is to design at 500-years ARI, for example, and check the design at 1,000-years ARI.

Note that the extremal distributions are quite flat and uncertainties will not be statistically high – affected as much by the spatial gradient issue.

Note that Cardno has not examined bias between the three types of data sets that were assembled for the operational and extremal analyses. However, in all cases, the best available wave parameter – height, period and direction, was adopted. Note also that although there would be parameter differences between measured and various hindcast-based parameters on a storm-by-storm basis, in a longer term statistical sense, there is consistency between Long Reef, Botany Bay and Port Kembla offshore data sets.

9.3 Design Wave Crest Levels

Wave crest heights have been estimated on a record by record basis by calculating the maximum wave height (adopting a relationship of $H_{max} = H_s \times 1.85$) and calculating the peak wave crest height above the still water level, based on the non-linear profile-fitting wave algorithm of Fenton (1990).

A time-series of peak crest levels has been derived by adding the peak crest height to the measured still water level from Fort Denison on a record-by-record basis at 30 minute intervals. A peak over threshold extreme value analysis has then been undertaken to estimate the extreme wave crest levels. Where data gaps were identified, data from another source was adopted – for example, wave height missing from the offshore Botany Bay WRB was replaced by the one from the Long Reef WRB site. Where overall data gaps were less than or equal to 6 hours, linear interpolation was adopted. Otherwise the gaps remained unfilled. Generally, there was no bias to these cases occurring during severe storms. In some other cases, notably historical storm events, hindcast data was available from previous investigations undertaken for Caltex in southern Botany Bay and was used to fill gaps, for example, the May 1974 storm. Note the offshore Botany Bay WRB was being serviced at the time of the May 1974 storm and hindcast data had been prepared using a calibrated whole of NSW wave model based on WaveWatch III and available meteorological data (NCEP), and considering the reliability of that data near the coastline.

Table 9-9 Present Day Design Wave Crest Levels

ARI (Years)	Peak Wave Crest Level (m AHD)	
	Kurnell A	La Perouse A
1	1.42	1.82
2	1.51	1.98
5	1.73	2.14
10	1.88	2.25
20	2.02	2.36
25	2.06	2.40
50	2.20	2.50
75	2.27	2.56
100	2.33	2.60
200	2.45	2.70
500	2.62	2.83
1,000	2.74	2.92

Based on the above assessment, the 1974 storm was the highest crest level event in the record at La Perouse. This event had an estimated peak wave crest level of 2.7m (AHD), which would be an approximate 200-years ARI event based on the EVA fit.

Similarly, at Kurnell the largest event was the June 2016 east coast low, which had an estimated crest level of 2.25m AHD. The 1974 storm was the second highest with an estimated crest level of just under 2.2m.

Note that ferry facilities at both sites were damaged by the May 1974 storm and these results are consistent with that damage outcome.

Note that there is some uncertainty in these wave crest analyses. Hence Cardno recommends that an air-gap of 0.3m be adopted in fixed structure design.

10 Hydrodynamic Modelling

10.1 Current Modelling System

Cardno have used the Delft3D model system to undertake the tidal current modelling required for this investigation. Delft3D is a hydrodynamic, sediment transport and water quality modelling system developed by Deltares (formerly Delft Hydraulics) in The Netherlands. Delft3D has been applied in major coastal and ocean investigations and engineering studies throughout Australia – including those for Port Botany, Port of Melbourne and at Port Hedland. In the last 10-years Delft3D has led modelling innovations such as coupled online wave and hydrodynamic forcing.

The Delft3D modelling system includes, among other features, wind, tide and wave forcing and is capable of using irregular, rectilinear or curvilinear coordinate systems that are used to describe the seabed bathymetry.

The site is suited to the curvilinear grid and domain decomposition systems, which have enabled a detailed description of the flow structure in the estuary.

Investigations generally begin with the Delft3D-FLOW (hydrodynamic) module. From Delft3D-FLOW details such as velocities and water levels can be provided as inputs to the other modules.

10.1.1 Hydrodynamic Numerical Scheme

The Delft3D FLOW module is based on the numerical finite-difference scheme developed by G. S. Stelling (1984) of the Delft University of Technology in The Netherlands.

The Delft3D Stelling Scheme arranges modelled variables on a staggered Arakawa C-grid. The water level points (pressure points) are designated in the centre of a continuity cell and the velocity components are perpendicular to the grid cell faces. Finite difference staggered grids have several advantages including:-

1. Boundary conditions can be implemented in the scheme as basic time-series.
2. It is possible to use a smaller number of discrete state variables in comparison with discretisations on non-staggered grids to obtain the same accuracy
3. Staggered grids minimise spatial oscillations in the water levels.

Delft3D can be operated in 2D (vertically averaged) or 3D mode.

Horizontal solution is undertaken using the Alternating Direction Implicit (ADI) method of Leendertse for shallow water equations.

10.1.2 Ability to Incorporate a Varying Mesh Size

As mentioned previously, bathymetric discretisation and modelling can be undertaken in Delft3D on a rectilinear or curvilinear grid, and includes domain decomposition. The Delft3D model is specifically written to undertake hydrodynamic flow and transport modelling arising from tidal and meteorological forcing on a curvilinear boundary fitted grid.

The curvilinear grid system enables grid sizes to vary so that better resolution can be used within the estuary and adjacent interconnecting bays and channels, with less resolution in the sea where less detail is required. Additionally, the curvilinear grid system can be better set-up to follow the flow streamlines and boundaries, thereby providing a better description of the current structure.

The domain decomposition module has been used also to prepare a fine grid area near the Kurnell and La Perouse sites in order to ensure that the hydrodynamic processes are resolved adequately.

10.1.3 Wetting and Drying of Intertidal Areas

Many estuaries and embayments contain shallow intertidal areas; consequently, Delft3D incorporates a wetting and drying algorithm for handling this phenomenon. Cardno have utilised Delft3D in many applications where inter-tidal flats exist. Through experience in these areas of application, Cardno use a method of careful refinement in the intertidal areas and appropriate setting of dry depths to minimise discontinuous movement of the boundaries. This process ensures oscillations in water levels and velocities are minimised and that the characteristics of the intertidal areas are modelled accurately.

10.2 Model Set-up

The downstream model boundary has been set in the open sea in a depth of about 70m and defined as a water level (predicted or measured tides) boundary. **Figure 10-1** describes the model grid and bathymetry applied to this study. The model was previously calibrated for Port Botany Expansion investigations (Lawson and Treloar, 2003), as well as Caltex Met-Ocean Investigations (Cardno, 2013).

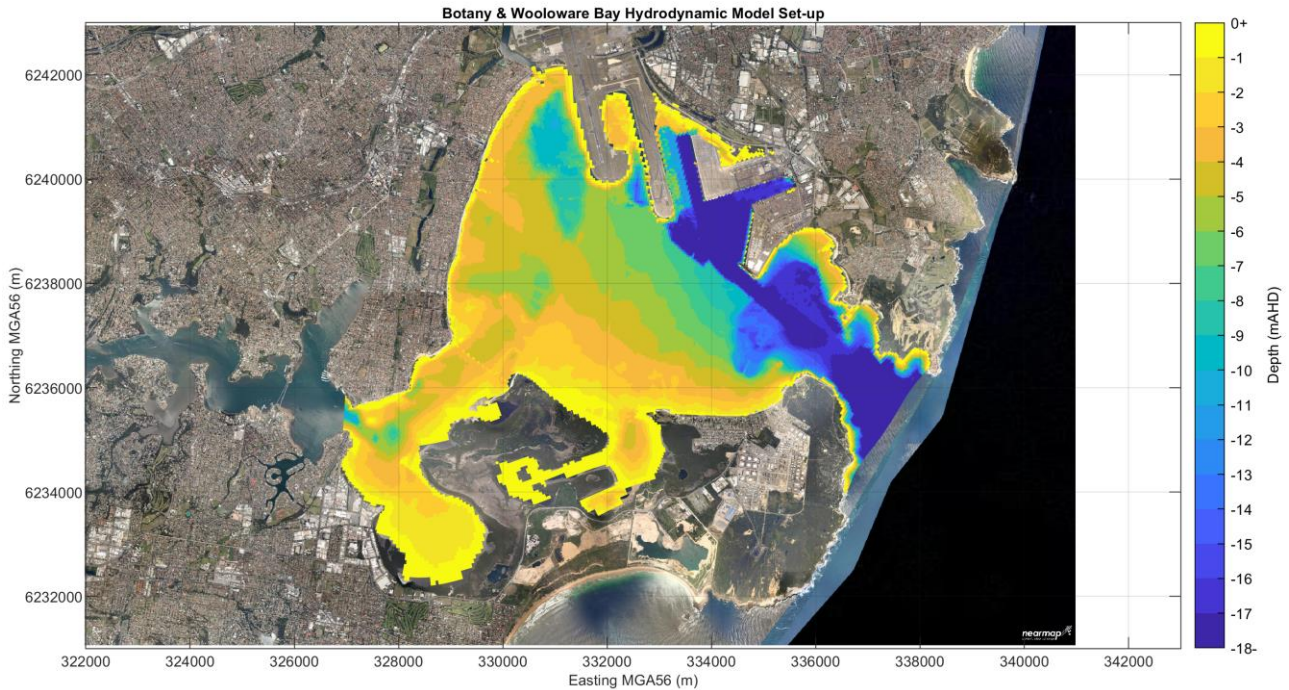


Figure 10-1 Botany and Woollooware Bays Hydrodynamic Model Set-up

10.3 Hydrodynamic Simulations

For this task, a 15 days tidal current simulation was undertaken, which covers a full spring/neap tidal cycle.

10.3.1 Results

Maps of the peak flooding and ebbing currents are presented in **Figures 10-2** and **10-3**. These plots show that currents tend to follow the direction of the shoreline at both sites, and the peak tidal currents during a spring tide are less than 0.3 m/s at the Kurnell wharf and 0.1 m/s at La Perouse.

Tidal current roses are presented in **Figure 10-4**. At Kurnell, currents typically flow towards the ENE during an ebbing tide and towards the WSW in a flooding tide. At this site, flooding currents are less than 0.2 m/s and ebbing currents less than 0.3 m/s.

At La Perouse, tidal currents tend to flow towards the SSW during an ebbing tide and towards the NNE during a flooding tide. At this site, currents are predicted to be small, rarely exceeding 5 cm/s, forming a large scale eddy

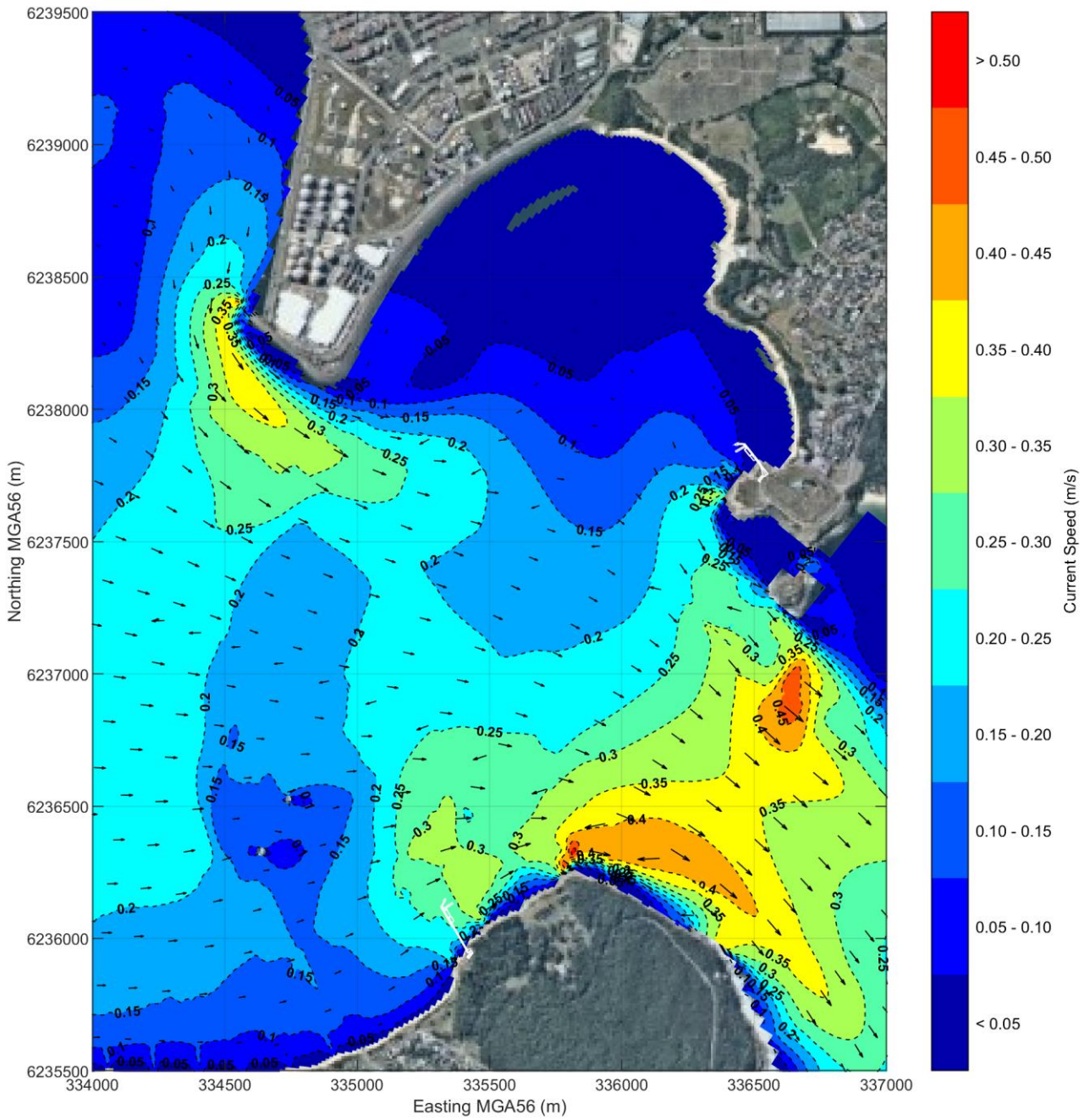


Figure 10-2 Map of Peak Ebbing Currents during the Simulation Period

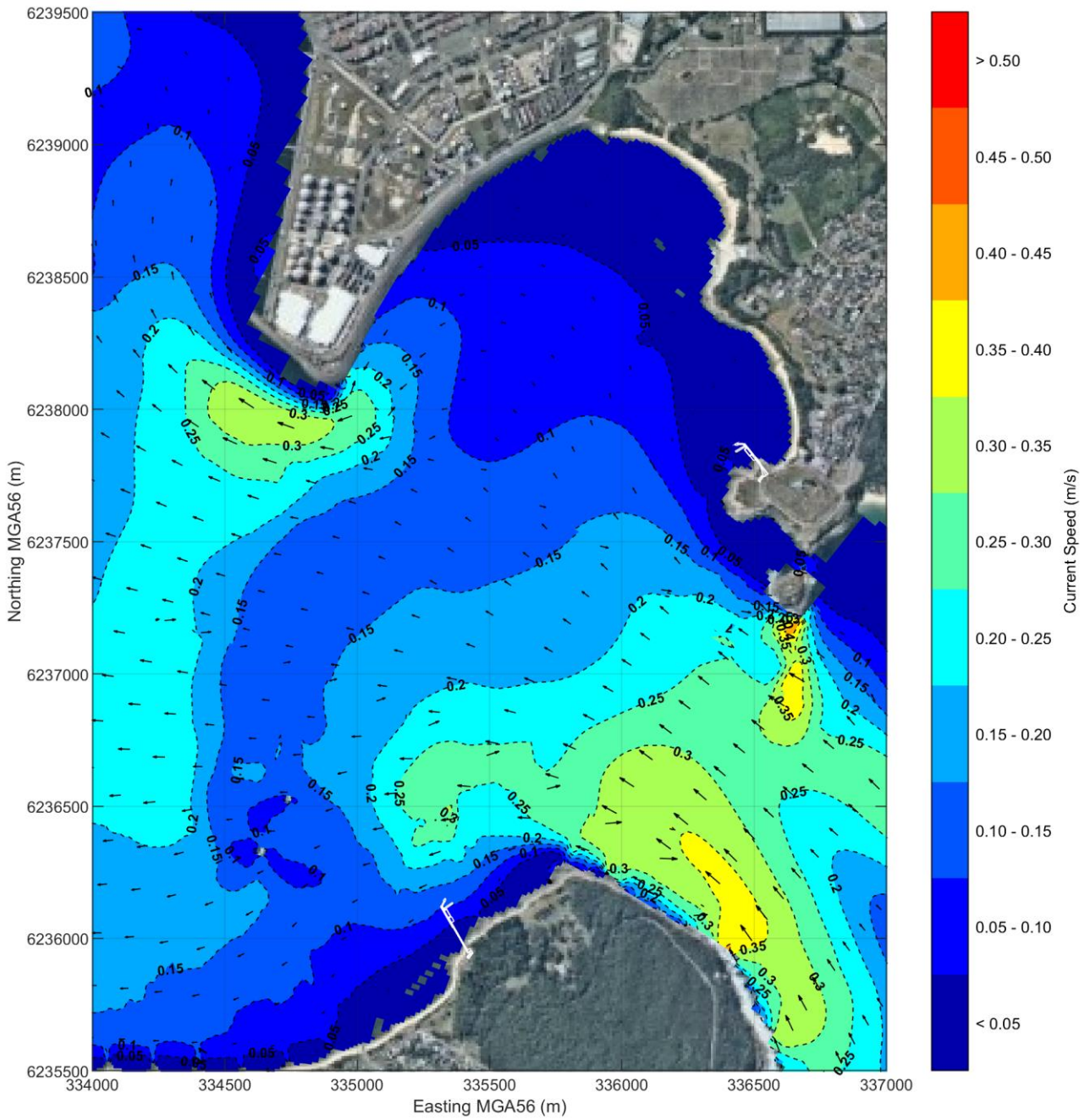


Figure 10-3 Map of Peak Flooding Currents during the Simulation Period

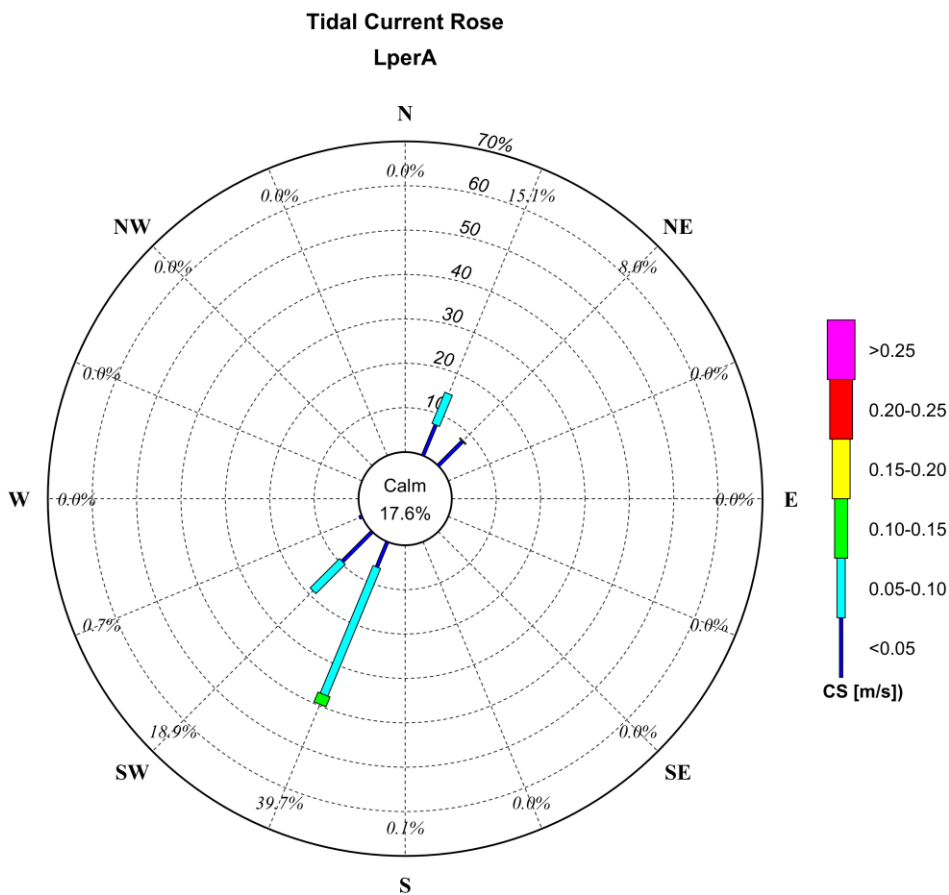
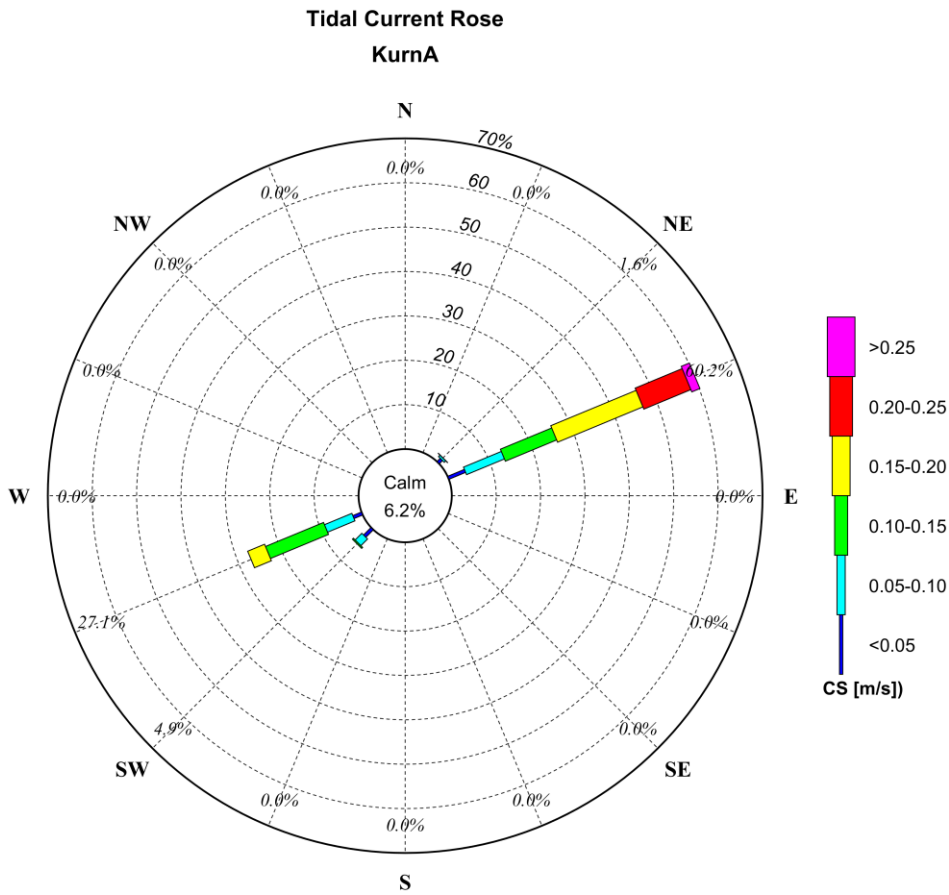


Figure 10-4 Tidal Current Roses at Kurnell (top) and La Perouse (bottom)

11 Concluding Remarks

As part of the business case development for the proposed Kamay to La Perouse Ferry Wharf development, Arup have commissioned Cardno to undertake a coastal processes assessment. The purpose of this assessment is to advise Arup of the met-ocean design and operational criteria of that project. As part of the study, Cardno has undertaken the following:-

- A data synthesis to inform the wave and hydrodynamic modelling (see **Section 4**);
- Analysed the local wave, water level and current processes data to provide a summary of the regional met-ocean operational and design parameters in the general Botany Bay entrance area (see **Section 5**);
- Numerical wave modelling in order to assess the local wave climate at the two sites, (see **Section 6**);
- Hindcast storm modelling and derivation of extreme wave conditions and associated storm tide levels for the preparation of design parameters at a range of ARI, (see **Sections 7 and 8**); and
- Numerical hydrodynamic modelling in order to assess local tidal generated current fields (see **Section 9**);

The proposed facilities will have no regional effects on coastal processes, being constructed as deck on pile structures, other than near any proposed shoreline abutments.

12 References

- Cardno (2013): MetOcean Study for the Caltex Wharf. Report (NA49913035 R001_v4). Prepared for Caltex Australia.
- DECCW (2009) NSW Sea Level Rise Policy Statement. Department of Environment, Climate Change and Water NSW.
- Fenton (1990). Non Linear Wave Theories. The Sea, Vol.9: Ocean Engineering Science, Eds. B. Le Méhauté and D.M. Hanes, Wiley, New York: 1990
- Holthuijsen, L., Booij, N. and Ris, R. (1993) A Spectral Wave Model for the Coastal Zone. Proceedings of 2nd International Symposium on Ocean Wave Measurement and Analysis, New Orleans, 630-641.
- Kulmar, M. (1995) Wave Direction Distributions off Sydney, New South Wales, 12th Australasian Coastal and Ocean Engineering Conference.
- Lawson & Treloar (2003) Proposed Expansion of Container Port Facilities in Botany Bay, NSW. Coastal Process and Water Resources Issues. Volume 3: Waves, Currents and Coastal process Investigations. Report J2076/R1999 Vol. 3.
- Manly Hydraulics Laboratory (1992): Mid New South Wales Coastal Region. Tide-Storm Surge Analysis. Report MHL 621.
- McInnes, K.L., Walsh, K.J., Whetton, P.H. and Pittock, A.B. (1998) The Impact of Climate Change on Coastal New South Wales – Final Report. CSIRO Atmospheric Research consultancy report for the National Greenhouse advisory committee, Aspendale, Victoria, viii+71pp.
- Monypenny, P. and Middleton, J. (1997) An Analysis of Winds at Sydney Kingsford Smith Airport. Australian Meteorological Magazine, Vol. 46, No. 4.
- MSB Sydney Ports Authority (1993) Sydney Airport - Parallel Runway, Coastal Processes Monitoring Stage 2A. Report KSA03.
- Phillips, N. A. (1957) A Co-ordinate System Having Some Special Advantages for Numerical Forecasting. Journal of Meteorology, 14, 184-185.
- Rijn, L.C. van, Walstra, D.J.R. and Van Ormondt, M. (2004) Description of TRANSPOR2004 and Implementation in Delft3D. WL | Delft Hydraulics, report Z3748.00.
- Roy, P. and Crawford (1979) Holocene Geological Evolution of Southern Botany Bay - Kurnell Region, Central NSW Coast. Records of the Geological Survey of NSW 20(2), pp159-250.
- Sand, S. (1982) Long Waves in Directional Seas. Journal of Coastal Engineering, Volume 6, Elsevier Scientific Publishing.
- Stelling, G.S. (1984) On the Construction of Computational Methods for Shallow Water Flow Problems. Tech. Rep. 35. Rijkswaterstaat.
- U.S. Army Corps of Engineers (2002) Coastal Engineering Manual. Engineer Manual 1110-2-1100, U.S. Army Corps of Engineers, Washington, D.C. (in 6 volumes).
- Willoughby, M.A. and Treloar, P.D. (1997) The Effects of Proposed Reclamation on Long and Short Wave Climates in Port Kembla Harbor, NSW. 13th Australasian Coastal and Ocean Engineering Conference
- Watson, P., and Lord, D. (2008) Fort Denison Sea Level Rise Vulnerability Study.

APPENDIX

A

PHYSICAL PROCESSES

General

The purpose of this section is to describe the physical processes that are important to the overall physiography of Botany Bay. These processes are:

- Waves
- Currents
- Water Levels
- Winds
- Sediment Transport – not discussed herein.

Wave Processes

Ocean waves that propagate to the study area may have energy in three distinct frequency bands. These are principally related to the generation and propagation of ocean swell (7 to 20 seconds) and local seas (less than 7 seconds), as well as infra-gravity waves. Large waves generated by a storm are generally categorised as wind waves because wind energy is still being transferred to the ocean. However, this distinction was not made in this study for offshore storm waves and they were considered as swell. Long waves (wave periods greater than 25 seconds) in Botany Bay generally occur during storms and are caused by wave grouping (Willoughby & Treloar, 1997). They are generally not important to this study because they do not affect coastal processes, but may affect moored ships.

Ocean waves are irregular in height and period and so it is necessary to describe wave conditions using a range of statistical parameters. In this study the following have been used:-

- H_{m0} significant wave height (H_s) based on M_0 where M_0 is the zeroth moment of the wave energy spectrum (rather than the time domain $H_{1/3}$ parameter).
- H_{max} maximum wave height in a specified time period – approximately $1.86 \times H_{m0}$
- T_p wave energy spectral peak period, that is, the wave period related to the highest ordinate in the wave energy spectrum – approximately $1.4 \times T_z$
- T_z average zero crossing period based on upward zero crossings of the still water line (seconds). An alternative definition is based on the zeroth and second spectral moments.
- $TH_{1/3}$ significant wave period – approximately $1.3 \times T_z$

Wave heights defined by zero up-crossings of the still water line fulfil the Rayleigh Distribution in deep water and thereby provide a basis for estimating other wave height parameters from $H_{1/3}$. In shallow water, that is, within Botany Bay, significant wave height defined from the wave spectrum, H_{m0} , is normally larger (typically 5% to 8%) than $H_{1/3}$ defined from a time series analysis. Otherwise height parameters H_1 and H_{10} , may be estimated from H_{m0} by the factors 1.67 and 1.27 respectively.

Ocean waves also have a dominant direction of wave propagation and directional spread about that direction that can be defined by a Gaussian or generalised cosine (\cos^n) distribution (amongst others), and a wave grouping tendency. Directional spreading causes the sea surface to have a more short-crested wave structure in deep water. Directional spread is reduced by refraction as waves propagate into the shallow, near shore regions and the wave crests become more parallel with each other and the seabed contours. Although neither of these characteristics is addressed explicitly in this study, directional spreading was included in the numerical wave modelling work.

Waves propagating into shallow water may undergo changes caused by refraction, shoaling, bed friction, wave breaking and, to some extent, diffraction. Wave reflection is important also in Yarra Bay.

Wave refraction is caused by differential wave propagation speeds. That part of the shoreward propagating wave which is in the more shallow water has a lower speed than those parts in deeper water. When waves approach a coastline obliquely these differences cause the wave fronts to turn and become more coast parallel. Associated with this directional change there are changes in wave heights. On irregular seabeds, wave refraction becomes a very complex process. Waves propagating over steep sided seabed slopes at a small angle to the seabed alignment, such as the Port Botany entrance channel, undergo a spatially rapid refraction process.

Waves propagating shoreward develop reduced speeds in shallow water. In order to maintain constancy of wave energy flux, (ignoring energy dissipation processes) their heights must increase. This phenomenon is termed shoaling and leads to a significant increase in wave height near the shoreline.

A turbulent boundary layer forms above the seabed with associated wave energy losses that are manifested as a continual reduction in wave height in the direction of wave propagation; leaving aside further wind input, refraction, shoaling and wave breaking. The rate of energy dissipation increases with greater wave height and reducing depth.

Wave breaking occurs in shallow water when the wave crest speed becomes greater than the wave phase speed. For irregular waves, this breaking occurs in different depths so that there is a breaker zone rather than a breaker line. Seabed slope, wave period and water depth are important parameters affecting the wave breaking phenomenon. As a consequence of this energy dissipation, wave set-up (a rise in still water level caused by wave breaking), develops shoreward from the breaker zone in order to maintain conservation of momentum flux. This rise in water level increases non-linearly in the shoreward direction and allows larger waves to propagate shoreward before breaking. Field measurements have shown that the slope of the water surface is normally concave upward. Wave set-up at the shoreline can be in the order of 15% of the equivalent deep-water significant wave height. Lower set-up occurs in estuarine entrances, but the momentum flux remains the same. Wave set-up is smaller where waves approach a beach obliquely, but then a longshore current can be developed. Wave grouping and the consequent surf beats also cause fluctuations in the still water level.

In a random wave field, each wave may be considered to have a period different from its predecessors and successors and the distribution of wave energy is often described by a wave energy spectrum. In fact, the whole wave train structure changes continuously and individual waves appear and disappear until quite shallow water is reached and dispersive processes are reduced. In developed sea states, that is swell, the Bretschneider modified Pierson-Moskowitz spectral form has generally been found to provide a realistic wave energy description. For developing sea states, the JONSWAP spectral form, which is generally more 'peaky', has been found to provide a better spectral description. Long waves have very irregular spectral forms.

For structural design in the marine environment it is necessary to define the H_{max} parameter related to storms having average recurrence intervals (ARI) of a pre-determined number of years. However, the expected H_{max} , relative to H_s in statistically stationary wave conditions, increases as storm/sea state duration increases. Based on the Rayleigh Distribution the usual relationship is:-

$$H_{max} = H_s * (0.5 * \ln Nz)^{0.5}$$

where Nz is the number of waves occurring during the time period being considered, where individual waves are defined by T_z

\ln is the natural logarithm.

This relationship has been found to overestimate H_{max} by about 10% in severe ocean storms. In shallow water the relationship is not fulfilled. In very shallow water H_{max} is replaced by the breaking wave height, H_b .

Waves propagating through an area affected by a current field are caused to turn in the direction of the current. The extent of this direction change depends on wave celerity, current speed and relative directions. Wave height is also changed. Opposing currents cause wave lengths to shorten and wave heights to increase and may lead to wave breaking. When the current speed is greater than one quarter of the phase speed, the waves are blocked. Conversely, a following current reduces wave heights and extends wave lengths.

Within the entrance channel to Botany Bay, flood and ebb tidal currents will move wave energy focal points.

Currents

Currents within Botany Bay are caused by a range of phenomena, including: -

- Astronomical Tides
- Winds
- River Discharges
- Coastal Trapped Waves and Other Tasman Sea Processes
- Near Shore Wave Processes
- Density Flows

The astronomical tides are caused by the relative motions of the Earth, Moon and Sun. The regular rise and fall of the tide level in the sea causes a periodic inflow (flood tide) and outflow (ebb tide) of oceanic water to the Bay and mixed oceanic and bay/river water from the Bay to the sea. A consequence of this process is the

generation of tidal currents. The volume of sea water that enters the Bay or leaves the Bay on flood and ebb tides, respectively, is termed the tidal prism; which varies due to the inequality between tidal ranges. The tidal prism is affected by changes in inter-tidal areas, such as reclamations, but not by dredged areas below low tide, such as navigation channels and trenches.

Wind forcing is applied to the water surface as interfacial shear, the drag coefficient and consequent drag force varying with wind speed. Momentum from the wind is gradually transferred down through the water column by vorticity, the maximum depth of this effect being termed the Ekman depth. At the surface, wind caused currents are in the direction of the wind, but in the southern hemisphere they gradually turn to the left of the wind direction until they flow in the opposite direction at the Ekman depth. Botany Bay is too shallow for this condition to develop fully and wind driven currents are affected by the seabed boundary layer and contours. Wind driven currents diminish with depth. Because wind forcing is applied at the water surface, the relative effect is greater in shallow water where there is less water column volume per unit plan area. Therefore, wind driven currents are greater in more shallow areas. Maximum surface current speed is in the order of 1% to 3% of the wind speed, depending on water depth. Where water is piled up against a coastline by wind forcing, a reverse flow develops near the seabed.

Density currents may be caused by freshwater inflows, for example, when the Georges River is in flood. The freshwater is more buoyant and tends to spread across the Bay surface until mixing with the ambient seawater occurs.

Coastal Trapped Waves (CTW) are long period wave phenomena that propagate northward along the continental shelf (Freeland *et al.*, 1986). These waves are irregular and cause approximate coast parallel currents and variations in water levels. They are trapped on the continental shelf by refraction and the Coriolis force – hence their wave heights are largest at the coastline. CTW are known to occur on the continental shelf of NSW and will affect observed water levels and currents in the Sydney – Botany Bay region.

The propagation of ocean waves (swell) into the near shore region leads to wave breaking and energy dissipation. Where waves propagate obliquely to the shoreline this process leads to the generation of a longshore current in the surf zone, and to some extent seaward of that line. These currents are of some importance to shoreline processes in the Bay generally.

Water Levels

Water level variations in the Bay and at the coastline result from one or more of the following natural causes:-

- Tides
- Wind Set-up and the Inverse Barometer Effect
- Wave Set-up
- Wave Run-up
- Fresh Water Flow
- Tsunami
- Greenhouse Effect
- Global Changes in Meteorological Conditions

Tides are caused by the relative motions of the Earth, Moon and Sun and their gravitational attractions. While the vertical tidal fluctuations are generated as a result of these forces, the distribution of land masses, bathymetric variation and the Coriolis force determine the local tidal characteristics.

In addition, the drop in atmospheric pressure, which accompanies severe meteorological events, causes water to flow from high pressure areas on the periphery of the meteorological formation to the low pressure area. This is called the 'inverse barometer effect' and results in water level increases up to 1cm for each hecta-Pascal (hPa) drop in central pressure below the average sea level atmospheric pressure in the area for the particular time of year, typically about 1010 hPa. The actual increase depends on the speed of the meteorological system and 1cm is only achieved if it is moving slowly. The phenomenon causes daily variations from predicted tide levels up to 0.05m. The combined result of wind set-up and the inverse barometer effect is called storm surge. When the meteorological event tracks over water at a speed equal to the long wave celerity, resonance may occur and the inverse barometer effect can be bigger than the normal inverse barometer effect. This process is included in the storm tide data prepared for the Sydney region.

Wave run-up is the vertical distance between the maximum height a wave runs up the beach or a coastal structure and the still water level, comprising tide plus storm surge. Additionally, run-up level varies with surf-beat, which arises from wave grouping effects. Wave set-up is implicitly included in wave run-up.

Tsunami are caused by sudden crustal movements of the Earth and are commonly, but incorrectly, called 'tidal waves'. They are very infrequent and unlikely to occur during a storm and so have not been included in this study. Nevertheless, in the context of events having recurrence intervals in the order of 100 years, one should keep this phenomenon in mind. They can cause sudden and significant currents that affect berthed ships.

Tidal planes derived from long-term records at Fort Denison, Sydney Harbour, are shown in **Table A.1**, (Manly Hydraulics Laboratory, 1992). Tidal planes for Botany Bay and the study area are similar to those for Sydney Harbour, (MSB Sydney Ports Authority, 1993). Tides in Botany Bay are semi-diurnal, that is, there are two high and two low tides each day, normally. On rare occasions there may be only one high or low tide because the lunar tidal constituents have a period of about 25 hours. There may also be a significant diurnal difference, that is, a significant difference between successive high tides and successive low tides.

Table A-1 Tidal Planes for Botany Bay

Tidal Plane	Water Level	
	m LAT	m AHD
Mean High Water Springs (MHWS)	1.61	0.69
Mean High Water Mark (MHWM)	1.48	0.56
Mean High Water Neaps (MHWN)	1.36	0.44
Mean Sea Level (MSL)	0.93	0.01
Mean Low Water Neaps (MLWN)	0.54	-0.39
Mean Low Water Springs (MLWS)	0.29	-0.64

Table A.2 presents extreme water levels for typical Average Recurrence Intervals (ARI), derived from Fort Denison Sea Level Rise Vulnerability Study (Watson and Lord, 2008). These levels exclude wave set-up and relate to locations seaward of the breaker zone.

Table A-2 Extreme Water Levels (Seaward of the Breaker Zone) – Excluding Projected SLR

Average Recurrence Interval	Water Level	
	m LAT	m AHD
0.02	1.89	0.965
0.05	1.97	1.045
0.10	2.02	1.095
1	2.16	1.235
2	2.20	1.275
5	2.24	1.315
10	2.27	1.345
20	2.30	1.375
50	2.34	1.415
100	2.36	1.435
200	2.38	1.455
500	2.39	1.465
1,000	2.40	1.475

Winds

Wind affects both the wave and current climates in Botany Bay. Wind data has been recorded at Sydney Airport since 1939 (Monypenny and Middleton, 1997).

The location and effects of airport development have changed since then. From 1939 to 16 August, 1994, a Dines anemometer was used to record 10-minute averages of wind speed and direction.

Since the early 1960's, at least, this anemometer was located on a 10m mast near the intersection of the east-west and north-south runways.

Recommended WMO clearances from buildings and other obstructions were maintained. During its period of service, the Dines anemometer was maintained well.

Since 16 August, 1994, wind data at the airport has been recorded using a Synchronic anemometer installed on a 10m mast near the threshold of the main north-south runway, which is more exposed than the previous Dines anemometer site.

Analyses of these wind records (Monypenny and Middleton, 1997) showed that there had been a gradual error (reduction) in wind speed recorded by the Dines anemometer. This reduction amounted to 2.6m/s by August, 1994. Monypenny and Middleton (1997) advise that a simplified linear adjustment be made to Sydney airport wind speeds up to 16 August, 1994 and this adjustment was made for this study.

More details are presented in the body of the report.

Climate Change Issues

For the purposes of this study, the regional coastal projections of climate change are discussed under the following sub-headings:

- Sea level rise (SLR);
- Wind;
- Frequency of extreme events; and
- Adopted climate change scenarios.

Sea Level Rise

At the regional scale, sea levels can be influenced by variations in ocean currents and in the atmosphere due to different wind regimes (McInnes *et al.*, 1998). Coastal responses to SLR can be highly variable and often unpredictable, and are greatly influenced by the local geomorphology. Temporary flooding/inundation associated with storm systems is generally of short duration, due to the infrequent and large-magnitude nature of these events, as well as the dependence of these processes on tide level, which varies from high to low water over 6 hours. On the other hand, the cumulative erosion and inundation of presently affected sites that would be associated with global SLR or land subsidence processes would be of longer duration and may be associated with low-magnitude events. Although the magnitude of future SLR may be relatively small in isolation, where severe storms coincide with elevated sea levels, wave attack and storm surge will result in significant effects on presently and newly vulnerable coastal areas.

Research into the long term SLR estimates for Australia indicates that the rate of SLR is slightly less than the global average. Church *et al.*, 2006 analysed two of Australia's longest tide gauge records: Fort Denison, Sydney, and Fremantle, in Western Australia. That study determined that the local SLR from 1950 to 2000 was 1.3 (± 0.5) mm/year, compared with a global average of 1.8mm/year. The difference is primarily to be due to the more frequent and intense El Niño events that have occurred since the mid-1970's, which caused lower sea-levels around Australia (Holper *et al.*, 2005).

The NSW OEH, in planning for climate change, produced a Sea Level Rise Policy Statement (DECCW, 2009a) that sets SLR planning benchmarks of 40cm by 2050 and 90cm by 2100 (relative to 1990 mean sea levels). These benchmarks are derived from both IPCC projections and CSIRO research. The manner in which they were calculated incorporates a range of variables, as shown in **Table A.3**. The SLR component is derived from the IPCC SRES A1F1 climate change scenario due to the fact that, in the last decade, the observed global average of sea level from satellite data is tracking along the upper bound of the Intergovernmental Panel on Climate Change (IPCC) projections. This document was withdrawn in 2012.

Table A.3: Water Level Components of SLR Planning Benchmarks (after DECCW, 2009a and b)

Component	2050	2100
SLR	30 cm	59 cm
Accelerated ice melt	(included above)	20 cm
Regional SLR variation	10 cm	14 cm
Rounding*	-	-3 cm
Total	40 cm	90 cm

According to AR5, the thermal expansion of the oceans and glacial melting have been the dominant contributors to 20th century global mean sea level rise. AR5 makes projections for global mean sea level rise during the 21st century. Projections are made for a number of different global greenhouse gas emissions scenarios, known as Representative Concentration Pathways (RCP's). AR5 states that "*It is very likely that the rate of global mean sea level rise during the 21st century will exceed the rate observed during 1971–2010 for all Representative Concentration Pathway (RCP) scenarios due to increases in ocean warming and loss of mass from glaciers and ice sheets*". The AR5 projections for mean sea level rise are reproduced in Figure A.1 and Table A.4.

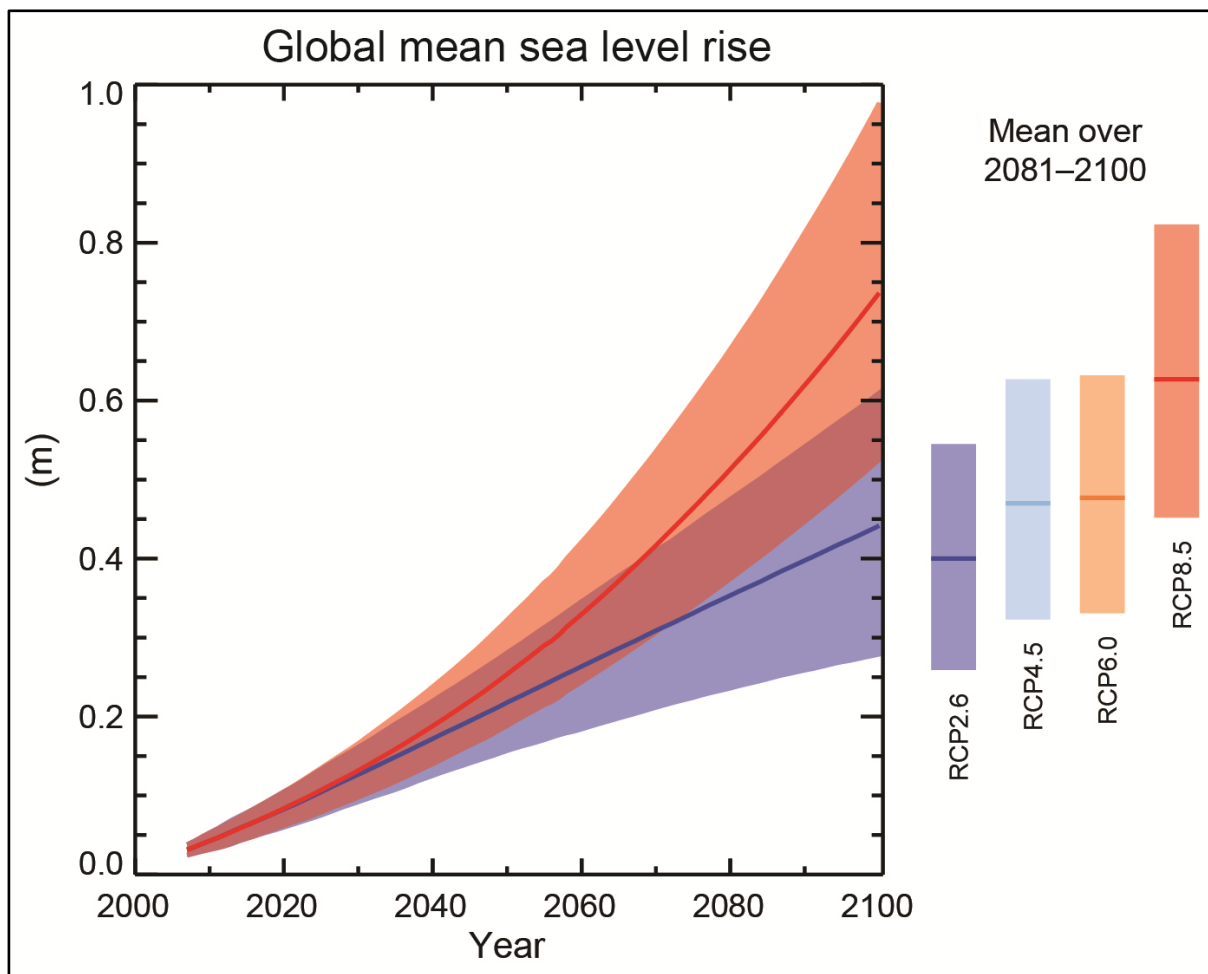


Figure A.1: AR5 (IPCC, 2018) GMSLR Projections

Table A.4: Global Mean Sea Level Rise Projections in AR5 (IPCC, 2018)

Scenario Name	Global Annual Greenhouse Gas Emissions Scenario	MSLR Mean Over 2046-2065 Mean and likely (>66% probability) range (m)	MSLR Mean Over 2081-2100 Mean and likely (>66% probability) range (m)	MSLR In 2100 Mean and likely (>66% probability) range (m)
RCP2.6	Emissions peak between 2010 and 2020, and decline substantially thereafter.	0.24 (0.17 to 0.32)	0.40 (0.26 to 0.55)	0.44 (0.28 to 0.61)
RCP4.5	Emissions peak around 2040, then decline.	0.26 (0.19 to 0.33)	0.47 (0.32 to 0.63)	0.53 (0.36 to 0.71)
RCP6.0	Emissions peak around 2080, then decline.	0.25 (0.18 to 0.32)	0.48 (0.33 to 0.63)	0.55 (0.38 to 0.73)
RCP8.5	Emissions continue to rise throughout the 21 st century.	0.30 (0.22 to 0.38)	0.63 (0.45 to 0.82)	0.74 (0.52 to 0.98)

For this study it is recommended that a value of 0.47m, interpolated from **Figure A.1** at 2075 for the mean RCP8.5 line, be adopted to represent the future sea level rise between **2000 and 2075, which is based on the mean RCP8.5 value**. This value can also be obtained from **Table A.4**, last row – SLR of 0.30m at 2055 and 0.63m at 2090, with 2075 being about midway between 2055 and 2090.

RCP8.5 is the scenario adopted by the NSW government.

Wind

At present, the prevailing winds in the Botany Bay area are from the south-east during the winter months and from the north-east and east during the summer months. During the day, sea breezes dominate (Hazelwood, 2007).

CSIRO, 2007 undertook a climate change study for NSW and concluded that predictions relating to wind changes for the state contained large uncertainty in most seasons. In general, mean wind-speed projections showed a tendency for increases across much of the state in summer, with decreases in wind from the north-east. In autumn, there was a tendency towards weaker winds from the south and east, and stronger winds from the north-west. In winter, increases in winds were from the north-west and south, with wind speeds decreasing elsewhere. Lastly, there was a general tendency for stronger winds to occur in spring across the state.

Extreme winds have similar patterns to mean wind speed changes in summer and autumn, although the magnitudes of the changes are larger; particularly over the continent due to frictional effects. In winter, the ocean region in the south of NSW showed a tendency for increasing extreme winds with only the north-east of NSW indicating decreasing winds (Hennessy *et al.*, 2004).

Frequency of Extreme Events

There is no current consensus on the effect of climate change on coastal storms in the Botany Bay region of NSW. While IPCC, 2007 warns of a potential increase in the frequency and intensity of coastal storms and cyclonic events, recent studies, for example, CSIRO, 2007 and McInnes *et al.*, 2007 present climate change predictions that indicate both increased and decreased wind speeds along the NSW coast, depending on the model and/or climate change scenario applied.

Botany Bay is not located in an active tropical cyclone region and even studies that predict the largest increase in the southern extent of the east Australia cyclone region due to climate change processes do not predict cyclones off the region within the next 50 to 100 years (CSIRO, 2007).

Of more importance for this area is the potential change in east coast low (ECL) event frequency and/or intensity due to climate change. Current understanding on ECL events is limited, although it is widely believed that the El Niño Southern Oscillation (ENSO) cycle has a significant influence on the frequency of ECL events. A study of ECLs along the Queensland coast identified that ECLs have doubled in frequency over the 30 years to 2000 (AGSO, 2000), most notably due to the 1970-1980 period of high frequency of events, and while it identifies that this is significant, it also makes the point that this “appears linked to broader climatic variations” such as the Southern Oscillation Index, rather than to climate change. Some of these meteorological formations move southward and affect the Sydney Region, or form locally.

Climate change models developed to date have not been able to investigate changes to wind conditions generated by small scale systems such as ECL events. CSIRO, 2007 concludes that for ECL events “model studies do not as yet indicate how the occurrence of east coast low pressure systems may change”.

Due to the lack of consensus related to climate change effects on the frequency and/or intensity of these events it is considered appropriate to adopt coastal storm conditions based on the current climatology and historical records. For the purposes of this study, the offshore design wave climate is based on measured offshore data from both the Manly Hydraulics Laboratory from 1992 combined with offshore Port Botany wave data and the more recent Port Botany directional wave data.

Adopted Climate Change Scenarios

For the purposes of this study it has been assumed that current tidal planes (relative to the rising mean sea level), wind prominence and storm intensity and frequency will remain unchanged into the future. Due to the uncertainty in the various climate change projections for these features it is considered appropriate to adopt conditions based on the current climatology and historical records; any implications for an alternative position would be very minor over the life of the current project.

APPENDIX

B

GLOSSARY OF TERMS

(AHD) Australian Height Datum	A common national plane of level corresponding approximately to mean sea level.
ADCP	Acoustic Doppler Current Profiler, seabed instrument that can measure currents through the water column and also wave conditions. Similar instruments include an AWAC.
Anemometer	Device that measures wind speed.
Arakawa C-Grid	Arakawa grid systems uses staggering. The Arakawa C-grid has vertical velocities on the middle of the left and right edges and horizontal velocities on the middle of the top and bottom edges.
ARI	Average Recurrence Interval
Astronomical Tides	Tides which are only influenced by the gravitational effect of the moon and the sun. Does not include climate, geography or other factors.
Atmospheric Boundary Layer	The lower part of the atmosphere where the presence of the Earth's surface is felt by (a modelled) wind, with its upper limit typically at altitude 150–500 m.
Australian Height Datum	A common national plane of level corresponding approximately to mean sea level.
Bathymetry	Depth profile of an area. Usually notated by amount of meters below mean sea level where negative signifies height above.
Batter Slope	Slope of for instance the side of a channel
Beach Nourishment	The placement of large quantities of good quality sand on the beach to advance it seaward.
Bed Load	That portion of the total sediment load that flowing water moves along the bed by the rolling or saltating of sediment particles.
Berth	Locations where ships may be moored.
Calibration	The process by which the results of a computer model are brought to agreement with observed data.
Catchment	The area draining to a site. It always relates to a particular location and may include the catchments of tributary streams as well as the main stream.
CD	Chart Datum, common datum for navigation charts - 0.92m below AHD in the Sydney coastal region. Typically Lowest Astronomical Tide.
Coastal Trapped Waves	Coastal Trapped Waves are long period wave phenomena that propagate along the continental shelf.
Computer Models	Digital models designed to simulate certain situations in reality.
Continental Shelf	Underwater extension of a continent which may stretch for many kilometres in length.

Coriolis Force	Fictitious force to account for the apparent deflection from a straight line of an object (or water particle) moving over the Earth's surface in a frame of reference on the Earth's surface due to the Earth's rotation.
Density Flow	Current due to water density (depending on temperature and salinity) gradients.
Diffraction	The curving of wave direction around an obstacle into the leeward side.
Discharge	The rate of flow of water measured in terms of volume per unit time. It is to be distinguished from the speed or velocity of flow, which is a measure of how fast the water is moving rather than how much is flowing.
Dispersive Transport	The transport of dissolved matter through the estuary by vertical, lateral and longitudinal mixing associated with velocity shear.
Diurnal	A daily variation, as in day and night.
Domain Decomposition	A numerical method which arrives at the solution by splitting the problem into smaller sub problems then iterating until boundary values are equal.
Dredging	Underwater excavation.
Ebb Tide	The outgoing tidal movement of water within an estuary.
Ekman Depth	The depth at which the current is opposite to the direction of the current at the surface, due to a (modelled) constant, steady wind.
Fetch	The length of the water over which wind has blown. Typically, the longer it is, the larger the wave.
Flood Tide	The incoming tidal movement of water within an estuary.
Geomorphology	The study of the origin, characteristics and development of land forms.
Groyne	A fixed structure which acts as a wall to sediment transport. Its effectiveness depends on the height, placement and length.
H 1/3	The top one third set of wave heights when ranked from highest to lowest.
Hindcasting	Inputting previous known data into a design model to see how close the results are to the known results.
H _{m0}	Significant wave height (H _s) based on where is the zero th moment of the wave energy spectrum (rather than the time domain H _{1/3} parameter).
H _s (Significant Wave Height)	H _s may be defined as the average of the highest 1/3 of wave heights in a wave record (H _{1/3}), or from the zero th spectral moment (H _{m0}), though there is a difference of about 5 to 8%.

Intertidal	Pertaining to those areas of land covered by water at high tide, but exposed at low tide, for example, intertidal habitat.
Inverse Barometer Effect	As air pressure lowers, the water level rises. For every 10hPa there is an inverse change of 0.1m.
Jetty	A breakwater designed to protect the coastline or a mooring facility for ships.
JONSWAP Spectrum	One-dimensional frequency spectrum for young sea states under idealised conditions (constant wind, straight coastline, deep water).
Local Sea	A sea state consisting of waves generated by local wind (as opposed to swell).
Long Shore Current	A current that moves parallel to the coast.
Mathematical/Computer Models	The mathematical representation of the physical processes involved in runoff, stream flow and estuarine/sea flows. These models are often run on computers due to the complexity of the mathematical relationships. In this report, the models referred to are mainly involved with wave and current processes.
MHL	Manly Hydraulics Laboratory
Model Verification	Checking the assumptions and equations behind a model to make sure the model is an accurate representation.
MSL	Mean Sea Level
Neap Tides	Tides with the smallest range in a monthly cycle. Neap tides occur when the sun and moon lie at right angles relative to the earth (the gravitational effects of the moon and sun act in opposition on the ocean).
NSW	New South Wales
Numerical Model	A mathematical representation of a physical, chemical or biological process of interest. Computers are often required to solve the underlying equations.
Peak Wave Height	The highest wave height in a group of waves.
Pierson - Moskowitz Spectrum	One-dimensional frequency spectrum for fully developed sea states under idealised conditions (constant wind, straight coastline, deep water).
Radiation Stress	The transport of wave-induced momentum.
Refraction	Waves bending into a direction normal to the shore due to approaching shallower depths. The part of the wave which reaches the shallow depth first moves slower allowing the deeper part to catch up.
Salinity	The total mass of dissolved salts per unit mass of water. Seawater has a salinity of about 35g/kg or 35 parts per thousand.

Saltation		The movement of sediment particles along the bed of a water body in a series of 'hops' or 'jumps'. Turbulent fluctuations near the bed lift sediment particles off the bed and into the flow where they are carried a short distance before falling back to the bed.
Sediment Load		The quantity of sediment moved past a particular cross-section in a specified time by estuarine flow.
Semi-diurnal		A twice-daily variation, for example, two high waters per day.
Shear Stress		The stress exerted on the bed of an estuary by flowing water. The faster the velocity of flow the greater the shear stress.
Shoaling		The variation of waves in their direction of propagation due to depth-induced changes of the group velocity in that direction. These changes in group velocity generally increase the wave amplitude as the waves propagate into shallower water.
Shoals		Shallow areas in an estuary created by the deposition and build-up of sediments.
Slack Water		The period of still water before the flood tide begins to ebb (high water slack) or the ebb tide begins to flood (low water slack).
Spring Tides		Tides with the greatest range in a monthly cycle, which occur when the sun, moon and earth are in alignment (the gravitational effects of the moon and sun act in concert on the ocean)
Storm Surge		The increase in coastal water levels caused by the barometric and wind set-up effects of storms. Barometric set-up refers to the increase in coastal water levels associated with the lower atmospheric pressures characteristic of storms. Wind set-up refers to the increase in coastal water levels caused by an onshore wind driving water shorewards and piling it up against the coast.
Surf Beat		In the surf zone, the combination of wave-induced set-up and wave groupiness generates low-frequency waves that radiate out to sea as infra-gravity waves.
Surf Zone		The section between the most seaward boundary of the breaker zone and waterline at the beach.
Swell		Regular, long-crested waves generated in a distant storm that have dispersed across the ocean.
Tidal Planes		A series of water levels that define standard tides, for example, 'Mean High Water Spring' (MHWS) refers to the average high water level of Spring Tides.
Tidal Prism		The total volume of water moving past a fixed point in an estuary during each flood tide or ebb tide.
Tidal Range		The difference between successive high water and low water levels. Tidal range is maximum during Spring Tides and minimum during Neap Tides.

Tides		The regular rise and fall in sea level in response to the gravitational attraction of the Sun, Moon and Earth.
T_{m01}		Mean wave period as calculated from the first and zeroth spectral moments of the wave energy frequency spectrum. T_{m01} normally 8% higher (approx.) than T_{m02} .
T_{m02}		Mean wave period as calculated from the second and zeroth spectral moments of the wave energy frequency spectrum. Generally equivalent to the time domain T_z parameter.
T_p		Wave energy spectral peak period; that is, the wave period related to the highest ordinate in the wave energy spectrum.
Tributary		Catchment, stream or river which flows into a larger river, lake or water body
T_s		The significant wave period.
Tsunami		Phenomena where a large volume of water is displaced to create a series of waves with large wavelengths. Can be caused by earthquakes, landslides, volcanic eruptions, etc.
T_z (Zero Crossing Period)		The average period of waves in a train of waves observed at a location.
Velocity Shear		The differential movement of neighbouring parcels of water brought about by frictional resistance within the flow, or at a boundary. Velocity shear causes dispersive mixing, the greater the shear (velocity gradient), the greater the mixing.
Wave Climate		Long term characterization of waves at a location over a number of years with respect to significant wave height, period, direction, etc.
Wave Energy Spectrum		The relationship between the distribution of energy and the frequency in waves.
Wave Grouping		An uninterrupted sequence of waves with wave heights higher than an arbitrarily chosen, but usually high, threshold value.
Wave Run-up		The vertical distance between the maximum height that a wave runs up the beach (or a coastal structure) and the still water level, comprising tide and storm surge.
Wave set-up		A rise in water level, particularly in the surf zone, to counteract the force exerted by a horizontal gradient in the radiation stress.

APPENDIX

C

PRELIMINARY LAYOUTS



Used for preliminary assessment purposes only. Not for construction

DRAWING COLOUR CODED - PRINT ALL COPIES IN COLOUR

**SENSITIVE - NSW GOVERNMENT
NOT FOR CONSTRUCTION**

1- KURNELL SITE PLAN
SCALE 1 : 2250

AMD	DESCRIPTION	DESIGNER SIGN./DATE	VERIFIED SIGN./DATE	APPROVED SIGN./DATE

CO-ORDINATE SYSTEM: MGA ZONE 56 HEIGHT DATUM: A.H.D SCALE: 1 : 2250



This drawing and the related information have been prepared by, or at the request of, Transport for NSW for a specific purpose and may not be used for any purpose other than the purpose intended by Transport for NSW. Transport for NSW does not provide any warranties and accepts no liability arising out of the use of this drawing or any of the related information for any purpose other than the intended purpose. This drawing is protected by copyright and no part of this drawing may be reproduced in any form without the express written permission of Transport for NSW.

ARUP
LEVEL 5, 151 CLARENCE STREET SYDNEY NSW 2000 T 61 2 9350 9300 www.arup.com

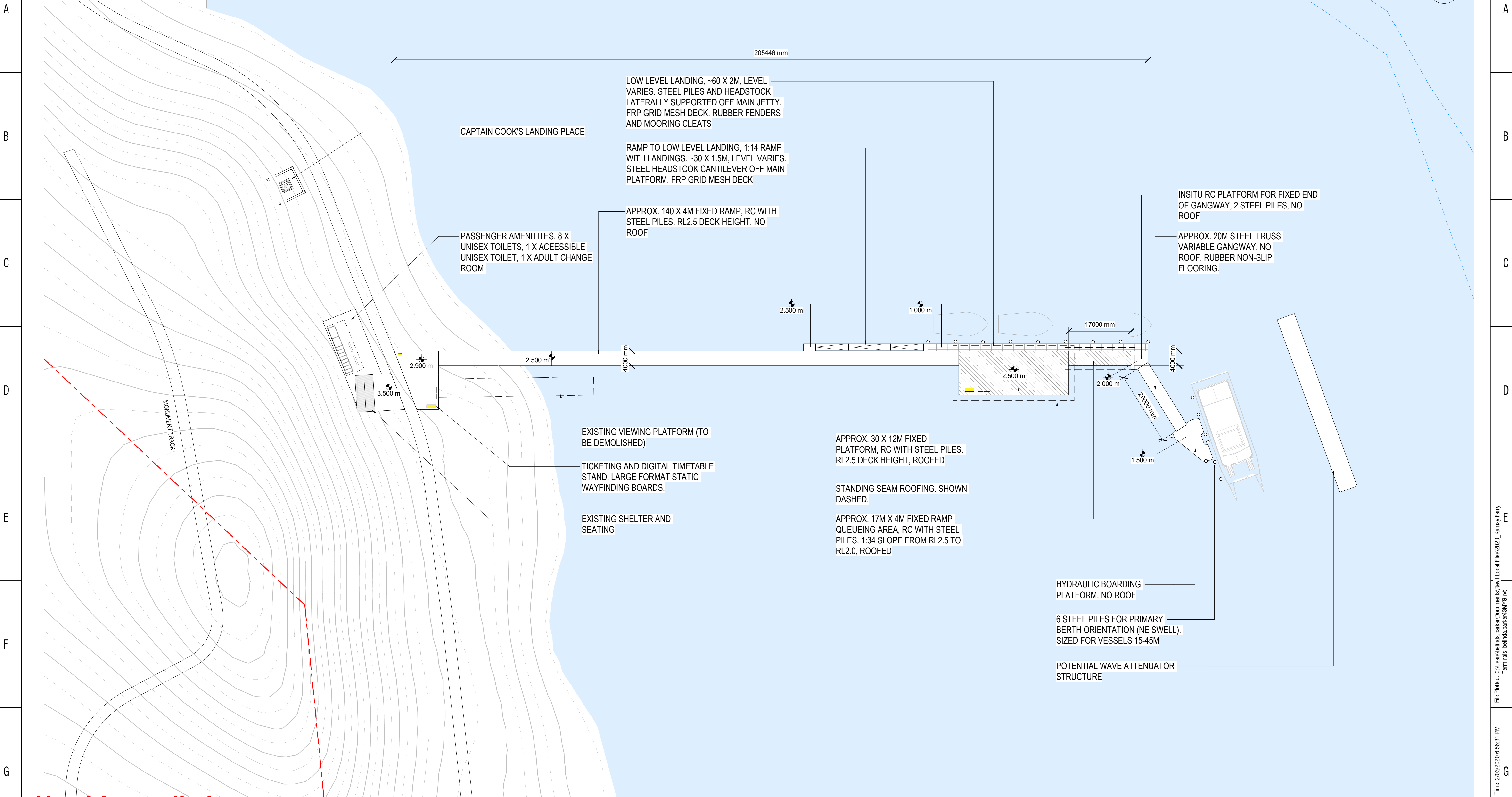
DRAWN _____
DESIGNED _____
DRG CHECK _____
DESIGN CHECK _____
APPROVED _____

WORK IN PROGRESS

KAMAY FERRY TERMINALS

KURNELL SITE PLAN

FILE No.	A1
STATUS	©
DRG No.	KFT01-ARUP-LPR-AR-DRG-000001
EDMS No.	



Used for preliminary assessment purposes only. Not for construction

DRAWING COLOUR CODED - PRINT ALL COPIES IN COLOUR

**SENSITIVE - NSW GOVERNMENT
NOT FOR CONSTRUCTION**

AMD	DESCRIPTION	DESIGNER SIGN./DATE	VERIFIED SIGN./DATE	APPROVED SIGN./DATE

CO-ORDINATE SYSTEM: MGA ZONE 56 HEIGHT DATUM: A.H.D SCALE: 1 : 500



ARUP

This drawing and the related information have been prepared by, or at the request of, Transport for NSW for a specific purpose and may not be used for any purpose other than the purpose intended by Transport for NSW. Transport for NSW does not provide any warranties and accepts no liability arising out of the use of this drawing or any of the related information for any purpose other than the intended purpose. This drawing is protected by copyright and no part of this drawing may be reproduced in any form without the express written permission of Transport for NSW.

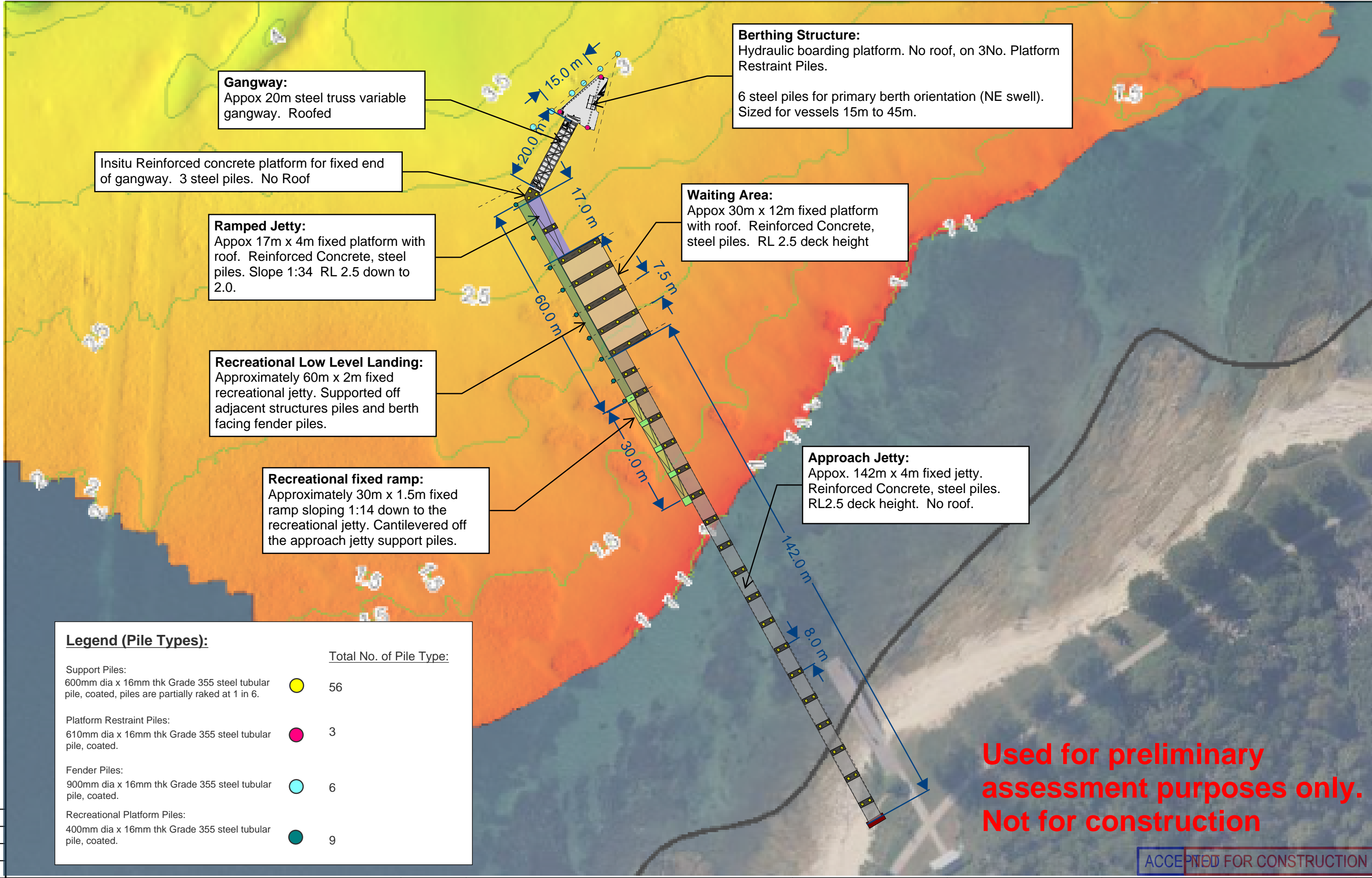
ARUP
LEVEL 5, 151 CLARENCE STREET SYDNEY NSW 2000 T 61 2 9320 6000 www.arup.com

DRAWN
DESIGNED
DRG CHECK
DESIGN CHECK
APPROVED

WORK IN PROGRESS

KURNELL WHARF GA PLAN - DESIRABLE OPTION
FILE No. _____
STATUS _____
DRG No. **KFT01-ARUP-LPR-ZZ-GF-DR-A-3Q01** EDMS No. _____

THIS DRAWING MAY BE PREPARED IN COLOUR AND MAY BE INCOMPLETE IF COPIED



Gangway:
Appox 20m steel truss variable gangway. Roofed

Berthing Structure:
Hydraulic boarding platform. No roof, on 3No. Platform Restraint Piles.
6 steel piles for primary berth orientation (NE swell). Sized for vessels 15m to 45m.

In situ Reinforced concrete platform for fixed end of gangway. 3 steel piles. No Roof

Ramped Jetty:
Appox 17m x 4m fixed platform with roof. Reinforced Concrete, steel piles. Slope 1:34 RL 2.5 down to 2.0.

Waiting Area:
Appox 30m x 12m fixed platform with roof. Reinforced Concrete, steel piles. RL 2.5 deck height

Recreational Low Level Landing:
Approximately 60m x 2m fixed recreational jetty. Supported off adjacent structures piles and berth facing fender piles.

Recreational fixed ramp:
Approximately 30m x 1.5m fixed ramp sloping 1:14 down to the recreational jetty. Cantilevered off the approach jetty support piles.

Approach Jetty:
Appox. 142m x 4m fixed jetty. Reinforced Concrete, steel piles. RL2.5 deck height. No roof.

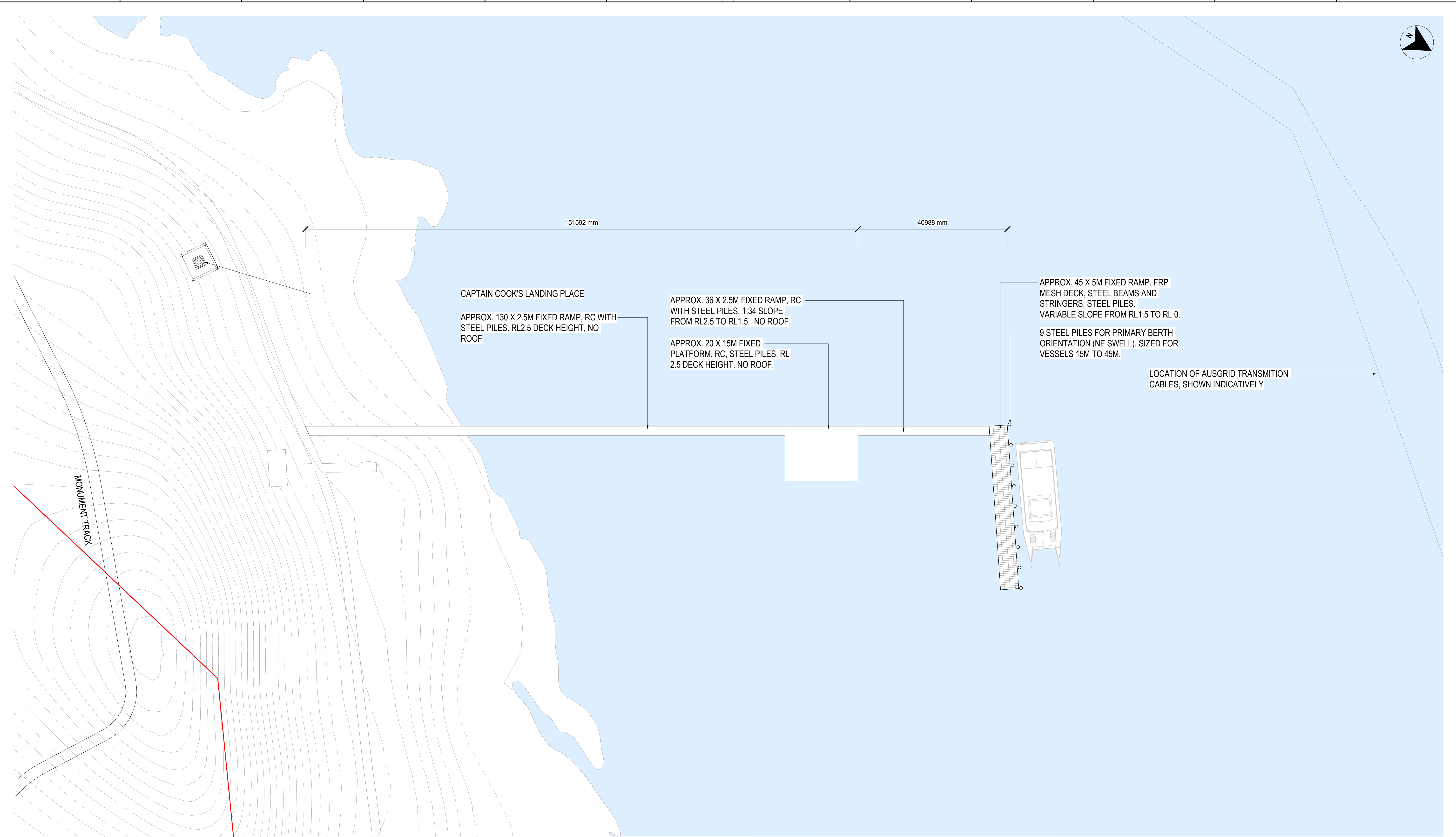
Legend (Pile Types):

	Total No. of Pile Type:
Support Piles: 600mm dia x 16mm thk Grade 355 steel tubular pile, coated, piles are partially raked at 1 in 6.	56
Platform Restraint Piles: 610mm dia x 16mm thk Grade 355 steel tubular pile, coated.	3
Fender Piles: 900mm dia x 16mm thk Grade 355 steel tubular pile, coated.	6
Recreational Platform Piles: 400mm dia x 16mm thk Grade 355 steel tubular pile, coated.	9

Used for preliminary assessment purposes only. Not for construction

ACCEPTED FOR CONSTRUCTION

DRAWING FILE LOCATION / NAME				DESIGN LOT CODE	DESIGN MODEL FILE(S) USED FOR DOCUMENTATION OF THIS DRAWING				PLOT DATE / TIME			PLOT BY			CLIENT			A3								
EXTERNAL REFERENCE FILES				REV	DATE	AMENDMENT / REVISION DESCRIPTION				WVR No.	APPROVAL	SCALES ON A3 SIZE DRAWING			DRAWINGS / DESIGN PREPARED BY			TITLE	NAME	DATE	NSW GOVERNMENT Transport Roads & Maritime Services					
												ARUP			CONSULT AUSTRALIA						PREPARED FOR					
												Member Firm Arup Pty Ltd ABN 18 000 995 165									RMS REGISTRATION No.					
												CO-ORDINATE SYSTEM			HEIGHT DATUM			DRG No.						ISSUE STATUS		
																					EDMS No.					
																					SHEET No.					
																					ISSUE					



Used for preliminary assessment purposes only. Not for construction

DRAWING COLOUR CODED - PRINT ALL COPIES IN COLOUR

**SENSITIVE - NSW GOVERNMENT
NOT FOR CONSTRUCTION**

AMD	DESCRIPTION	DESIGNER SIGN./DATE	VERIFIED SIGN./DATE	APPROVED SIGN./DATE

CO-ORDINATE SYSTEM: MGA ZONE 56 HEIGHT DATUM: A.H.D SCALE: 1 : 500



Transport for NSW



This drawing and the related information have been prepared by, or at the request of, Transport for NSW for a specific purpose and may not be used for any purpose other than the purpose intended by Transport for NSW. Transport for NSW does not provide any warranties and accepts no liability arising out of the use of this drawing or any of the related information for any purpose other than the intended purpose. This drawing is protected by copyright and no part of this drawing may be reproduced in any form without the express written permission of Transport for NSW.

ARUP

LEVEL 5, 151 CLARENCE STREET SYDNEY NSW 2000 T 61 2 9320 9320 www.arup.com

DRAWN _____
DESIGNED _____
DRG CHECK _____
DESIGN CHECK _____
APPROVED _____

KURNELL WHARF GA PLAN - MINIMUM OPTION

FILE No. _____ A1
STATUS _____ ©
DRG No. **KFT01-ARUP-LPR-ZZ-GF-DR-A-3Q01** EDMS No. _____



1- LA PEROUSE SITE PLAN
SCALE 1 : 1500

DRAWING COLOUR CODED - PRINT ALL COPIES IN COLOUR

SENSITIVE - NSW GOVERNMENT
NOT FOR CONSTRUCTION

AMD	DESCRIPTION	DESIGNER SIGN./DATE	VERIFIED SIGN./DATE	APPROVED SIGN./DATE

CO-ORDINATE SYSTEM: MGA ZONE 56 HEIGHT DATUM: A.H.D SCALE: 1 : 1500



This drawing and the related information have been prepared by, or at the request of, Transport for NSW for a specific purpose and may not be used for any purpose other than the purpose intended by Transport for NSW. Transport for NSW does not provide any warranties and accepts no liability arising out of the use of this drawing or any of the related information for any purpose other than the intended purpose. This drawing is protected by copyright and no part of this drawing may be reproduced in any form without the express written permission of Transport for NSW.

ARUP
LEVEL 5, 151 CLARENCE STREET SYDNEY NSW 2000 T 61 2 9350 9300 www.arup.com

DRAWN _____
DESIGNED _____
DRG CHECK _____
DESIGN CHECK _____
APPROVED _____

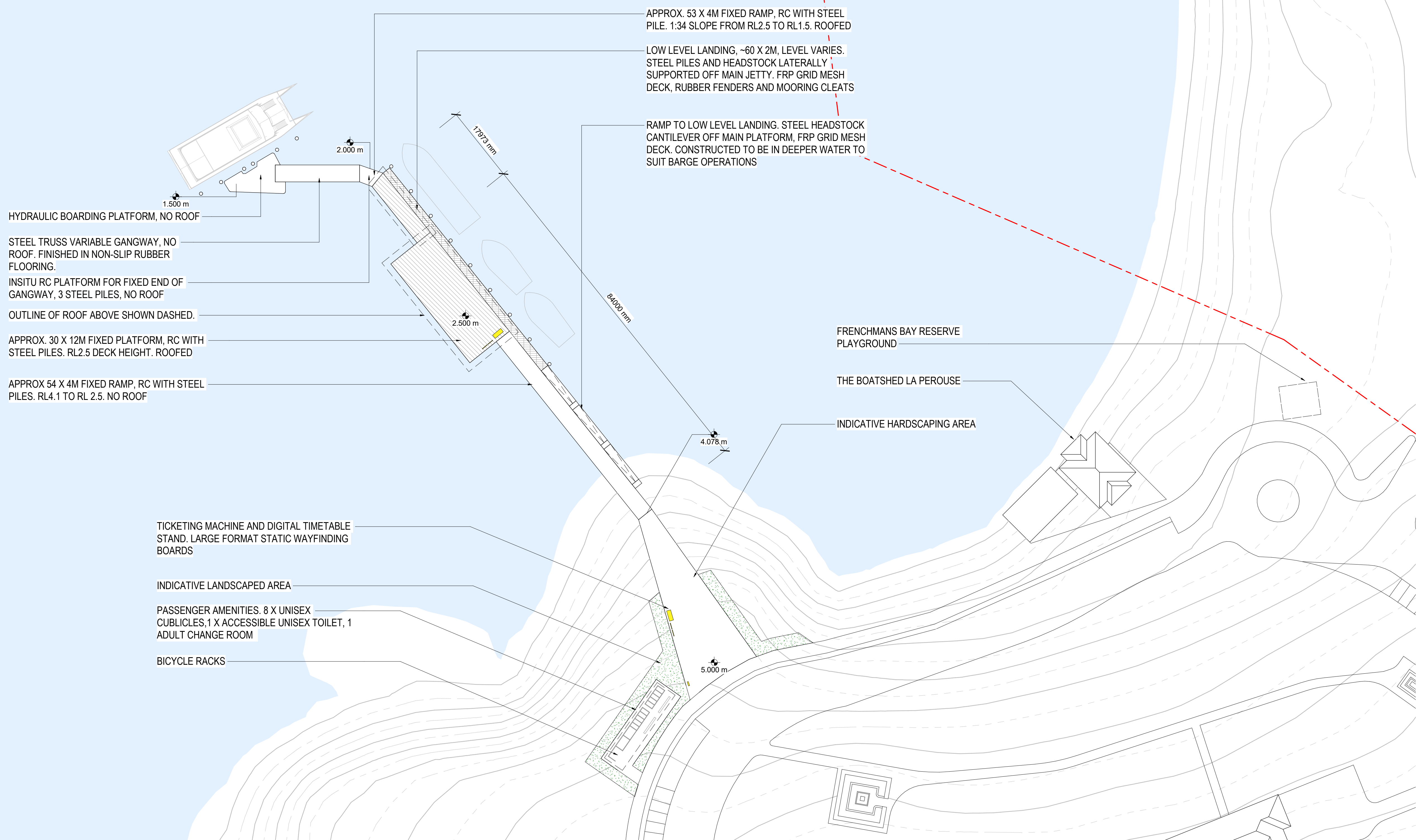
WORK IN PROGRESS

KAMAY FERRY TERMINALS	
LA PEROUSE SITE PLAN	
FILE No.	A1
STATUS	©
DRG No. KFT01-ARUP-LPR-AR-DRG-000002	EDMS No.



A
B
C
D
E
F
G
H

A
B
C
D
E
F
G
H



HYDRAULIC BOARDING PLATFORM, NO ROOF

STEEL TRUSS VARIABLE GANGWAY, NO ROOF. FINISHED IN NON-SLIP RUBBER FLOORING.

INSITU RC PLATFORM FOR FIXED END OF GANGWAY, 3 STEEL PILES, NO ROOF

OUTLINE OF ROOF ABOVE SHOWN DASHED.

APPROX. 30 X 12M FIXED PLATFORM, RC WITH STEEL PILES. RL2.5 DECK HEIGHT. ROOFED

APPROX 54 X 4M FIXED RAMP, RC WITH STEEL PILES. RL4.1 TO RL 2.5. NO ROOF

APPROX. 53 X 4M FIXED RAMP, RC WITH STEEL PILE. 1:34 SLOPE FROM RL2.5 TO RL1.5. ROOFED

LOW LEVEL LANDING, -60 X 2M, LEVEL VARIES. STEEL PILES AND HEADSTOCK LATERALLY SUPPORTED OFF MAIN JETTY. FRP GRID MESH DECK, RUBBER FENDERS AND MOORING CLEATS

RAMP TO LOW LEVEL LANDING. STEEL HEADSTOCK CANTILEVER OFF MAIN PLATFORM. FRP GRID MESH DECK. CONSTRUCTED TO BE IN DEEPER WATER TO SUIT BARGE OPERATIONS

TICKETING MACHINE AND DIGITAL TIMETABLE STAND. LARGE FORMAT STATIC WAYFINDING BOARDS

INDICATIVE LANDSCAPED AREA

PASSENGER AMENITIES. 8 X UNISEX CUBICLES, 1 X ACCESSIBLE UNISEX TOILET, 1 ADULT CHANGE ROOM

BICYCLE RACKS

FRENCHMANS BAY RESERVE PLAYGROUND

THE BOATSHED LA PEROUSE

INDICATIVE LANDSCAPING AREA

Used for preliminary assessment purposes only. Not for construction

DRAWING COLOUR CODED - PRINT ALL COPIES IN COLOUR

SENSITIVE - NSW GOVERNMENT NOT FOR CONSTRUCTION

AMD	DESCRIPTION	DESIGNER SIGN./DATE	VERIFIED SIGN./DATE	APPROVED SIGN./DATE

CO-ORDINATE SYSTEM: MGA ZONE 56 HEIGHT DATUM: A.H.D SCALE: 1 : 500



This drawing and the related information have been prepared by, or at the request of, Transport for NSW for a specific purpose and may not be used for any purpose other than the purpose intended by Transport for NSW. Transport for NSW does not provide any warranties and accepts no liability arising out of the use of this drawing or any of the related information for any purpose other than the intended purpose. This drawing is protected by copyright and no part of this drawing may be reproduced in any form without the express written permission of Transport for NSW.

ARUP
LEVEL 5, 151 CLARENCE STREET SYDNEY NSW 2000 T 61 2 9300 9300 www.arup.com

DRAWN _____
DESIGNED _____
DRG CHECK _____
DESIGN CHECK _____
APPROVED _____

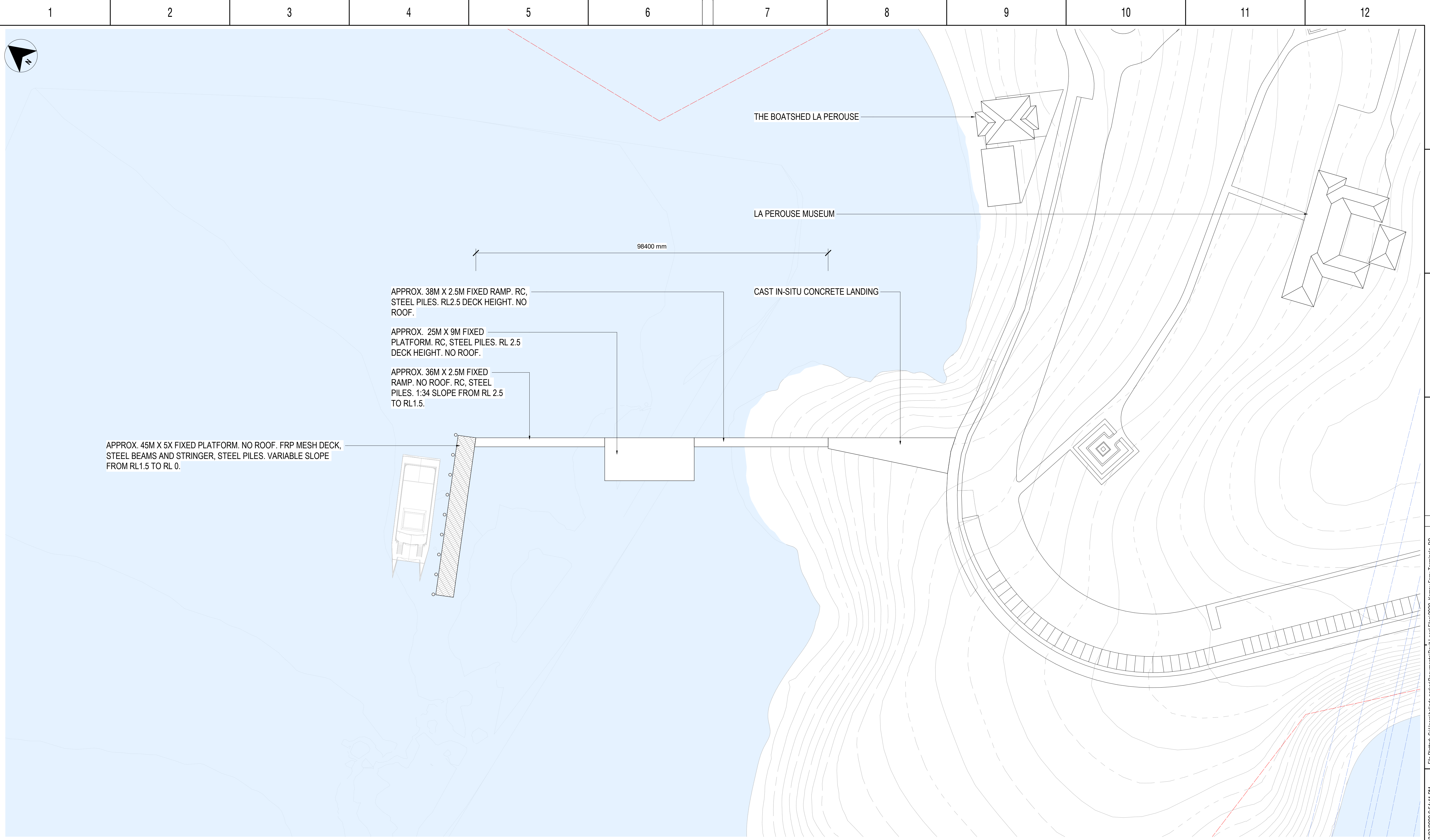
WORK IN PROGRESS

LA PEROUSE GA PLAN - DESIRABLE OPTION

FILE No. _____ A1

STATUS _____ ©

DRG No. KFT01-ARUP-LPR-ZZ-01-DR-A-3Q01 EDMS No. _____



APPROX. 45M X 5X FIXED PLATFORM. NO ROOF. FRP MESH DECK, STEEL BEAMS AND STRINGER, STEEL PILES. VARIABLE SLOPE FROM RL1.5 TO RL 0.

APPROX. 38M X 2.5M FIXED RAMP. RC, STEEL PILES. RL2.5 DECK HEIGHT. NO ROOF.

APPROX. 25M X 9M FIXED PLATFORM. RC, STEEL PILES. RL 2.5 DECK HEIGHT. NO ROOF.

APPROX. 36M X 2.5M FIXED RAMP. NO ROOF. RC, STEEL PILES. 1:34 SLOPE FROM RL 2.5 TO RL1.5.

THE BOATSHED LA PEROUSE

LA PEROUSE MUSEUM

CAST IN-SITU CONCRETE LANDING

98400 mm

Used for preliminary assessment purposes only. Not for construction

DRAWING COLOUR CODED - PRINT ALL COPIES IN COLOUR

**SENSITIVE - NSW GOVERNMENT
NOT FOR CONSTRUCTION**

DESIGN MODEL FILE(S): Model Name.rvt

AMD	DESCRIPTION	DESIGNER SIGN./DATE	VERIFIED SIGN./DATE	APPROVED SIGN./DATE

CO-ORDINATE SYSTEM: MGA ZONE 56 HEIGHT DATUM: A.H.D SCALE: 1 : 500



This drawing and the related information have been prepared by, or at the request of, Transport for NSW for a specific purpose and may not be used for any purpose other than the purpose intended by Transport for NSW. Transport for NSW does not provide any warranties and accepts no liability arising out of the use of this drawing or any of the related information for any purpose other than the intended purpose. This drawing is protected by copyright and no part of this drawing may be reproduced in any form without the express written permission of Transport for NSW.

ARUP
LEVEL 5, 151 CLARENCE STREET SYDNEY NSW 2000 T 61 2 9320 6320 www.arup.com

DRAWN _____
DESIGNED _____
DRG CHECK _____
DESIGN CHECK _____
APPROVED _____

WORK IN PROGRESS

LA PEROUSE GA PLAN - MINIMUM OPTION

FILE No. _____ A1
STATUS _____ ©
DRG No. **KFT01-ARUP-LPR-ZZ-01-DR-A-3Q01** EDMS No. _____

File Plotted: C:\Users\shelinda.parker\Documents\Revit Local Files\2020_Kamay Ferry Terminals_DD_Min_Labels.parker3WVG.rvt

Plotted Date & Time: 2/03/2020 6:54:41 PM

Plotted by: ELOISE LEOPOLD

APPENDIX

D

KURNELL WAVE CLIMATE

See attached Excel Document, **AppendixD_KurnellWaveModelling.xlsx**

Available upon request

APPENDIX

E

LA PEROUSE WAVE CLIMATE

See attached Excel Document, **AppendixE_LaPerouseWaveModelling.xlsx**

Available upon request

APPENDIX

F

CROSSING POINTS WAVE CLIMATE

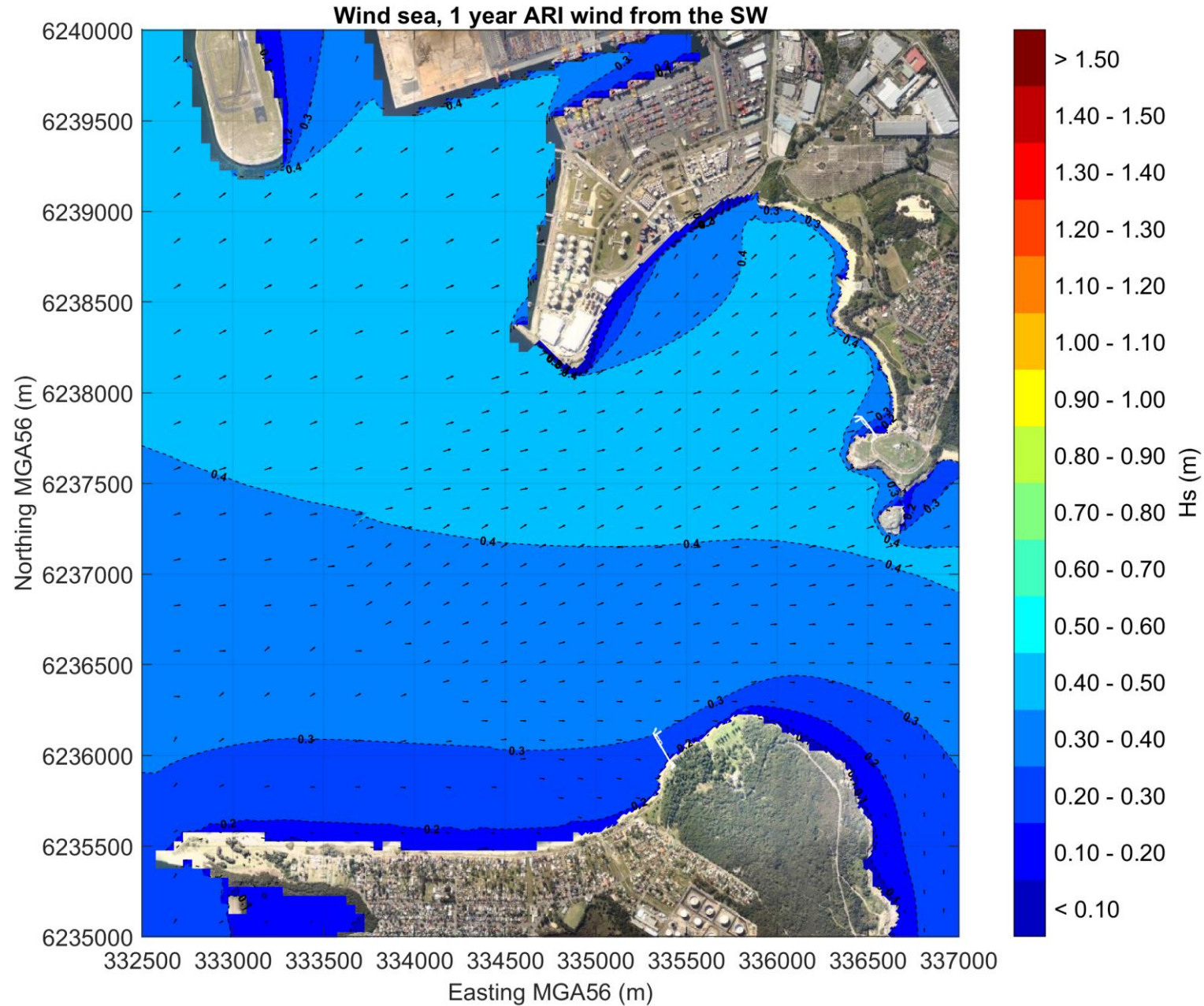
See attached Excel Document, **AppendixF_CrossingWaveModelling.xlsx**

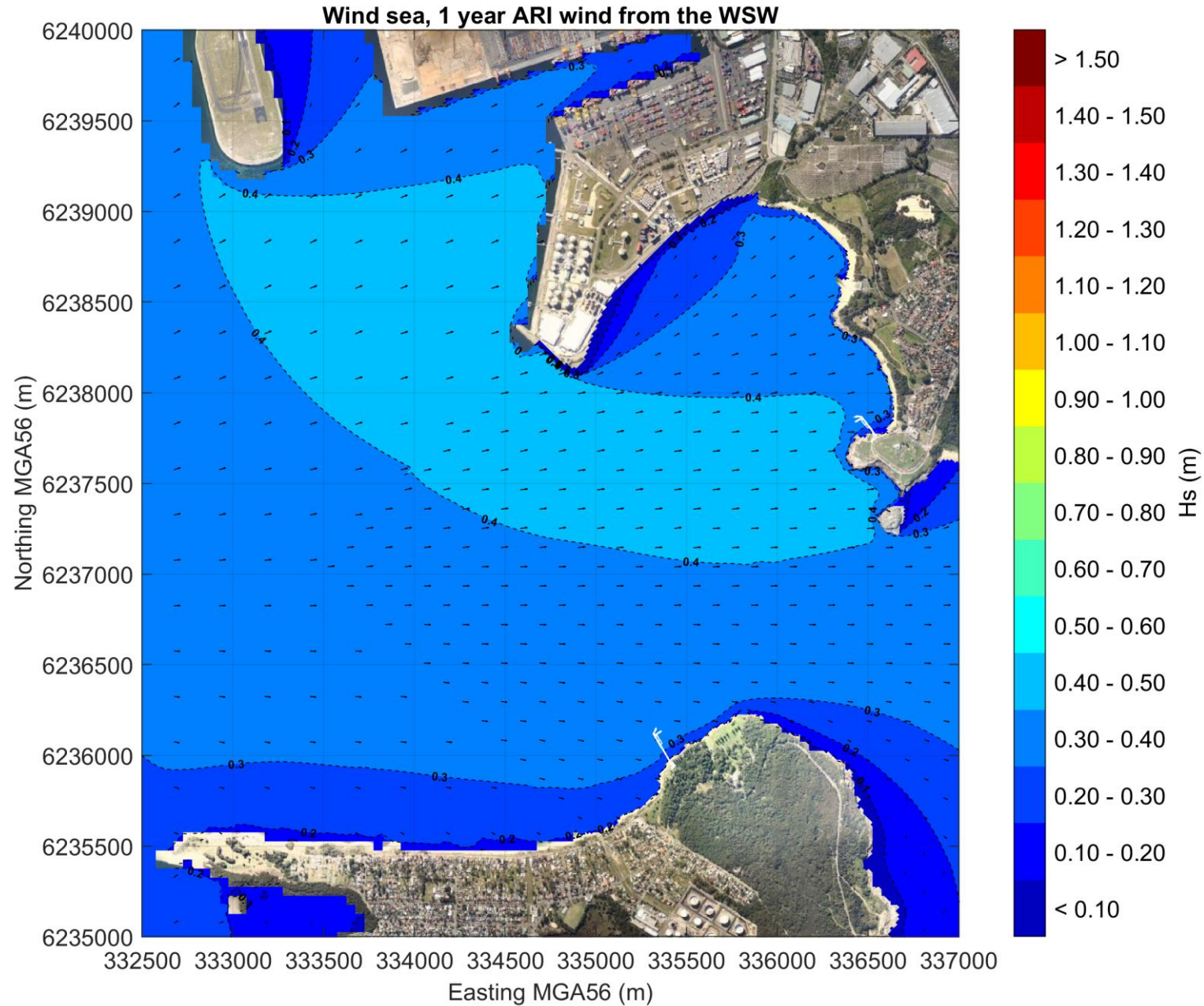
Available upon request

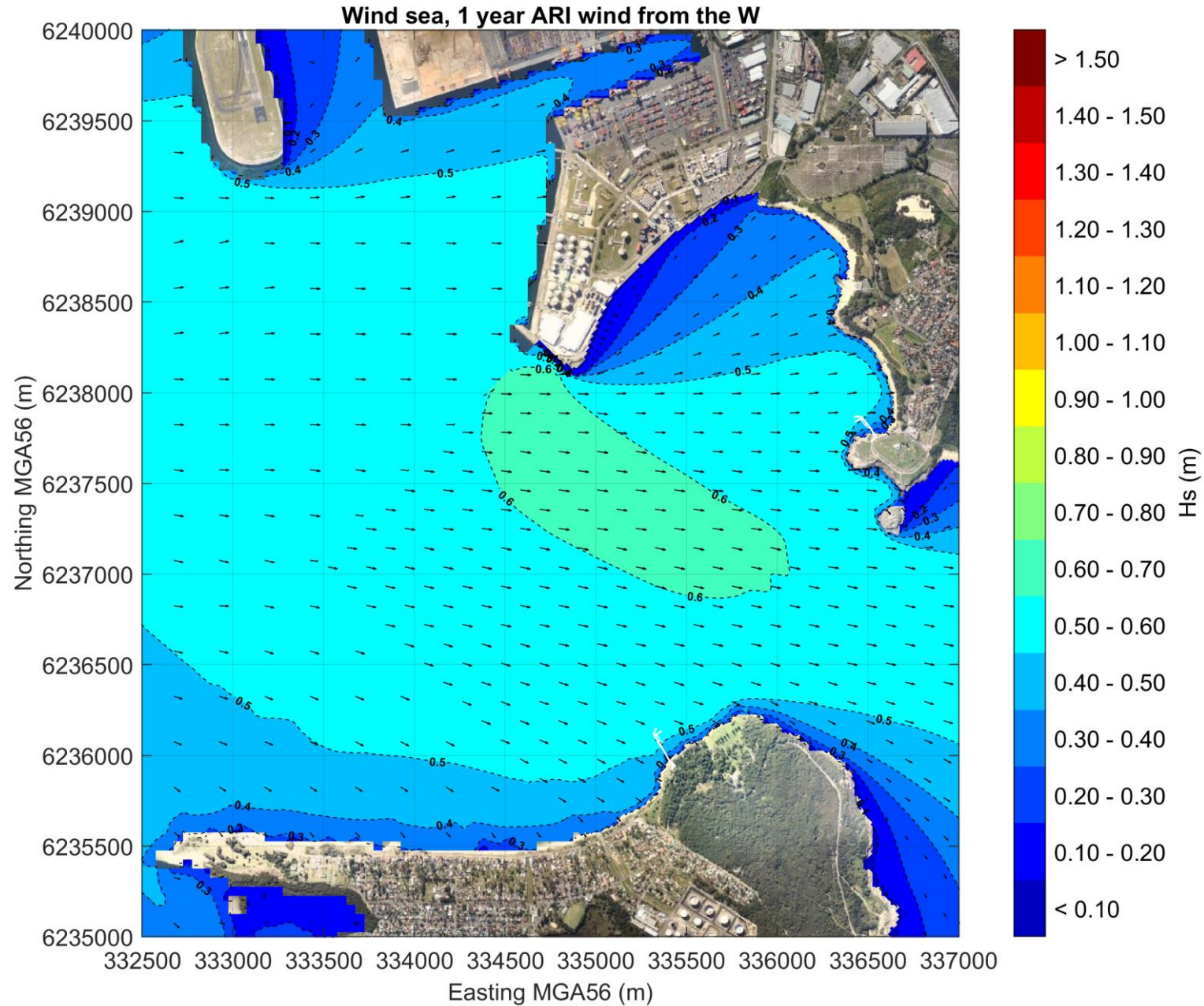
APPENDIX

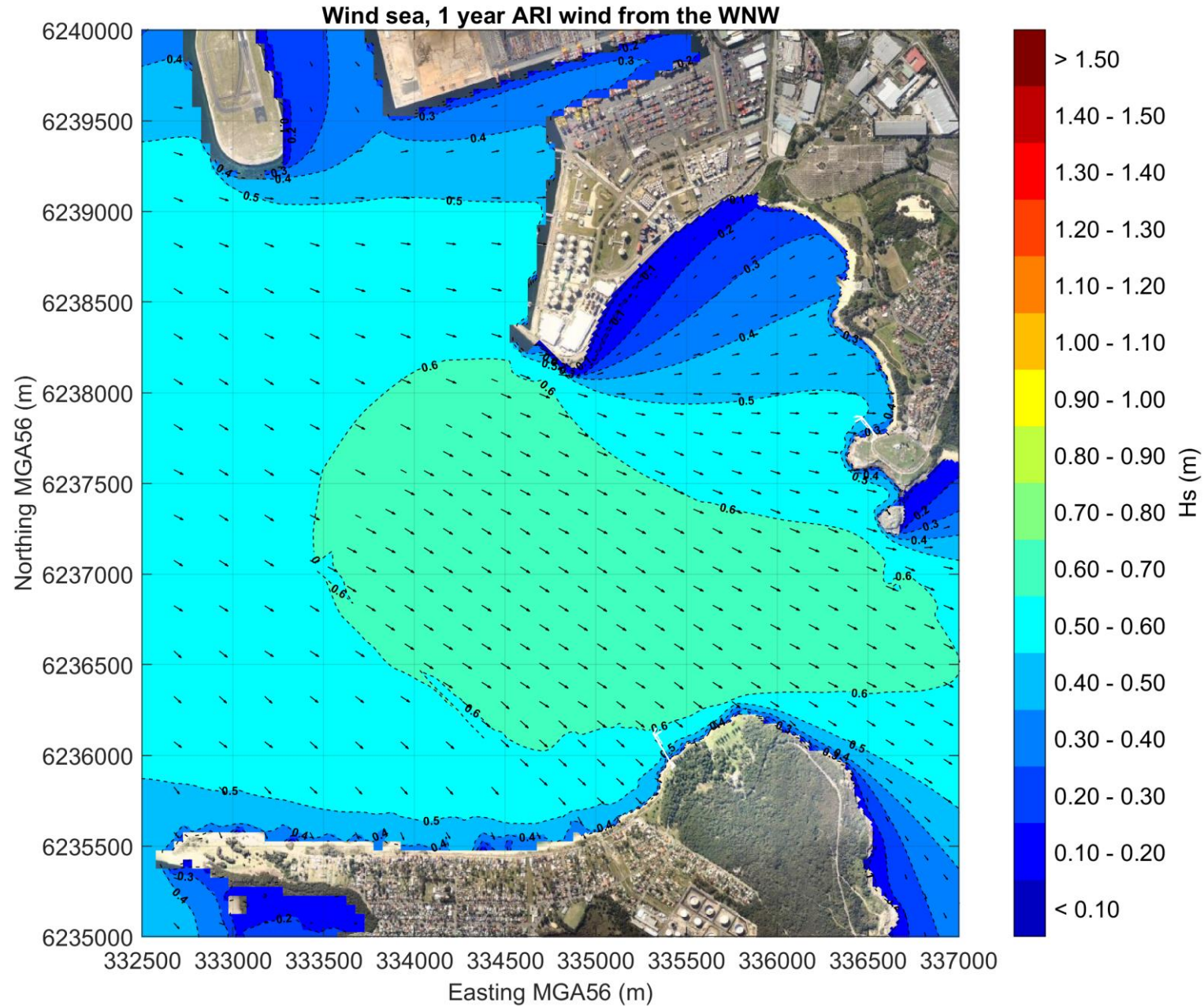
G

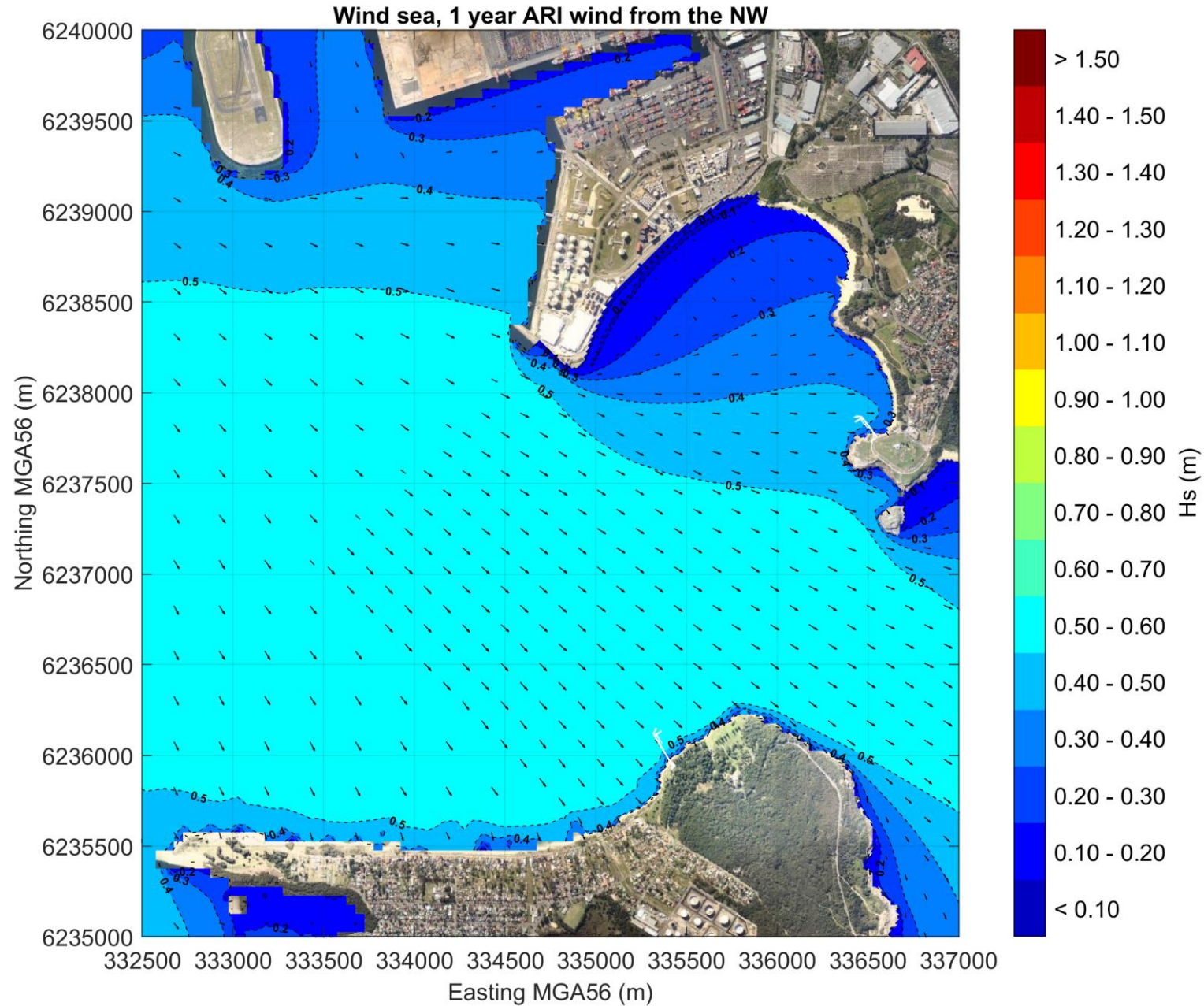
SEA WAVE MODELLING PLOTS

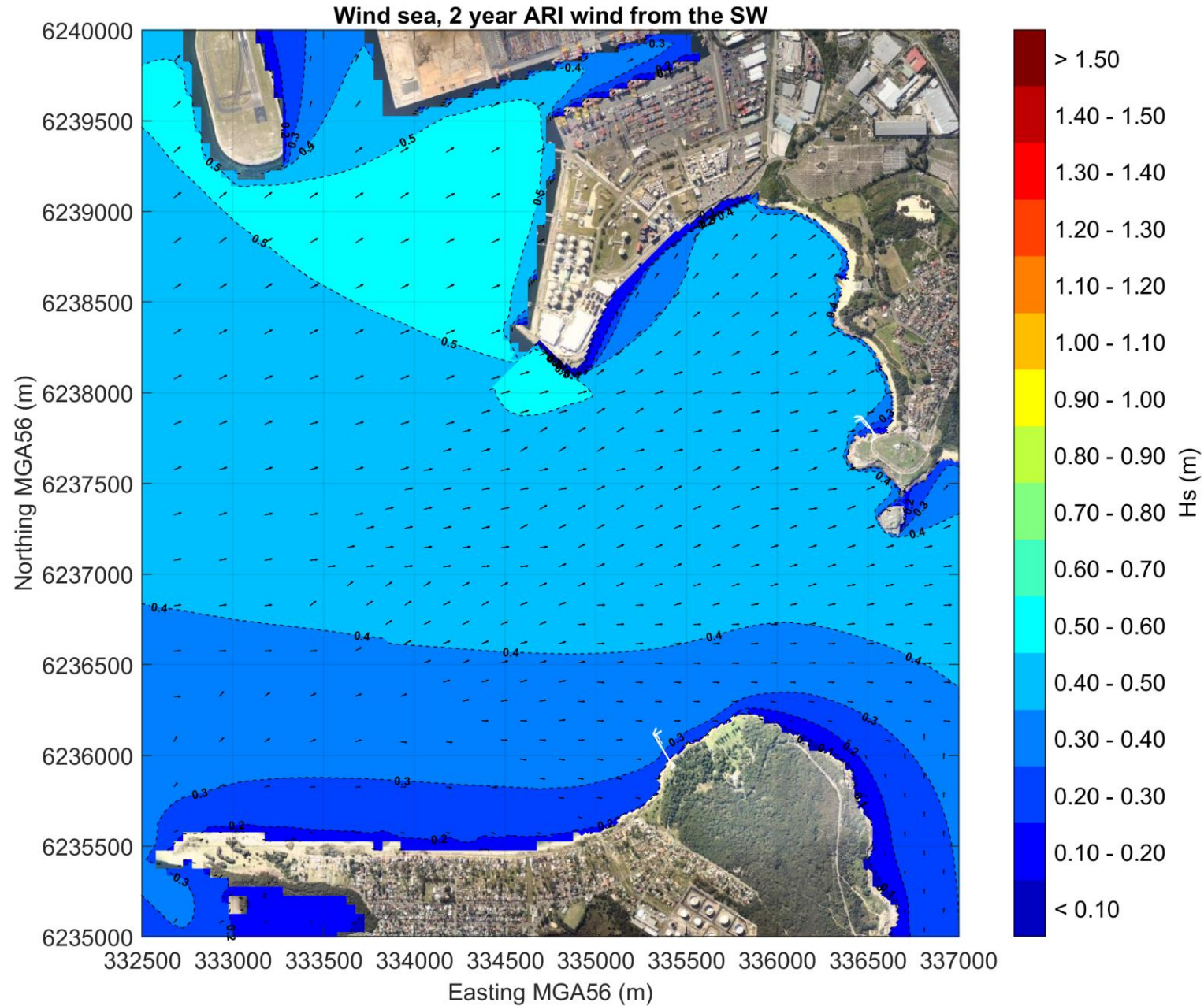


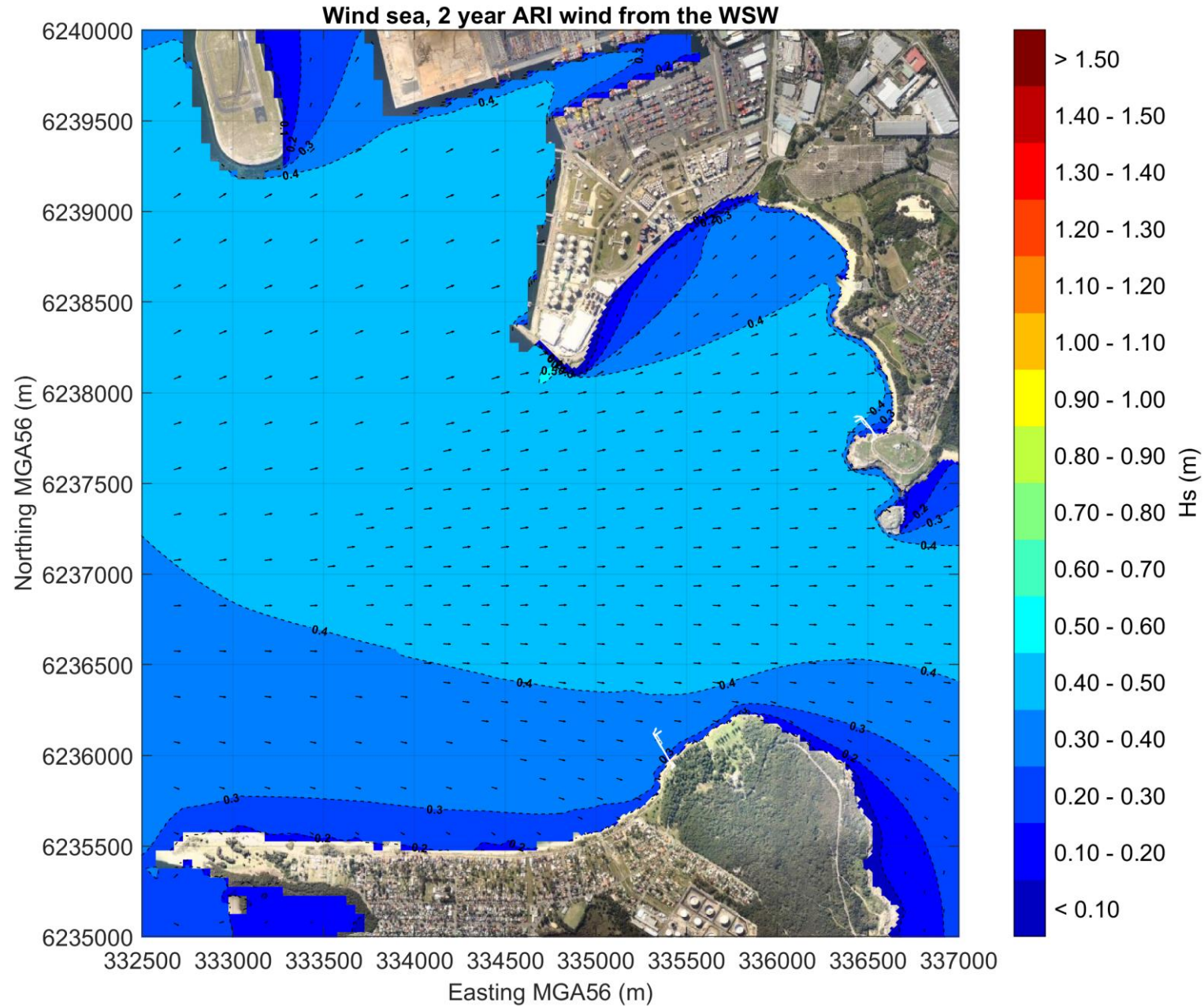


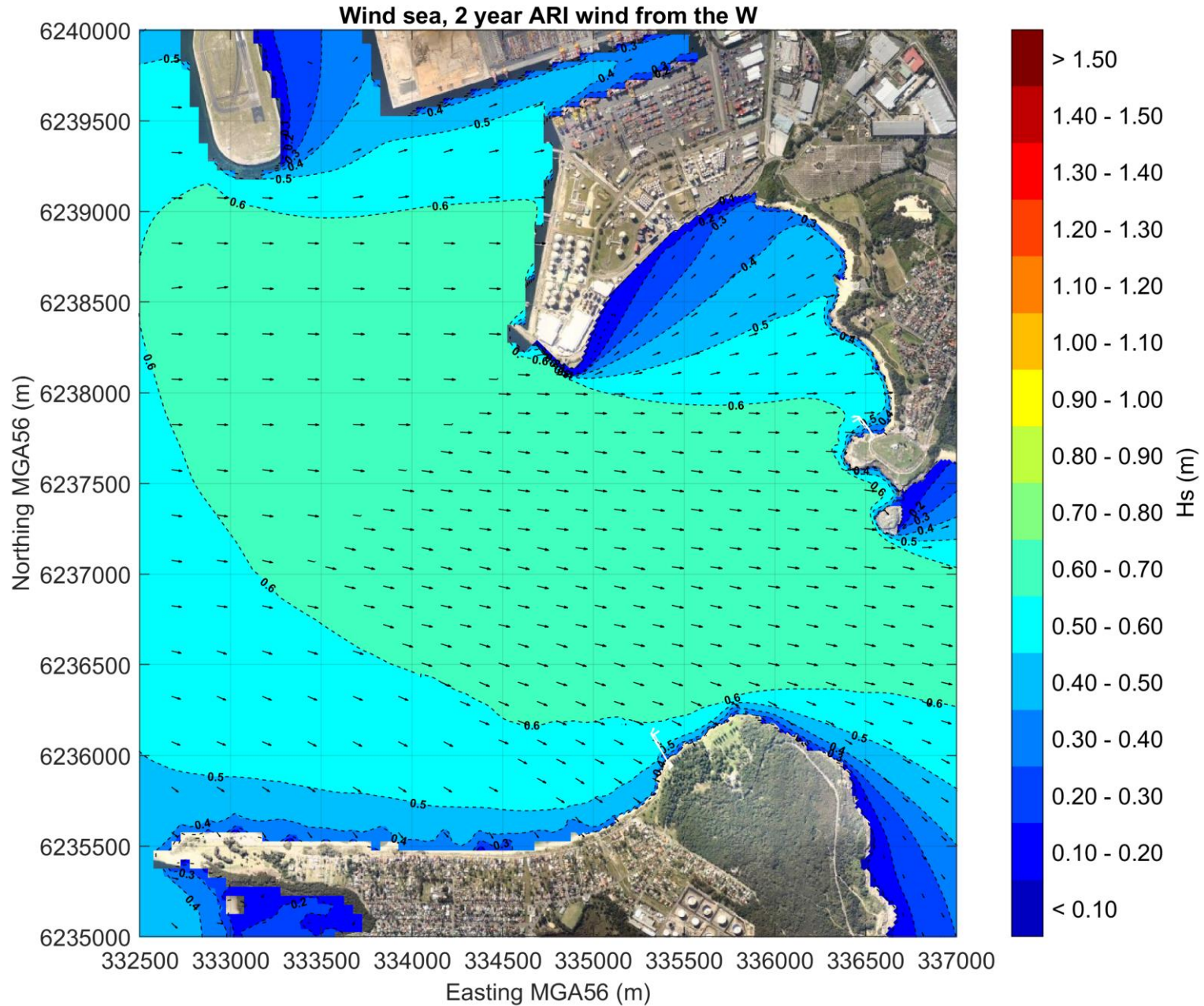


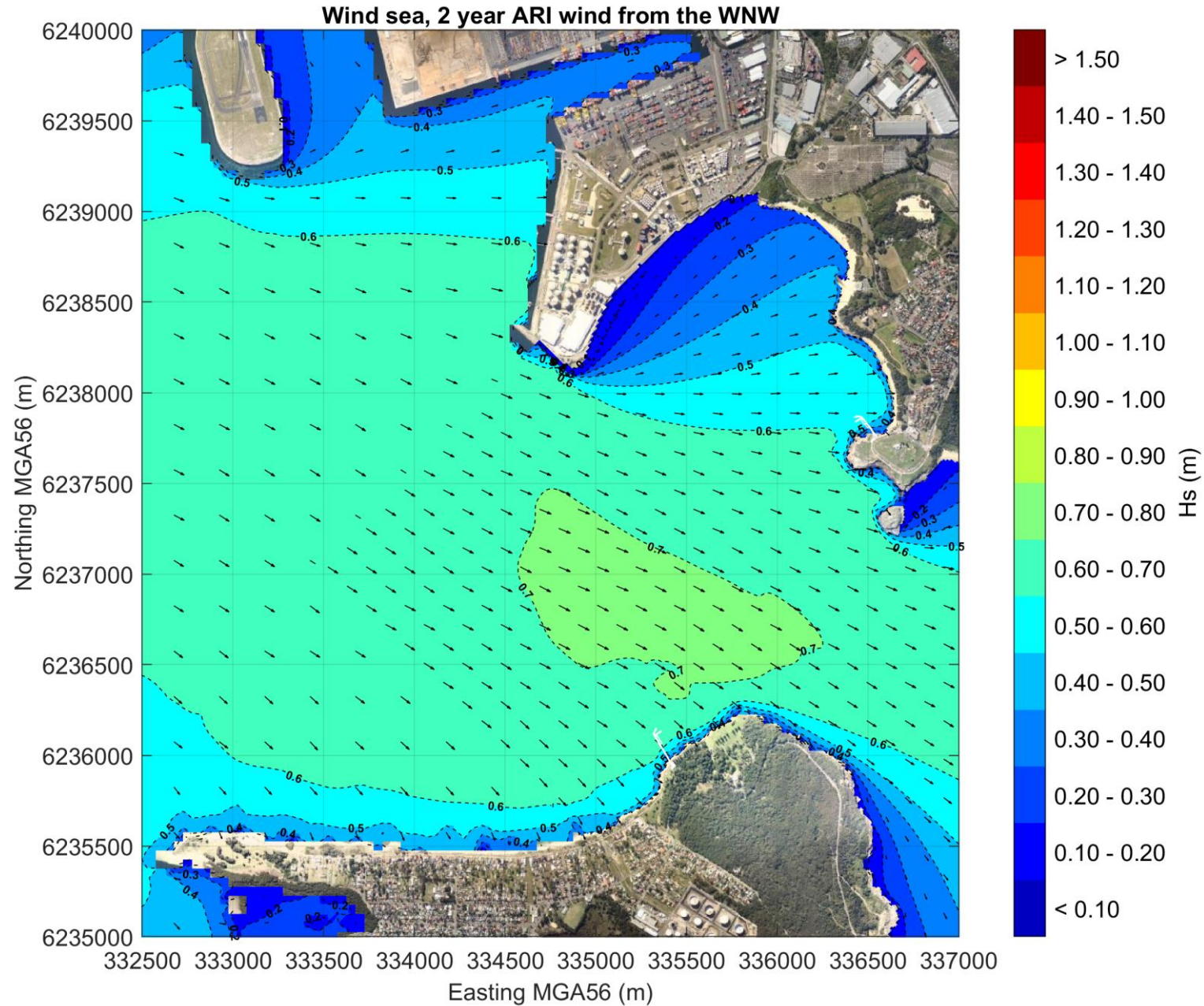


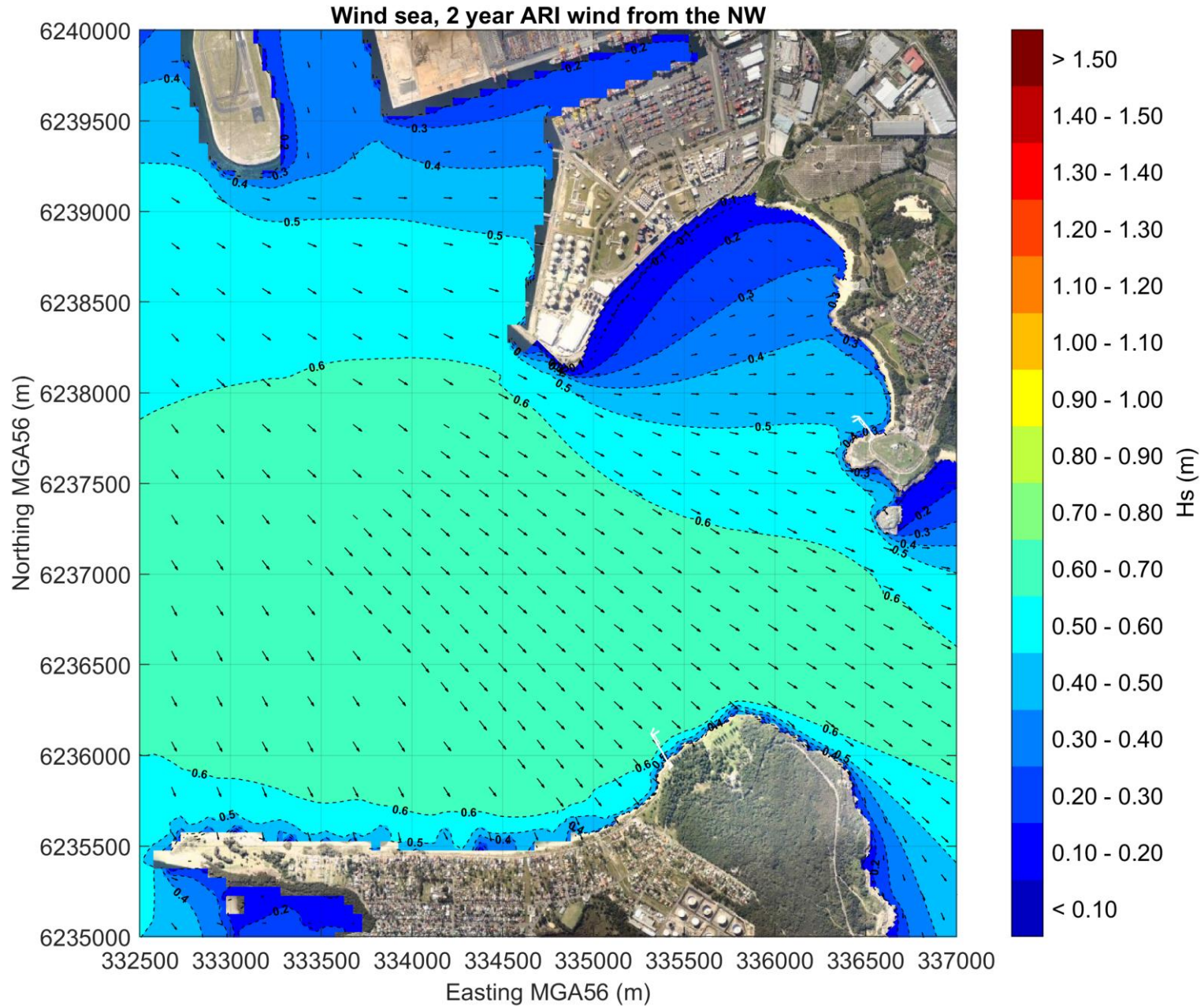


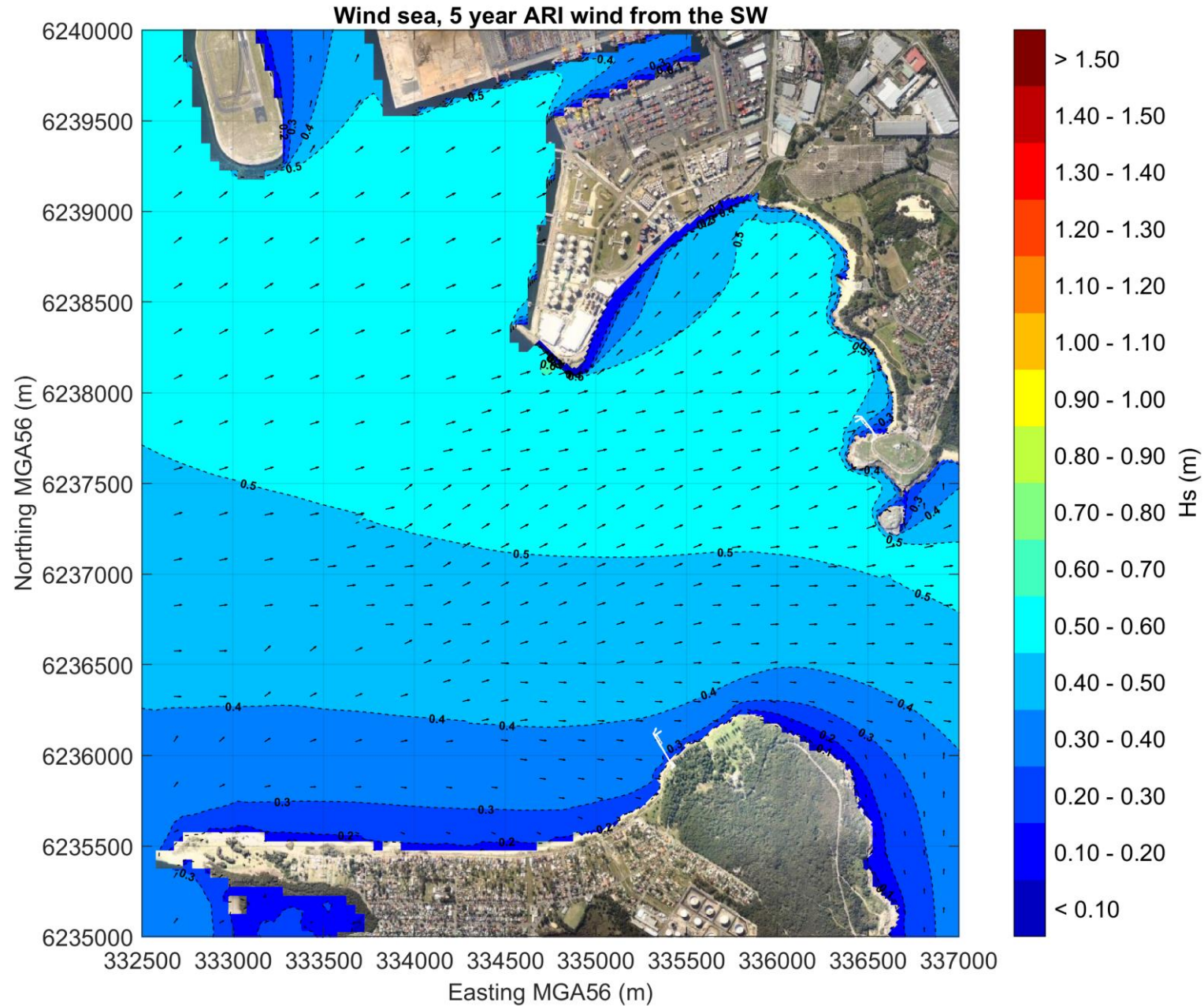


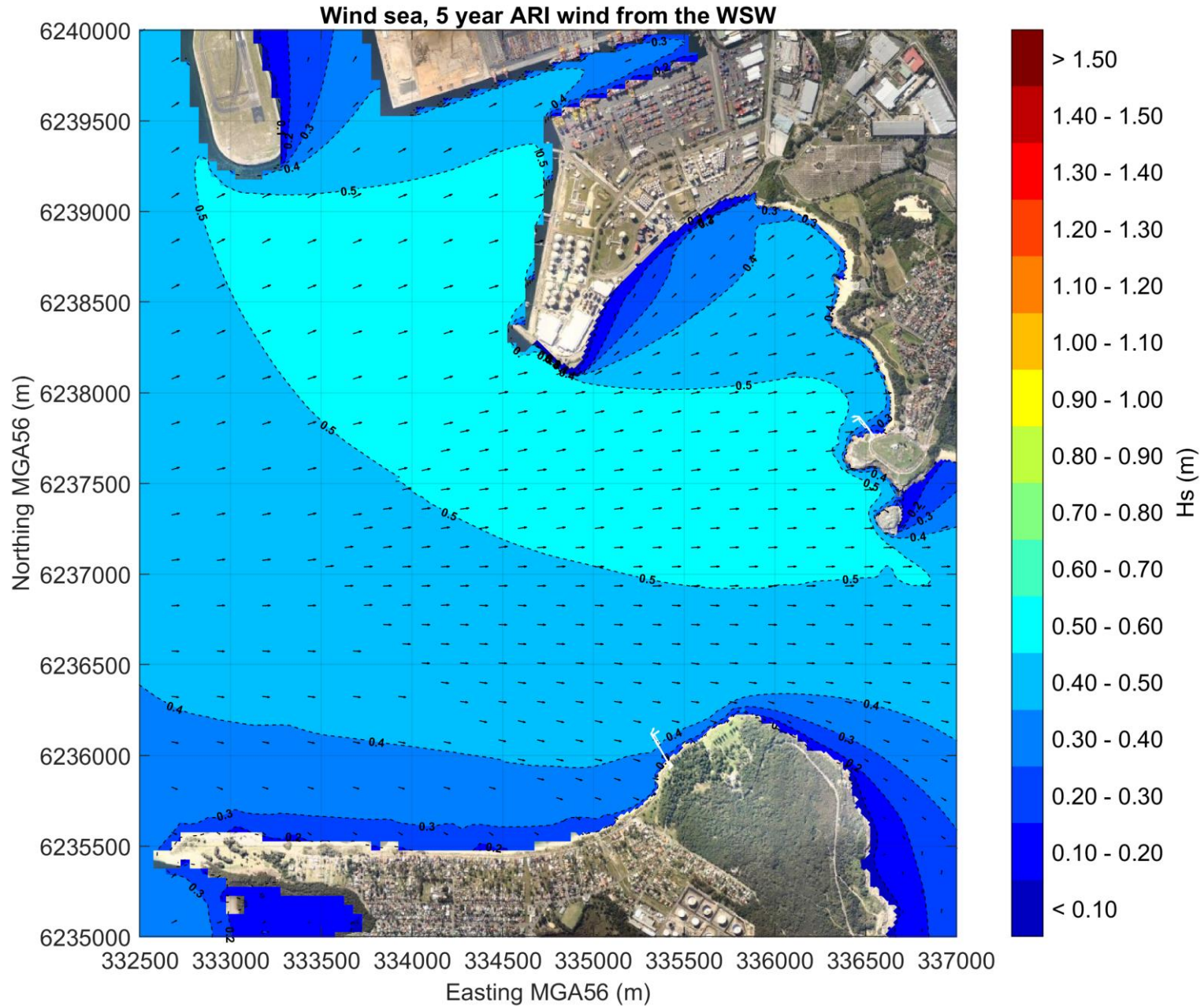


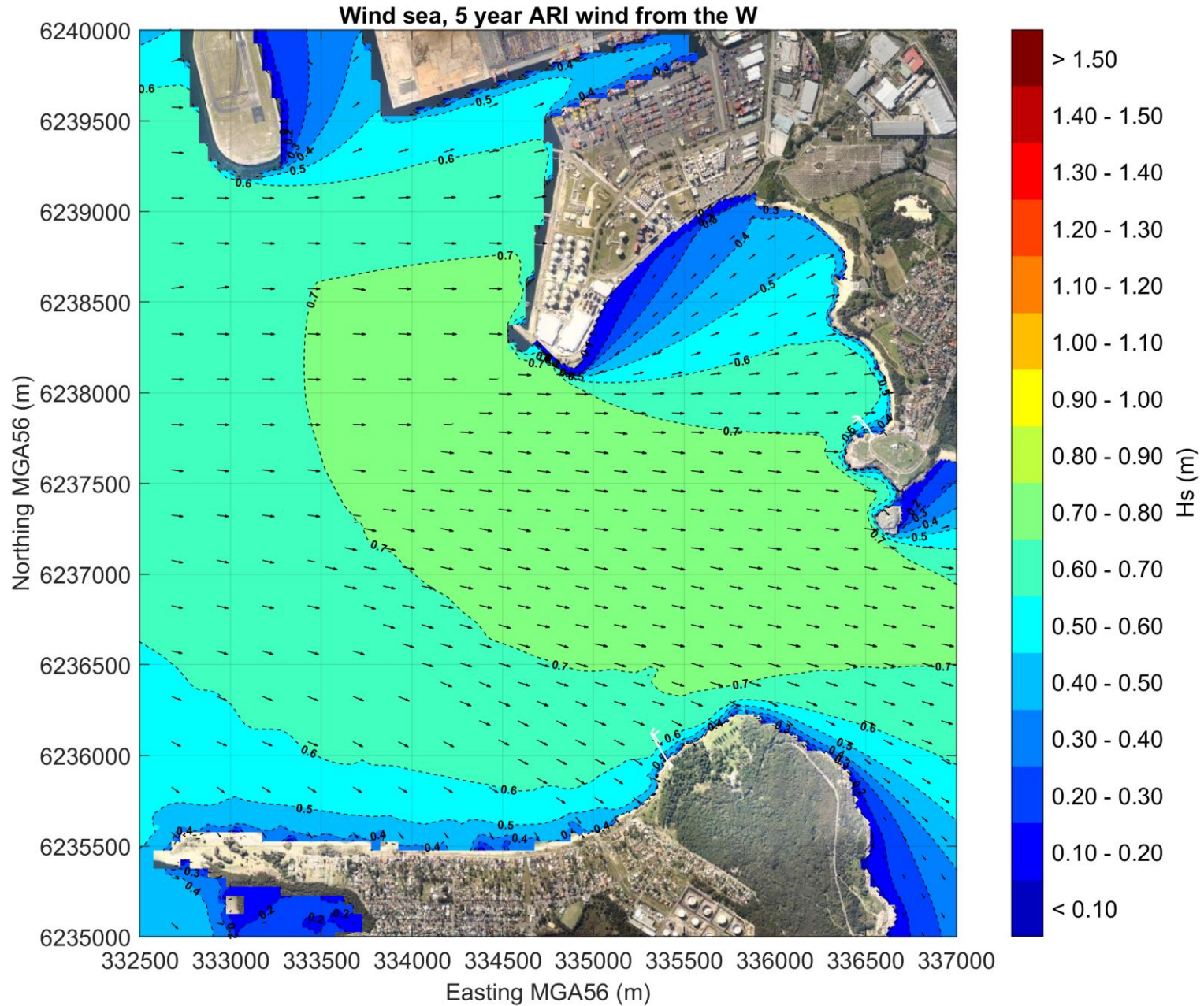


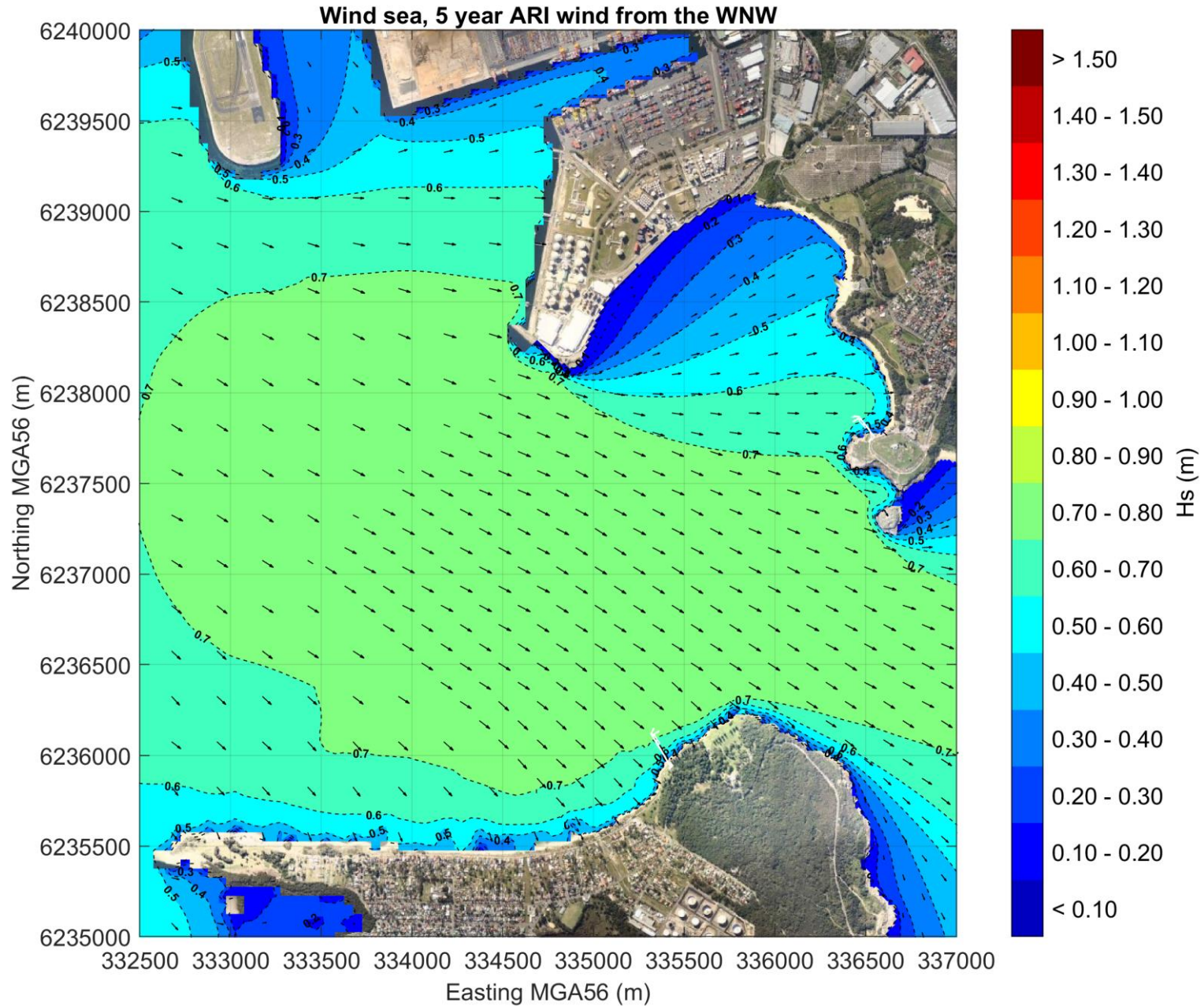


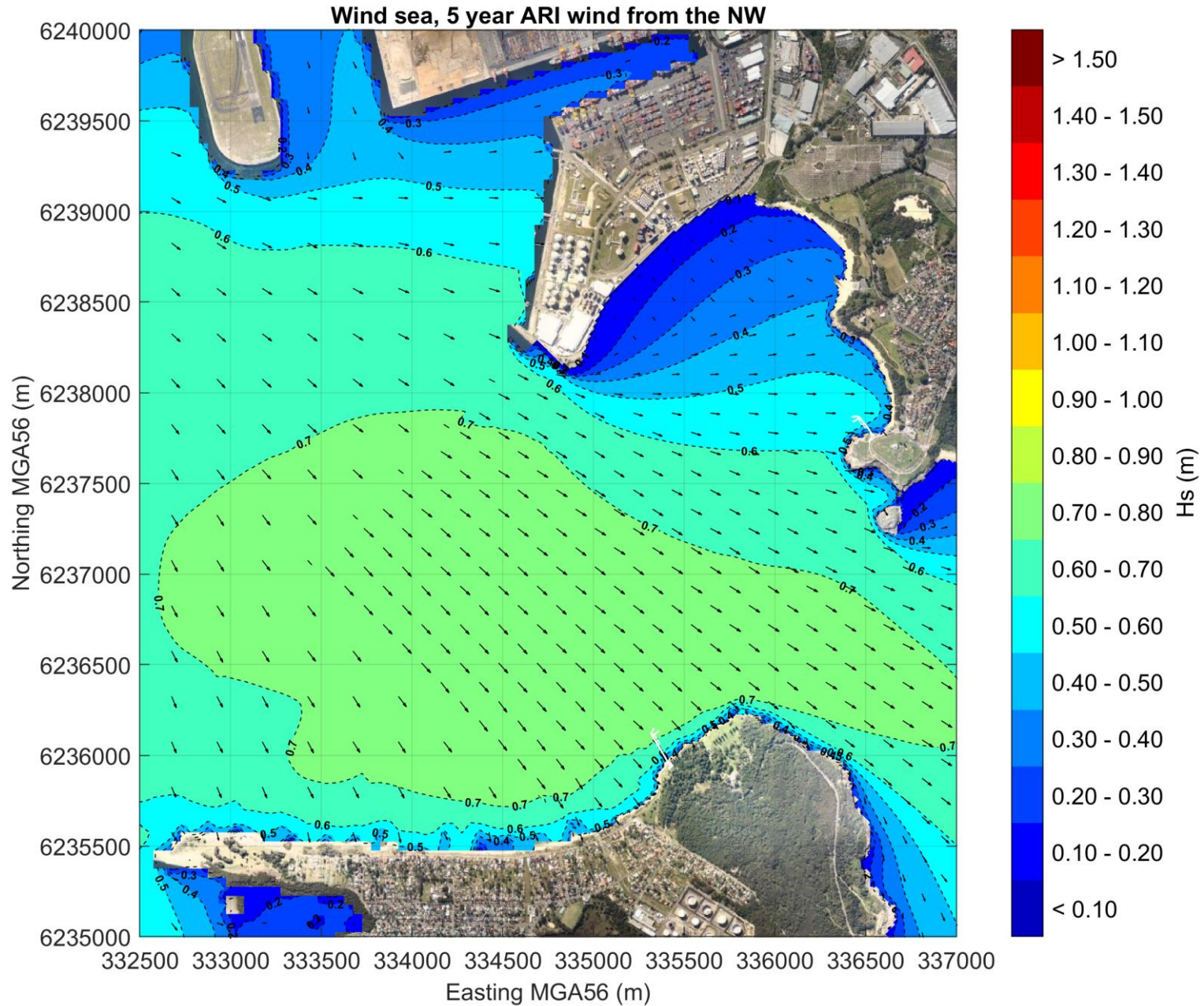


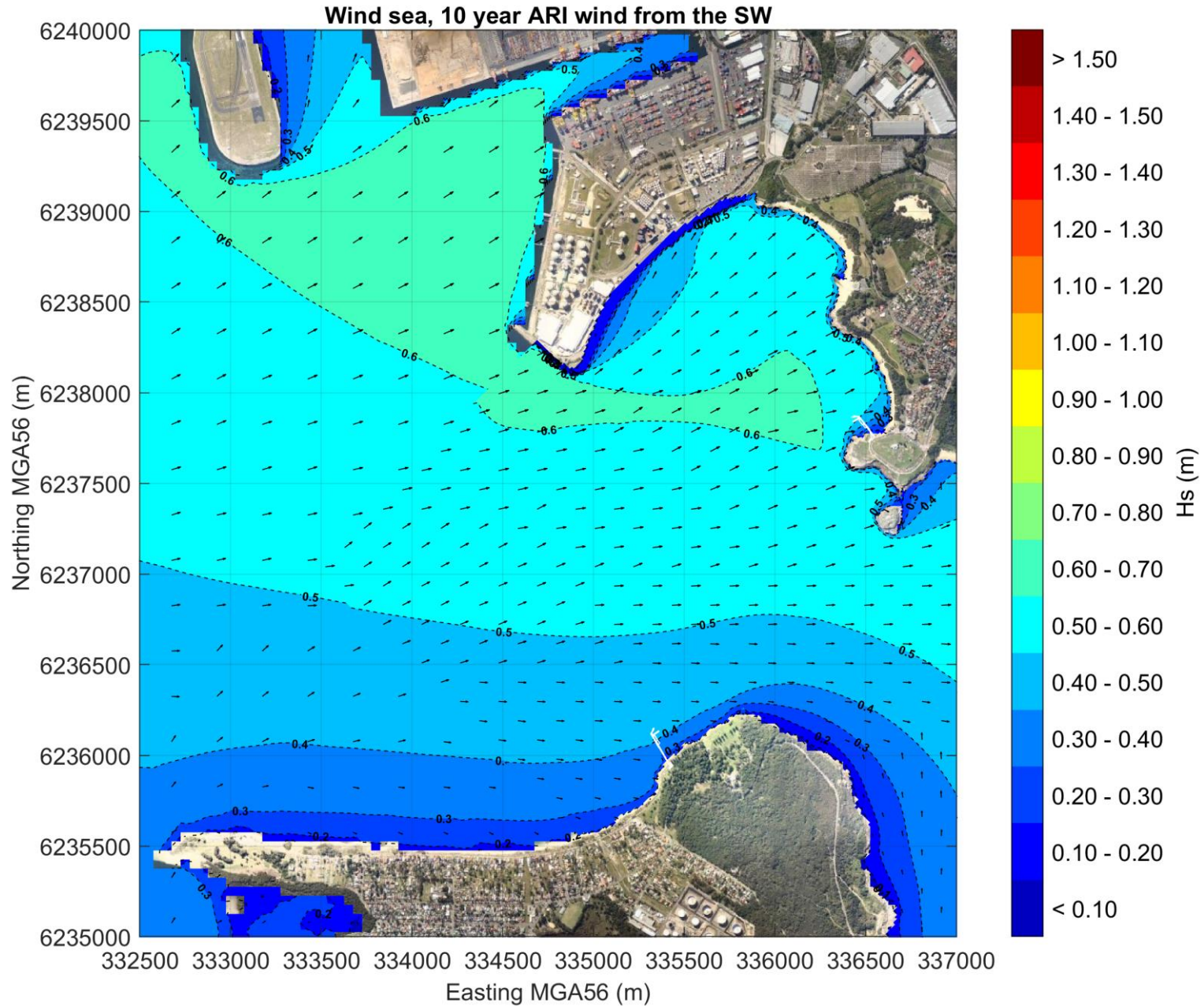


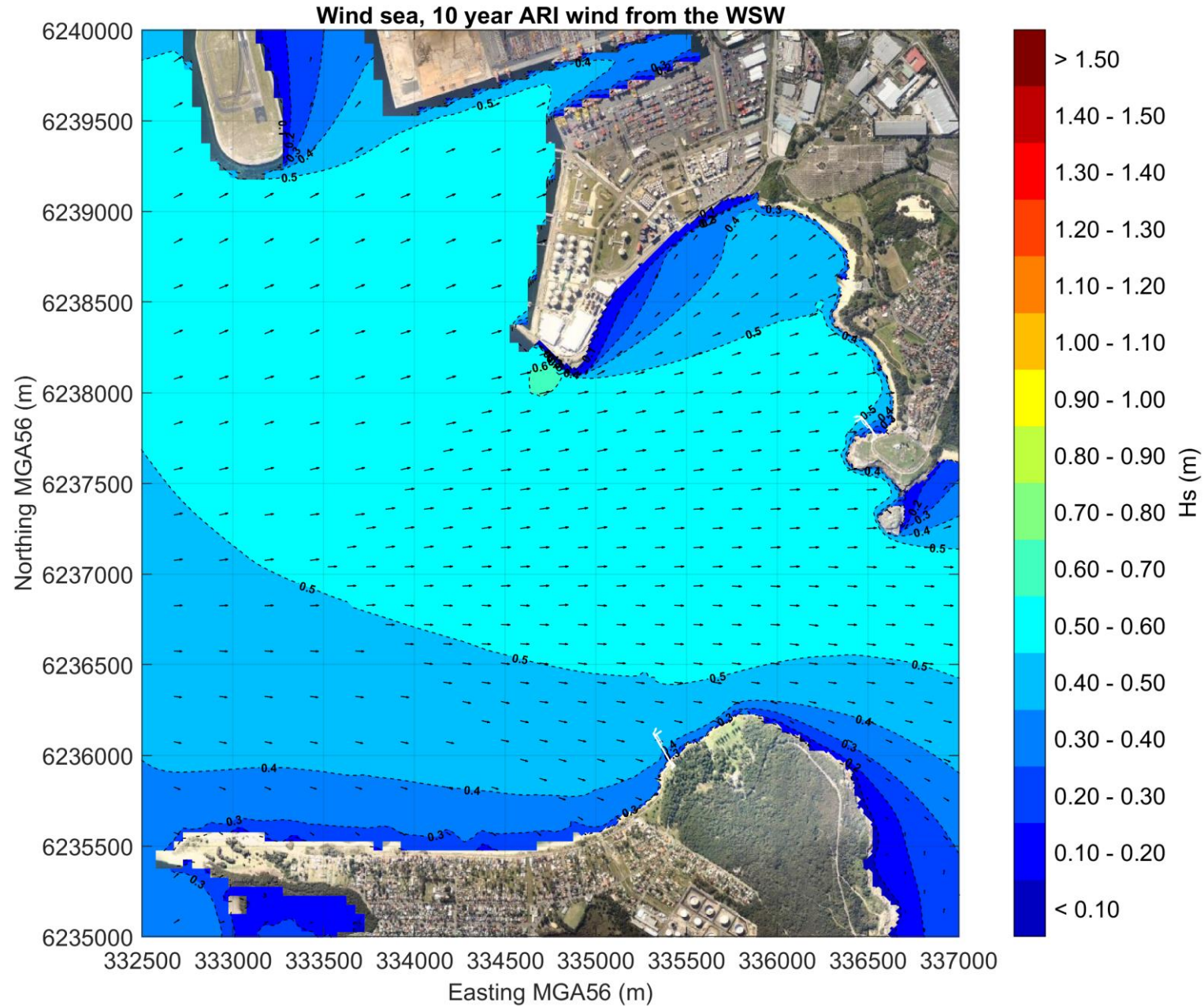


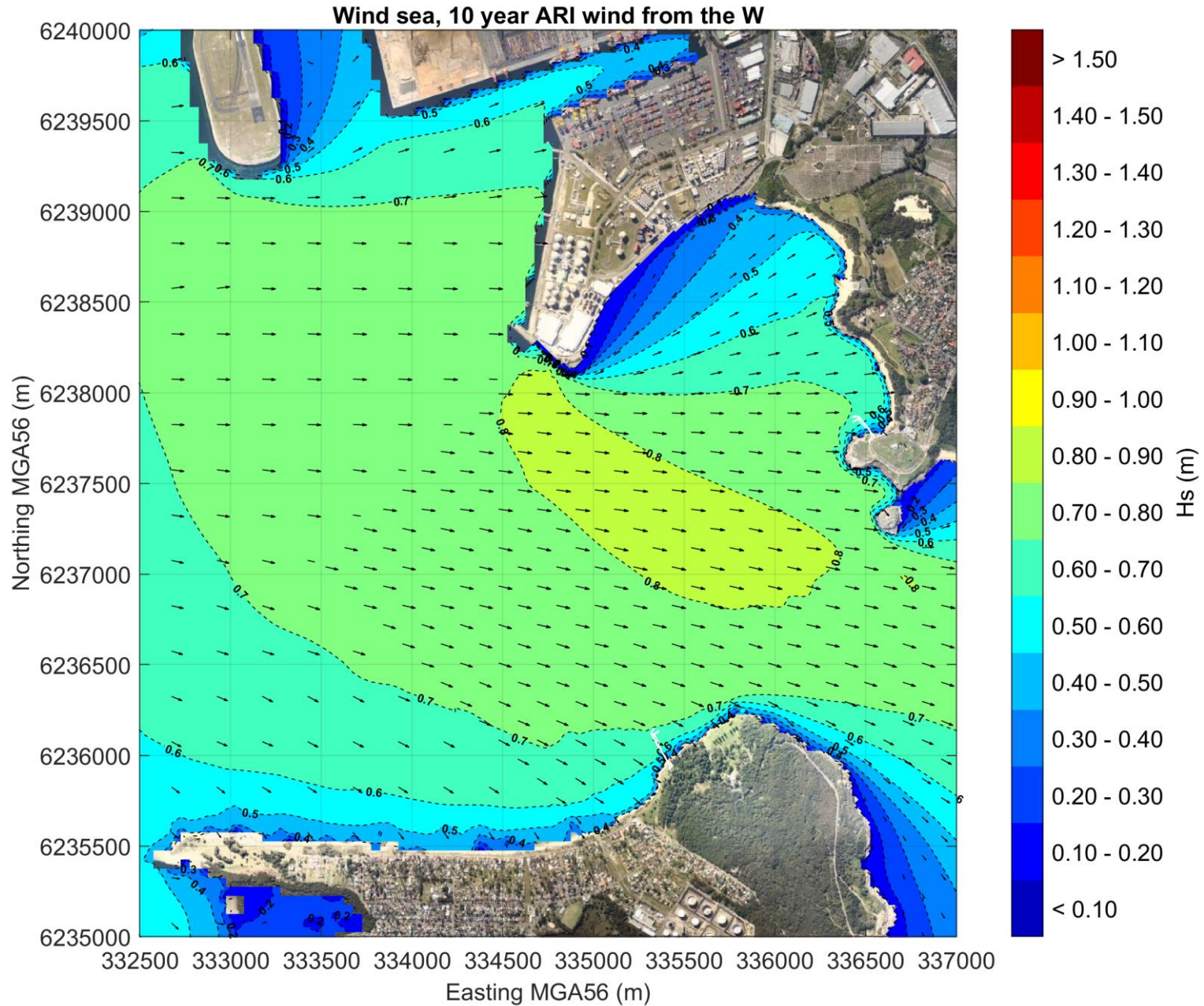


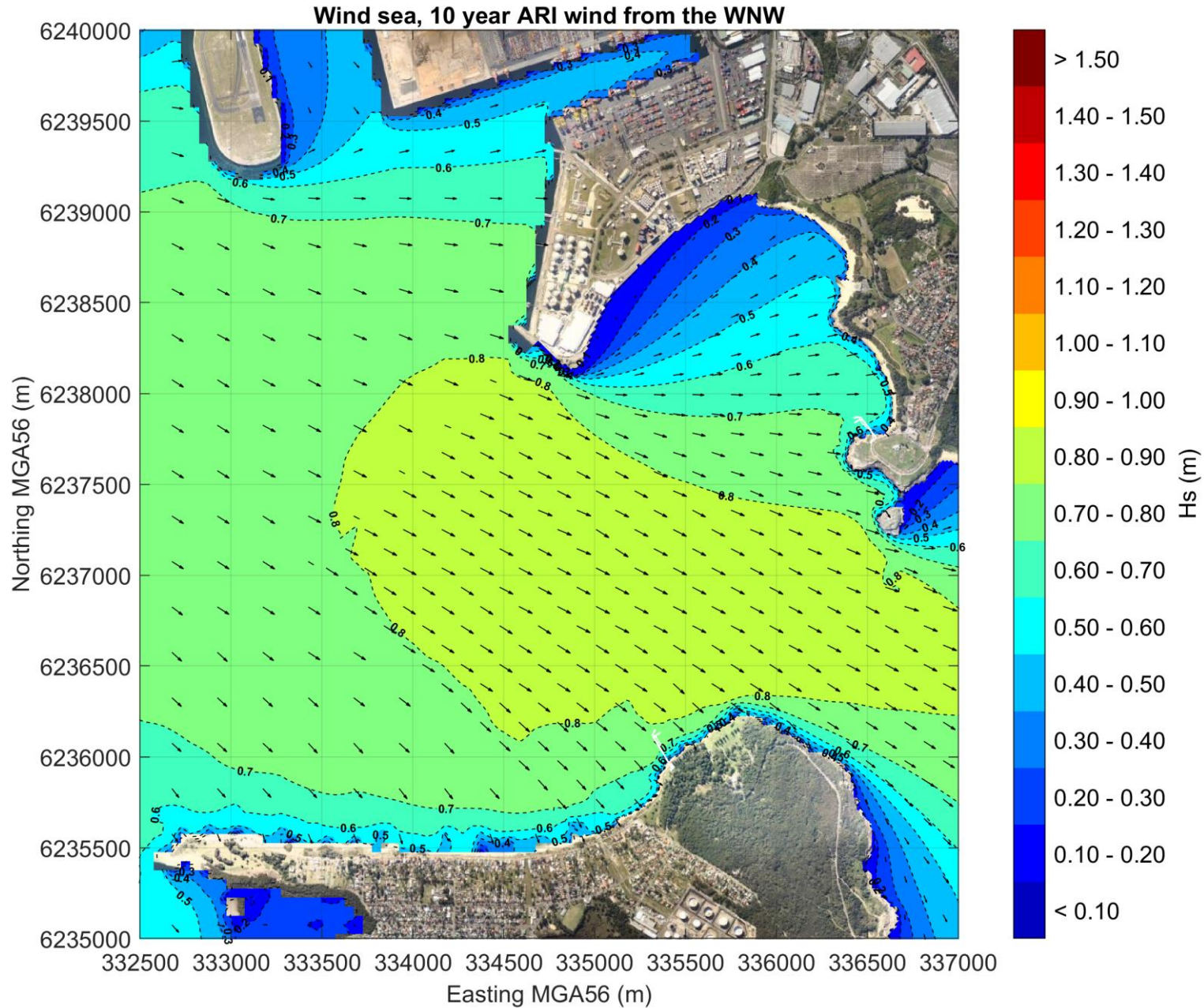


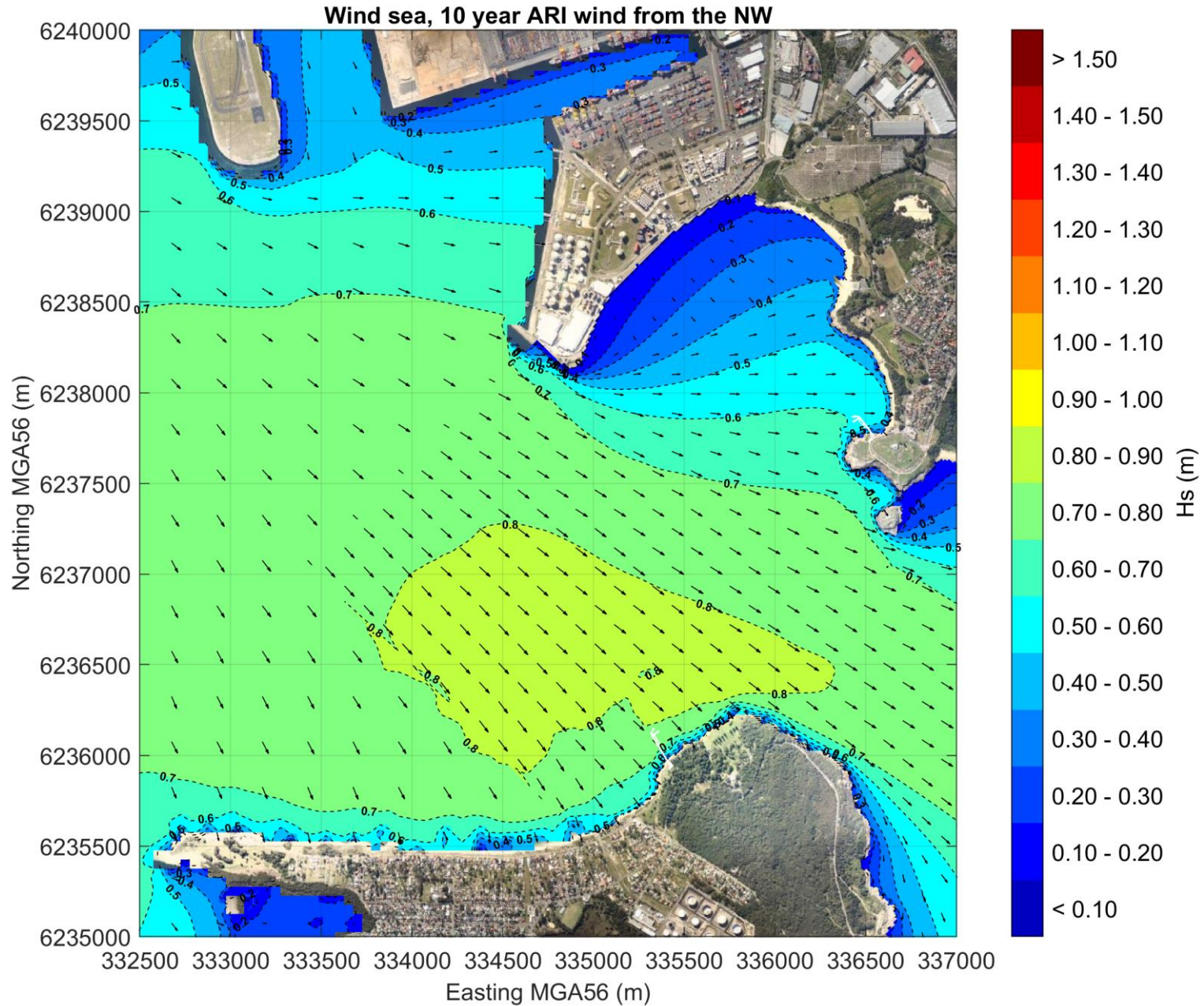


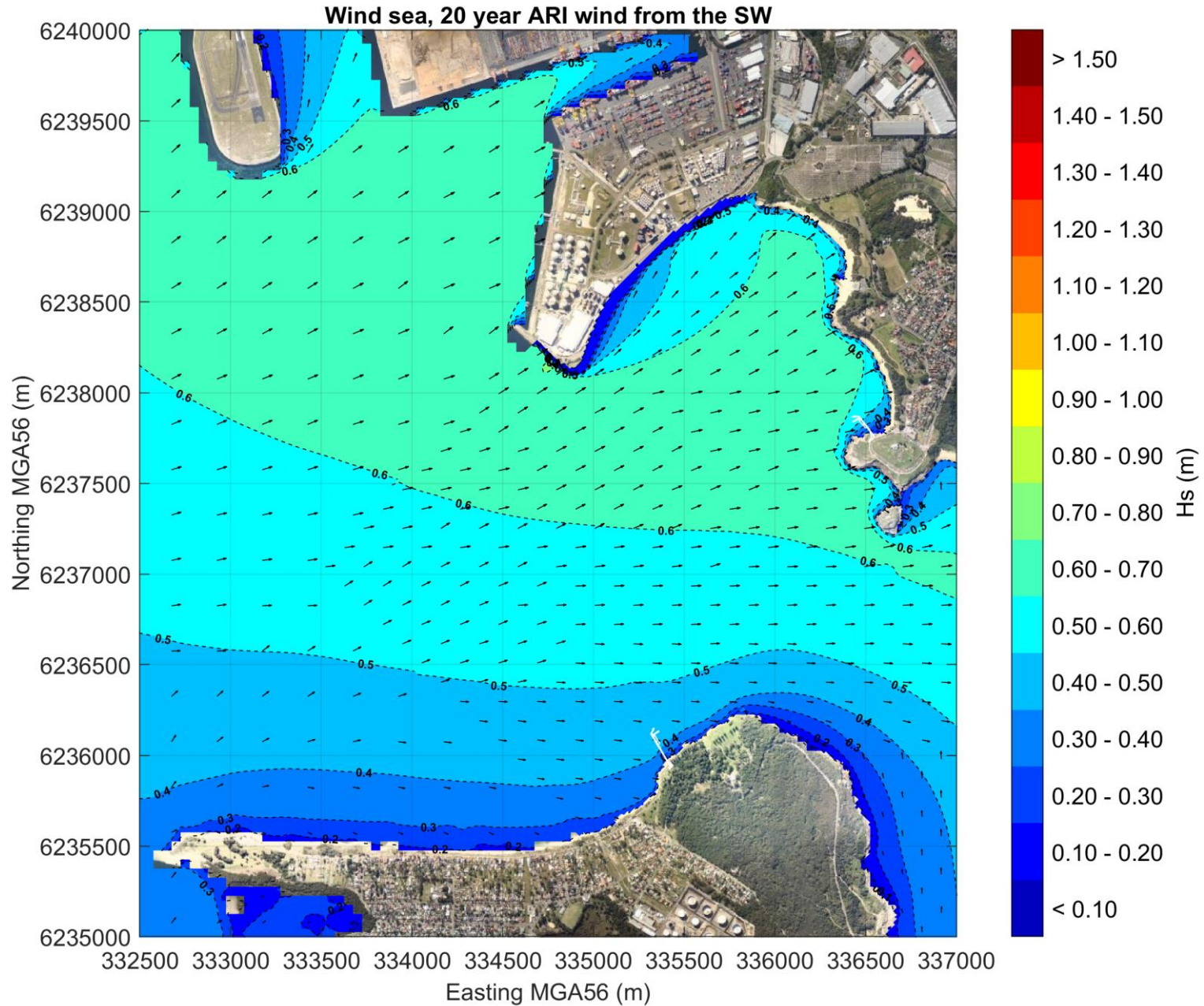


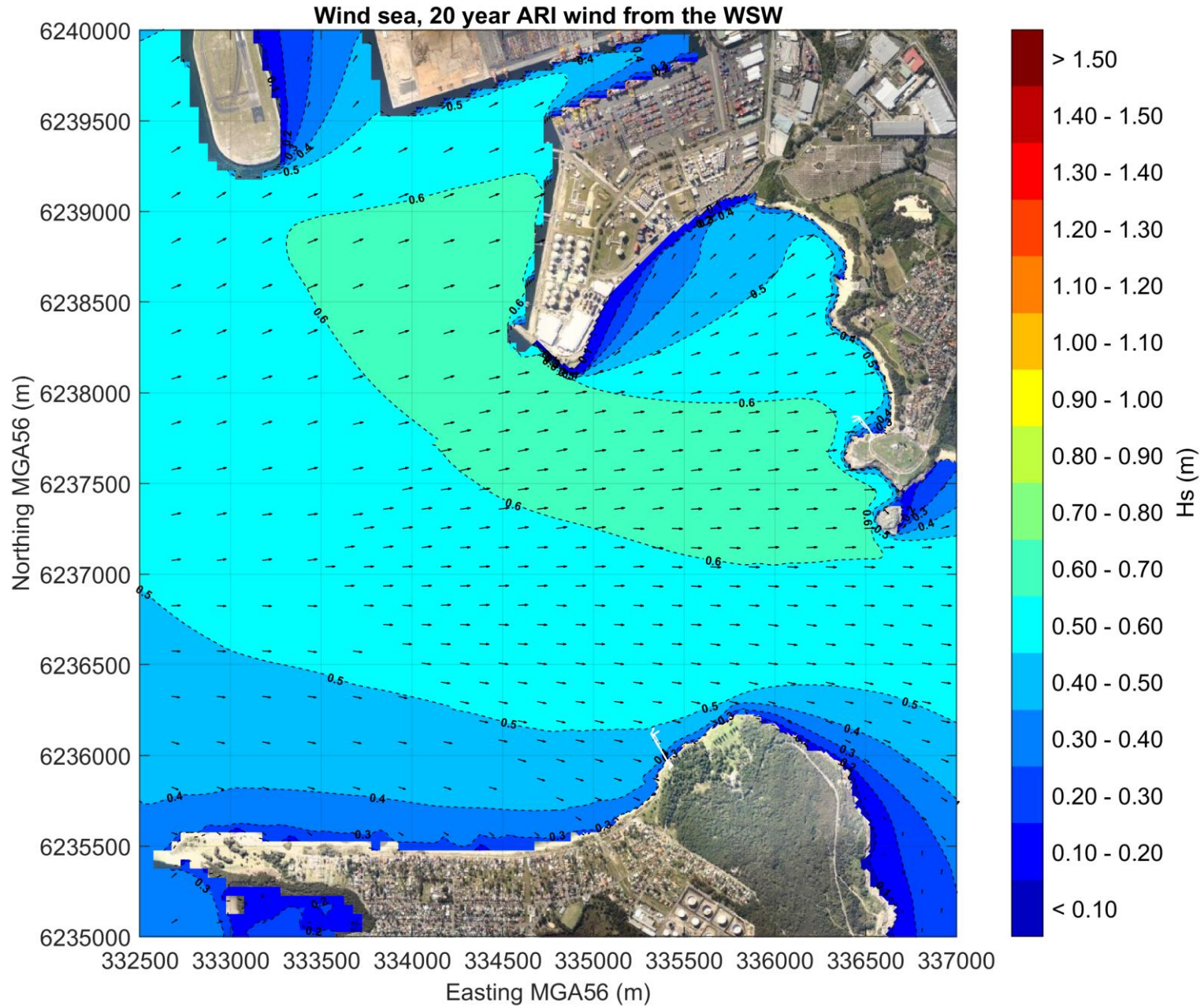


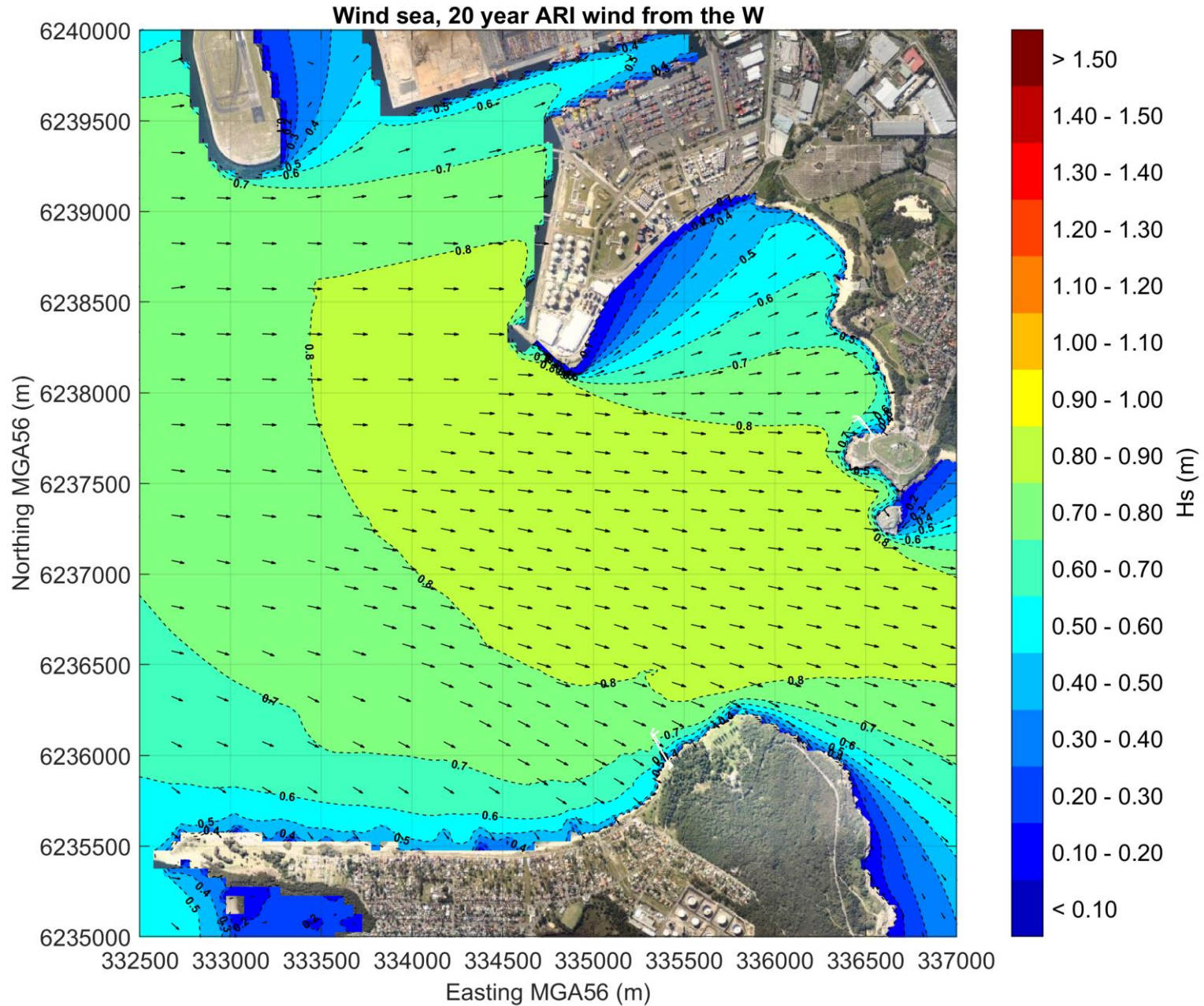


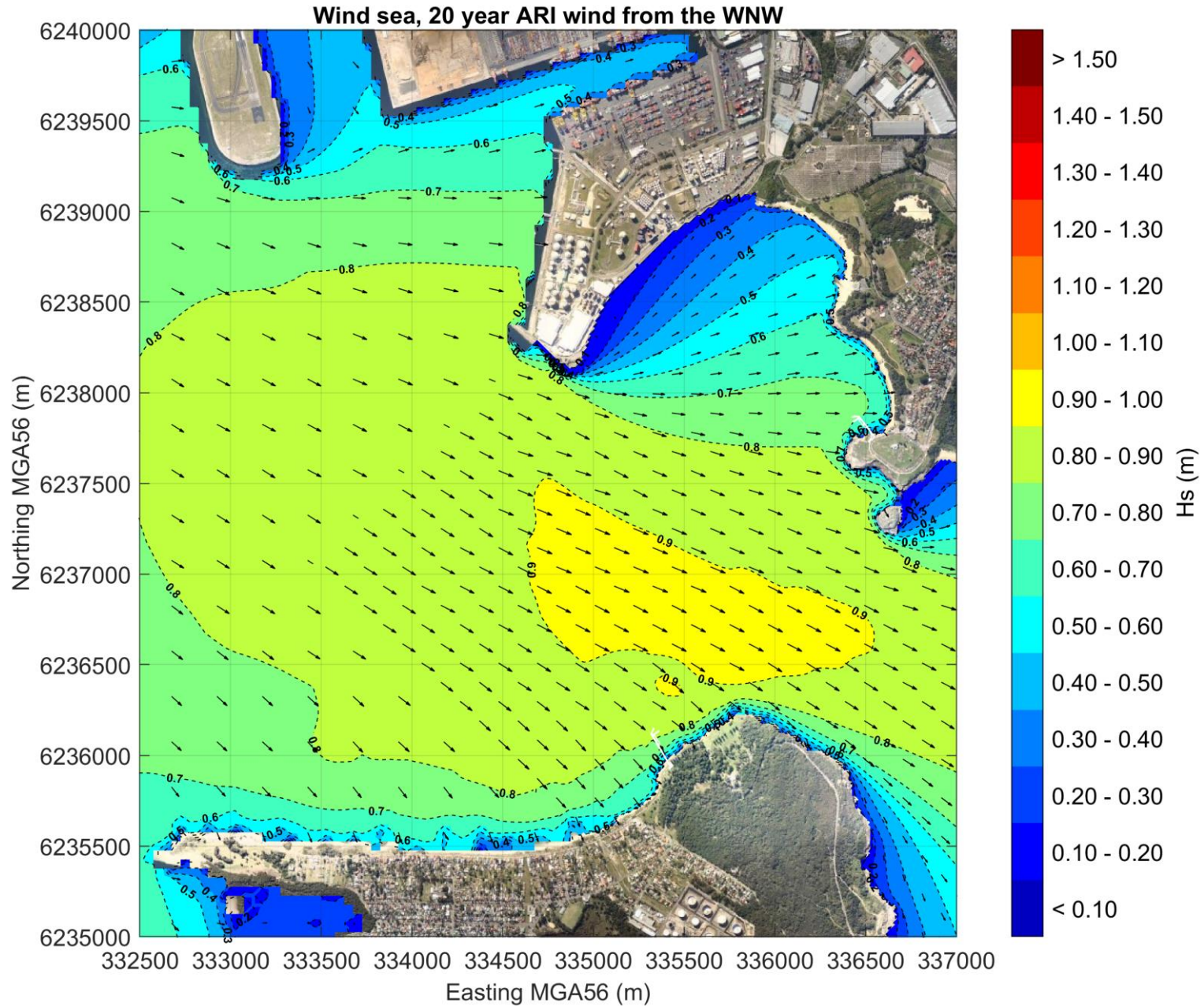


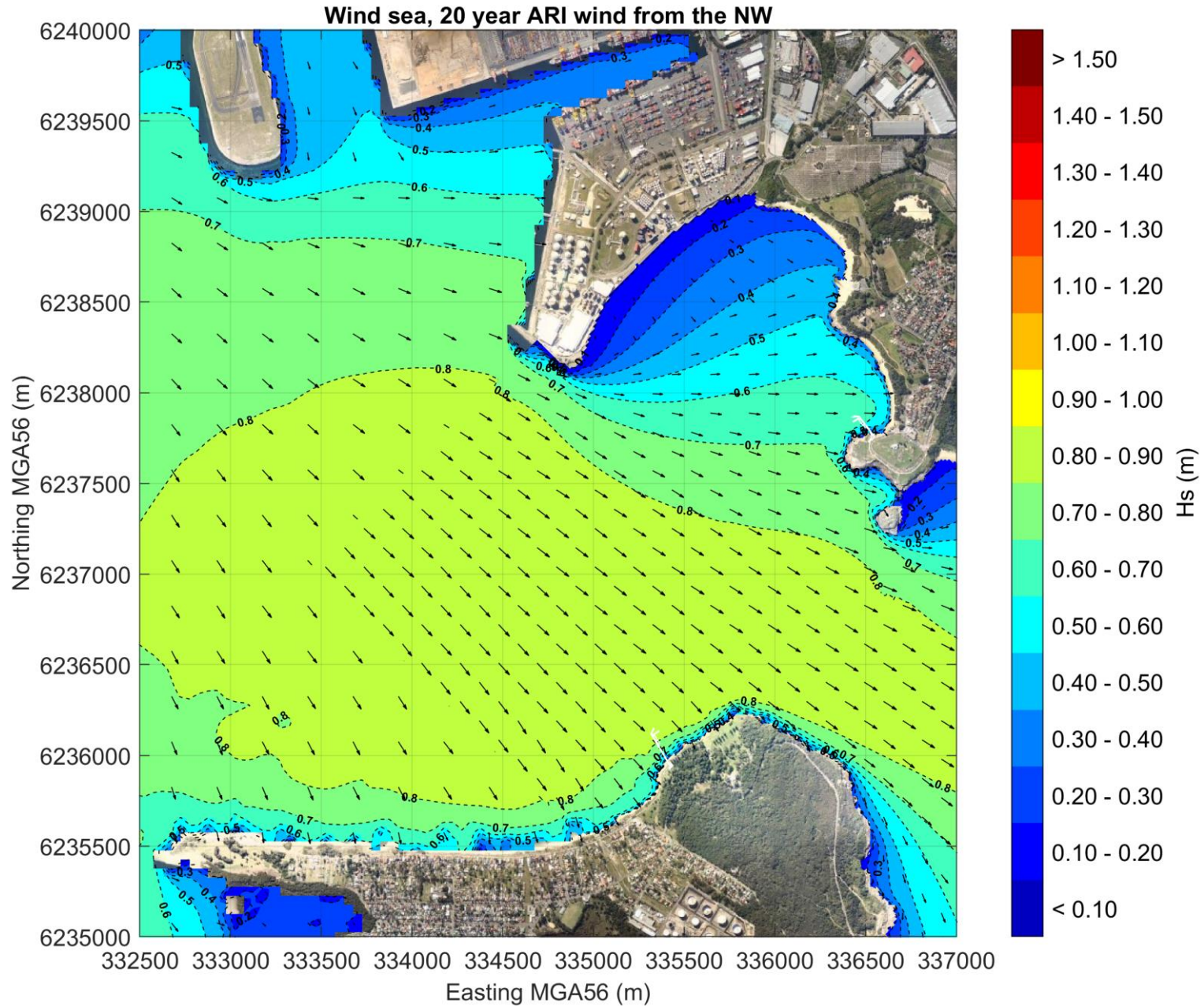


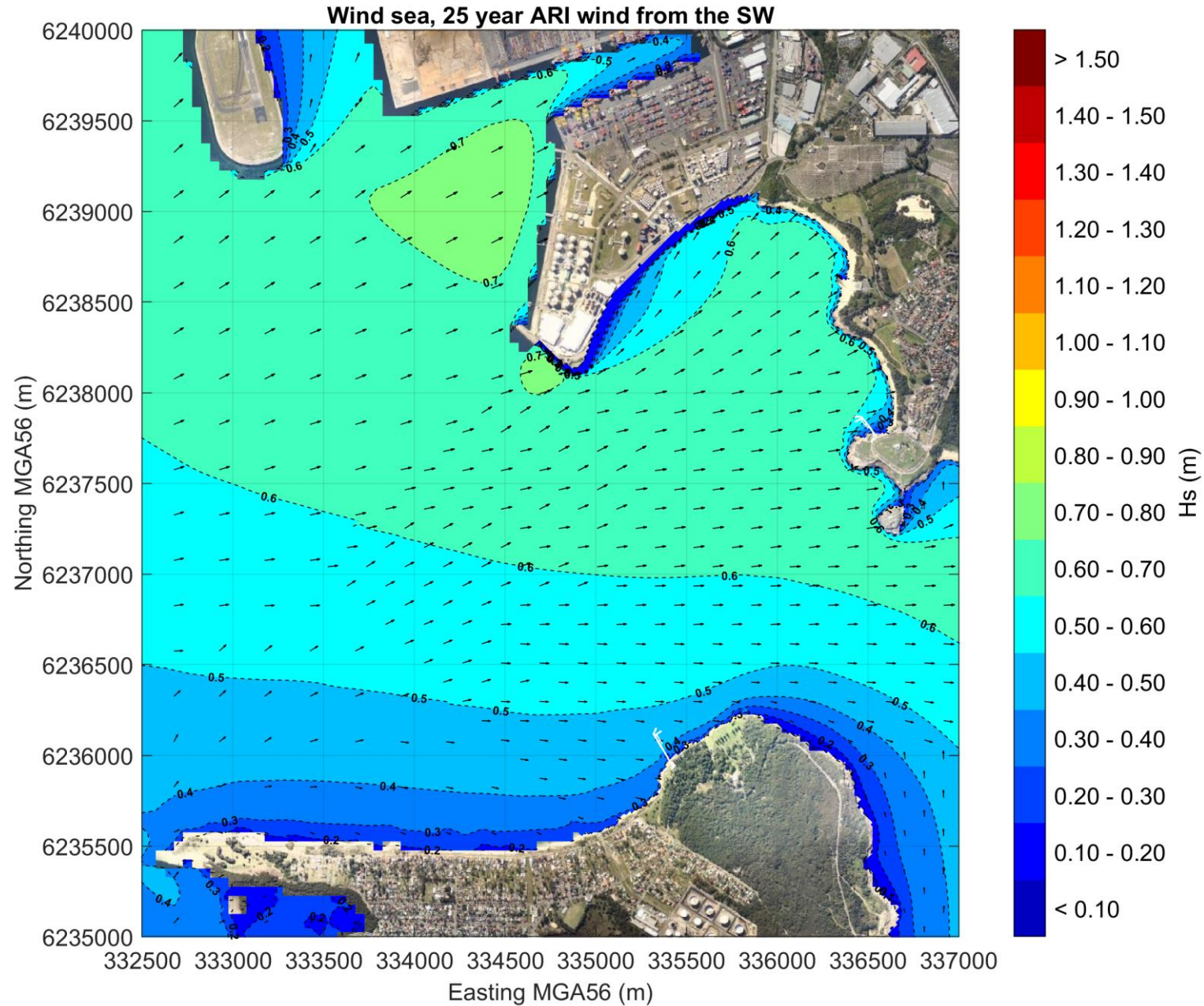


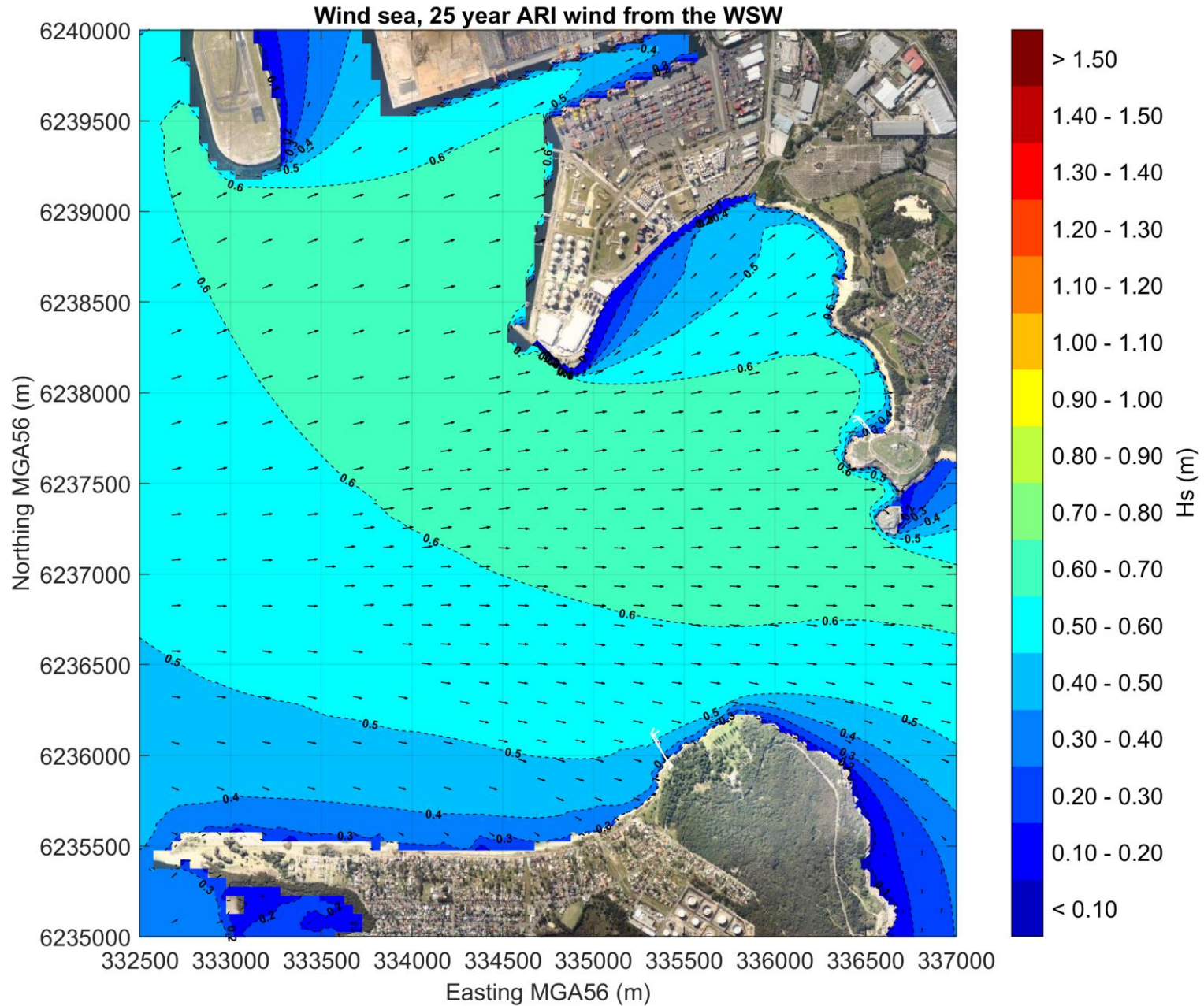


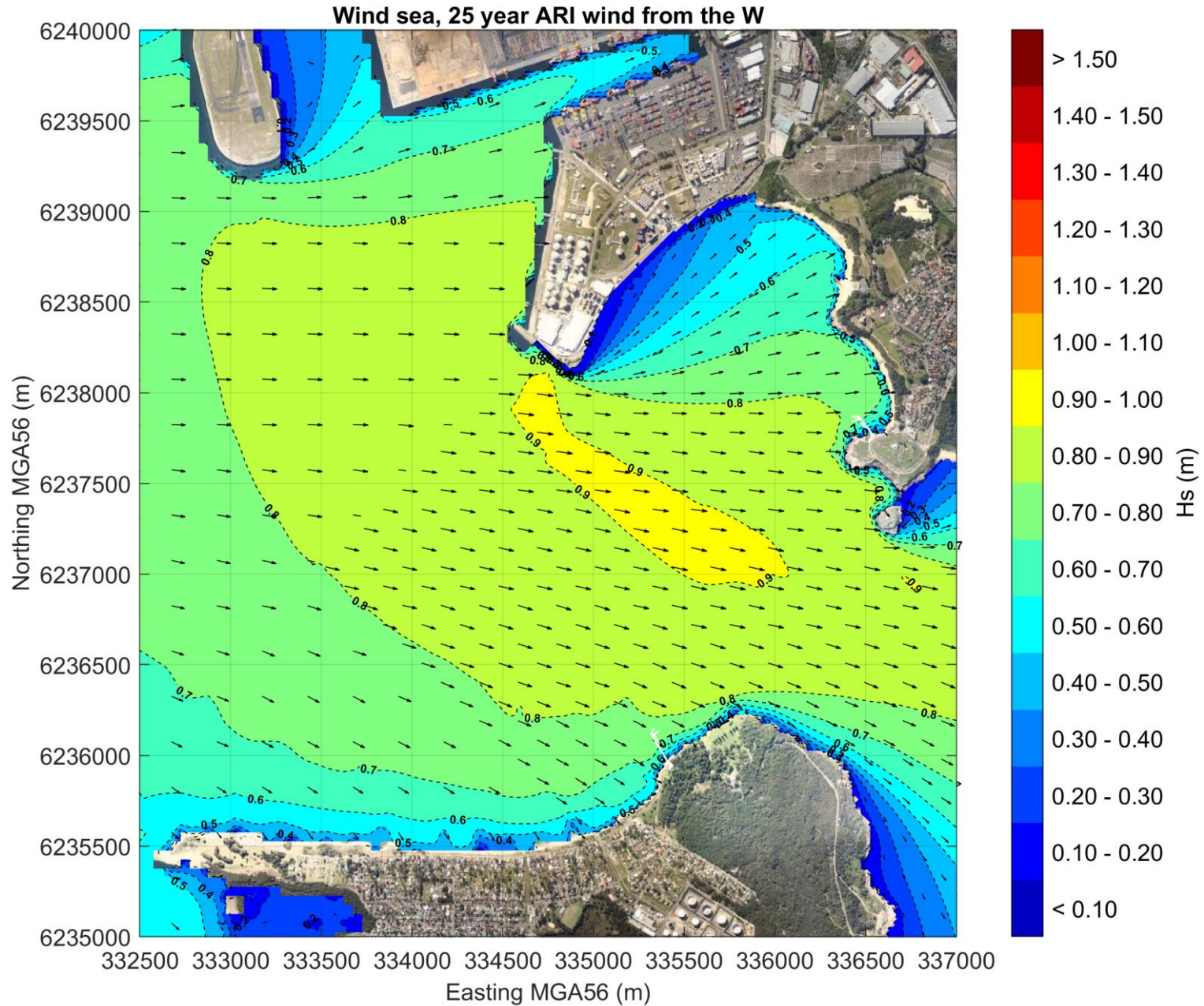


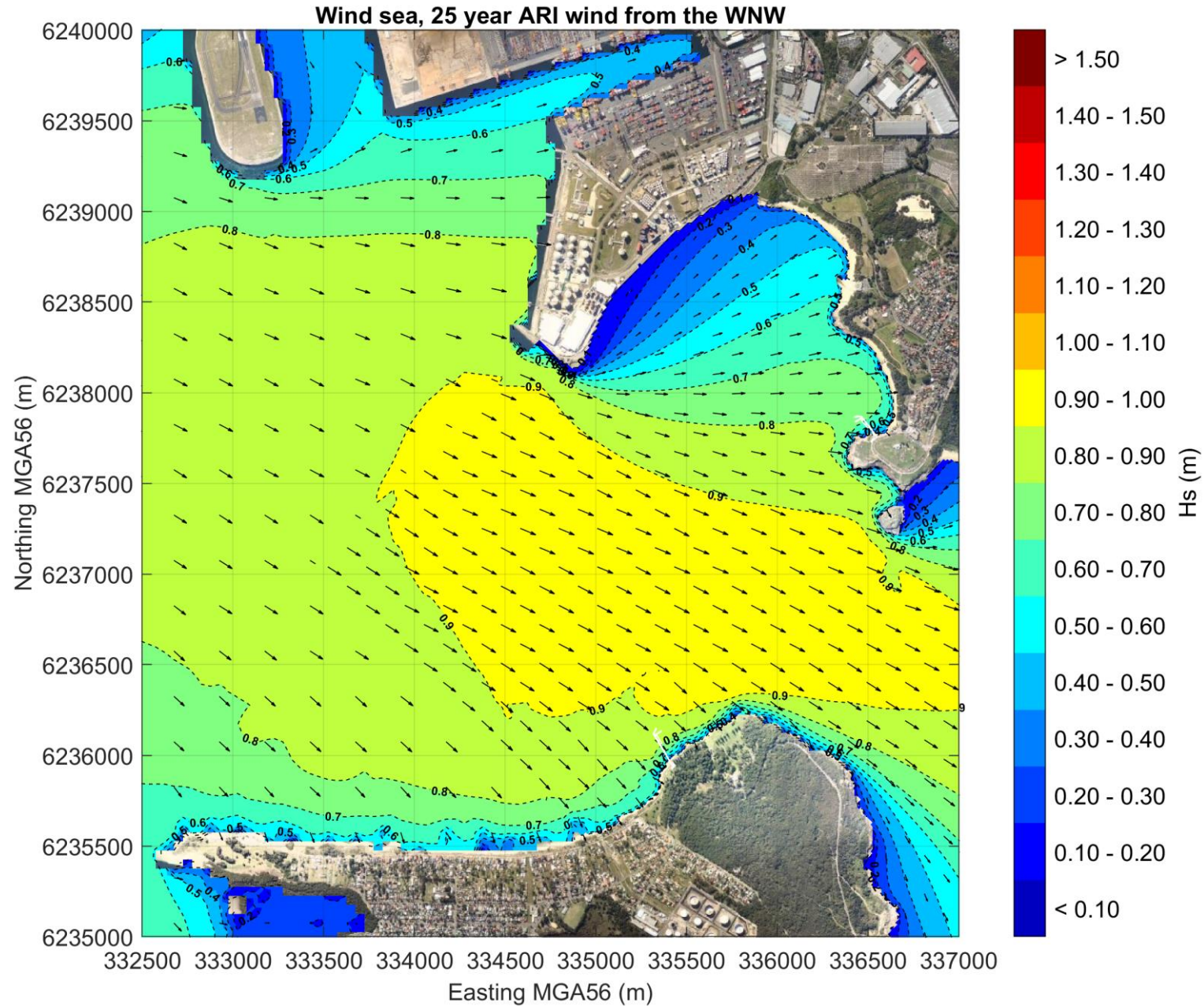


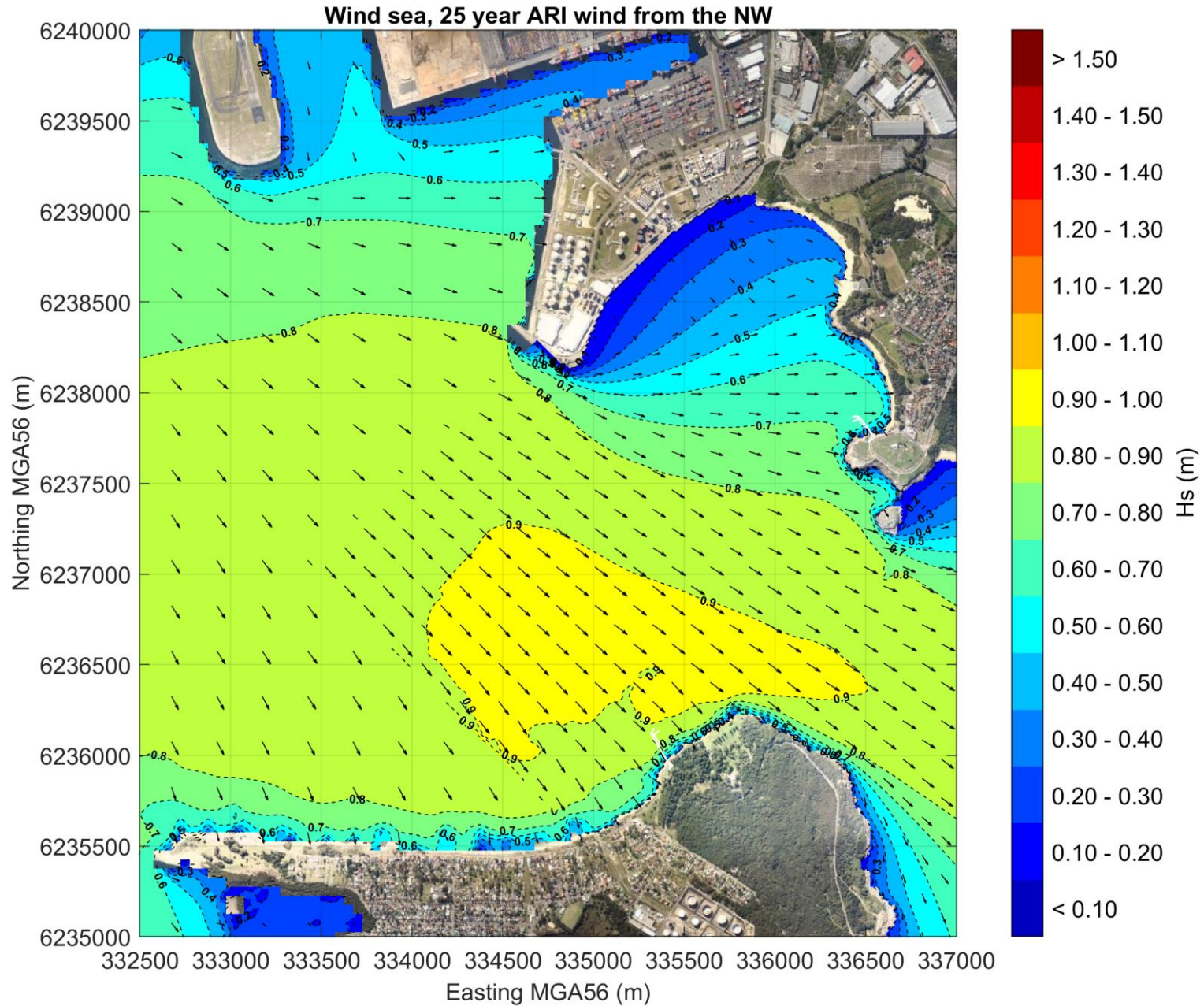


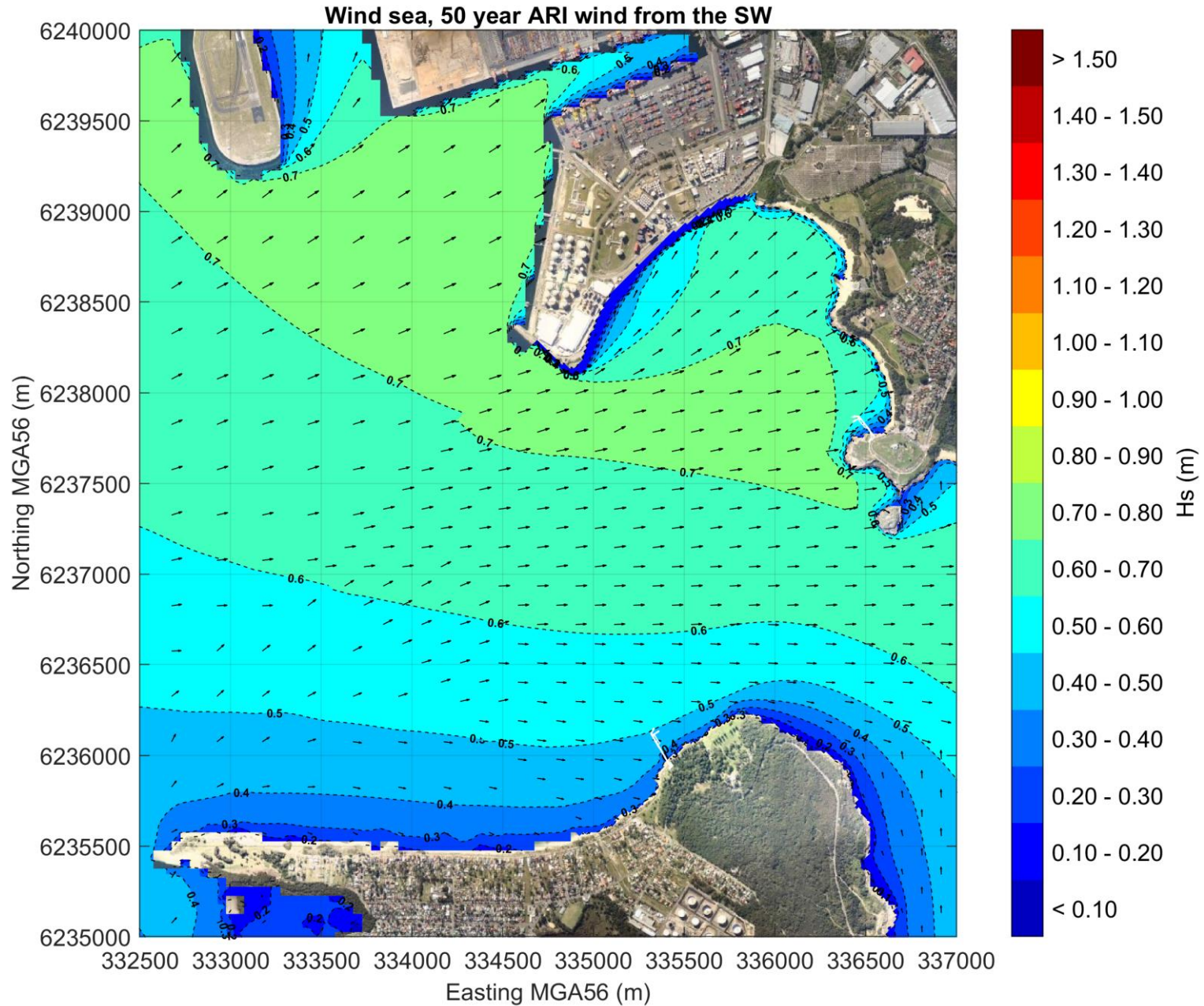


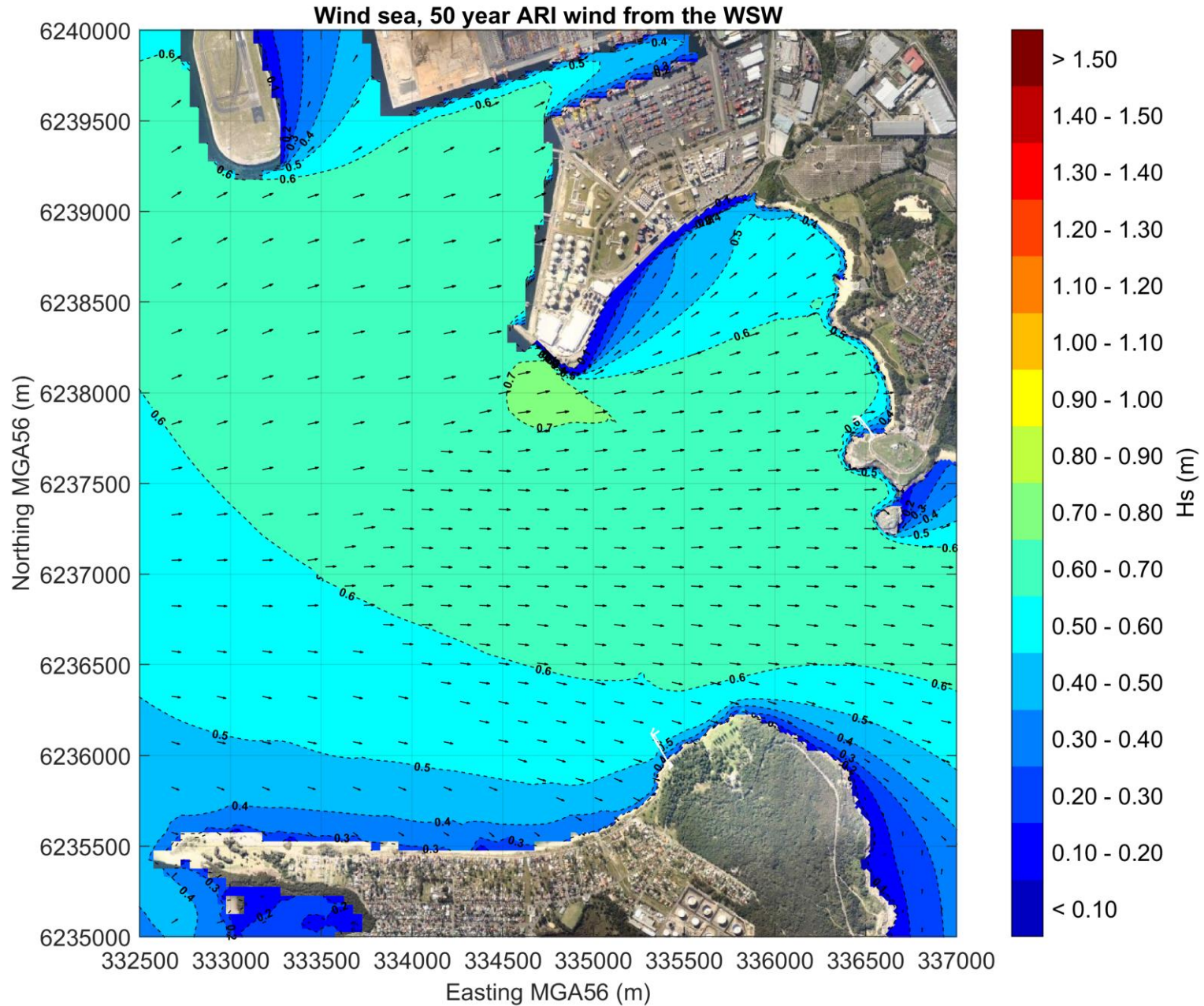


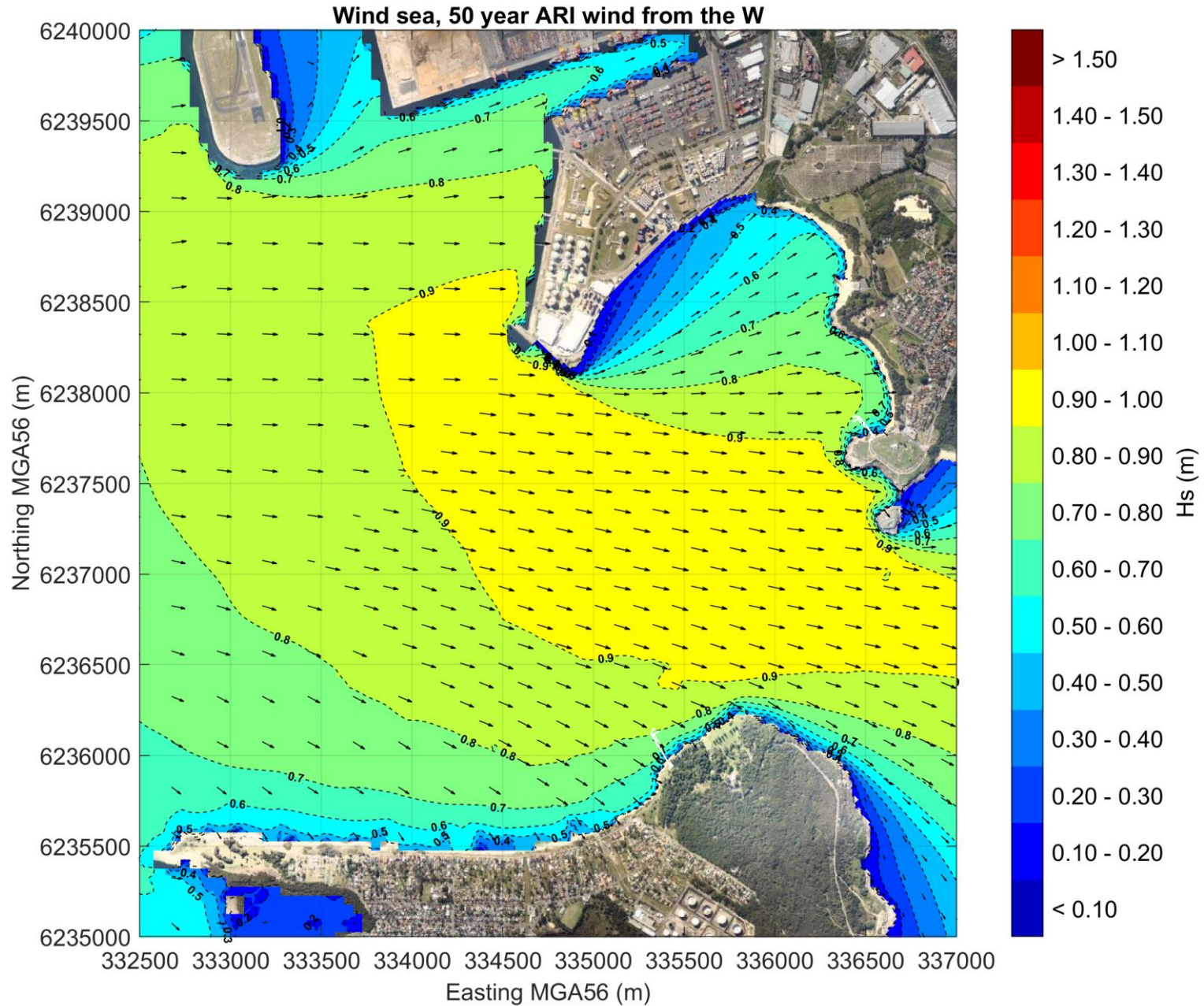


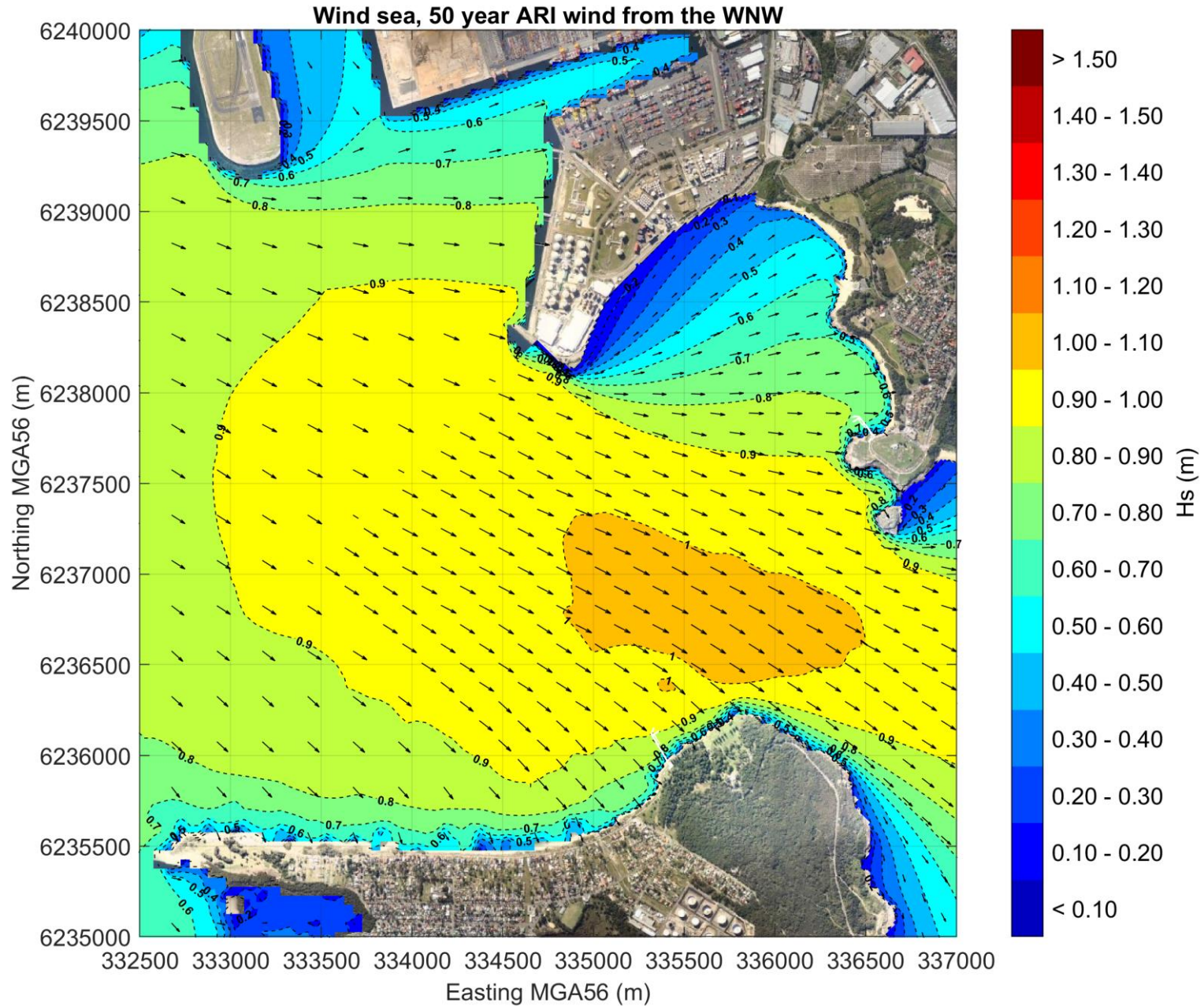


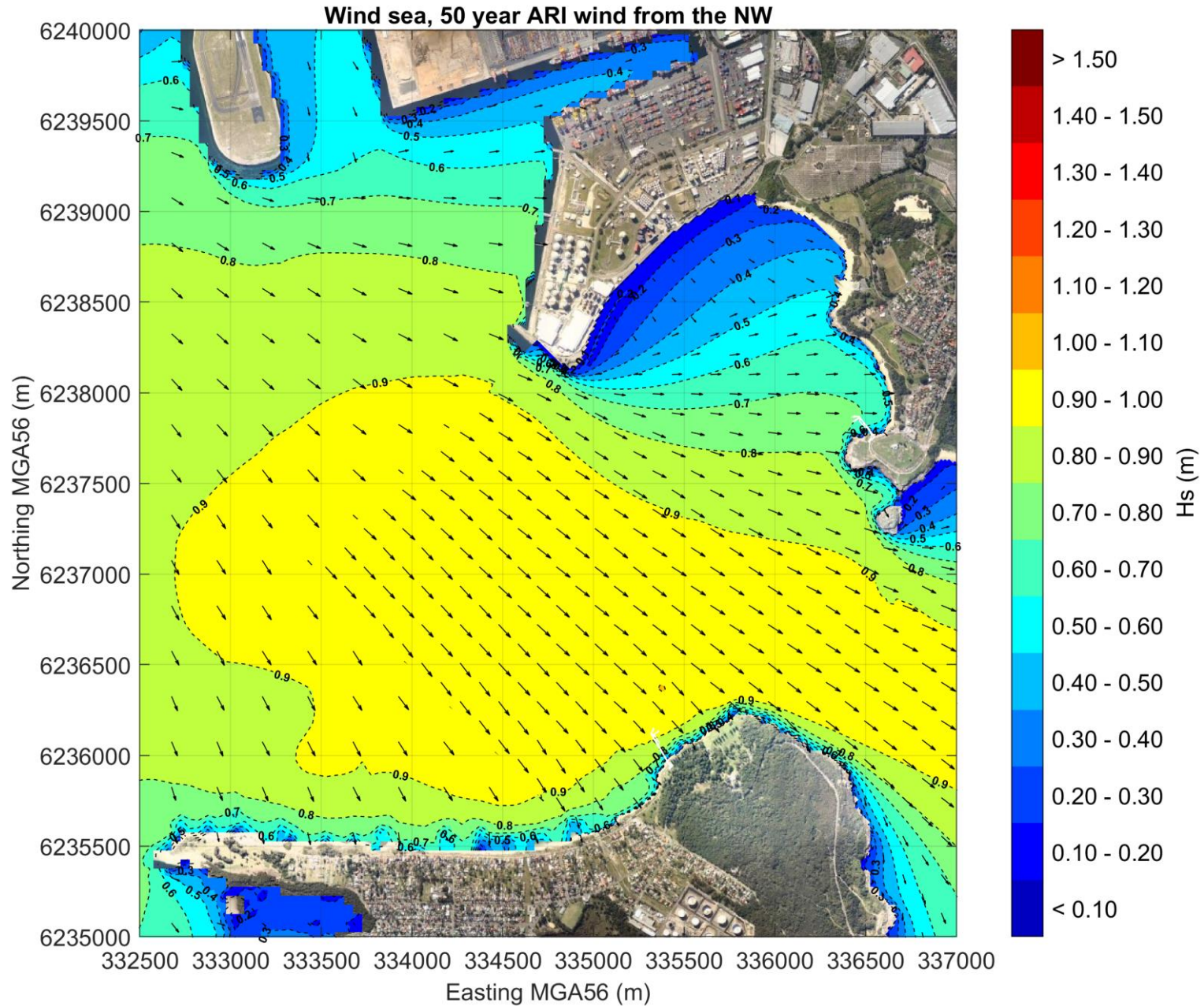


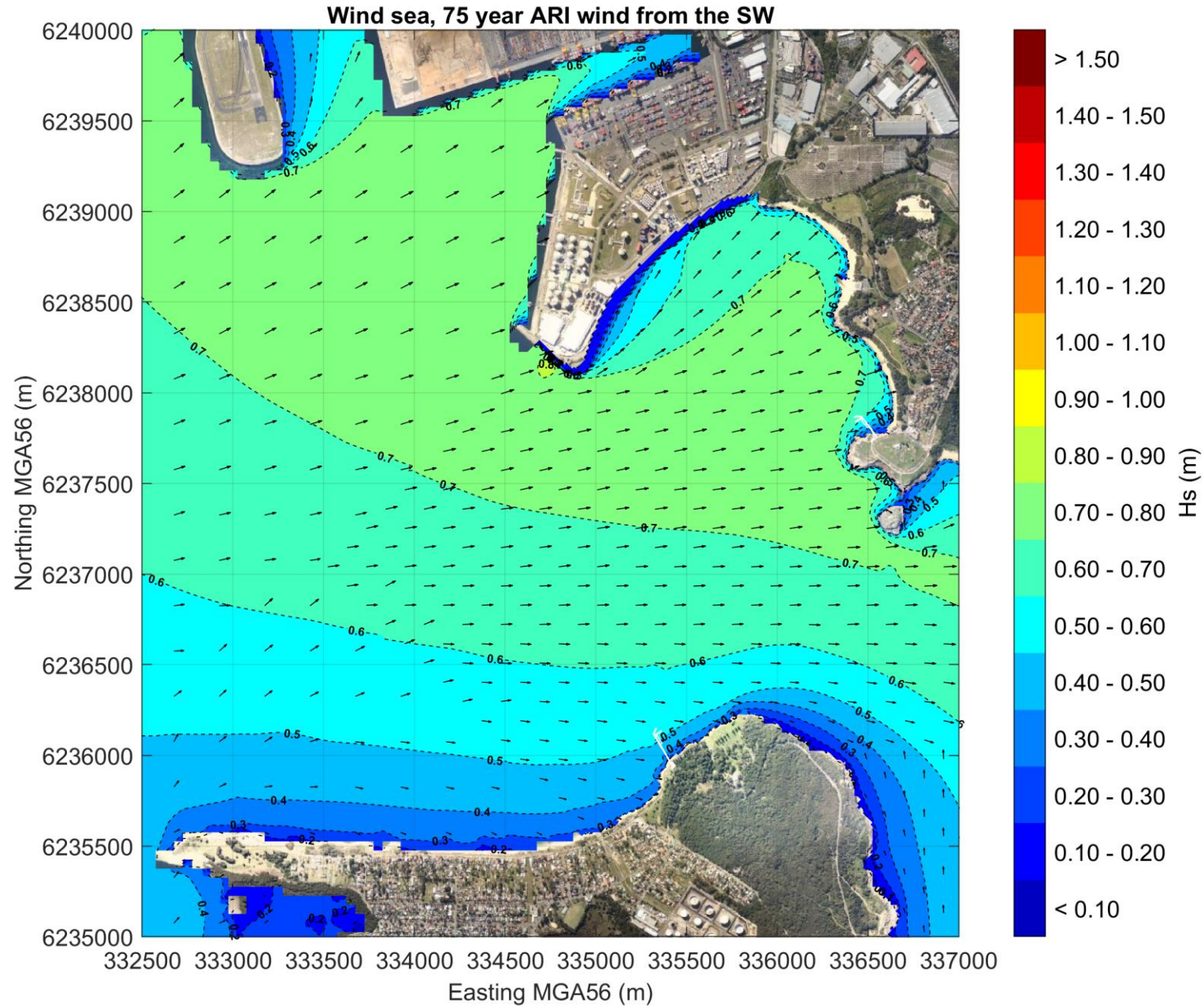


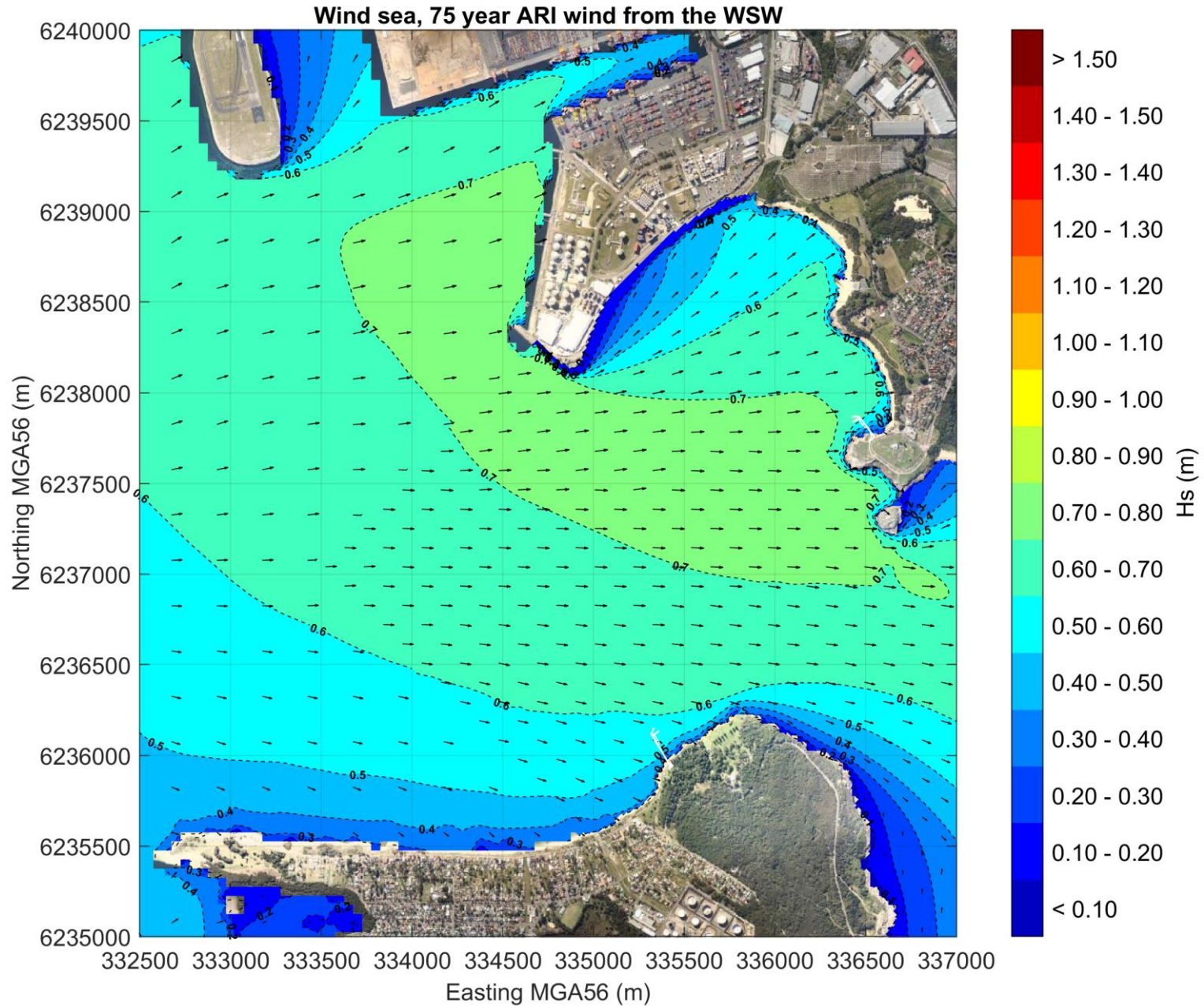


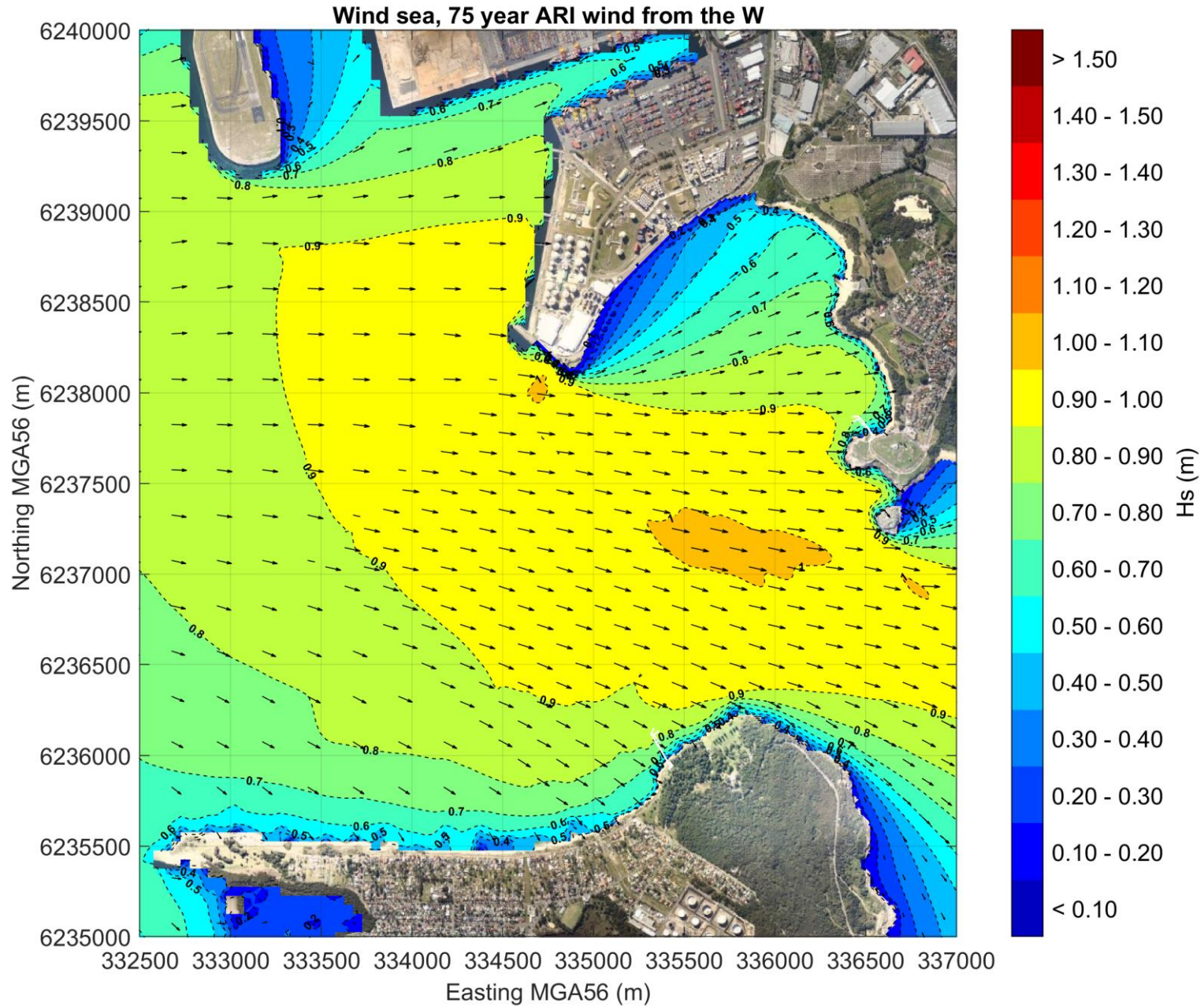


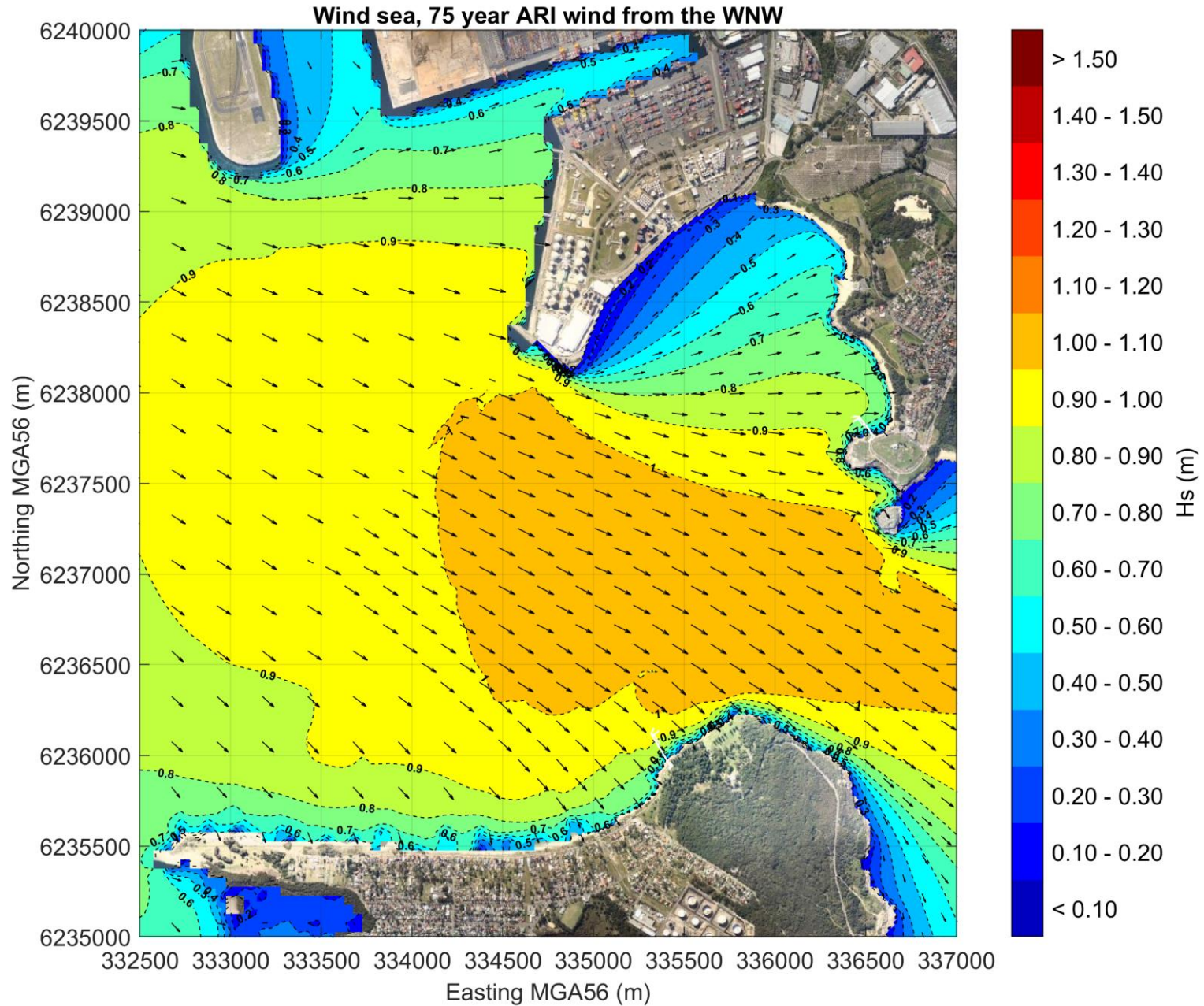


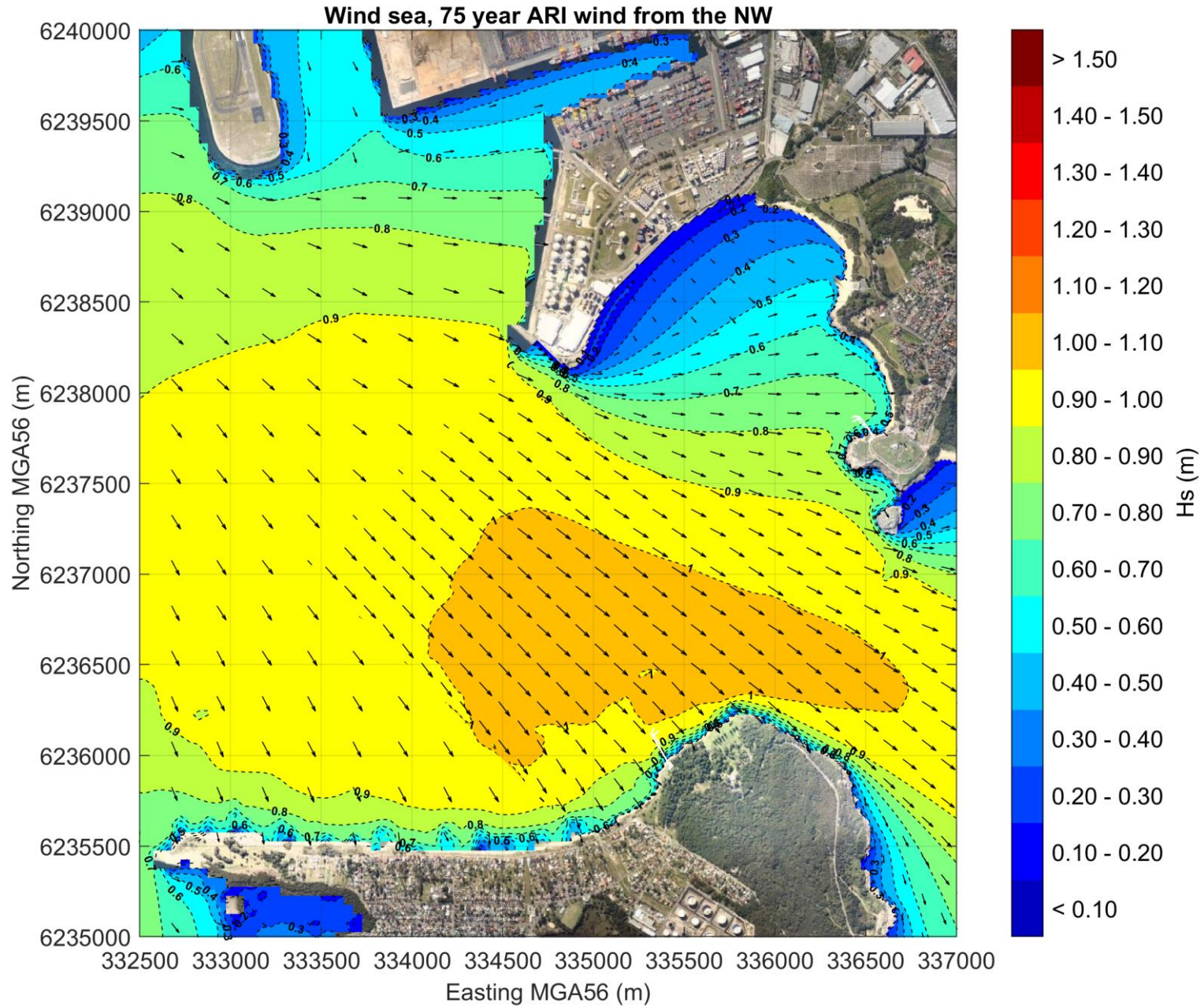


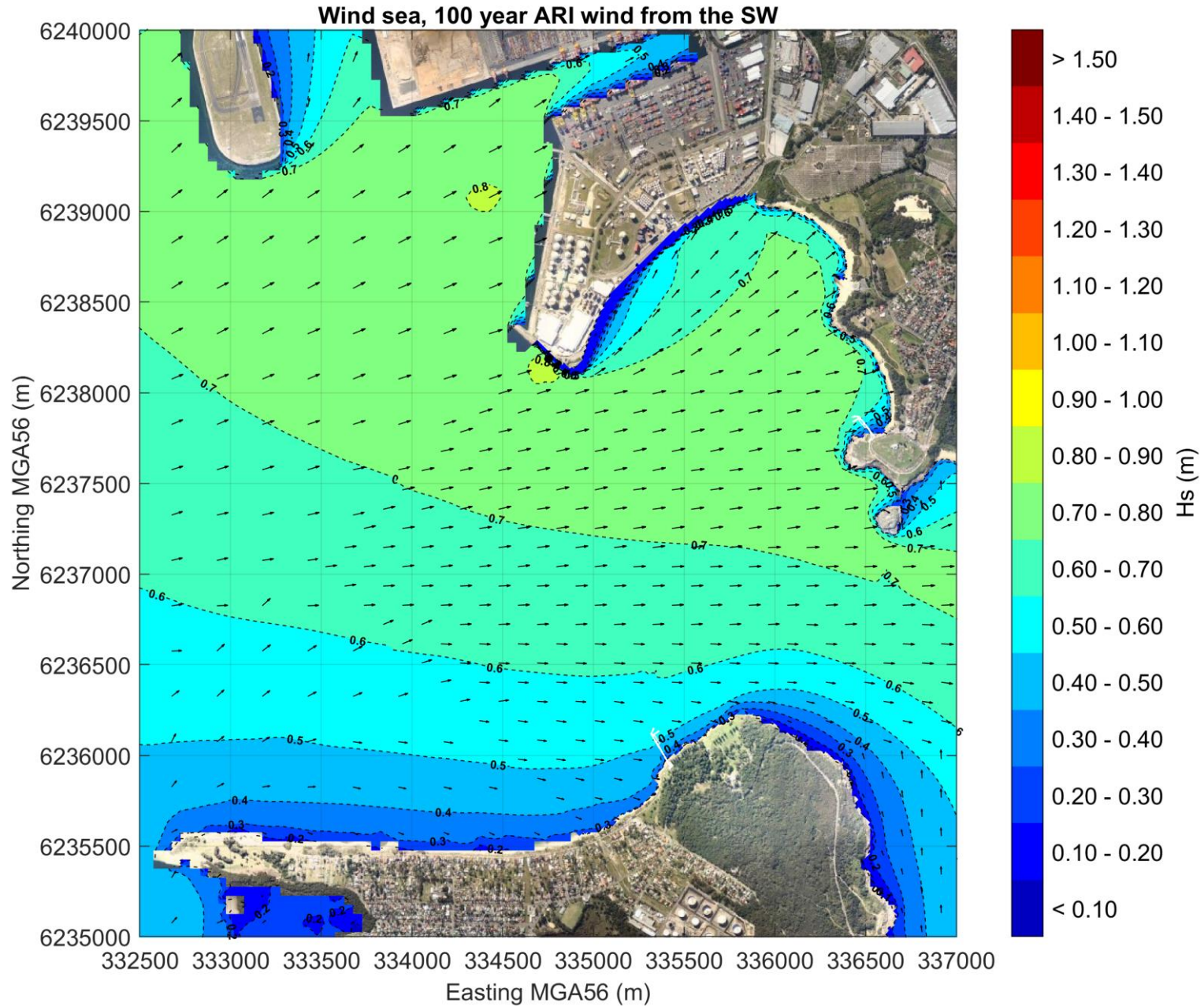


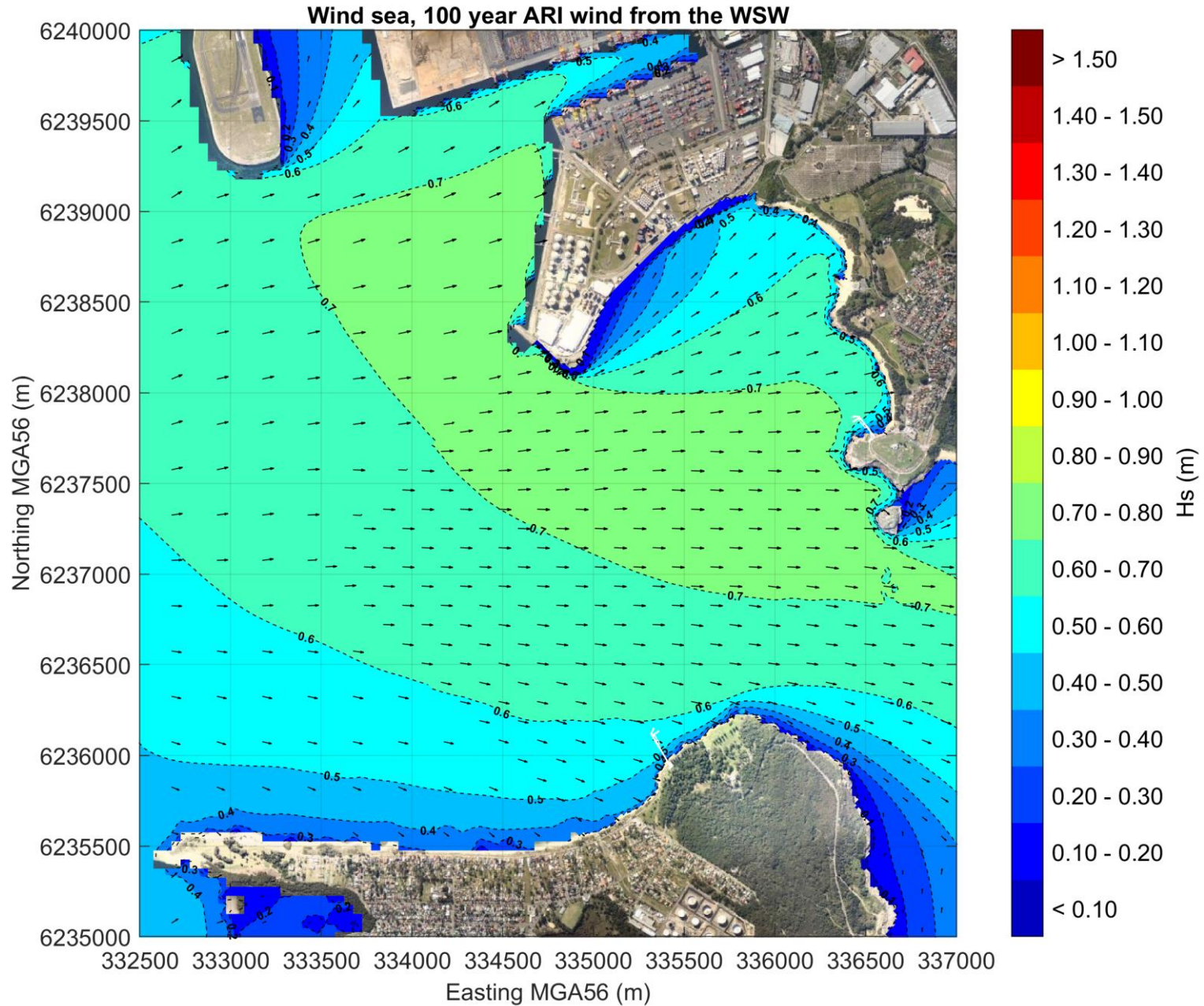


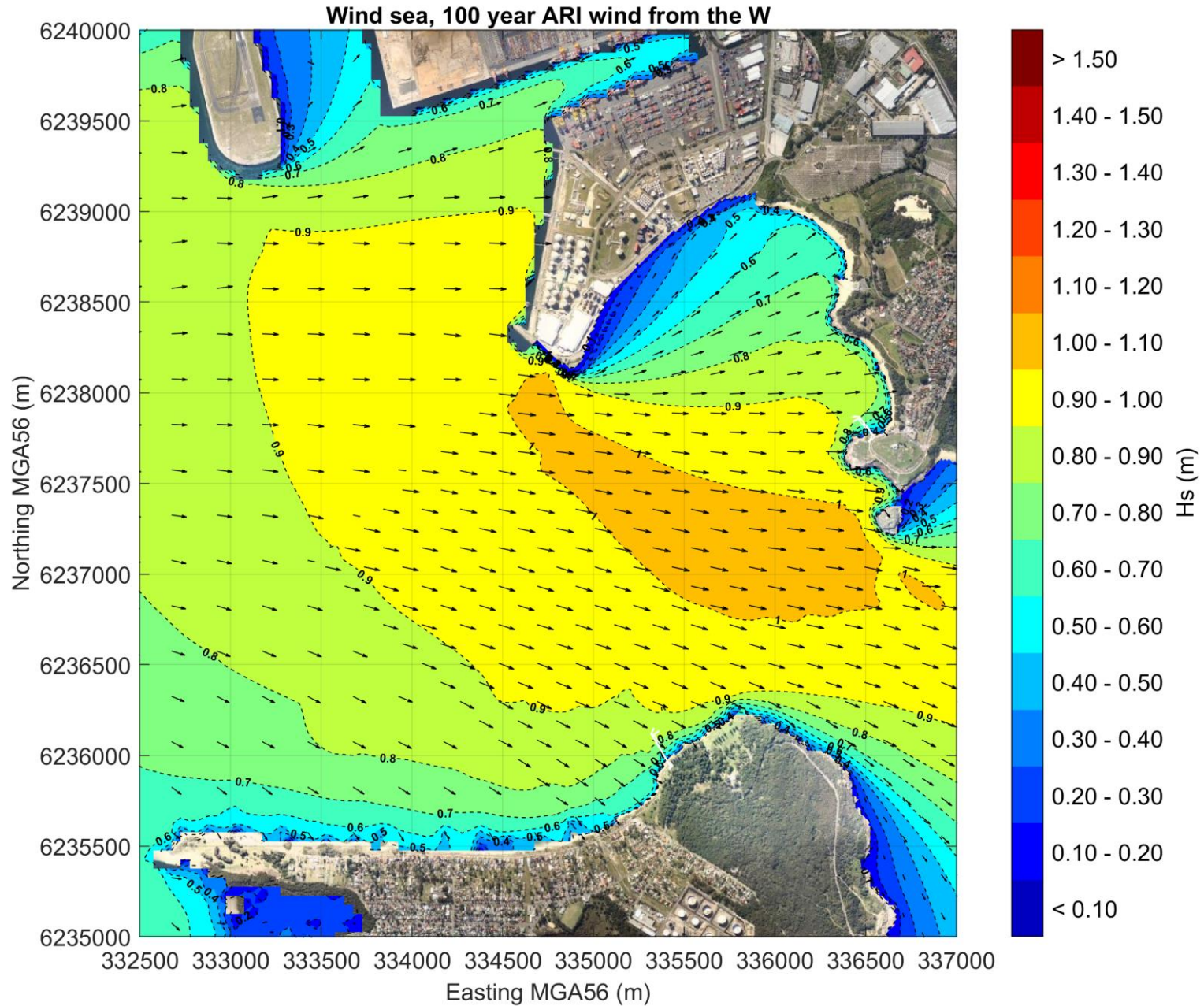


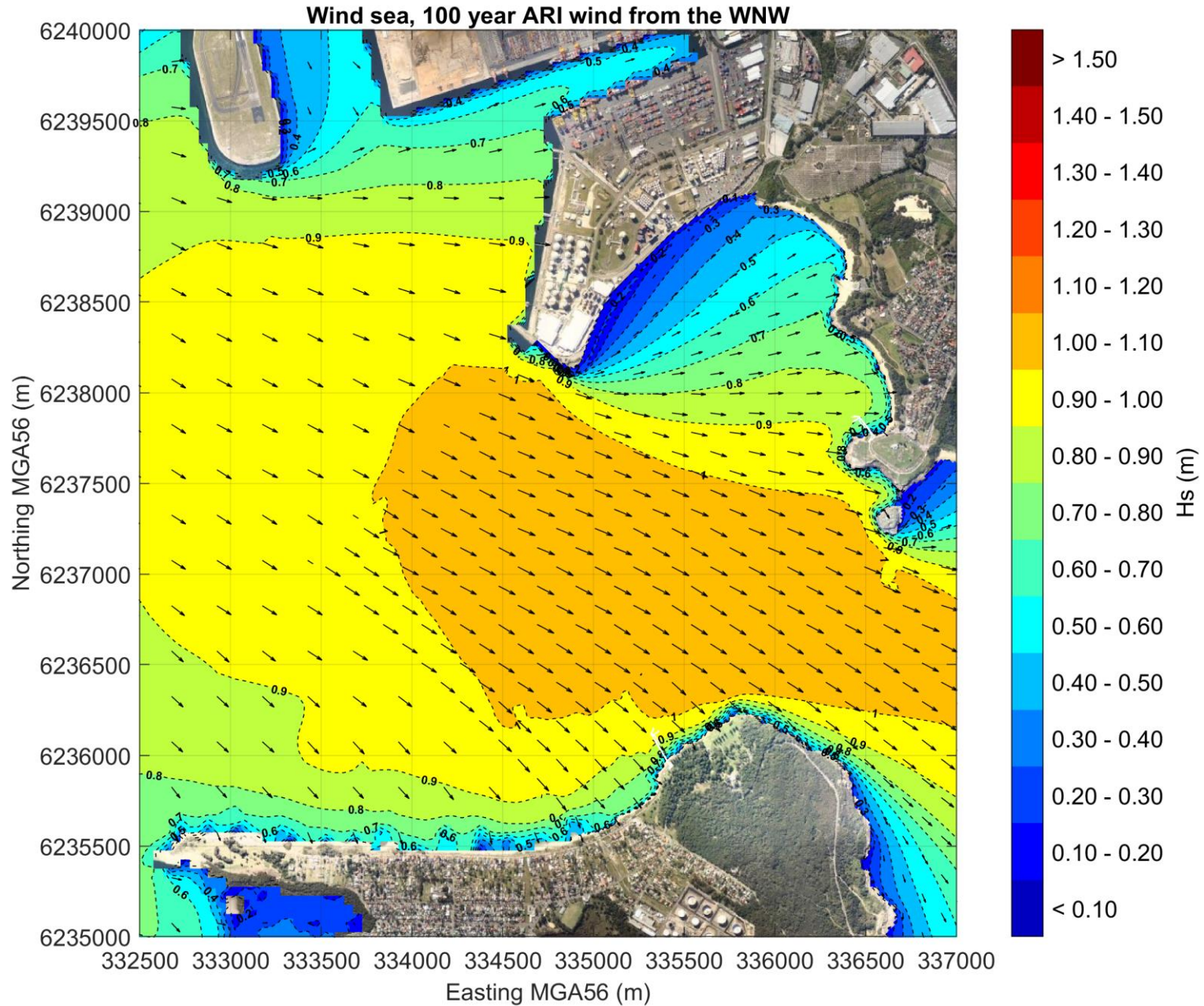


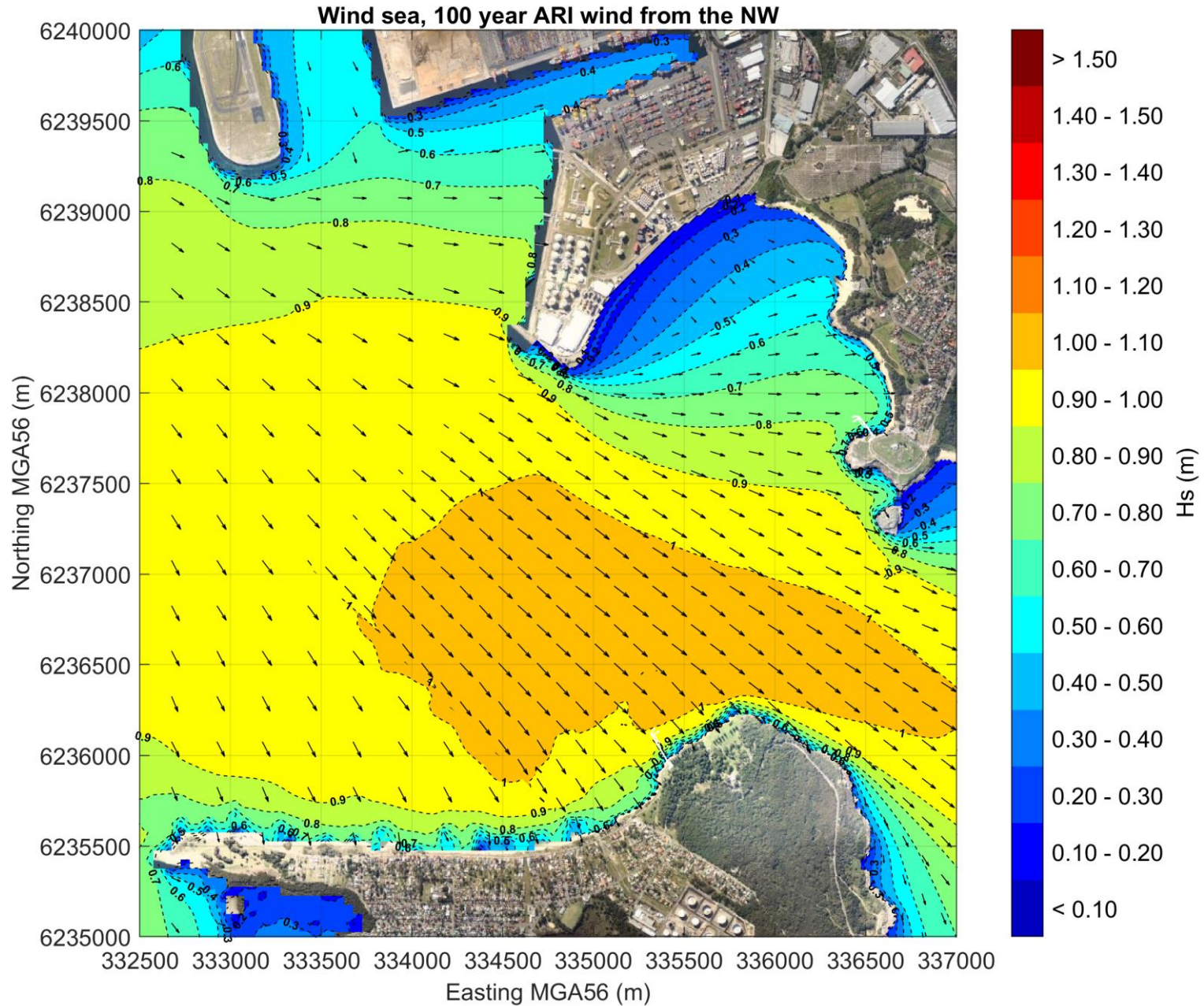


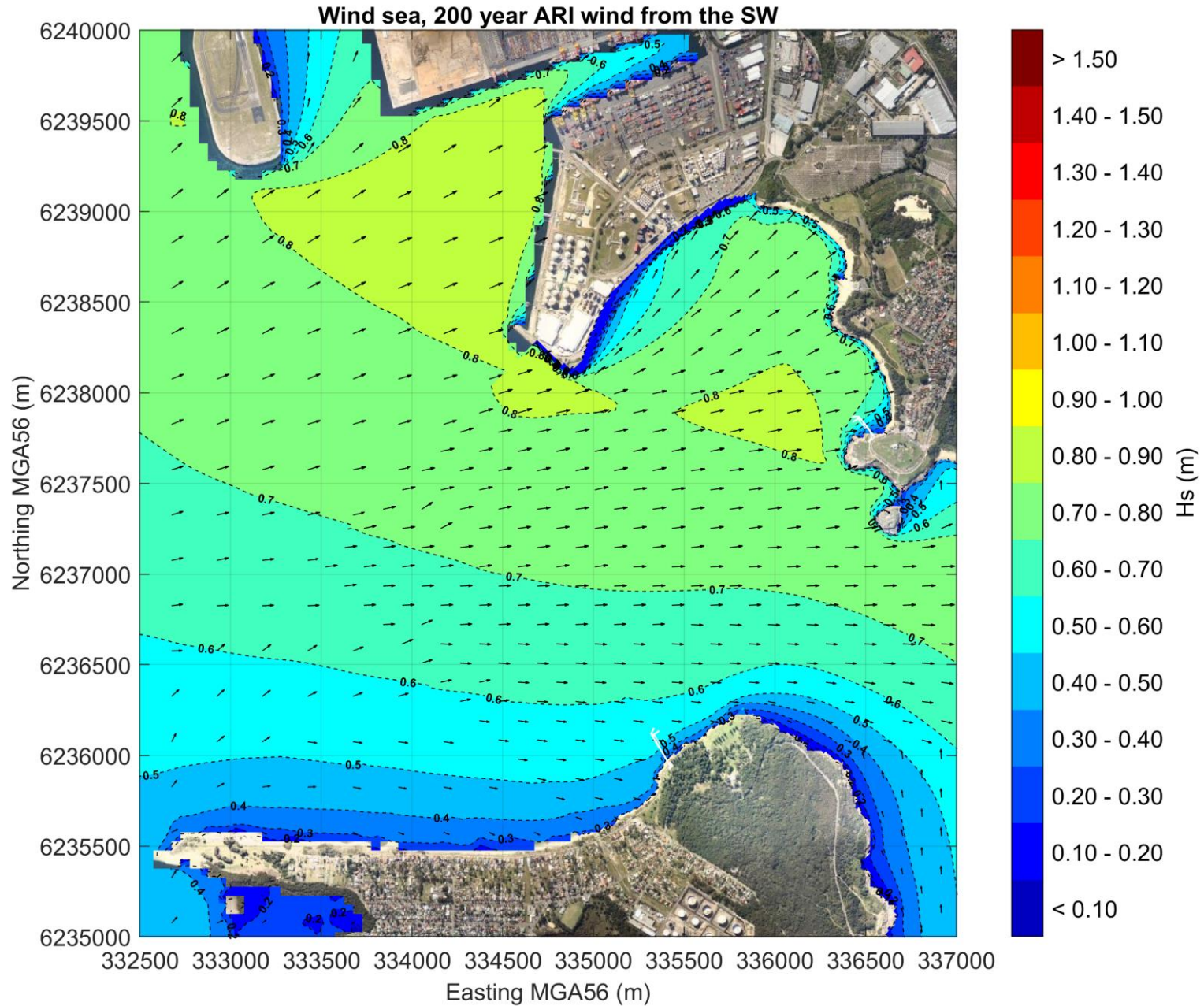


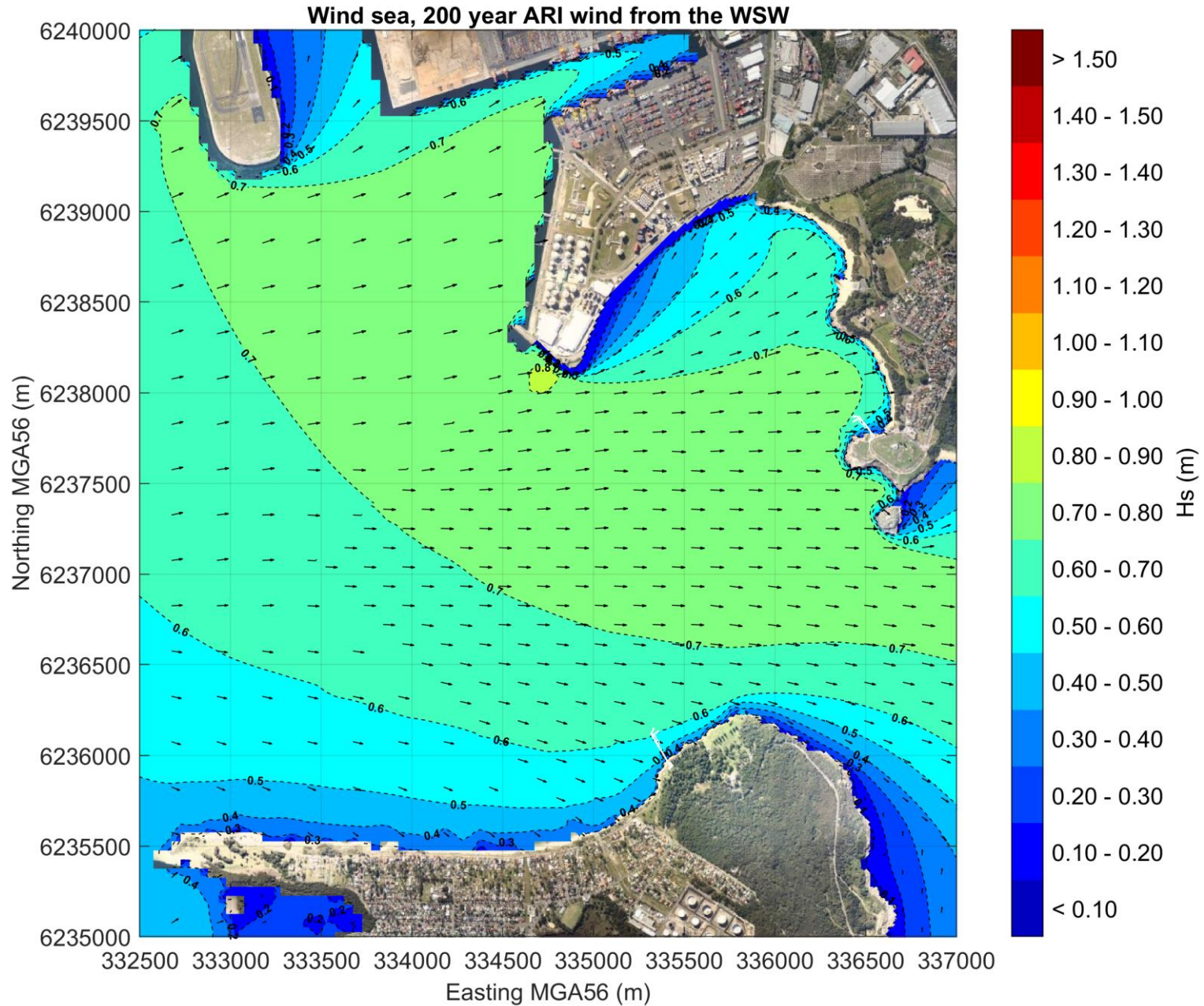


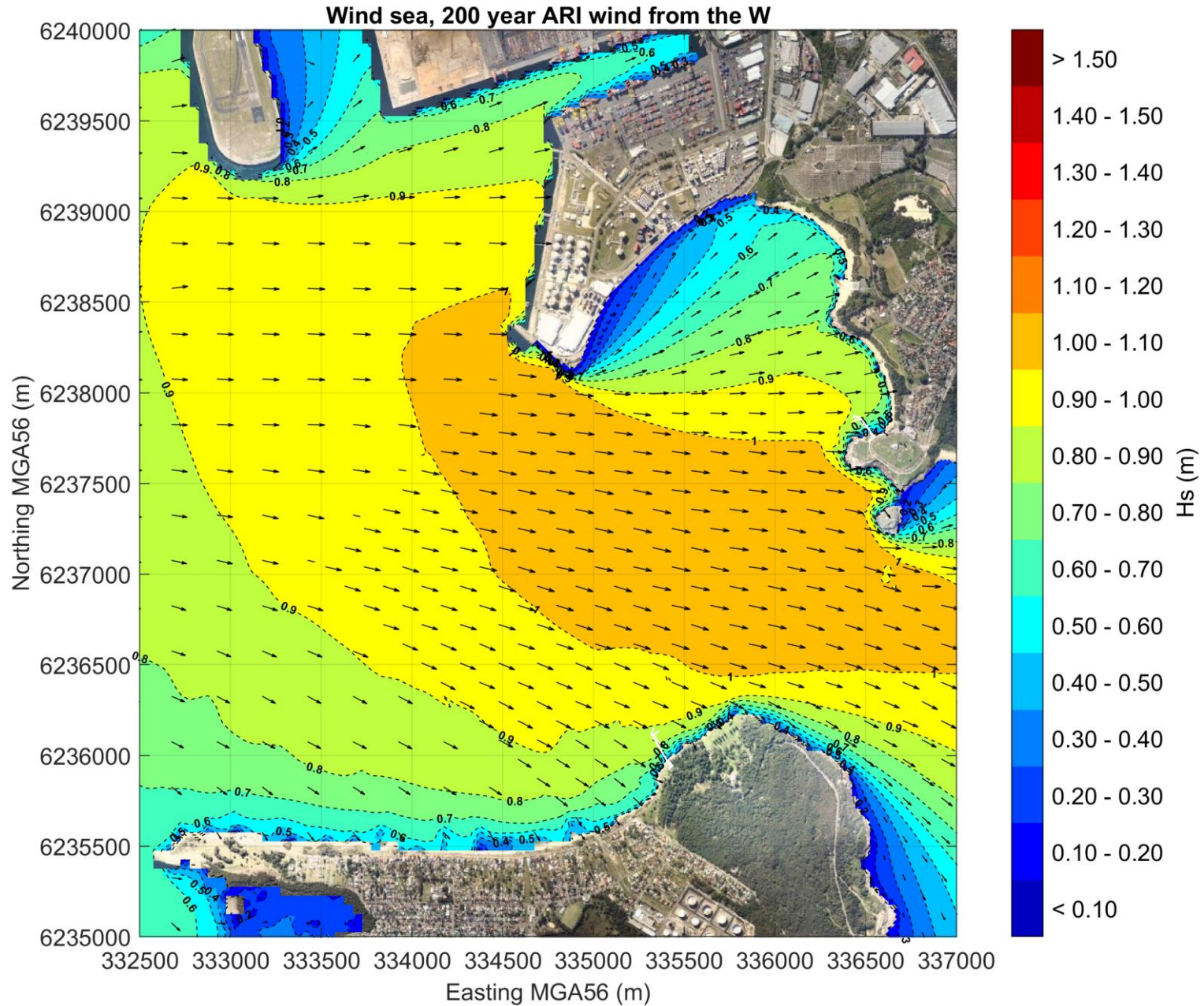


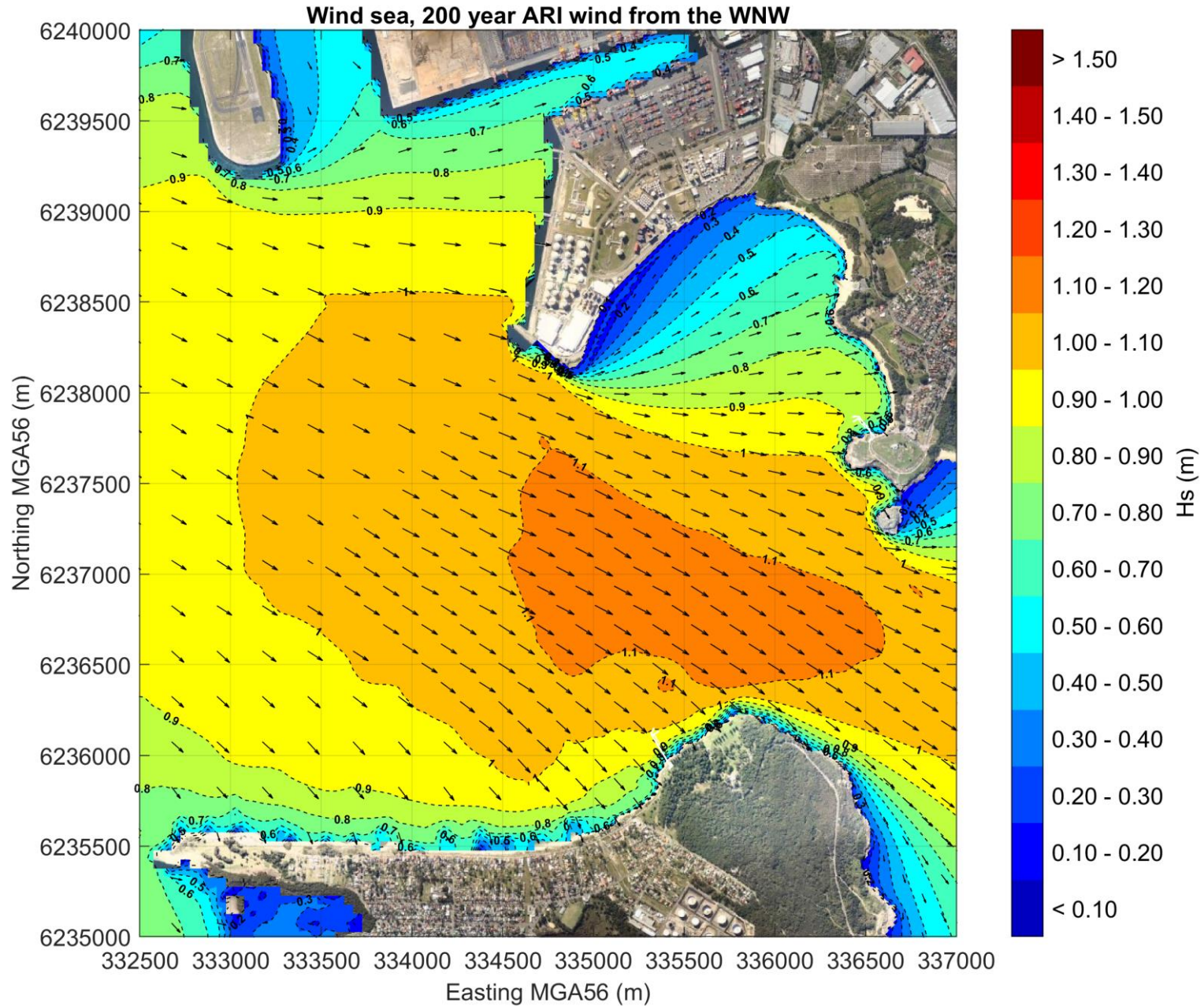


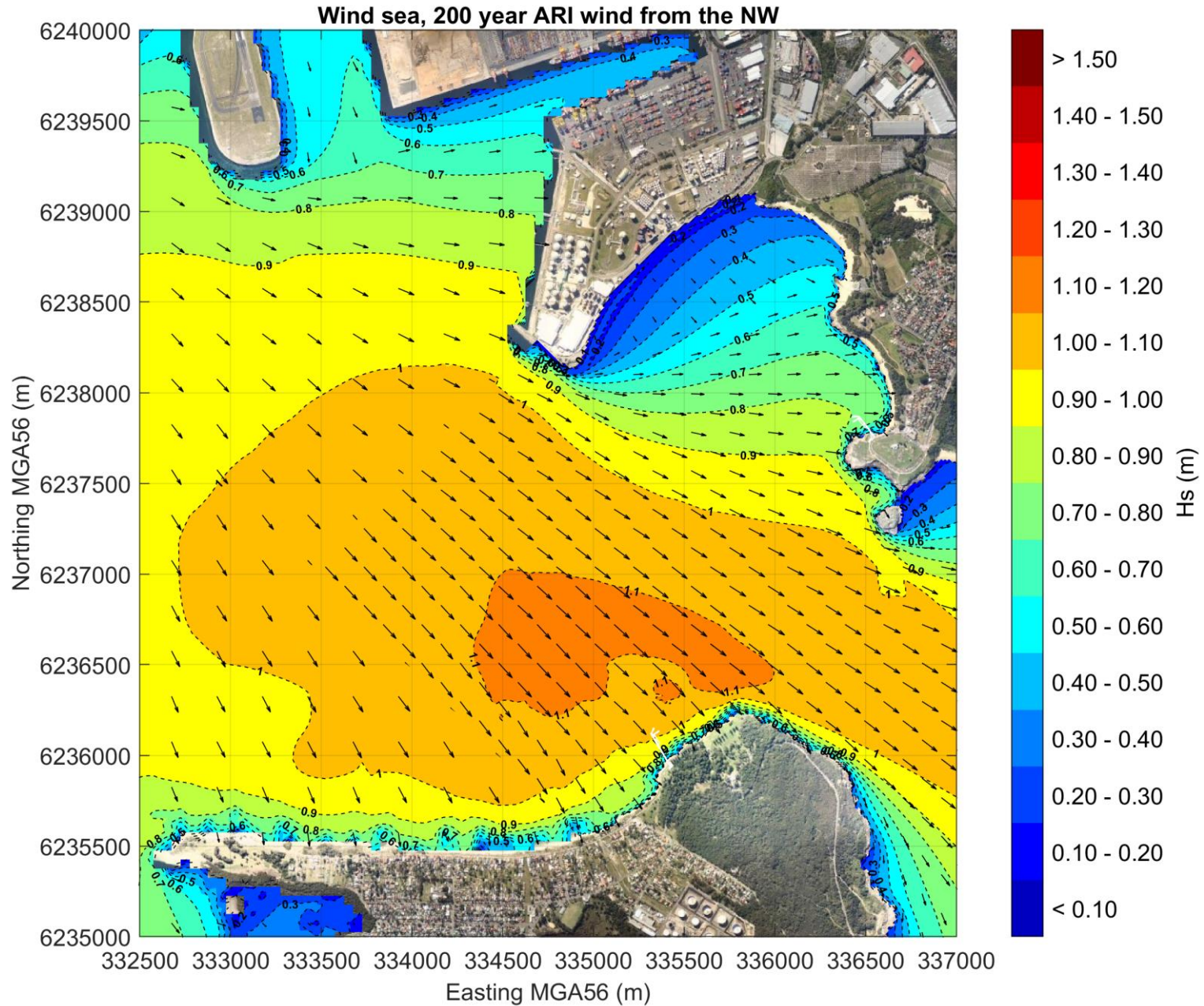


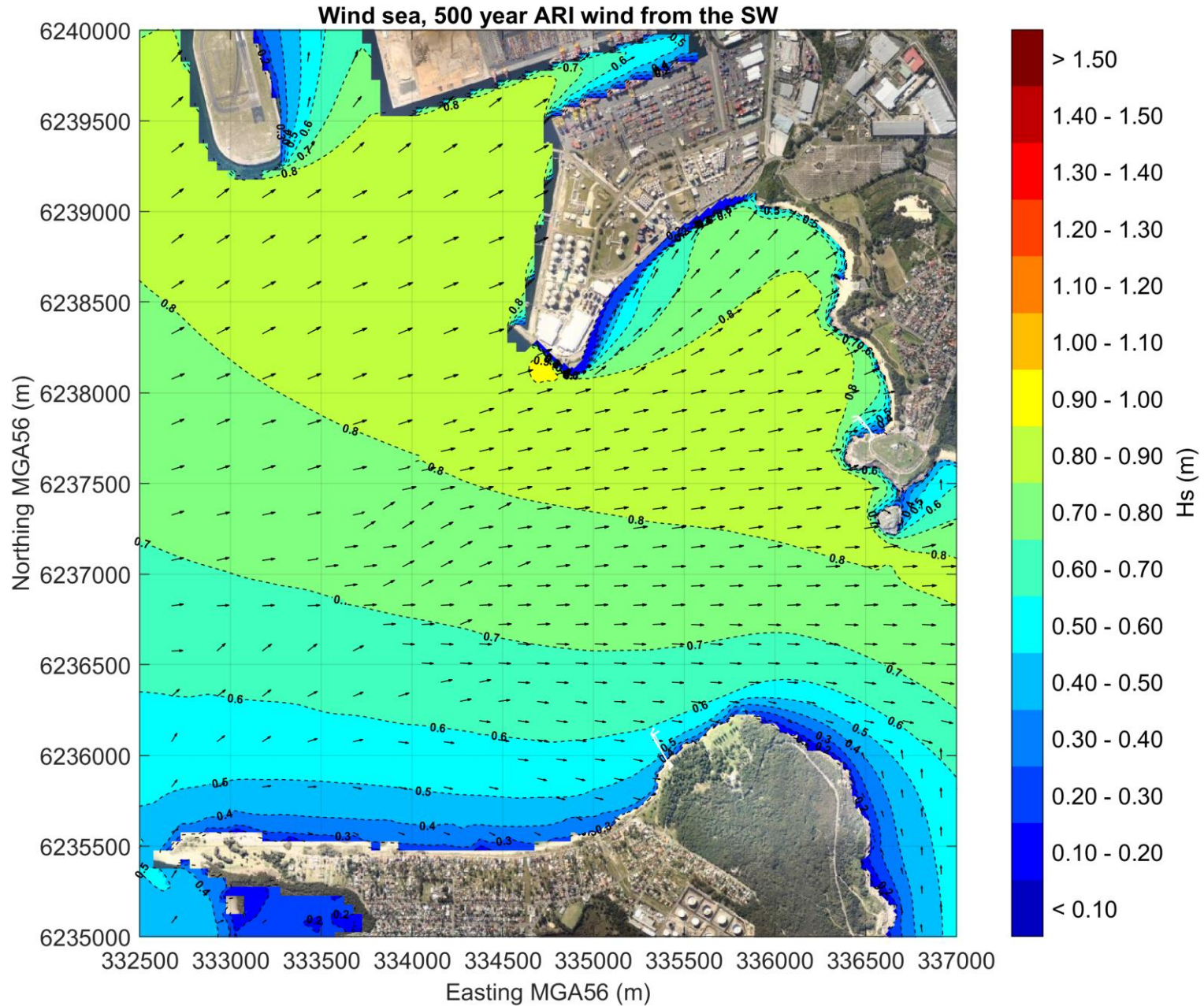


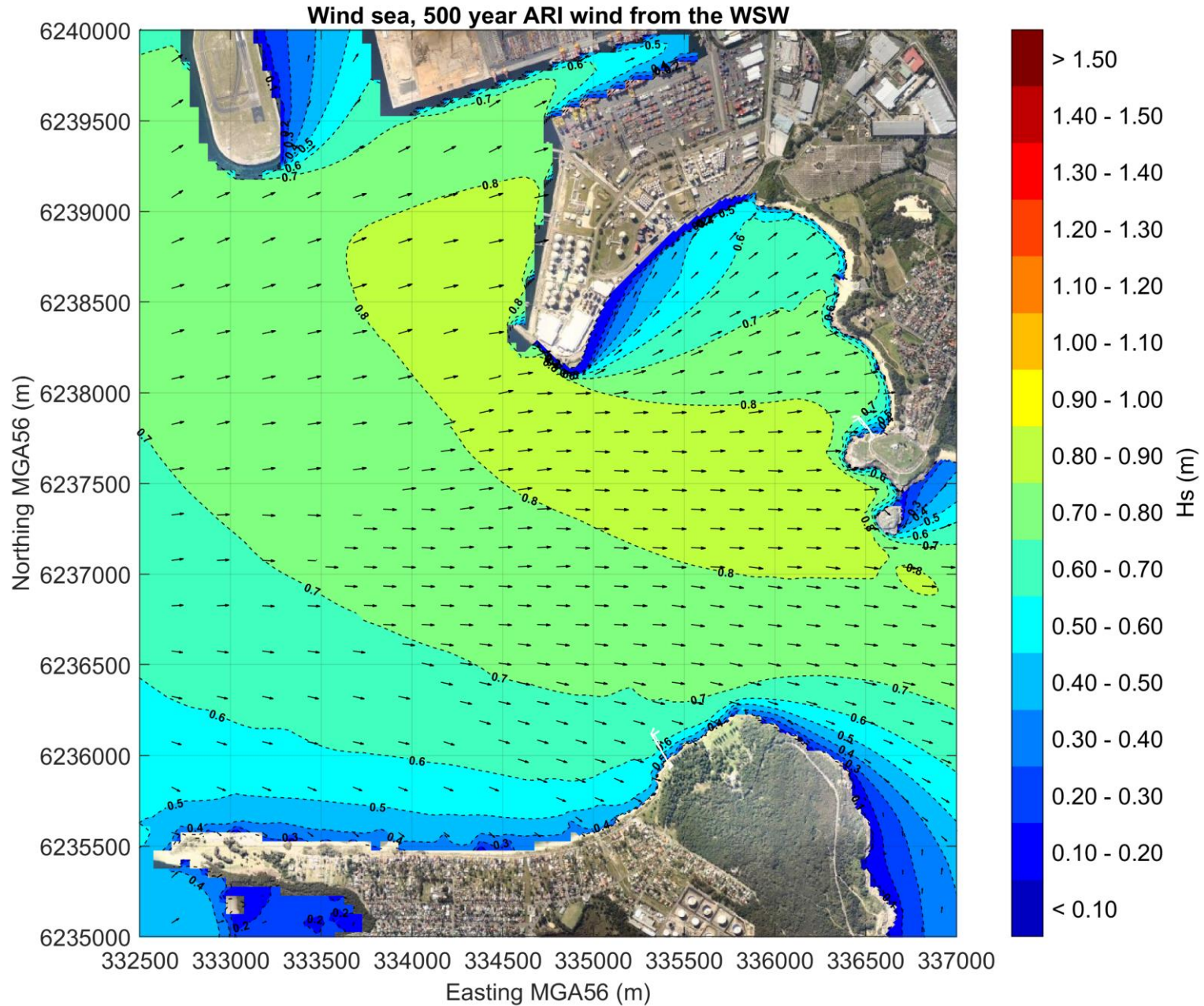


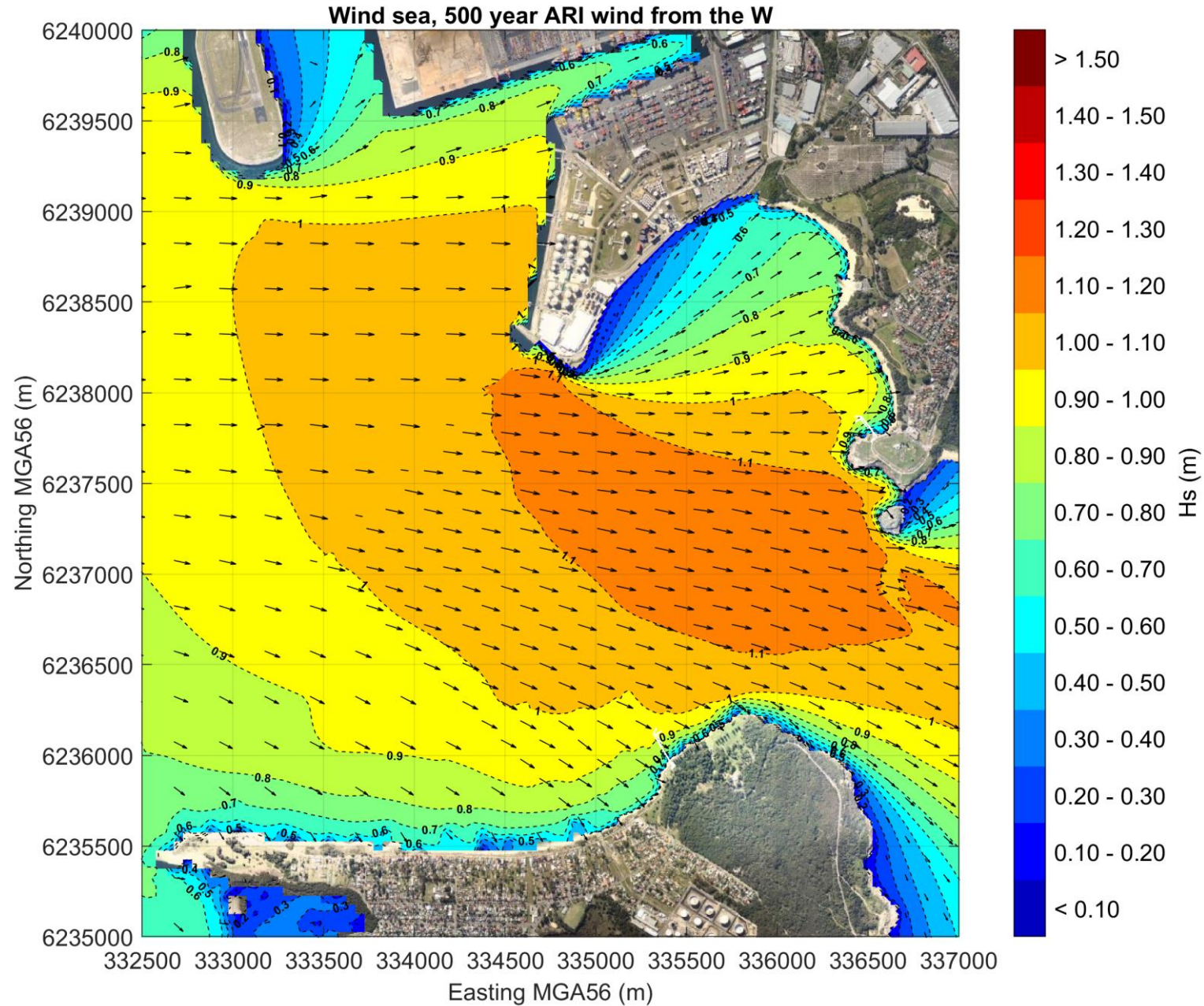


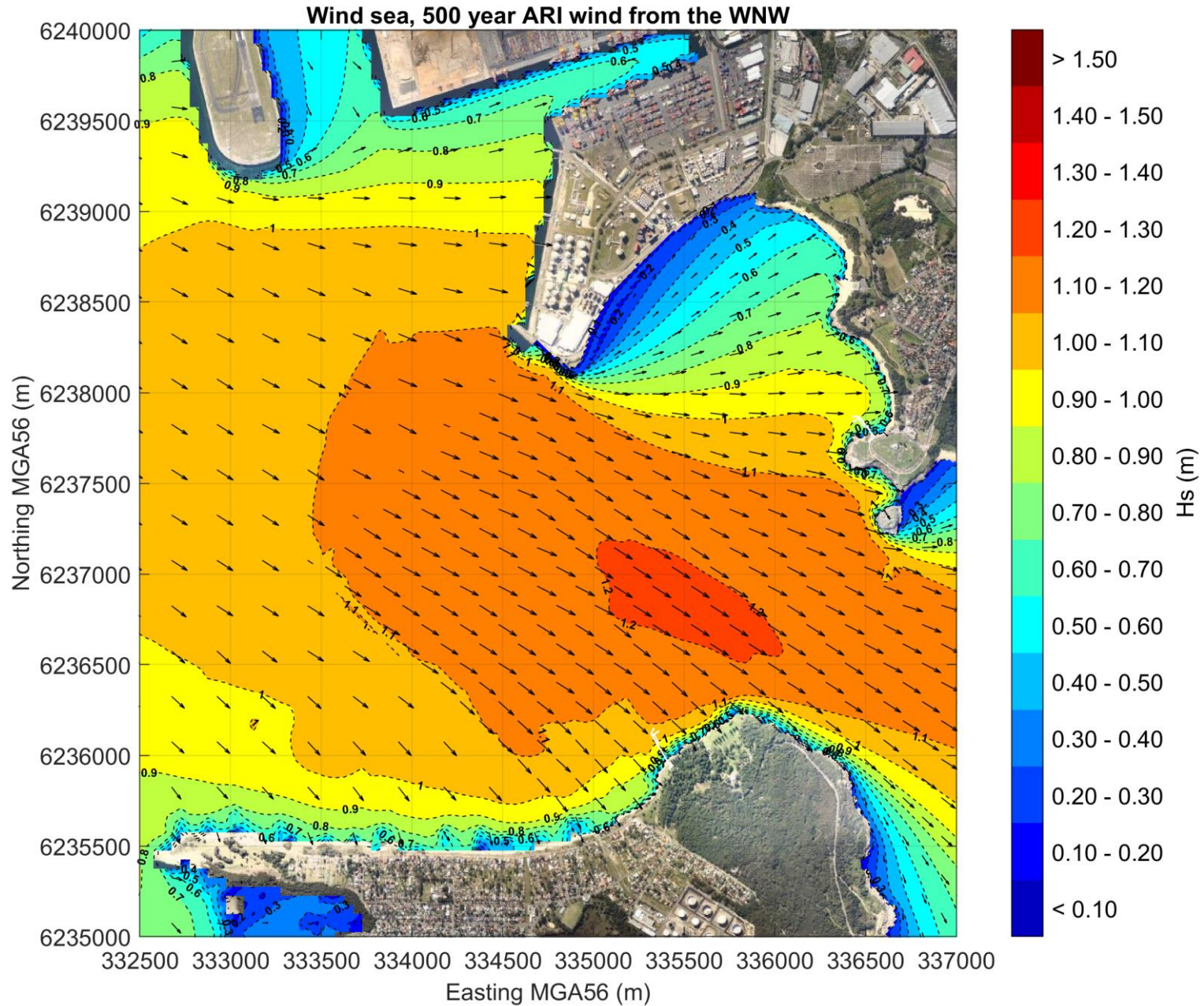


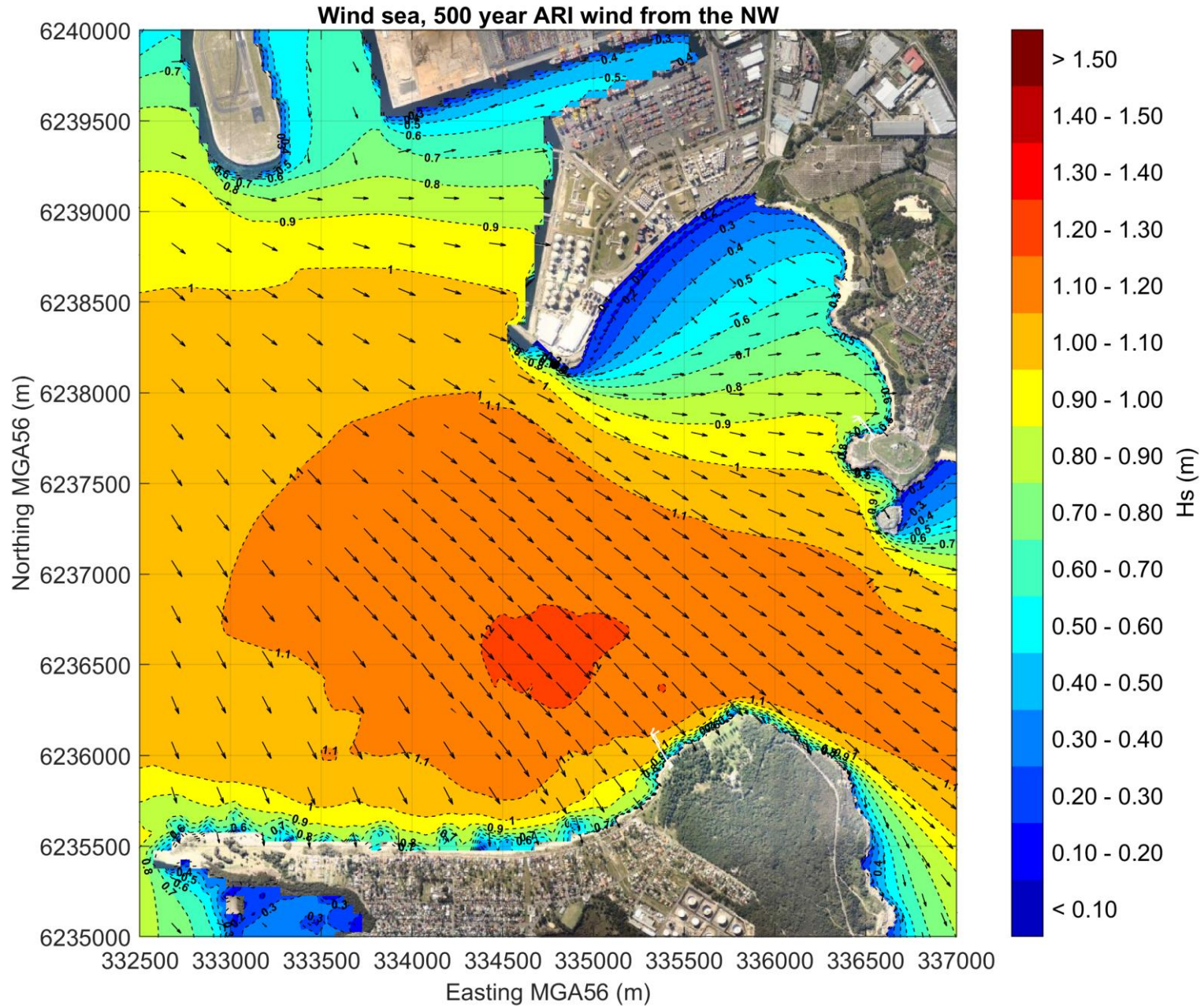


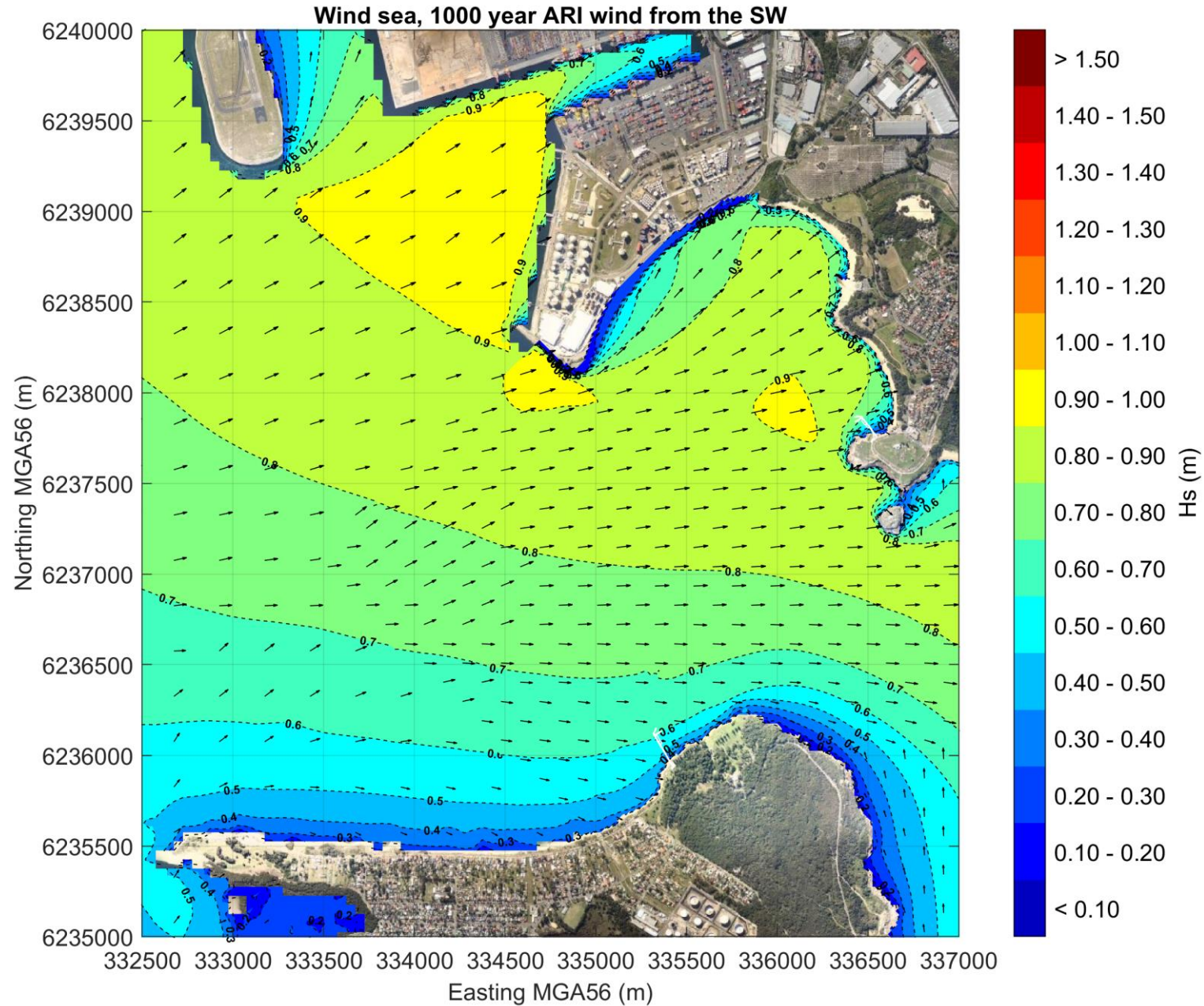


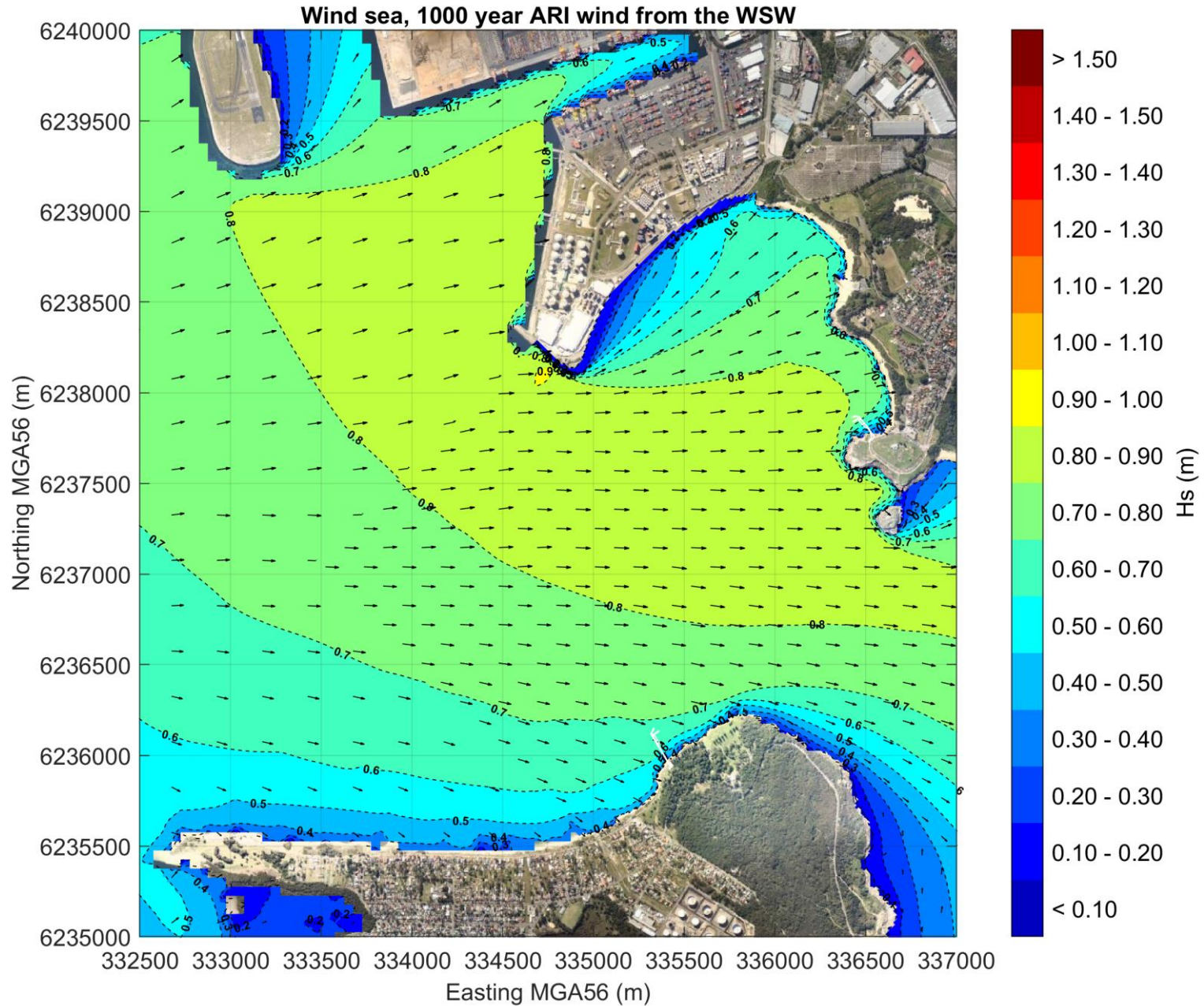


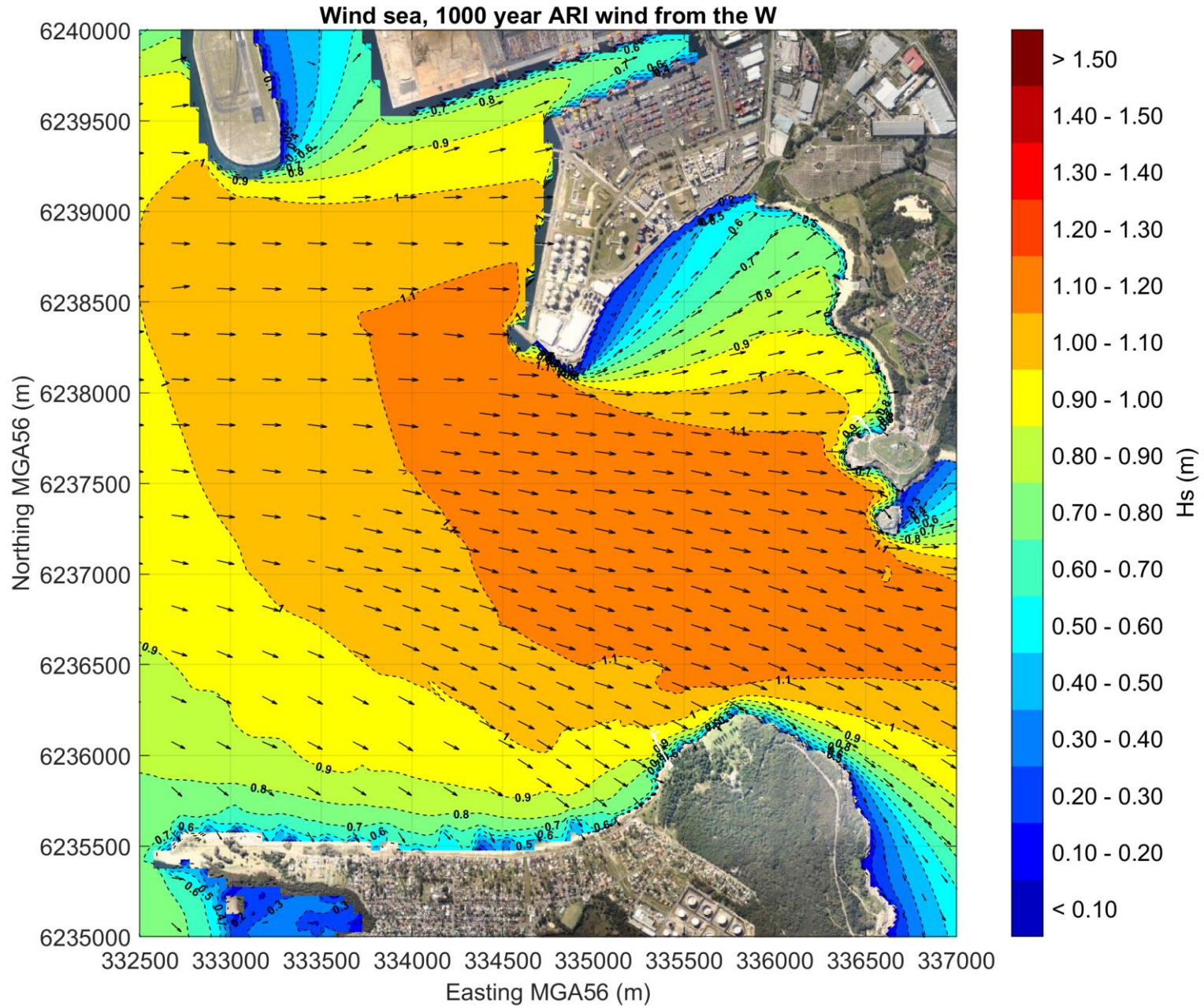


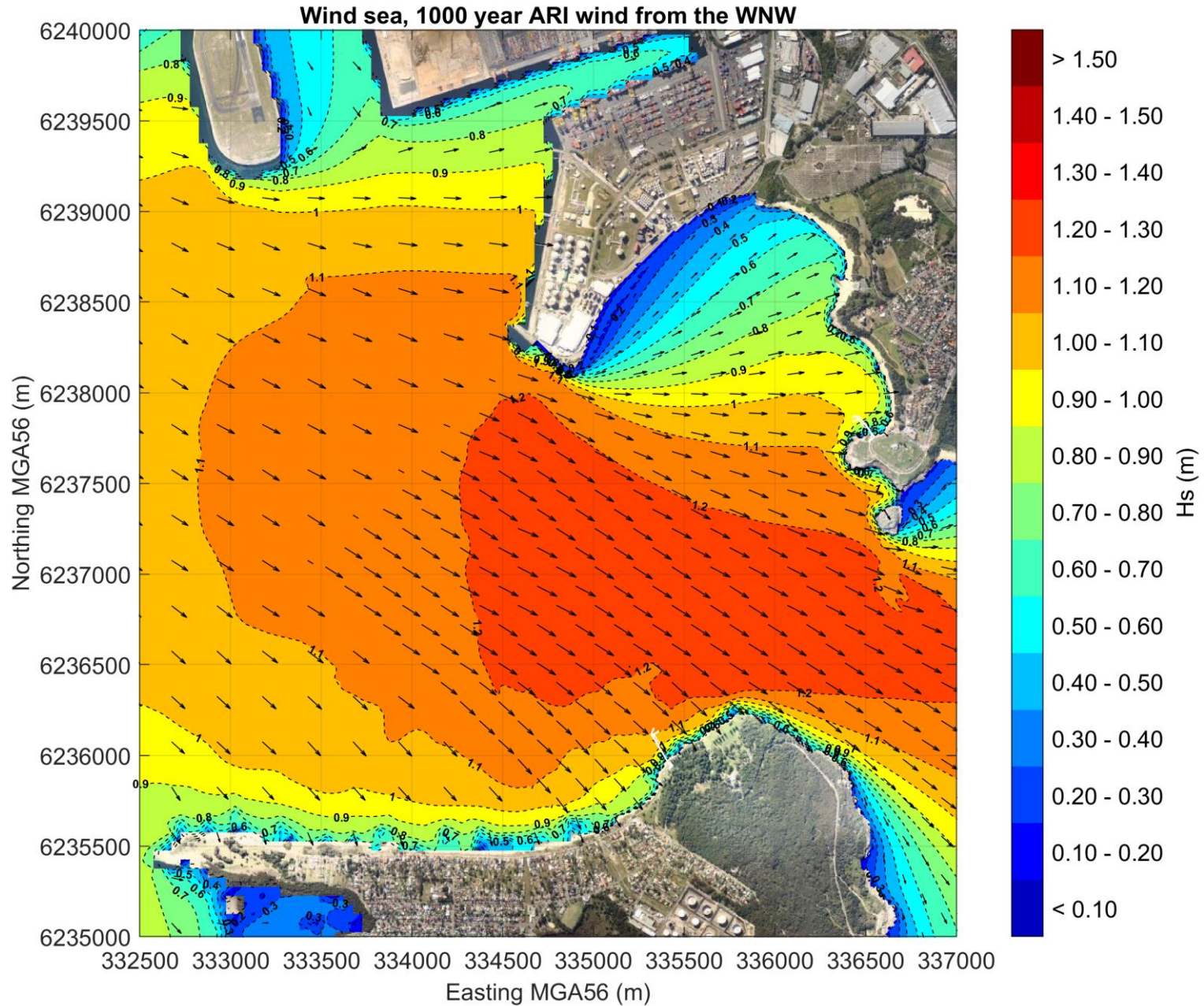


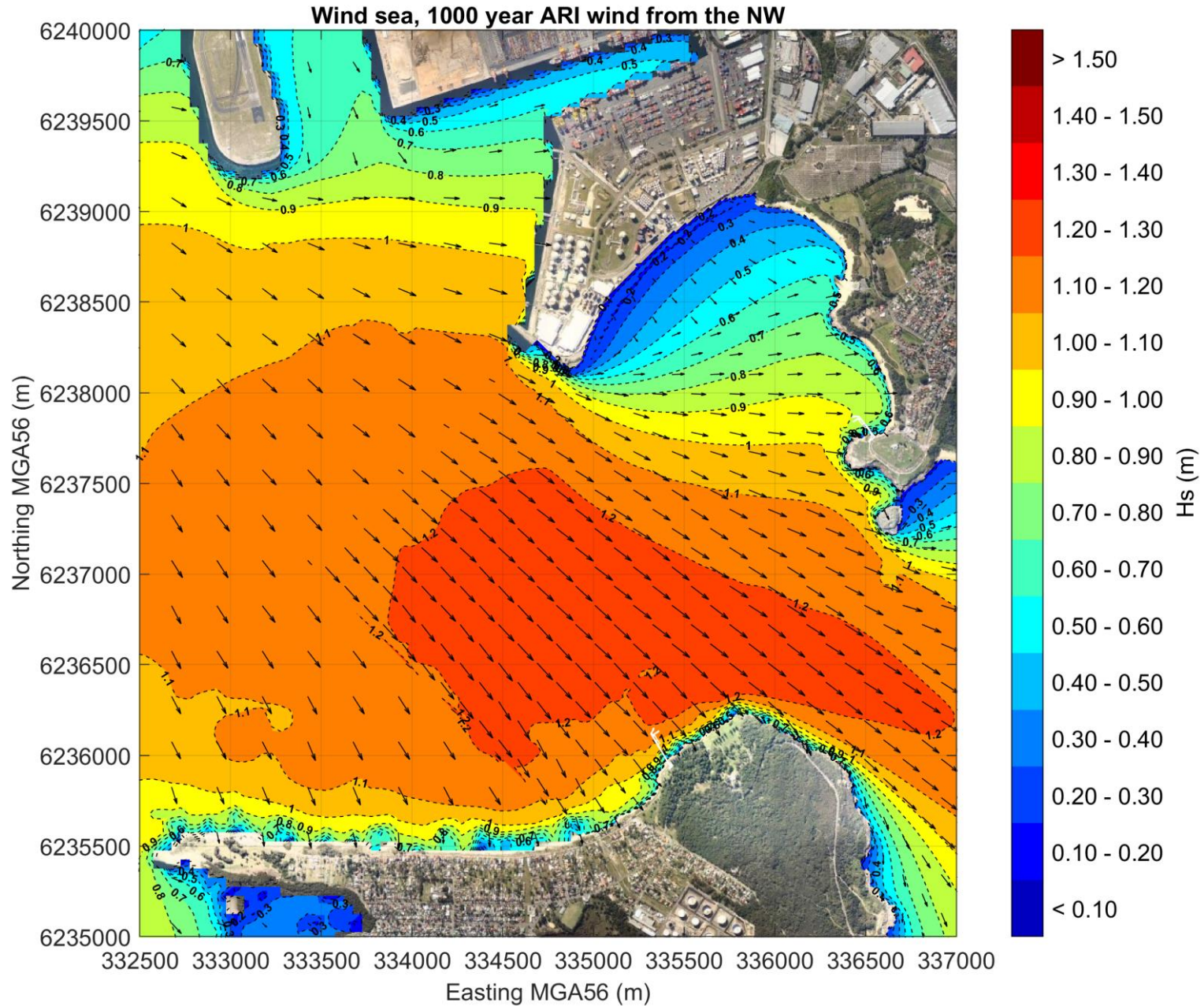












About Cardno

Cardno is a professional infrastructure and environmental services company, with expertise in the development and improvement of physical and social infrastructure for communities around the world. Cardno's team includes leading professionals who plan, design, manage and deliver sustainable projects and community programs. Cardno is an international company listed on the Australian Securities Exchange [ASX:CDD].

Contact

Level 9 - The Forum
203 Pacific Highway
St Leonards NSW 2065
Australia

Phone +61 2 9496 7700
Fax +61 2 9439 5170

Web Address
www.cardno.com

Appendix D

Shoreline Impact Assessment (2020)

Technical Memorandum

Title	Kamay Ferry Wharves Shoreline Impact Assessment	
Client	ARUP	Project No AWE200187
Date	29-07-2020	Status Final
Author	Chris Scraggs	Discipline Coastal
Reviewer	Doug Treloar	Office Sydney

1.1 Background

As part of the proposed Kamay Ferry Wharves project in Botany Bay, a shoreline near-perpendicular causeway is being proposed at the Kurnell wharf site (refer **Figure 1-1**) as part of access facilities to the berth. The causeway is proposed to be constructed from the back-beach at the shoreline and extend out to the -2m AHD contour as a rock 'groyne'.

This memo outlines the potential impacts to sediment transport, and to the surrounding shoreline due to construction of the causeway. This assessment has focussed on an analysis of aerial imagery and the nearshore wave climate to predict likely changes to the shoreline. A sediment transport and coastal processes model, such as LITPACK, has not been applied to this study, given the complex foreshore geometry and rock shelf/perched beach nature of the shoreline, and it would therefore not be expected to be able to adequately resolve the shoreline processes.

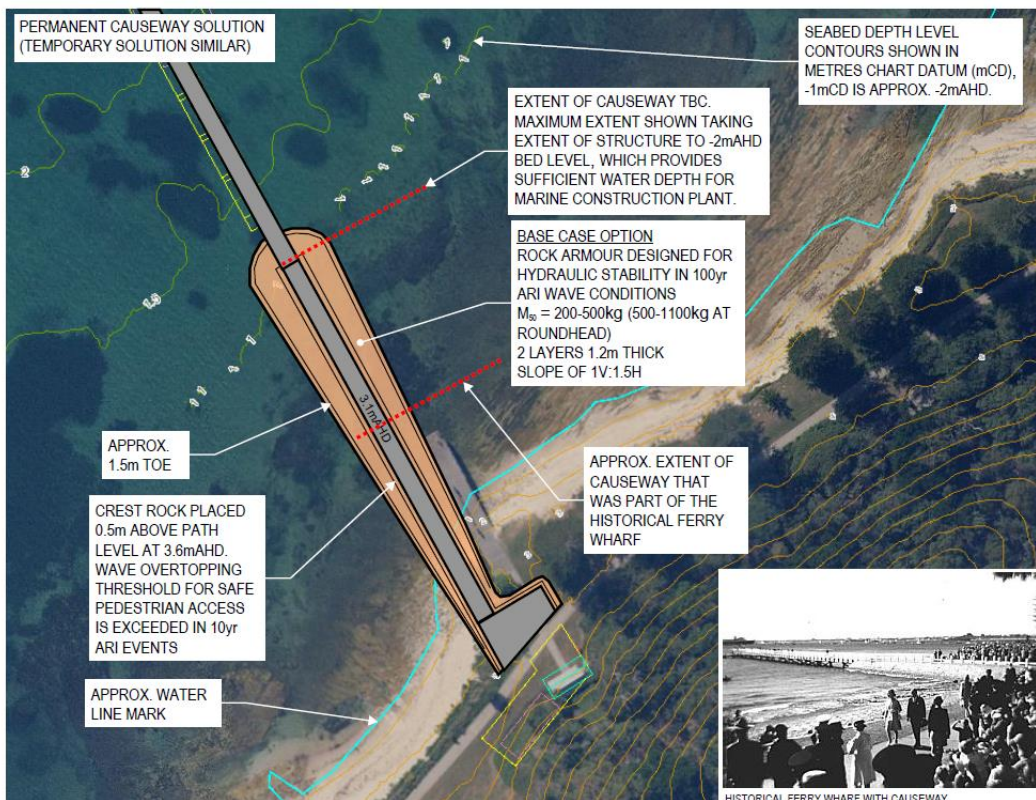


Figure 1-1 Proposed Causeway and Jetty at Kurnell

The site is located on the southern shore of Botany Bay, at Kurnell in the Meeting Place Precinct within the Kamay Botany National Park. The beach along this section of coastline is perched on an intertidal rock shelf, as shown below in **Figure 1-2**. Given the perched nature of the beach, the volume of sand available for transport will be limited, and can only occur during periods of high water levels. However, in some places the back-beach is formed from sand that only occasionally, during rare, severe storms, forms part of active beach processes.

The area has been noted as undergoing recent erosion (Mott MacDonald, 2018). Mott Macdonald undertook a site visit to the area and noted significant erosion scarps along the foreshore, which was threatening a number of Norfolk Island Pines, as shown in **Figure 1-3**. The size of these trees confirms that they have been there undamaged for some decades. Based on Mott MacDonald's site-visit observations, and a preliminary assessment of historical aerial photographs, they recommended the construction of a buried seawall to protect the adjacent land from erosion. Note that Cardno's report does not address that matter, only the likely effects of the proposed causeway.

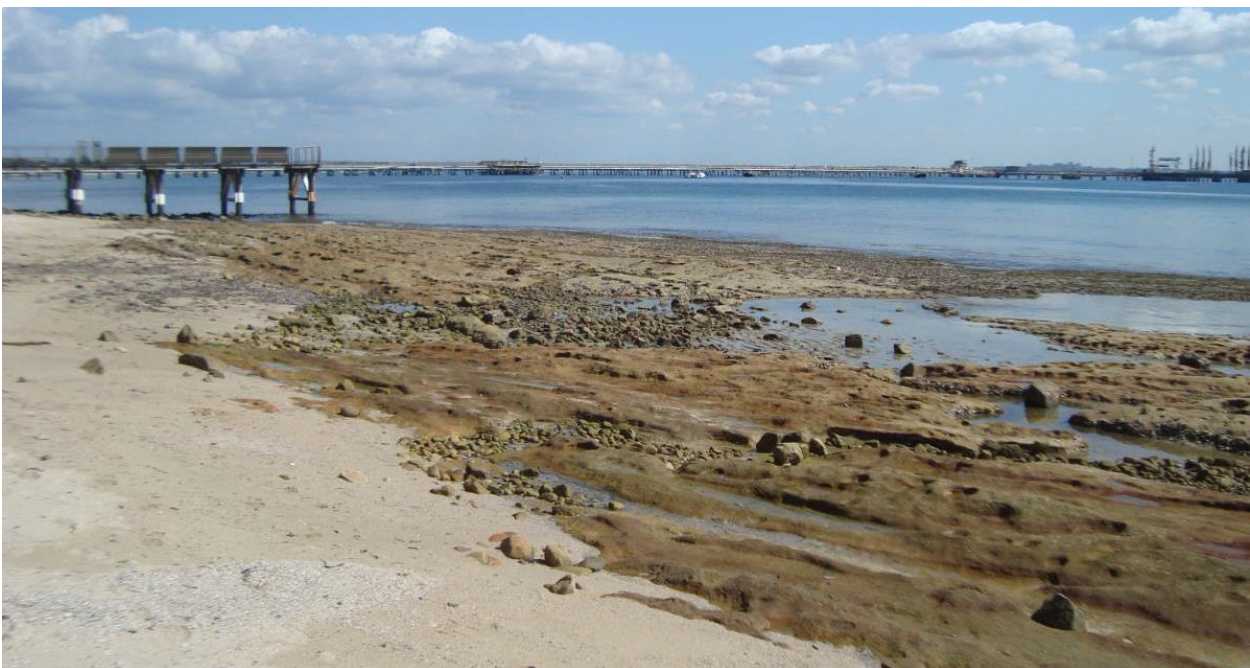


Figure 1-2 Foreshore adjacent to the Proposed Causeway (Mott Macdonald, 2018)



Figure 1-3 Erosion Scarp in 2018, the Proposed Location of the Kurnell Ferry Wharf can be seen in the Background

1.2 Site Visit 16-07-2020

Cardno's principal coastal engineer undertook a site visit to the Kurnell site at a time near low water on Thursday 16 July 2020 to assess the current condition of the shoreline and to provide further information for this assessment. The site visit was carried out at low tide to ensure access to the shoreline.

The site visit coincided with large offshore waves from the south-east ($H_s=3.6\text{m}$, $T_p=12\text{s}$, $DIR=148^\circ\text{N}$ based on the Botany Bay offshore Waverider Buoy).

Key observations from the site visit were:

1. Nearshore wave conditions, at Kurnell were small, likely to be less than 0.5m at the time of the site visit;
2. The beach at the site is perched on a rock shelf, with only very small patches of sand visible on the foreshore, indicating that longshore sediment transport is likely to be very small due to the unavailability of mobile sand in the active foreshore zone (**Figure 1-4**);
3. Large GSC sandbags have been used to construct a 'temporary' seawall on the northern side of the proposed causeway. These have been constructed as a single layer of approximately 5T sand-filled containers (refer to **Figure 1-5**).
4. The GSC bag wall does not quite abut the existing jetty, but rather terminates in an area with rock rubble, leaving a small gap between the jetty and the bags. (**Figure 1-6**) The rubble in this area is not large, and predominantly pebble sized, and as such may be washed away during a large storm event;
5. An old sandstone wall protects the footpath on the southern side of the proposed causeway. This wall appears to be in a generally good state, but some sections of the wall need repair due to dislodged sandstone blocks (**Figures 1-7 and 1-8**).



Figure 1-4 Image looking towards the proposed causeway location



Figure 1-5 GSC Sandbags protecting the Norfolk Island Pines



Figure 1-6 GSC wall Termination adjacent to the Jetty



Figure 1-7 Sandstone Wall protecting the Footpath



Figure 1-8 Example of Missing Blocks from the Sandstone Wall

1.3 Aerial Imagery Assessment

In order to assess the cause of the erosion along the beach, historical aerial imagery has been analysed. High resolution Nearmap imagery has been used covering the period between 2009 and 2020.

The vegetation lines in the images have been traced in GIS as a proxy for shoreline position, and the general trends over that eleven years period have been assessed.

The aerial imagery indicates that the erosion noted by Mott MacDonald was caused by the June 2016 east coast low (ECL) event. This shoreline change can be seen in **Figures 1-9, 1-10** and **1-11** below. The vegetation-line assessment from the imagery indicates that between 2009 and May 2016 the shoreline remained stable, with only slight changes (variations of up to 5m during this period) in the vegetation line noted in some areas. The Nearmap images used in this assessment are appended to this technical note.

Two successive images captured in 29 April 2016 and 16 June 2016 show the erosion caused by the June 2016 east coast low. The vegetation line receded by between 3m and 6m over the study area. However, the imagery post-2016 shows that the shoreline has been slowly recovering, and has only recently reached its pre-2016 ECL position (**Figure 1-6**). Note that this ECL was one of the most severe in terms of erosion at this site because of its offshore ENE wave direction and associated high water level. Peak Hs exceeded 6m for about 24 hours, with peak storm tide of about 1.3m AHD – based on MHL’s Long Reef Waverider buoy and the RAN HMAS Penguin tide gauge. Not since May 1974 had there been such a severe ENE ECL in the Sydney region.

The above analysis indicates that the main cause of erosion along this section of coastline is due to rare ENE wave-caused storm erosion, which is predominantly a cross-shore process. The beach recovery is also relatively slow, indicating only low long-shore drift close to the shoreline, because beach-building swell is quite low. Low longshore transport is also indicated by the nearshore rock shelf, visible seagrass beds close to shore and the (relatively) minor shoreline changes due to the groyne on Silver Beach to the east of the Caltex jetty – no significant accumulation of sand on the eastern side of the groyne field since its construction in the mid-1970s.



Figure 1-9 Change in the Vvegetation Line between 2009 and May 2016 (image is from November 2009)



Figure 1-10 Change in the Vegetation Line between 26 May and 16 June 2016 (image is from 16 June 2016)



Figure 1-11 Change in the Vegetation Line between June 2016 and April 2020 (image is from 12 April 2020)

1.4 Weighted Mean Wave Direction

Cardno has undertaken an assessment of the potential impacts of the proposed causeway on the adjacent beach due to altered wave directions that would be caused by the presence of the causeway. Potential long term morphological impacts to the beach, specifically changes to the alignment/orientation of the beach due to altering the prevailing directionality of the incident wave energy at the shoreline may occur. This has been assessed through analysis of the Energy Weighted Mean Wave Direction (EWMWD) at several output points along the shoreline both sides of the proposed causeway for the existing and developed cases. Changes to the mean wave direction at the shoreline could reasonably be expected to result in long term shoreline recession/accretion along the beach (depending on the nature and magnitude of any changes).

This assessment involved:

1. Re-running the SWAN wave model described in the coastal processes study to extract wave conditions along the foreshore along the -1.0m AHD bed level contour;
2. Updating the SWAN model to include the proposed causeway and re-running the long-term wave climate; and
3. Calculating the energy weighted mean wave direction for eight locations along the regional coastline for the pre and post developed cases;

Figure 1-12 presents an aerial image of the site, overlaid with the computed weighted mean wave directions for the existing case and the developed case. This figure shows that the weighted mean wave directions for both cases indicate a very low net sediment transport rate due to the wave direction being nearly perpendicular to the shoreline. The calculated weighted mean wave directions at each of the nearshore output locations are presented in **Table 1-1**. Only very minor changes to the weighted mean wave direction are predicted by the model at points D and E (less than 0.05 degree change in direction).



Figure 1-12 Pre and Post Development Energy Weighted Mean Wave Directions

Table 1-1 Calculated Pre and Post Development Energy Weighted Mean Wave Direction

Point	Energy Weighted Mean Wave Direction ($^{\circ}$ N)		
	Existing	Developed	Impact
A	354.83	354.83	0.00
B	344.56	344.56	0.00
C	341.21	341.21	0.00
D	327.18	327.14	-0.04
E	346.12	346.12	0.01
F	337.30	337.31	0.00
G	301.20	301.20	0.00
H	313.55	313.55	0.00

1.5 Impacts Due to the Causeway

The site visit, aerial imagery and modelling indicate that the longshore sediment transport rate in this shoreline area is low, and any change to the very nearshore wave climate is localised to the causeway. Any short-term impacts to the shoreline due to the causeway are therefore expected to be very localised.

Although the longshore drift is small, the causeway is still likely to result in long term changes to the shoreline in its immediate vicinity due to the blocking of longshore drift and change in near shore wave direction, albeit small. This impact is likely to be a gradual accretion of the beach to the east of the causeway, and possible erosion immediately to the west. It is unlikely to affect Silver Beach, however, the beach immediately west of the causeway, near Point D in **Figure 1-7** is likely to receive slightly less sand once the causeway is built. Based on the recent site inspection, the rock rubble on the beach at the site of the proposed causeway appears to be acting as an informal groyne by blocking longshore sediment transport. The proposed causeway is likely to block no additional longshore sediment (because of the very narrow perched beach) and is expected to have only slight impacts on coastal erosion on downdrift beaches.

It is noted that the footpath immediately south-west of the proposed causeway is currently very close to the foreshore, and could be considered to be at high risk of coastal erosion. The risk to the footpath would be higher once the causeway is constructed. This footpath is currently protected by a sandstone wall – hence, it is recommended that the integrity of the wall be investigated and repairs carried out as required to ensure the footpath is not undermined in the future.

Aerial Imagery



























AWE200187:CJS
23 June 2021

22



Yours sincerely,

A handwritten signature in blue ink, appearing to read "Chris Scraggs".

Chris Scraggs
Service Area Lead - Coastal
for Cardno
Direct Line: +61 2 9024 7184
Email: christopher.scraggs@cardno.com.au